MOSCOW ENGINEERING PHYSICS INSTITUTE

ACTIVATION STUDY IN THE ATLAS DETECTOR

V.A.Klimanov, E.I.Kulakova, M.N.Morev, V.K.Sakharov

ISTC Project #1800
I quarter (April-June 2001)

Abstract

Some previous studies carried out in separate parts of the ATLAS detector has shown that the dose rate due to induced activity may be rather high, that will create certain difficulties during maintenance of the detector. So that a comprehensive study of activation is necessary in the detector as a whole. This note reports on results obtained in evaluating the induced activity in the ATLAS detector. Dose rates from the Disk Shielding Plug and Forward Shielding Bridge were evaluated as well. Both activation induced by low energy neutrons and high energy hadrons are taken into consideration.

Moscow, 5 July 2001

1. Introduction

Shielding and equipment are activated by elementary particles during LHC operation. Induced radioactivity depends on flux, energy spectra of particles, activation (radioactive nucleus production) cross-section, concentration of target nuclei in the material, exposure time, and time after shut down.

Interactions of hadrons with stable nuclei produce most contribution to induced radioactivity. From the methodical point of view, its is convenient to divide the energy range onto two sub-ranges: (1) from thermal energies to 20 MeV, and (2) above 20 MeV. The point is that different processes of radionuclide production predominate in the energy ranges. At energy below 20 MeV, neutron induced reactions like (n,γ), (n,p), (n,α), and (n,2n) predominate. While, at energy above 20 MeV hadron induced reactions (x,Spall), were *X* is proton, neutron, Pi+, or Pi- are most important. The division is also convenient due to different representation and availability of activation cross-sections. Neutron cross-sections are studied well for energy below 20 MeV as widely used in reactor applications. For energy above 20 MeV activation cross-sections are usually studied in less detail. As a rule, only protons cross-sections are studied well enough and used as a conservative estimation for other particles.

The note reports on the results achieved during the first phase of implementation of the ISTC #1800 project. The basic aims for the phase are preparation of necessary data sets and codes for a further comprehensive study of induced activity and doses in the ATLAS detector. The following preliminary results are given:

- Distribution of induced activity against R and Z axes for widely used materials like carbon, aluminum alloys, cast iron, stainless steel, and copper alloys;
- Equivalent dose rate around JD Plug and JF Bridge.

2. The simulations

Induced activity

It is convenient to use activation integral for calculation of induced activity. The integral, calculated per one target nuclear, shows the rate of a nuclear reaction:

$$q = \int_0^\infty \sigma(E)\varphi(E)\,dE\,,$$

where, ***σ(E)*** - activation cross-section, ***φ(E)*** - flux of particles.

Having solved the balance equation for the number of radioactive atoms, one could come to the formula for activity per unit volume

$$A_v = nq\left(1-\exp(-\lambda T)\right)\exp(-\lambda t) \qquad (1)$$

where λ is the decay constant, $\lambda = \ln(2)/T_{1/2}$;
n - number of target nuclei per unit of volume;
T - is exposure time in the steady flux;
t - time after shut down.

At that, we disregard the burning-out processes for both stable and target nuclei. The same expressions one could formulate for the daughter radioactive nuclei produced by

radioactive decay of the radionuclide-product of nuclear reaction. Practically, it is enough to consider a mass-chain of three radioactive nuclei, as there is not a radionuclide with half decay exceeding few hours, which would have a longer mass-chain.

In the case the flux cannot be considered as steady in time, its possible to approximate it with a step-wise function of time. So that, the formula (1) will transform into the following:

$$A_{\text{v}} = \frac{nq_{nom}}{W_{nom}}\left\{\sum_{j=1}^{J} W_j\left(1-\exp(-\lambda\Delta T_j)\right)\exp\left(-\lambda\ (t+T-\sum_{i=1}^{j}\Delta T_i)\right)\right\} \qquad (2)$$

where q_{nom} - is activation integral calculated for the nominal W_{nom} luminosity; W_j – luminosity during the time period ΔT_j; $T = \sum_{j=1}^{J} T_j$ - full exposure time.

Number of target nuclei per unit volume in formulas (1) and (2) are calculated using:

$$n = P\rho N_A / A, \qquad (3)$$

where, P - natural abundance of the isotope in natural material; ρ - density; N_A – Avogadro constant; A- atomic weight of the element.

Volume activity can be expressed in terms of contact dose rate - dose rate at the surface of a semi-infinite source uniformly contaminated with volume activity A_v.

Any radionuclide emitting ***I*** gamma rays with different energy E_{0i}, MeV, and absolute intensity n_i, photons per decay, will produce contact dose rate $\dot{H}$, Sv/h:

$$\dot{H} = \frac{2\pi\Gamma_H A_v}{\mu_{en}^{S}(\bar{E})\rho} 3600\cdot 10^4, \qquad (4)$$

where $\mu_{en}^{S}(\bar{E})$, cm^2/g, - mass energy attenuation coefficient for average energy $\bar{E}$ emitted by the radionuclide; ρ- is density of material, g/cm^3.

Γ_H, $\frac{Sv\cdot m^2}{Bq\cdot s}$, – so-called "gamma-factor", which is constant for the radionuclide:

$$\Gamma_H = \frac{\sum_{i=1}^{I}\left(E_{0i} n_i \mu_{en,m}^{tiss}(E_{0i}) w\right) 1.602\cdot 10^{-13}}{4\pi}. \qquad (5)$$

$\mu_{en,m,i}^{tiss}(E_{0i})$ - mass energy attenuation coefficient for energy E_{0i} emitted by the radionuclide in the biological tissue, m^2/kg;

w= 1 Sv/Gy - tissue weighting factor for photons;

Factor 1.602E-13 is used to transform energy E_{0i} from MeV to Joles.

If the source contains more than one radionuclide, then the contact dose will be the sum for all the radionuclides.

Another value, which can be used for characterization of emitting power of a radioactive source is so-called "gamma-equivalent", which is a product of gamma-factor by activity. Gamma-equivalent is equal to the dose from a point-wise radioactive source with activity A at the distance 1 m. For example, volume gamma-equivalent can be calculated by the formula

$$k_{e,v} = A_v \Gamma_v \qquad (6)$$

There exists a direct relation between the gamma-equivalent and contact dose rate:

$$\dot{H} = \frac{2\pi k_{e,v}}{\mu_{en}^{S}(\bar{E})\rho} 3600 \cdot 10^{4} \qquad (7)$$

The described methods for simulation of induced activity and dose characteristics (contact dose rate and gamma-equivalent) have been implemented in the ACTIVATION-2 code [1,2]. Additionally, the code allow to calculate a distributed volume source which is used in the study as input for simulation of photons transport with widely used codes DOT-III [3] and MCNP [4]. The ACTIVATION-2 code is equally applicable for study of both low energy neutrons and high-energy hadron activation if relevant group activation cross-sections libraries are available.

3. Input data

In order to calculate specific induced activity one should know:

- flux of incident particles;
- concentration of target nuclei;
- cross-section of nuclear reactions producing radioactive nuclei;
- operation scenario: time of operation ***T*** and time of cooling ***t***.

Status of input data

1) Fluxes	**Available**
2) Concentration of target nuclei and geometry;	for high energy activation - are **available** from GEANT/GCALOR geometry file - bulky items, such as shielding, are represented rather well; for thermal neutron activation - **incomplete**- concentration of impurities are taken conservative
3) Cross-section of nuclear reactions producing radioactive nuclei	for low energy neutrons - **available** for high energy hadrons - **incomplete**- proton cross-sections are used
4) Operation scenario	**General assumptions** are made; more details on maintenance procedure and operation history are needed for further study of doses

Fluxes

Fluxes in the region 0<R<12 m, 0<Z<24 m, together with a readback procedure, were produced by Mike Shupe with GEANT/GCALOR. The following data available [5]:

- Fluxes on 10 cm x 10 cm grid

1. High energy neutrons above 20 MeV;
2. Fast neutrons - 2.19 MeV to 20 MeV;
3. Intermediate neutrons - 3.78 keV to 2.19 MeV;
4. Moderated neutrons - 0.414 eV to 3.78 keV;
5. Thermal neutrons - 10E-5 to 0.414 eV;

6. Protons above 20 MeV;
7. Pi minus above 20 MeV;
8. Pi plus above 20 MeV;
9. Stars, threshold 50 MeV.

- Neutron spectra on 100 cm x 100 cm grid, 61 energy groups.
- Charged hadron spectra on 50 cm x 50 cm grid, 21 energy groups:

1. protons,
2. π- pions,
3. π+ pions.

The data was calculated for latest baseline geometry of February 2001. Totally, 1505 events were processed.

Cross-sections

Cross-sections of nuclear reactions producing radioactive nuclei are usually available in form of data libraries.

Historically, neutron cross-sections, ranging from thermal energies up to 20 MeV, are studied rather well, because they are extensively used in fission reactor applications. There are number sources available, e.g ENDF, JANDL, IRDF.

Calculated proton cross-sections for threshold reactions are available up to energy 100 MeV (MENDL-2 data library for nuclear activation and transmutation). Proton reaction data up to energy 10 GeV are also available in the form of experimental or calculated data compilations for a limited list of materials [6,7].

Cross-section data set for protons was prepared in the same energy group structure as fluxes. By now the data set includes Be, C, Al, Mn, Fe, Ni, Cu, Au. For other elements we use cross-sections of material with a most close atomic number. For example, in the study we use cross-sections for Cu instead of Zn.

There were no pions reaction data found so far. For the purpose of this study, proton cross- sections are used for all hadrons with energy above 20 MeV. The estimation is rather valid for neutrons and results in certain conservatism for pions (up to 30%), that can be concluded from the energy dependence of hadrons inelastic cross-sections.

Concentrations

Concentration of target nuclei were taken from various sources. Most informative are results of neutron activation analysis, though available only for a restricted number of materials. Other possible sources can be either real specifications of materials or industrial specifications like ASTM, and so on [8].

It is very often, that impurities at level of 100-1000 ppm may produce major contribution to activation due to thermal and moderated neutrons. For example, the most sensitive impurity in ferrous materials is cobalt. Its content ranges from 30 ppm to 150 ppm in carbon steel, and from 150 ppm to 2000 ppm in stainless steel. It is Co-60 (reaction Co-59(n,.)Co-60) that will determine doses from stainless steel after few years of operation. Other sensitive elements are Ag and Sb, for example in copper and solder.

Concentrations of elements in some materials used for the study are summarized in Table 1.

Operation scenario

For the purpose of this study there is no need in detail specifying LHC operation history. It is assumed, for the short term operation scenarios (less than one year), that LHC is operated at high luminosity during T and then is shut down during time t. For long-term operation scenarios, 120 days per year run at high luminosity was assumed and the rest of the year LHC is shut down.

For the further study of dose rates, it is necessary to establish maintenance scenarios, including realistic LHC operation history, access locations, and time after shut down. Work time at access locations should be specified as well, to enable doses estimations.

Geometry

For these studies, of interest are the JD Plug and JF Bridge designs. As the design has not been finalized yet, the latest version of GEANT/GCALOR geometry description file of February 2001 was used. Some details of design and materials were taken from private communications.

- JD plug materials were taken cast iron and brass (90% Cu, 10% Zn). For design features see Fig.1.
- JF bridge is the lowest part of removable Forward shielding. Material was taken gray cast iron. The design was taken from a latest proposal.

4. Results

Activation of carbon, 2000 Series Aluminum Alloy, 5000 Series Aluminum Alloy, Cast Iron, Stainless Steel 304 type, Copper Alloy (UNS C19500), and Commercial Bronze 220 have been studied. Two-dimension activity distributions for every single material are given at fig. 2-85. The fields shows the areas, where an item made of given material of interest would be highly radioactive (above 100 μSy/h in terms of surface dose rate), radioactive (from 100 μSy/h to 10 μSy/h), and slightly radioactive (from 10 μSy/h to 0.1 μSy/h). The color data represents relative contribution of low energy neutrons to the total contact dose. The activation fields were calculated for T=30 days and t=1 day and 5 days; T=100 days and t=1 day, 5 days, 30 days, and 100 days; T= 10 years and t= 1 day, 5 days, 30 days, 100 days, 200 days, and 2 years.

The dose rates around JD Plug and JF bridge were calculated for T=30 days, 100 days, 5 years, and 100 years; time after shut down is 1 day and 5 days.

Dose rates around JD Plug were calculated with DOT-III radiation transport code. The dose rates around the plug due to high-energy hadrons are given at Table 2 and for low energy neutrons at Table 3. Results are given averaged over volumes 10 cm x 10 cm.

It is known that a discrete ordinate code like DOT can result in significant inaccuracy being implemented for geometry with localized source surrounded with low-density material like air due to the so-called "ray-effects". So, in order to estimate the related inaccuracy, some calculations were carried out for the same geometry with MCNP code. The dose rates from high-energy hadrons around the plug calculated for T=30 days and t= 1 day are given on Table 4. Statistical error do not exceeds 10% in every volume. The discrepancy do not exceeds 30% for all the volumes.

Dose rate inside Forward Shielding was calculated with DOT-III radiation transport code and a simple calculations code was developed to calculate doses from JF bridge, which

was represented as a set of surface sources. The dose rates around JF Bridge due to high-energy hadrons are given at Table 5 and due to low energy neutrons at Table 6.

5. Conclusions

Levels of induced activity in the ATLAS detector are significant. At the locations most close to the Z-axis, the contact dose rate may reach hundreds mSv/h. In these regions high energy hadrons usually produce a relatively high contribution, though low energy neutrons activation cannot be neglected even in this regions. For example, thermal and intermediate energy neutrons produce a considerable activation in copper for few days after shut down.

Dose rate in the plug region does not exceed some mSv/h. At 1 day after shut down contribution of high-energy hadrons activation exceed by a factor of 2 the contribution of low energy neutrons and neutron induced activation promptly decreases with time as half decay of most important activation product ^{64}Cu is 12.7 hours. This fact requires well-defined and optimized access maintenance procedures. Dose rates around JF Bridge seems to be of no concern. At the side surface the doses will not exceed few tens μSv/h, and most contribution produce the inner layers. Dose rate at front surfaces will be about 500 μSv/h. So that, certain precautions during handling the bridge are necessary.

6. Acknowledgements

The authors would like to thank M.Shupe for calculation of hadron fluxes and V.Hedberg for many useful discussions.

References

1. Borisov S.E., Kudryavtseva A.V., Leschenko A.V. at. al. VVER-500 as a source of induced activity resulting from decommissioning. Atomic Energy, Translated from Russian Original Vol.77, No.4, October, 1994. ISSN 1063-4258. pp.802-807.
2. Engovatov I.A., Mashkovich V.P., Orlov Yu.V. at.al. Radiation Safety under Decommissioning of Nuclear Reactors of Civilian and Mililitary Purposes/ ISTC Project #465-97.
3. Mynat F., Engle W.Jr., Gritzner M. et.al. The DOT-III Two-Dimentional Discreate Ordinates Transport Code. ORNL-TM-4280, 1973.
4. J.F.Briesmeister,Ed., MCNP -A General Monte Carlo N-Particle Transport Code, Vertion 4A, Los Alamos National Laboratory Report, LA-12625, 1995
5. ~shupe/w1/morev/flux_morev_jdcu.dat
6. A.S.Botvina, A.V.Dementyev, o.N.Smirnova, N.M.Sobolevsky. International Codes and Models Intercomparison for Intermediate Energy Activation Yields. Report of the Institute for Nuclear Research of RAN. Moscow, 1995
7. V.G.semenov, N.M.Sobolevsky. Approximation of Radionuclides Production Cross-Sections in Proton Induced Nuclear Reactions. Report on ISTC Project #187. Moscow, 1998
8. www.engineering-e.com/datamat/index.html; www.matls.com

Table 1

Concentrations of elements in materials, %

Element	Gray cast iron, ASTM A 48 Class 40, cast iron	Stainless steel Type 304	5000 Series Aluminum Alloy	2000 Series Aluminum Alloy	Copper, UNS C19500	Commercial Bronze 220	Carbon
C	3.5	0.08					100
Mg			4.5	0.02			
Al			94.8	93			
Si			0.4	0.2			
Ti			0.15	0.1			
V				0.15			
Cr	0.45	19	0.25				
Mn	0.9	2	1	0.4			
Fe	95	71	0.4	0.3	1.5		
Co	0.015(*)	0.2			0.8		
Ni	0.2	10.5					
Cu	0.4		0.1		97	90	
Zn			0.25	0.1		10	
Zr				0.25			
Mo	0.1						
Sn					0.6		

* Conservative assumption.

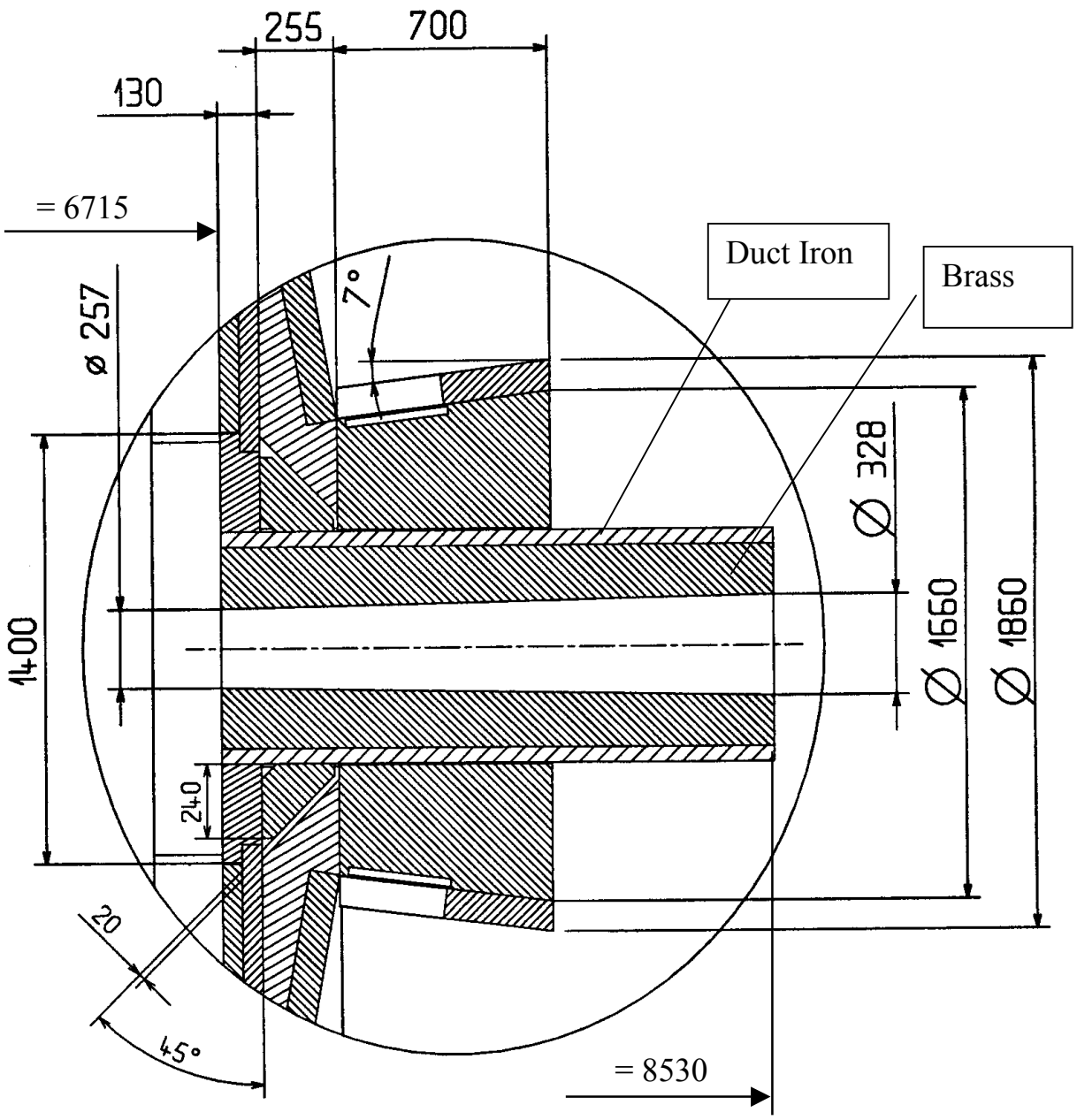

Fig.1. Disc Shielding plug.

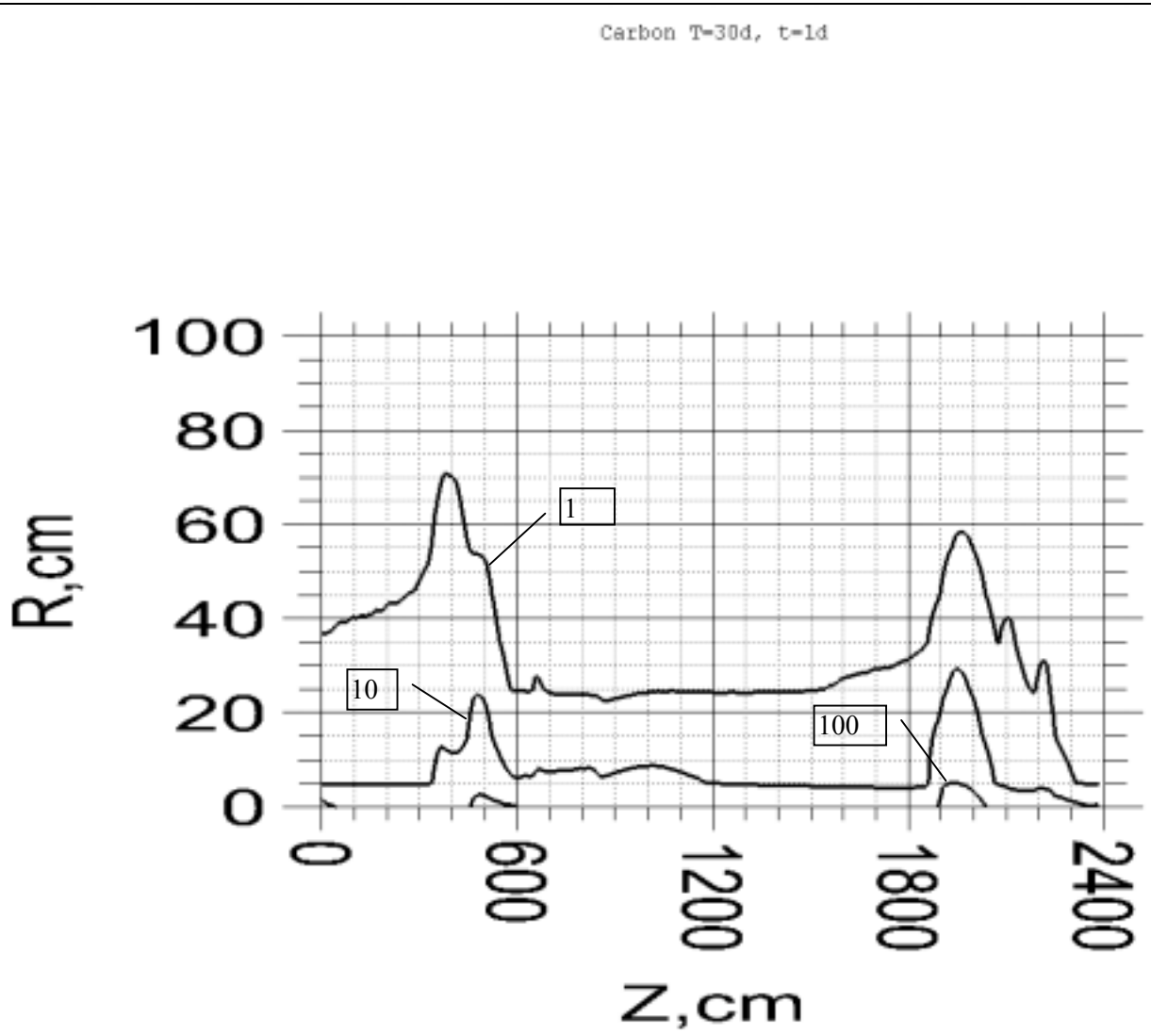

Fig .2. Distribution of induced radioactivity in carbon calculated at T=30d, t=1d. The levels show contact dose rate in μSv/h.

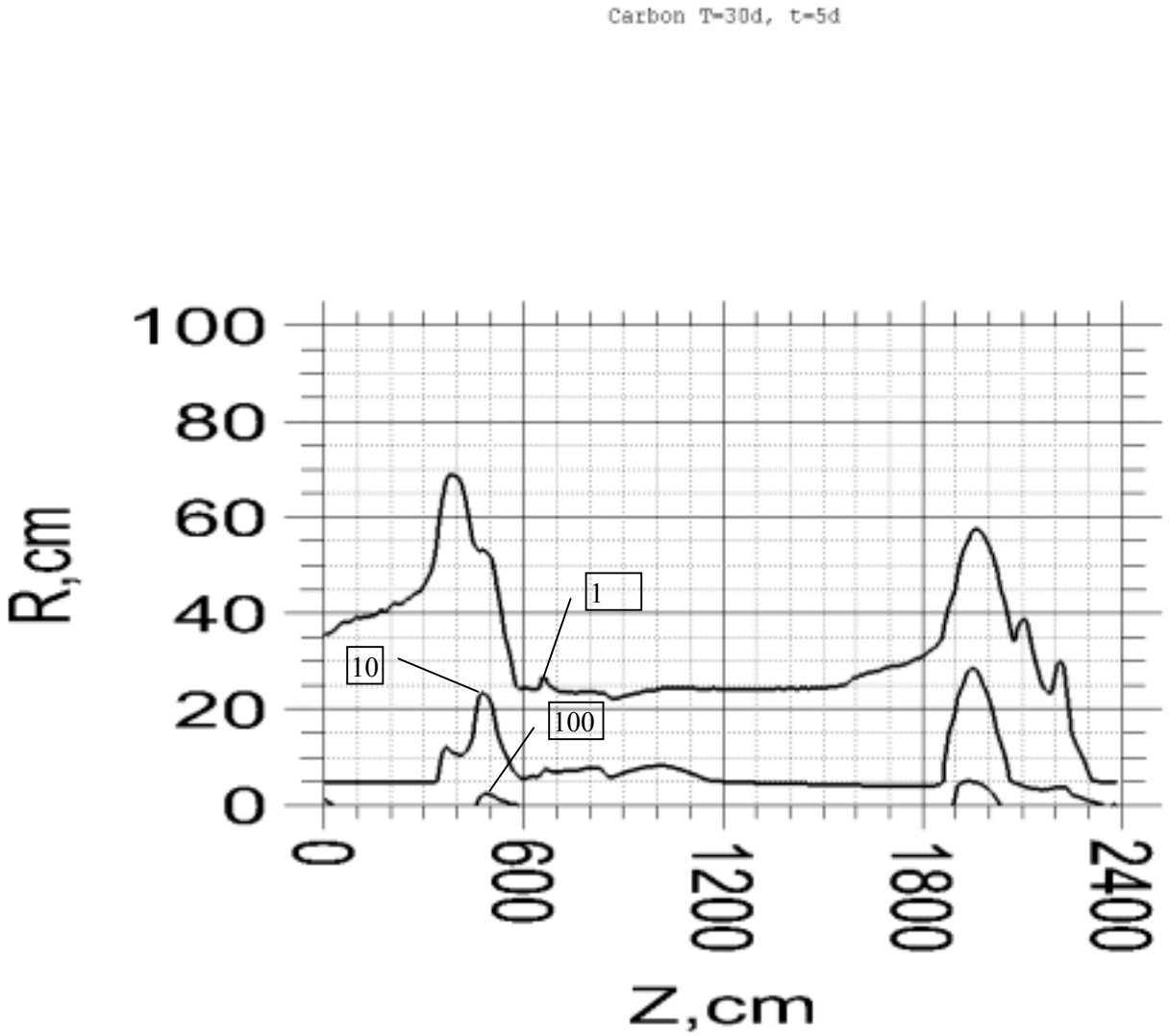

Fig .3. Distribution of induced radioactivity in carbon calculated at T=30d, t=5d. The levels show contact dose rate in μSv/h.

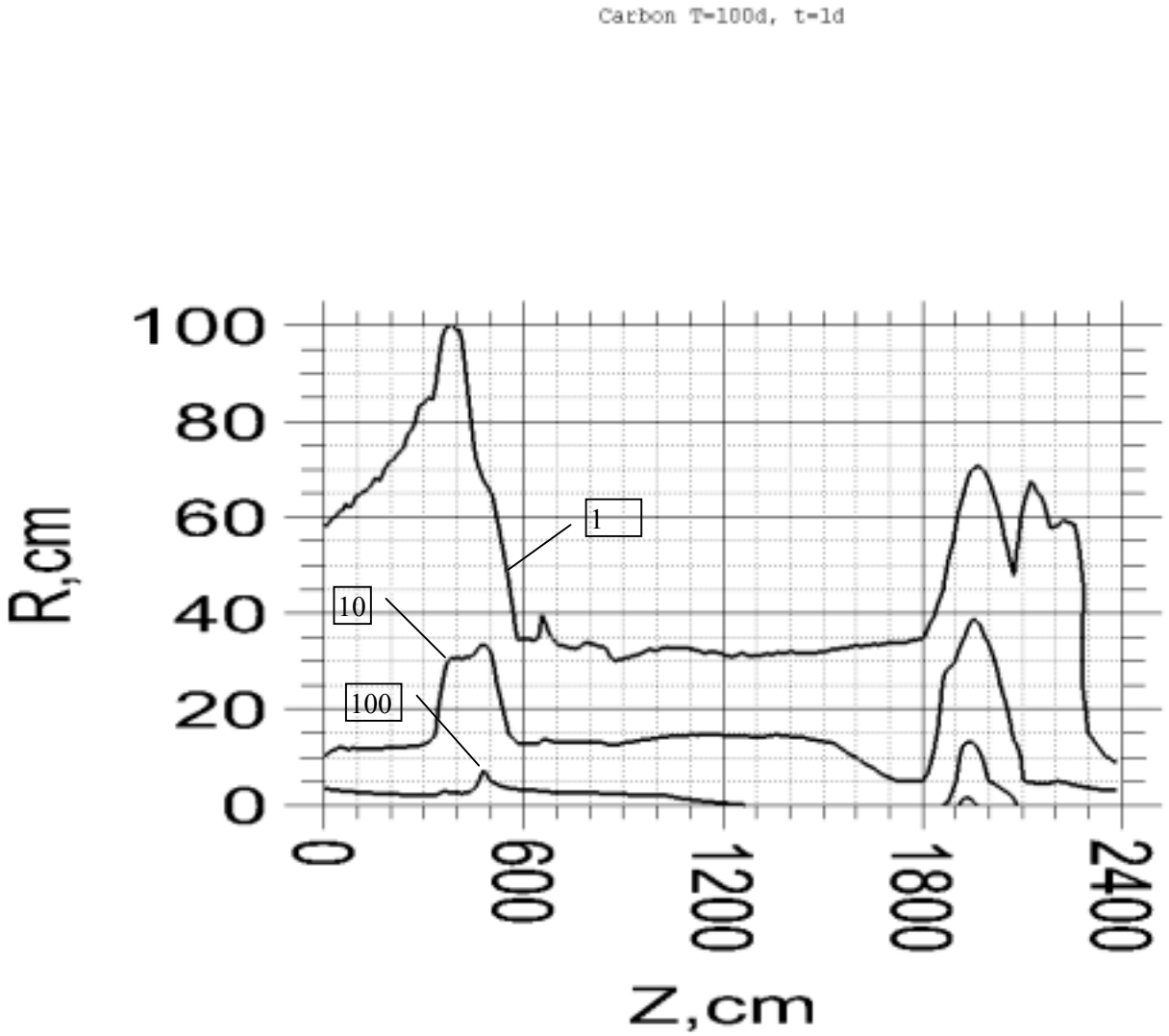

Fig .4. Distribution of induced radioactivity in carbon calculated at T=100d, t=1d. The levels show contact dose rate in μSv/h.

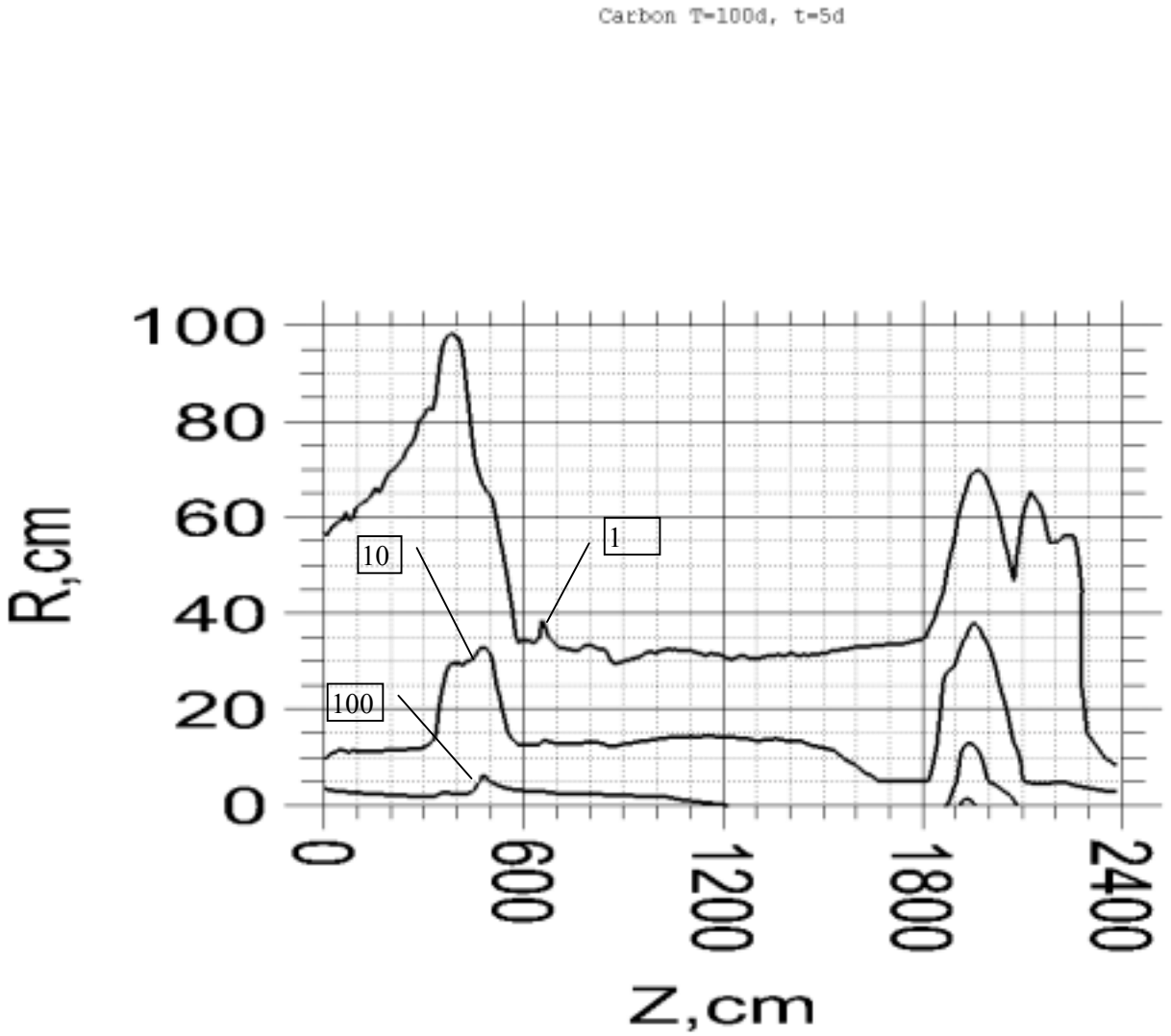

Fig .5. Distribution of induced radioactivity in carbon calculated at Carbon T=100d, t=5d. The levels show contact dose rate in μSv/h.

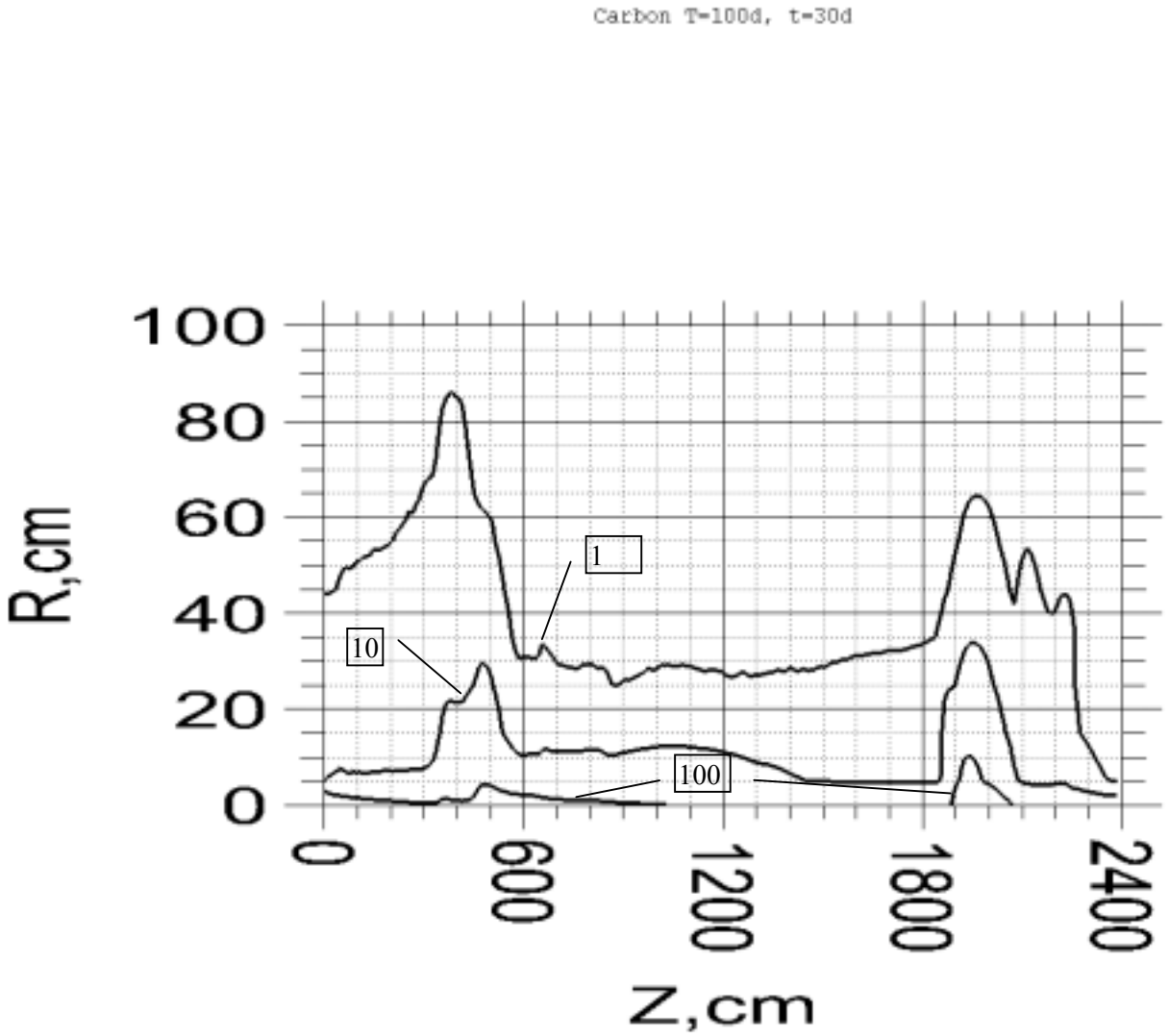

Fig .6. Distribution of induced radioactivity in carbon calculated at T=100d, t=30d. The levels show contact dose rate in μSv/h.

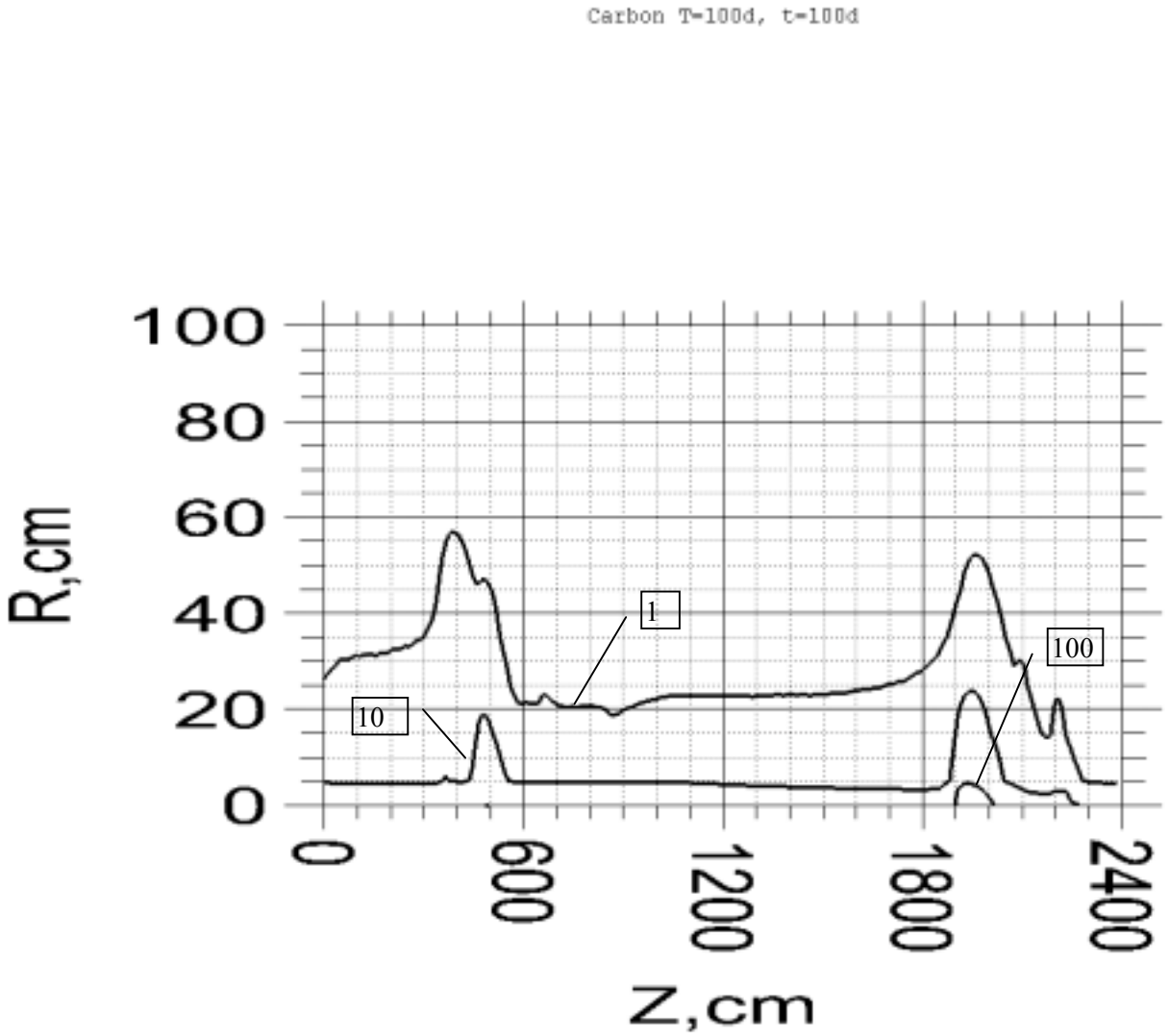

Fig .7. Distribution of induced radioactivity in carbon calculated at T=100d, t=100d. The levels show contact dose rate in μSv/h.

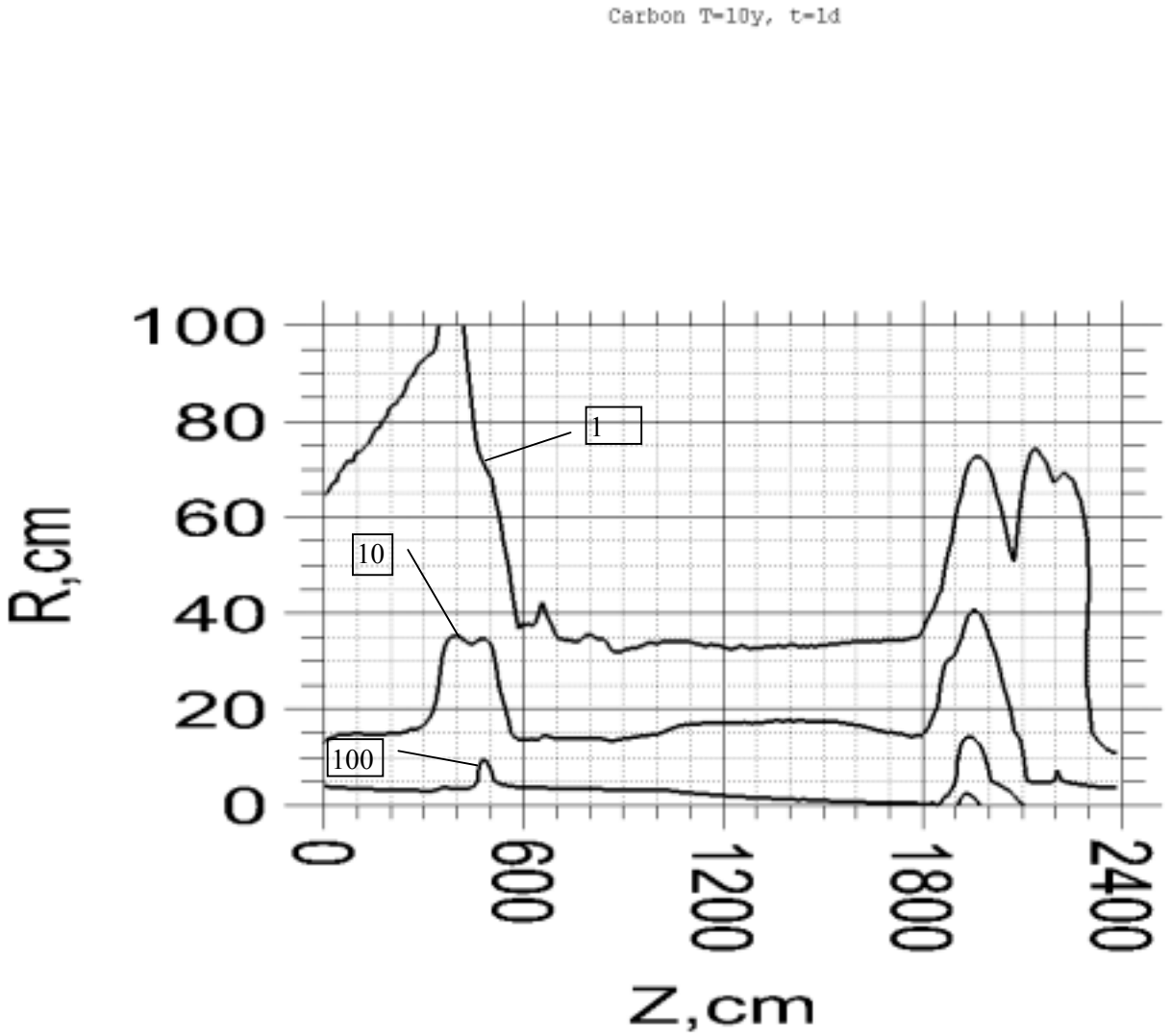

Fig .8. Distribution of induced radioactivity in carbon calculated at T=10y, t=1d. The levels show contact dose rate in μSv/h.

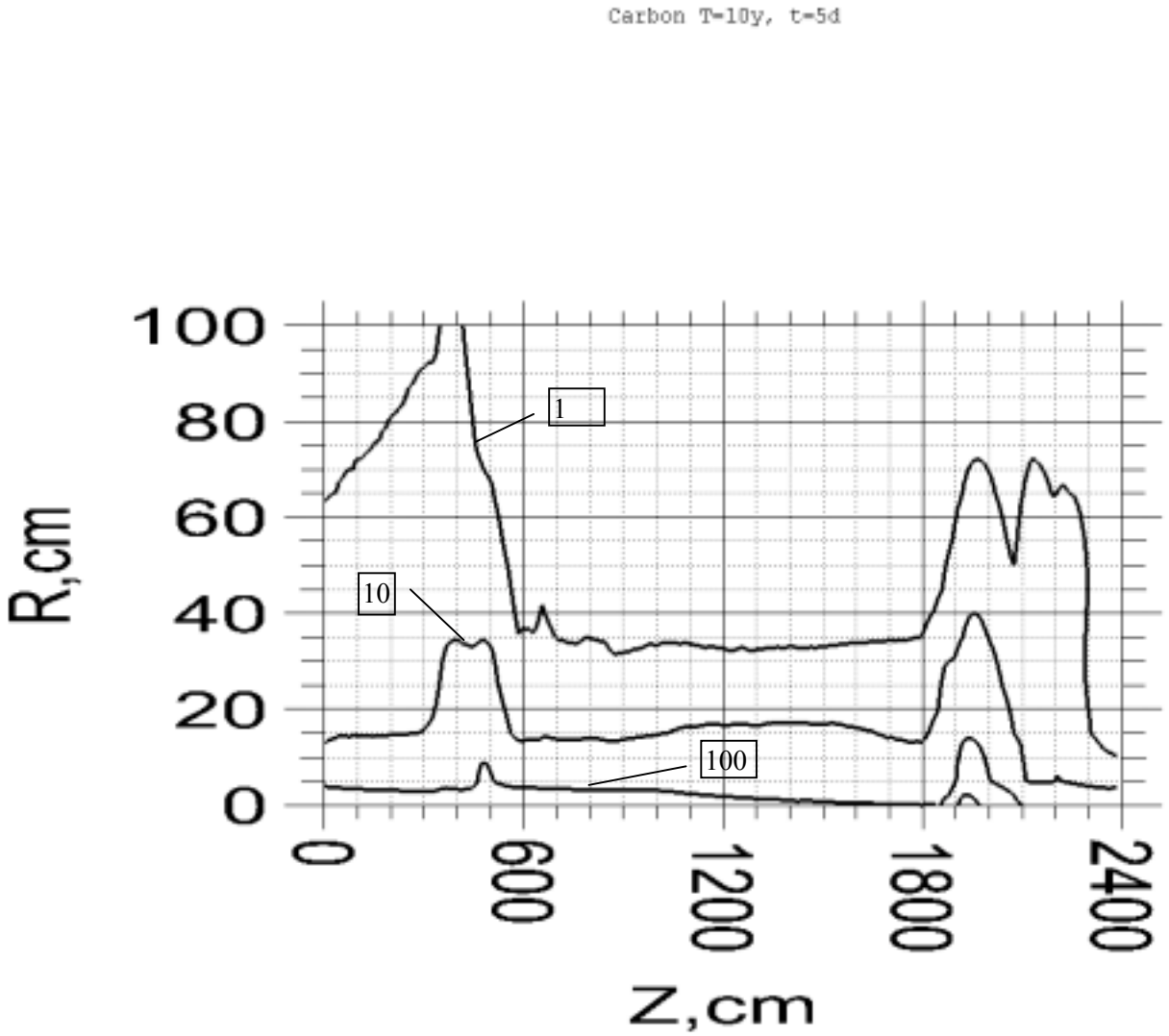

Fig .9. Distribution of induced radioactivity in carbon calculated at T=10y, t=5d. The levels show contact dose rate in μSv/h.

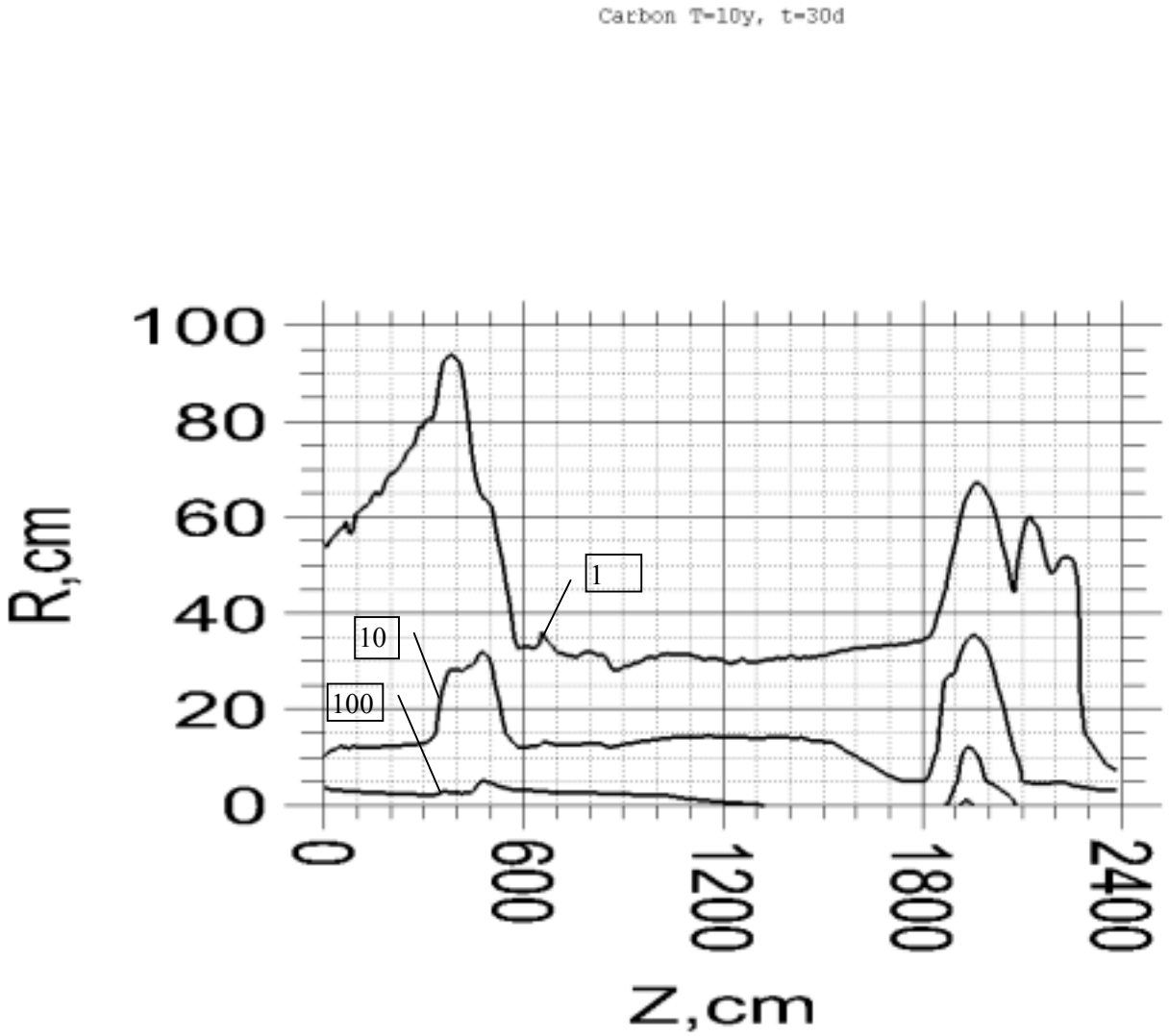

Fig. 10. Distribution of induced radioactivity in carbon calculated at T=10y, t=30d. The levels show contact dose rate in μSv/h.

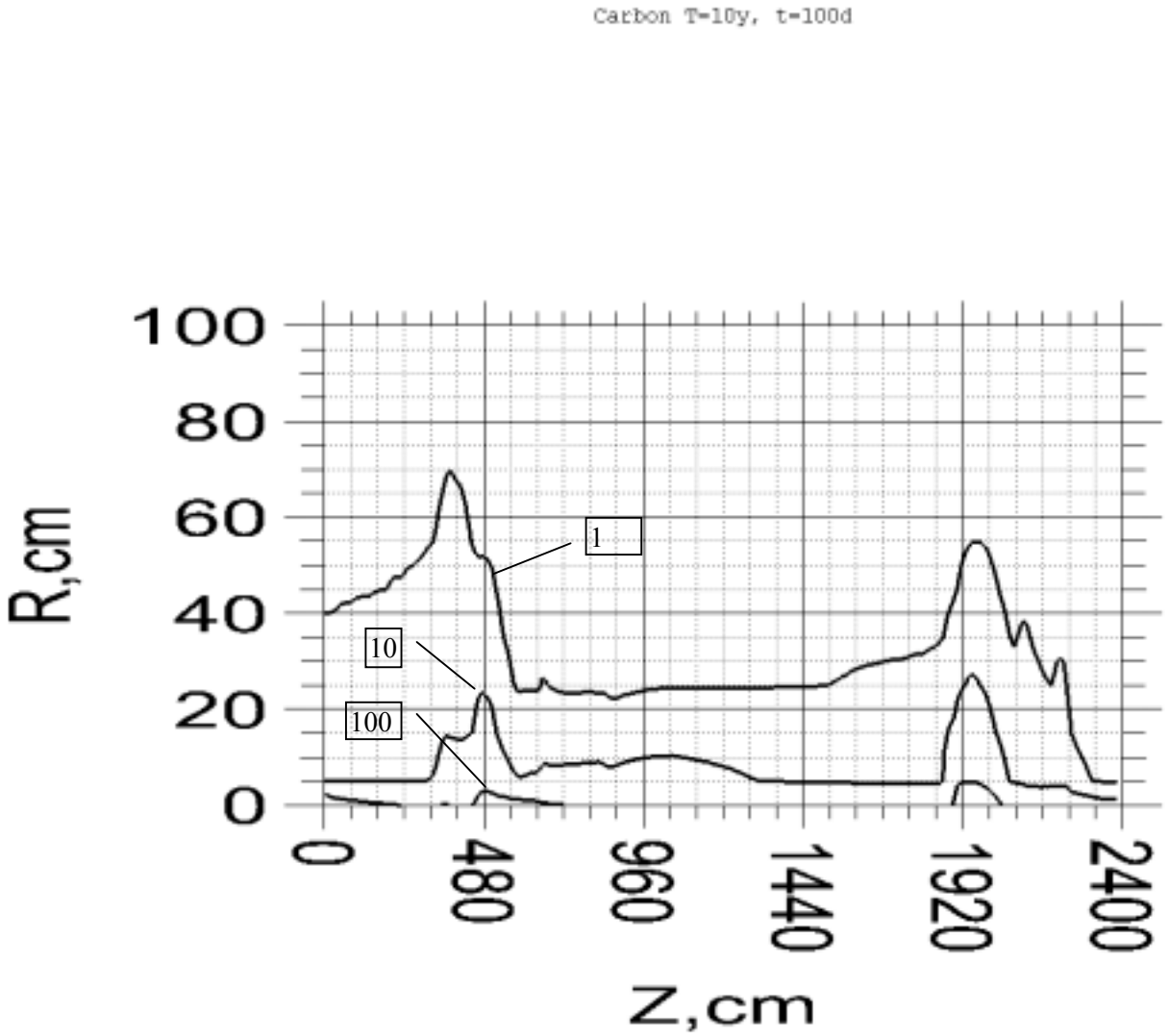

Fig. 11. Distribution of induced radioactivity in carbon calculated at T=10y, t=100d. The levels show contact dose rate in μSv/h.

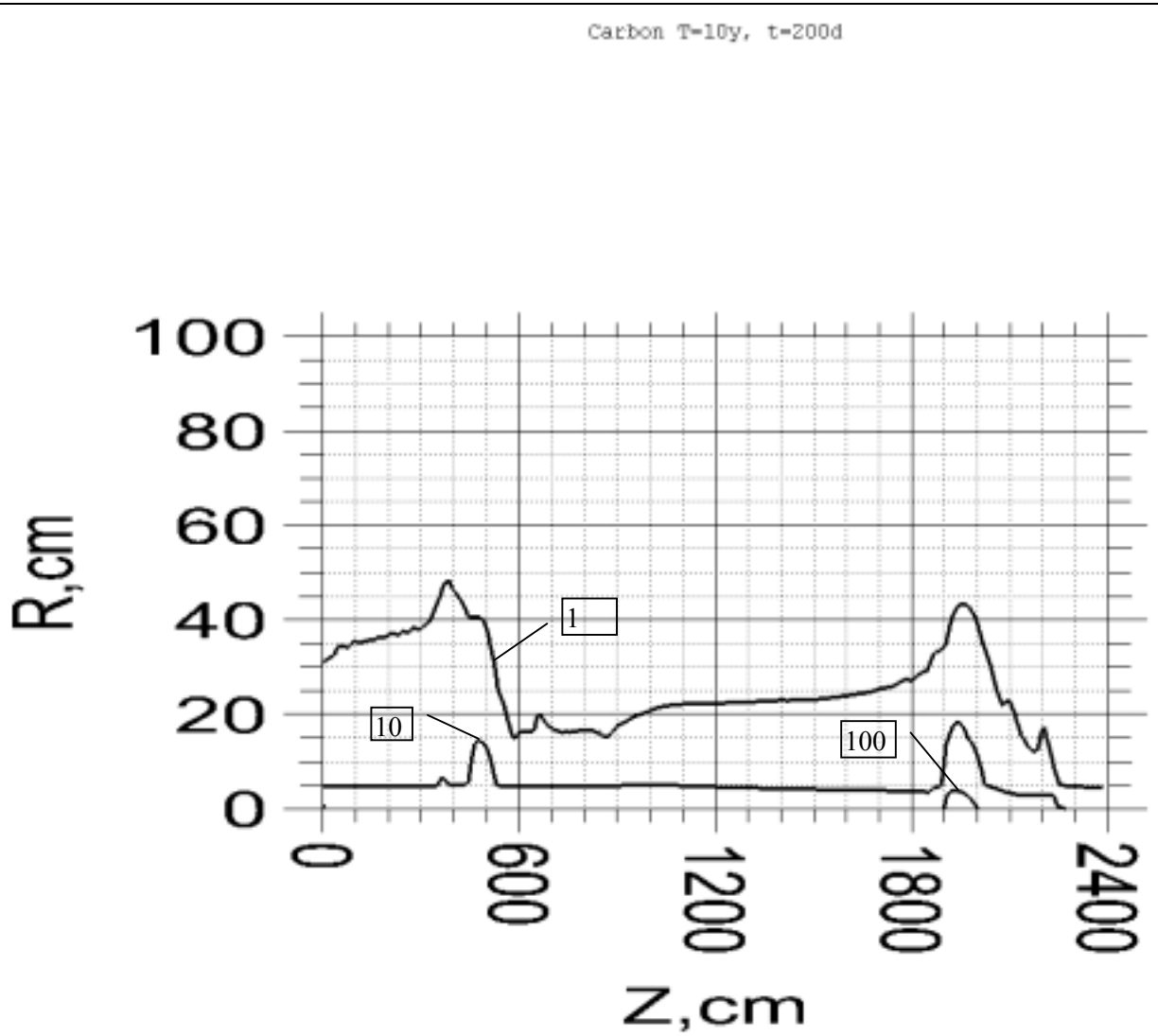

Fig. 12. Distribution of induced radioactivity in carbon calculated at T=10y, t=200d. The levels show contact dose rate in μSv/h.

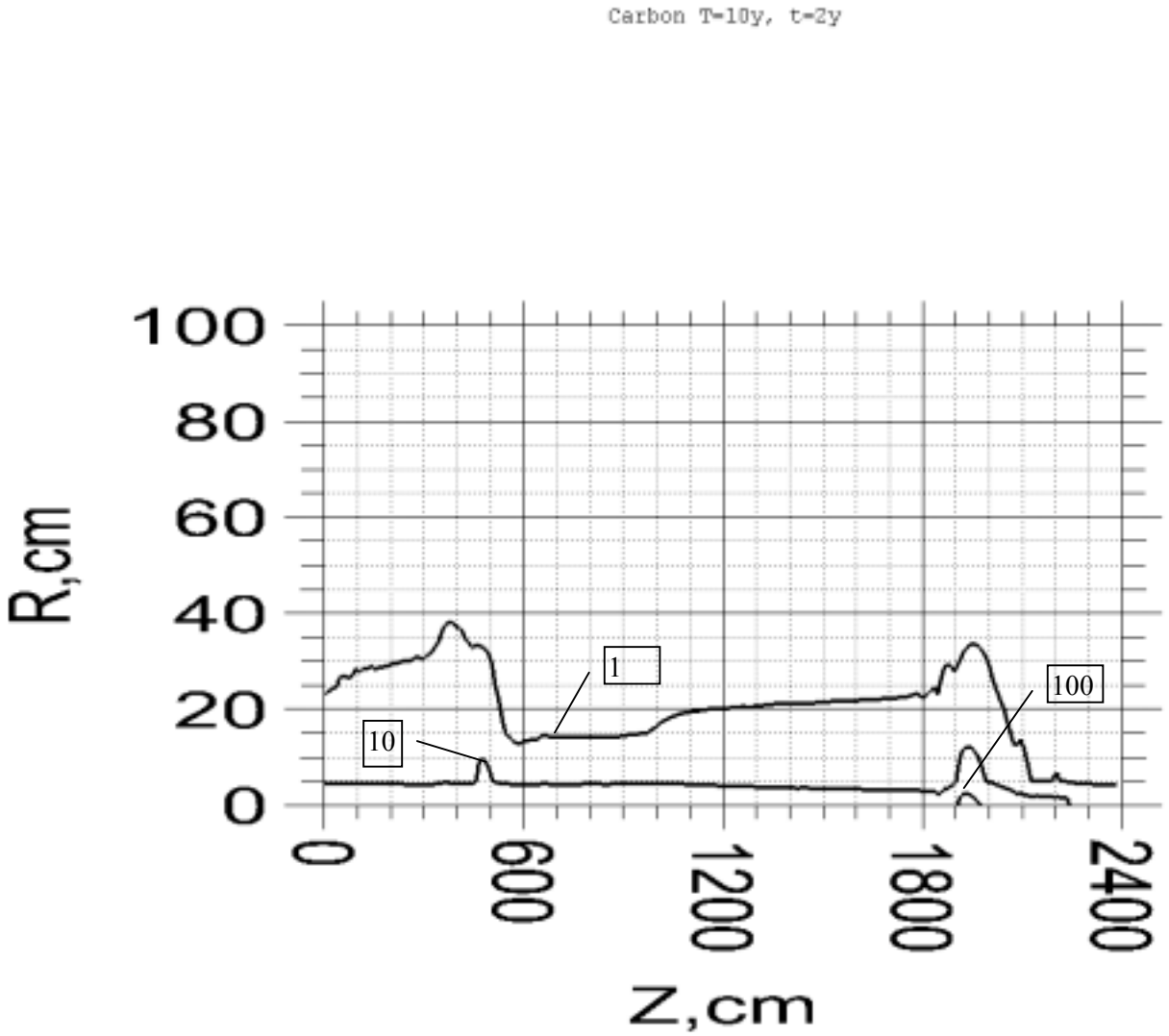

Fig. 13. Distribution of induced radioactivity in carbon calculated at T=10y, t=2y. The levels show contact dose rate in μSv/h.

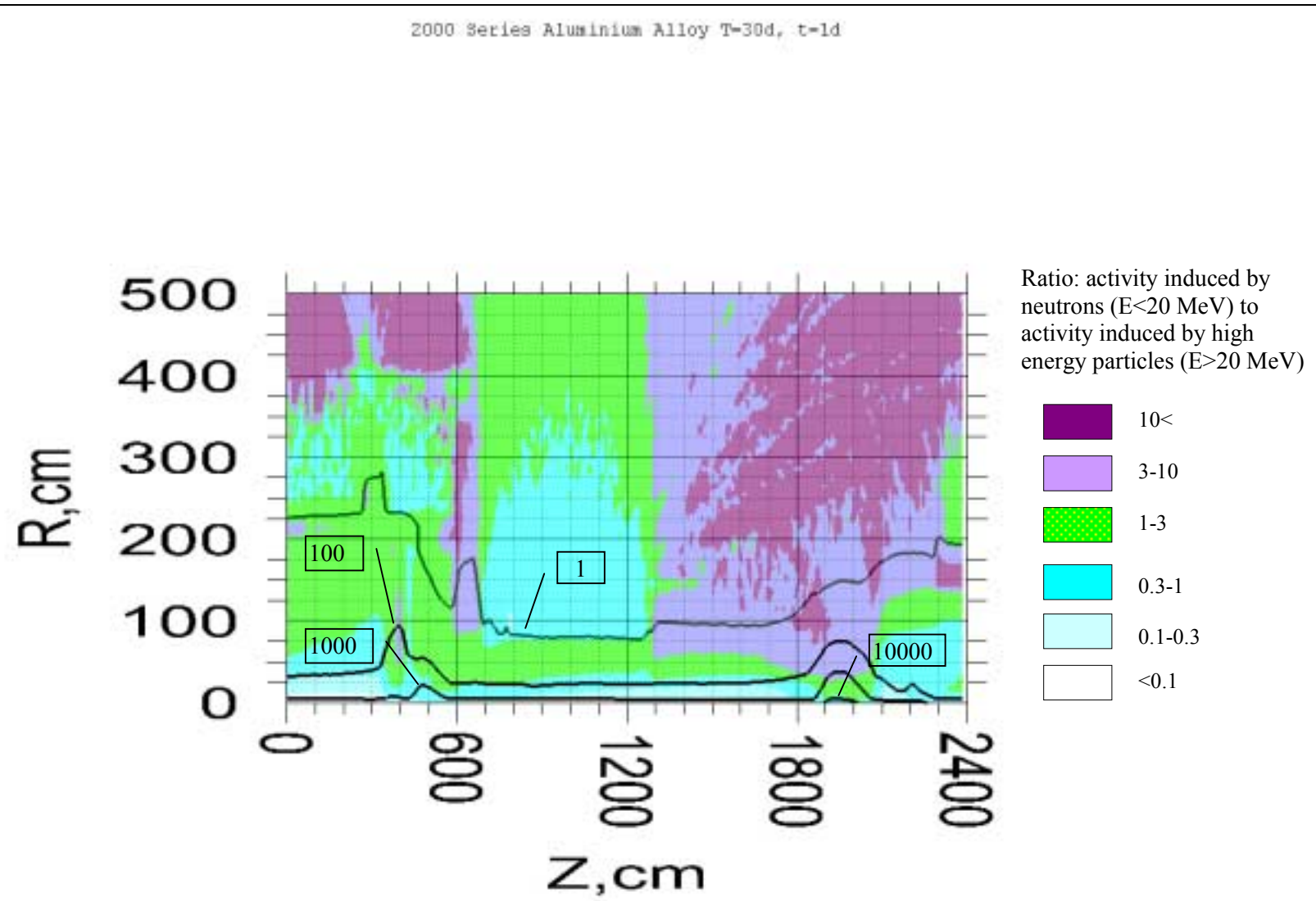

Fig .14. Distribution of induced radioactivity in 2000 Series Aluminum Alloy calculated at T=30d, t=1d. The levels show contact dose rate in μSv/h.

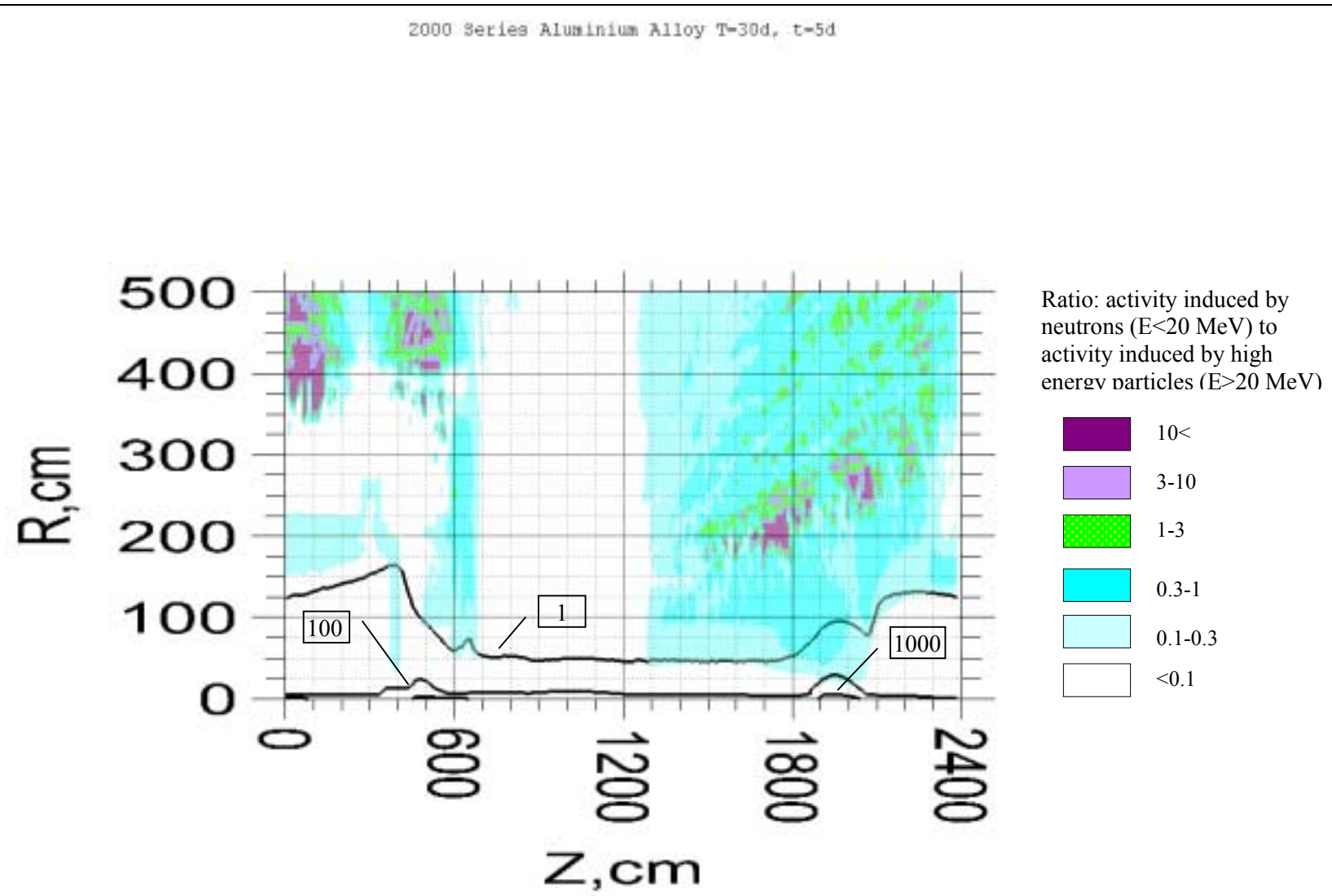

Fig .15. Distribution of induced radioactivity in 2000 Series Aluminum Alloy calculated at T=30d, t=5d. The levels show contact dose rate in μSv/h.

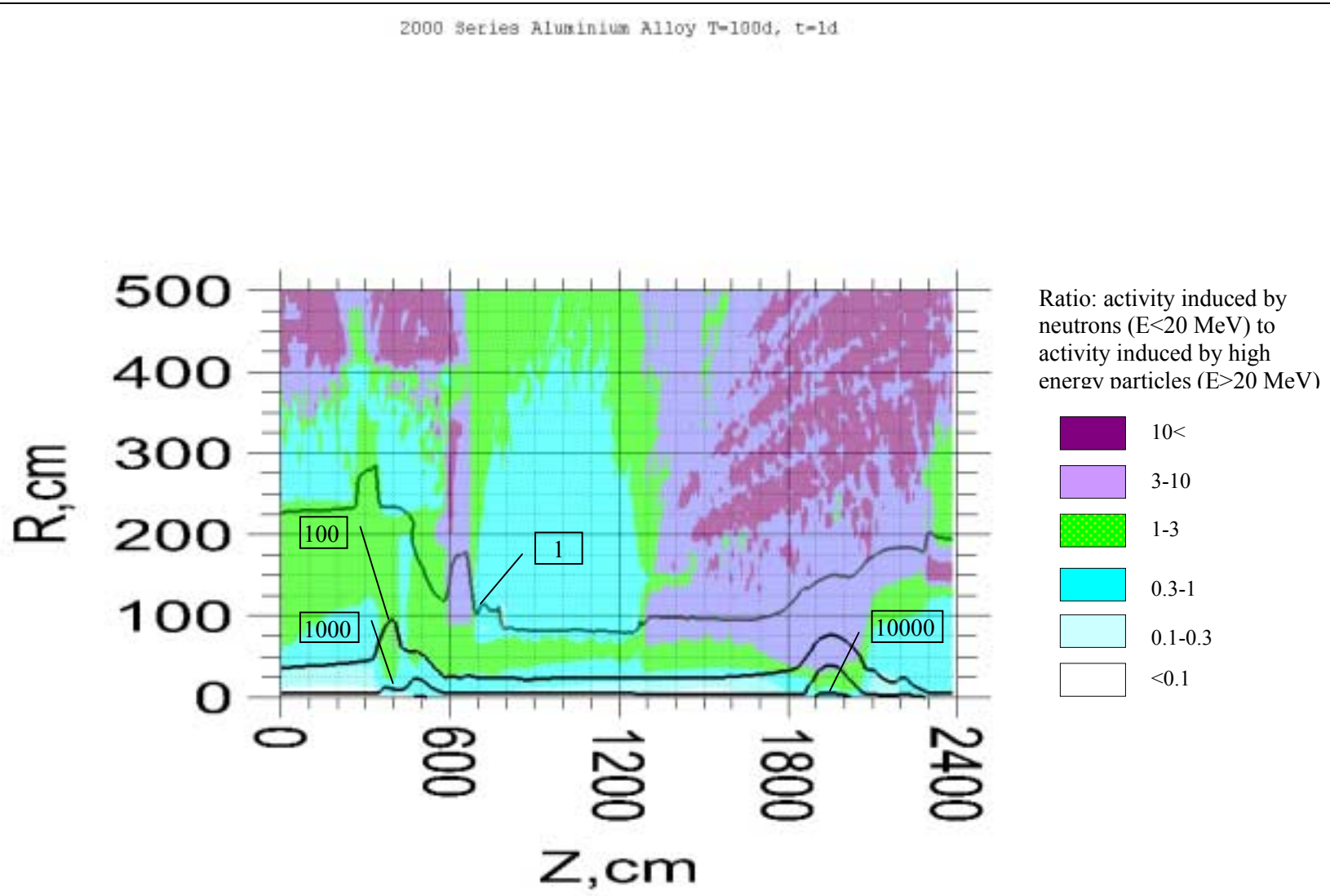

Fig .16. Distribution of induced radioactivity in 2000 Series Aluminum Alloy calculated at T=100d, t=1d. The levels show contact dose rate in μSv/h.

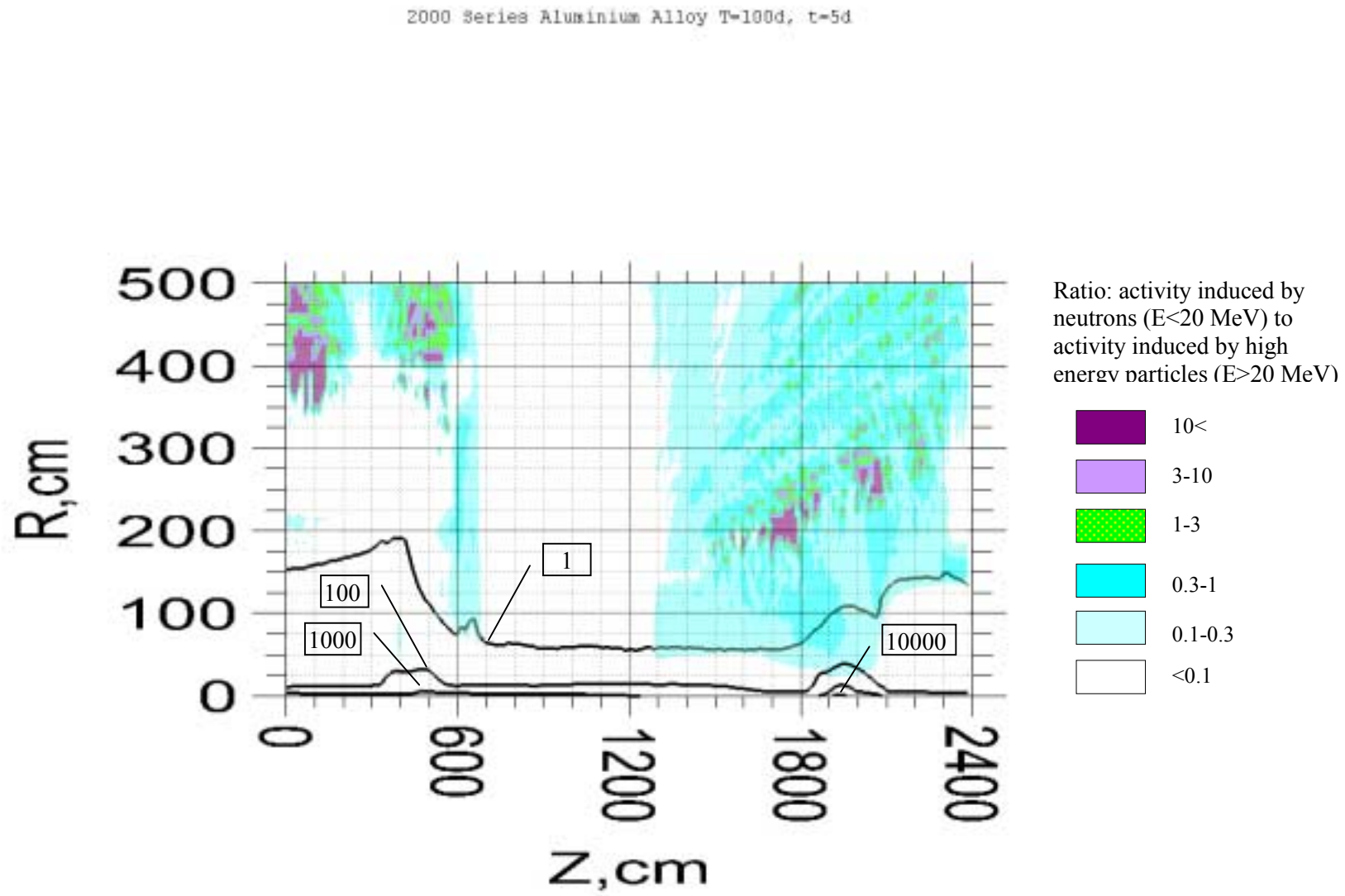

Fig .17. Distribution of induced radioactivity in 2000 Series Aluminum Alloy calculated at T=100d, t=5d. The levels show contact dose rate in μSv/h.

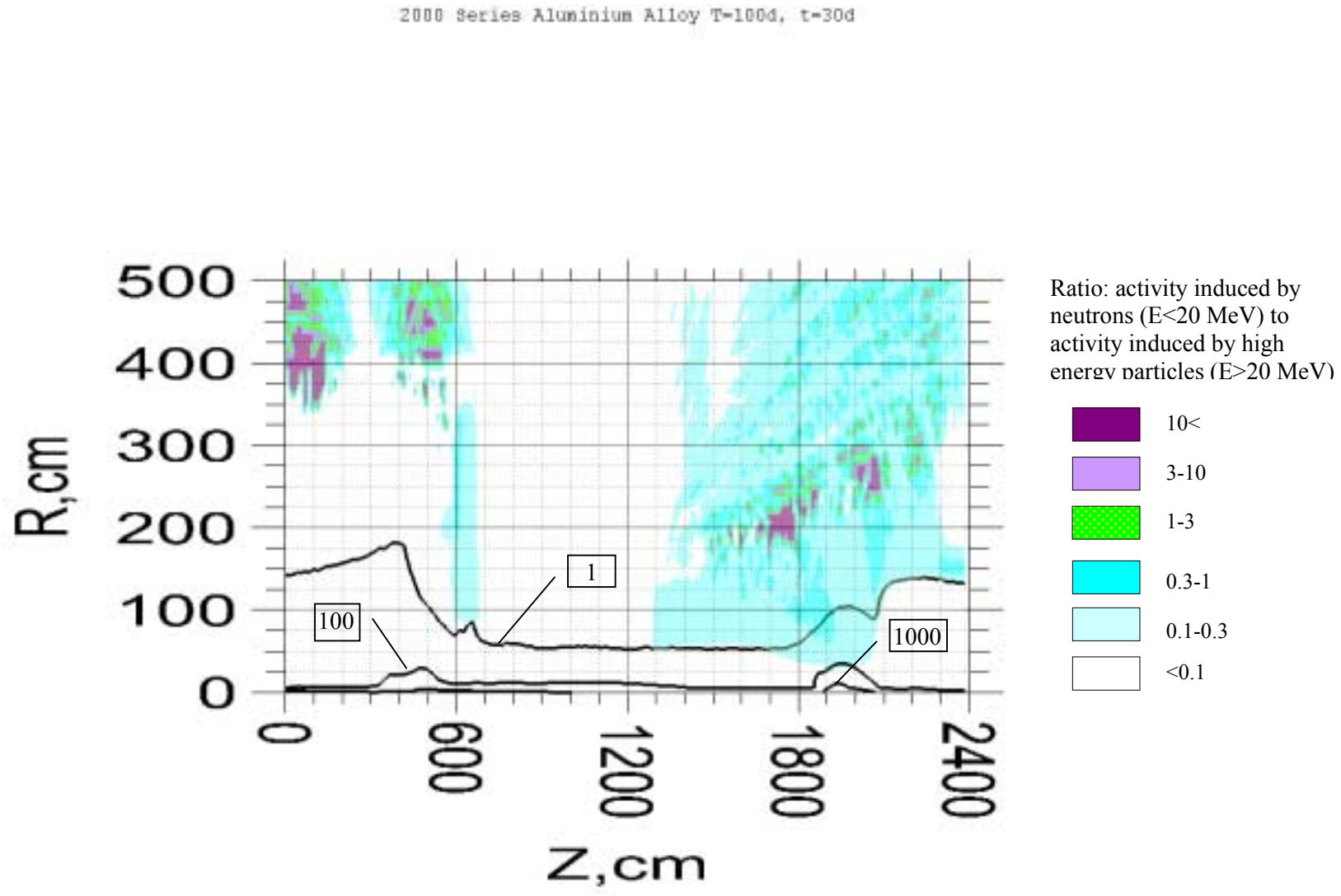

Fig .18. Distribution of induced radioactivity in 2000 Series Aluminum Alloy calculated at T=100d, t=30d. The levels show contact dose rate in μSv/h.

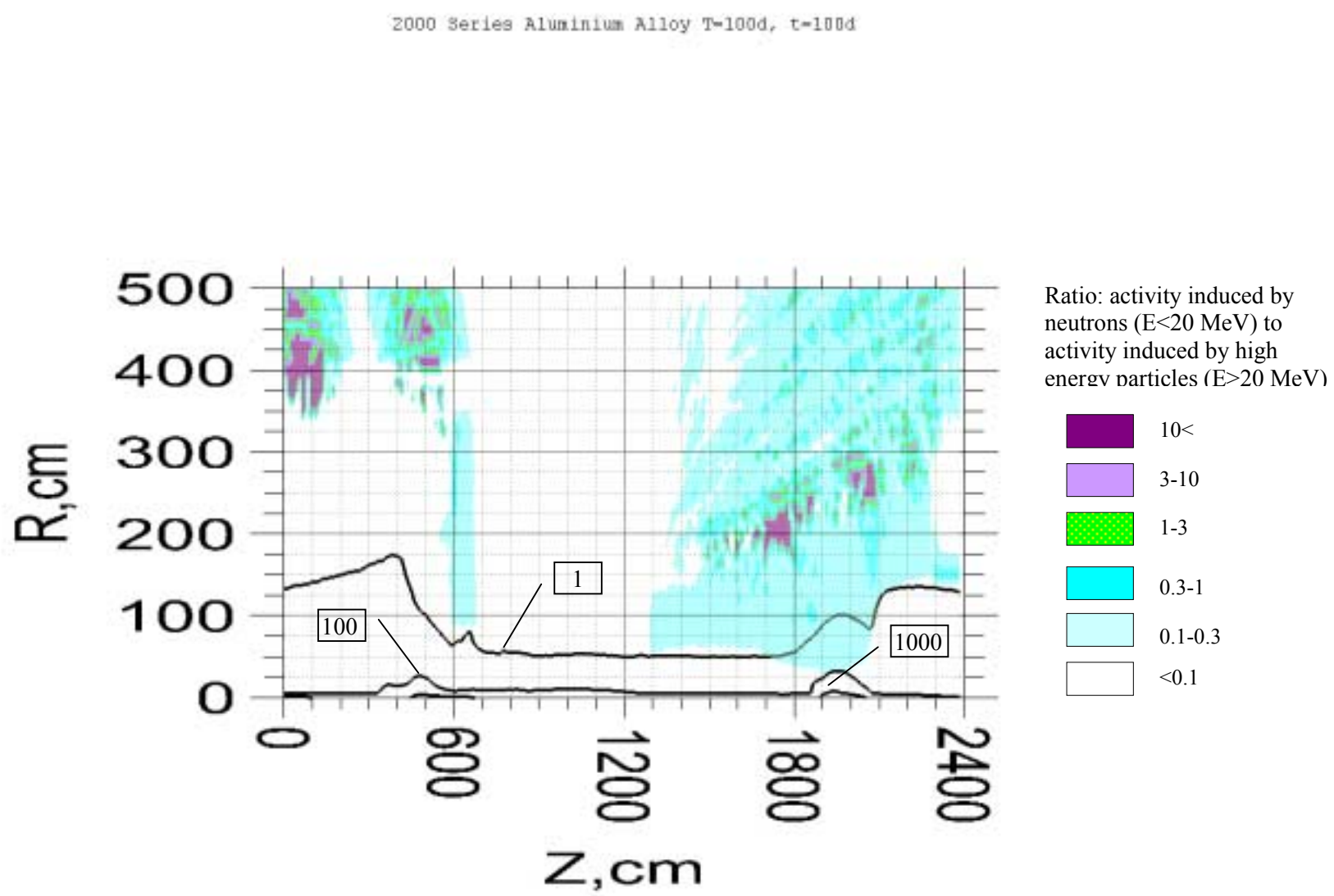

Fig .19. Distribution of induced radioactivity in 2000 Series Aluminum Alloy calculated at T=100d, t=100d. The levels show contact dose rate in μSv/h.

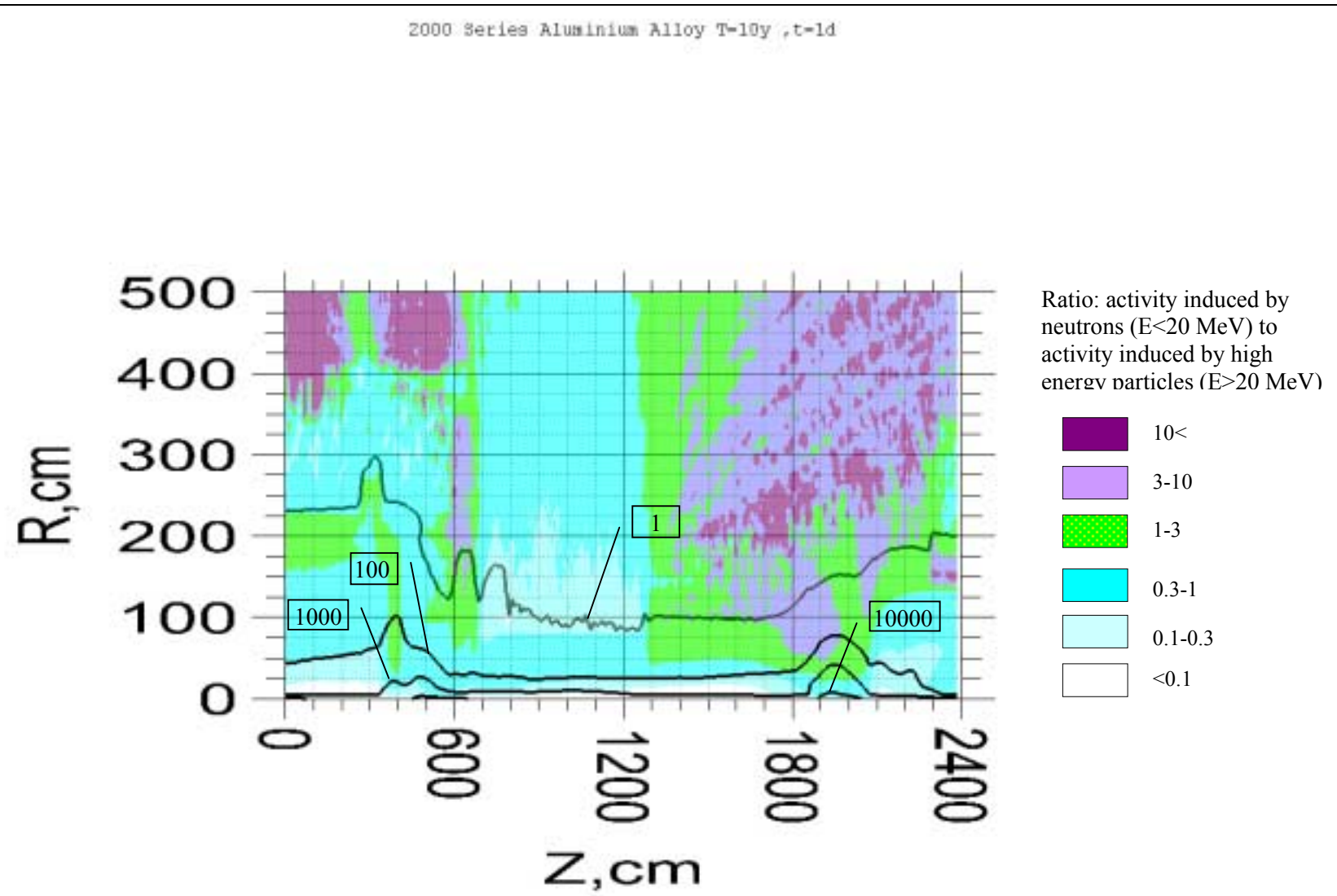

Fig .20. Distribution of induced radioactivity in 2000 Series Aluminum Alloy calculated at T=10y, t=1d. The levels show contact dose rate in μSv/h.

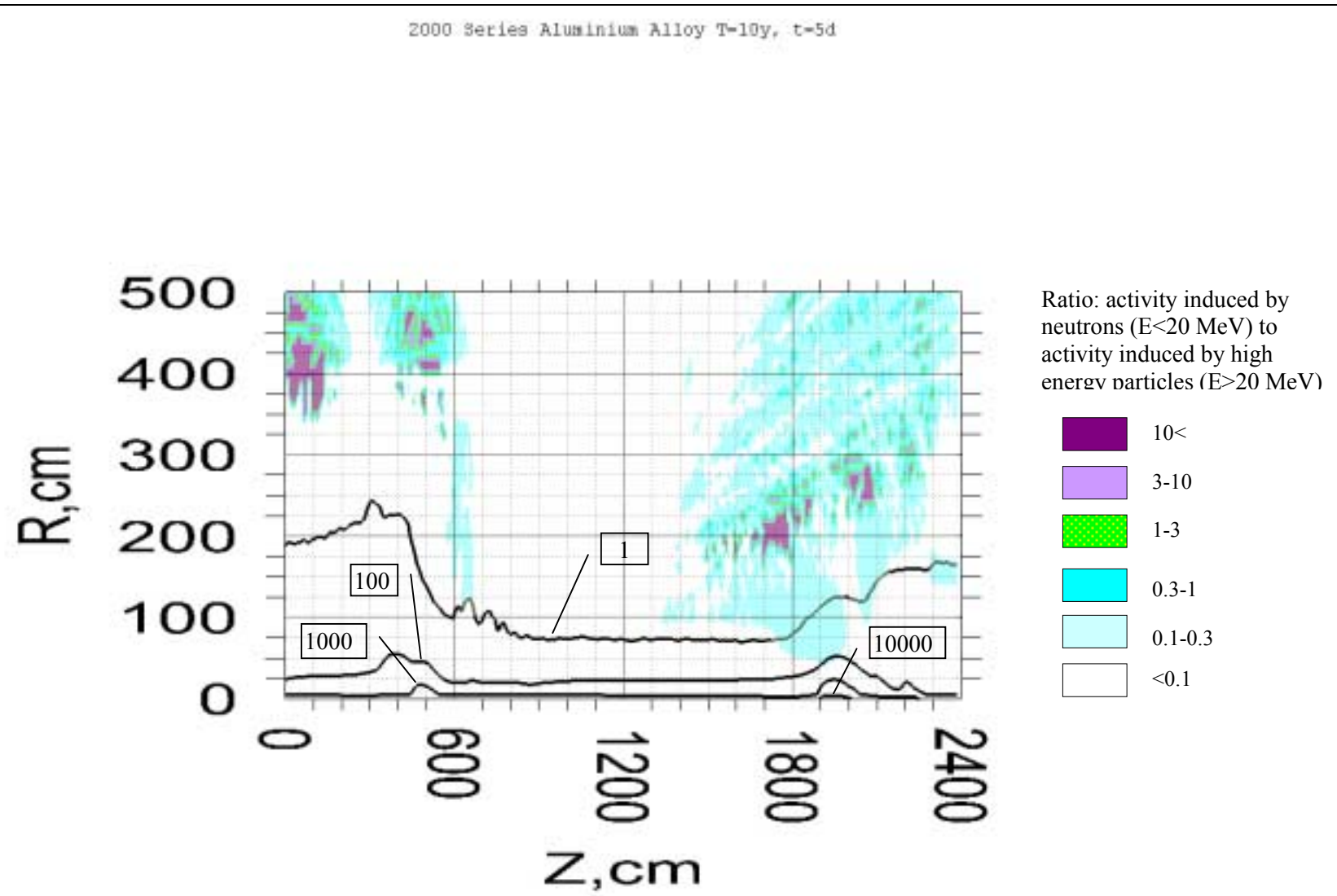

Fig .21. Distribution of induced radioactivity in 2000 Series Aluminum Alloy calculated at T=10y, t=5d. The levels show contact dose rate in μSv/h.

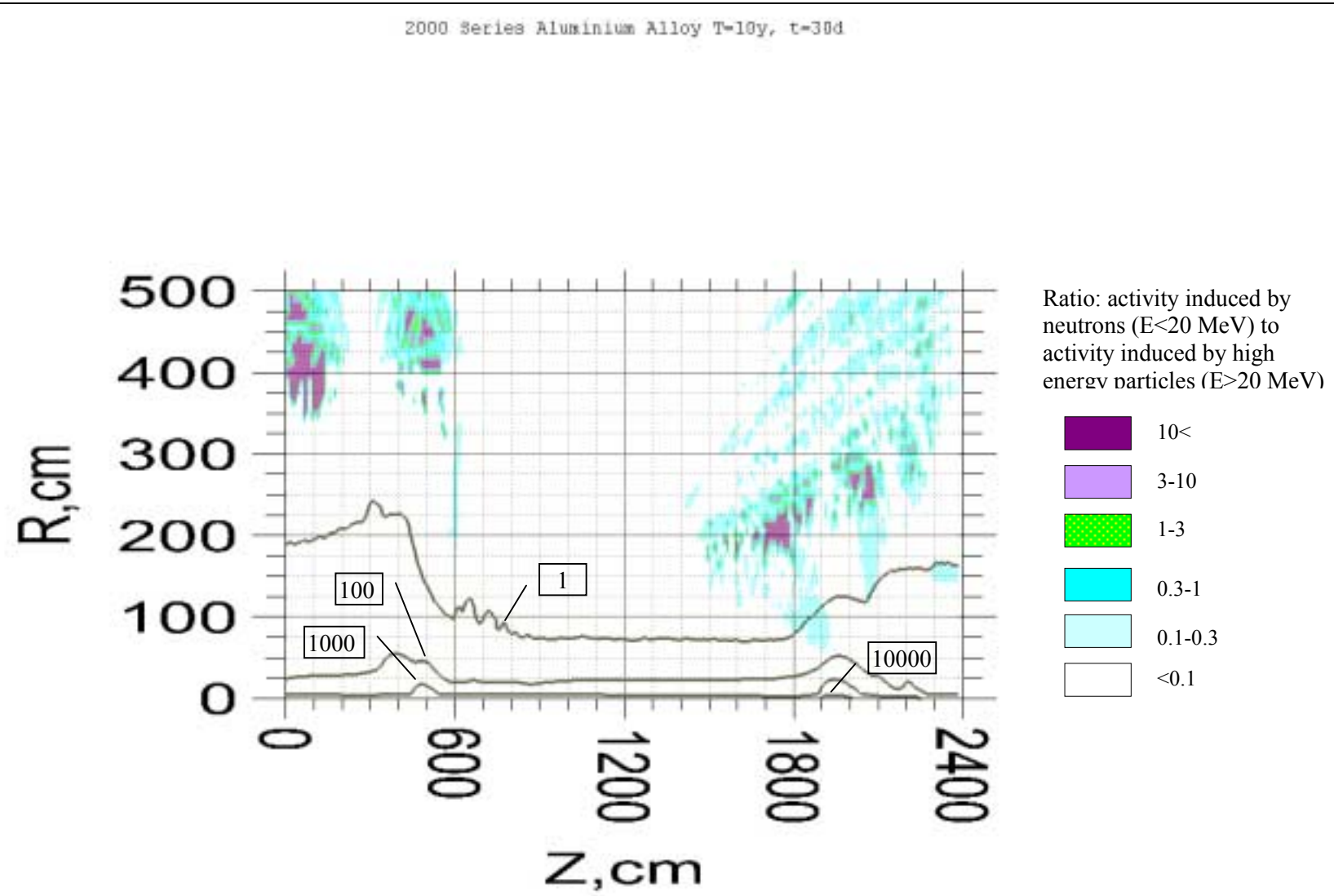

Fig .22. Distribution of induced radioactivity in 2000 Series Aluminum Alloy calculated at T=10y, t=30d. The levels show contact dose rate in μSv/h.

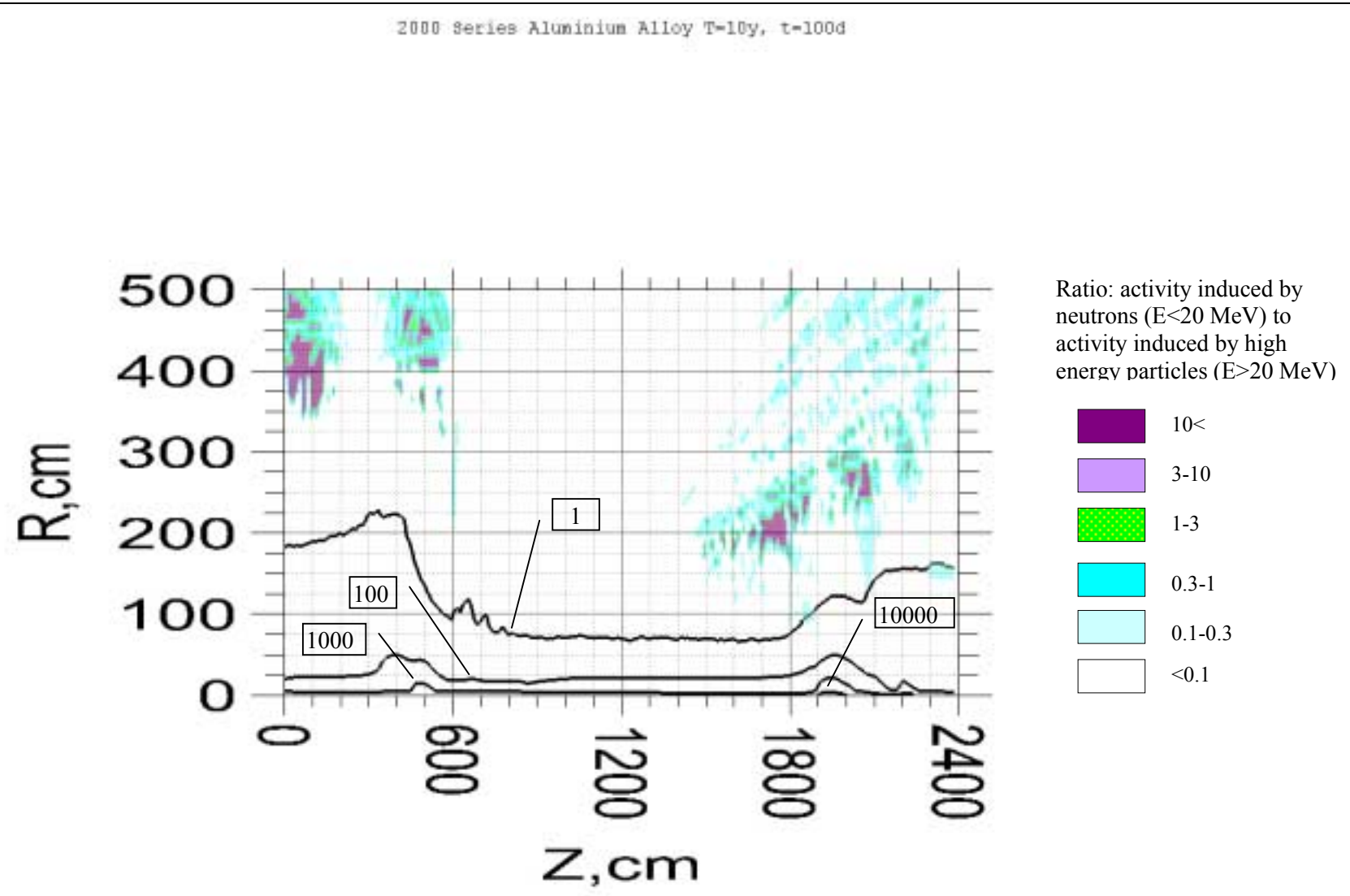

Fig .23. Distribution of induced radioactivity in 2000 Series Aluminum Alloy calculated at T=10y, t=100d. The levels show contact dose rate in μSv/h.

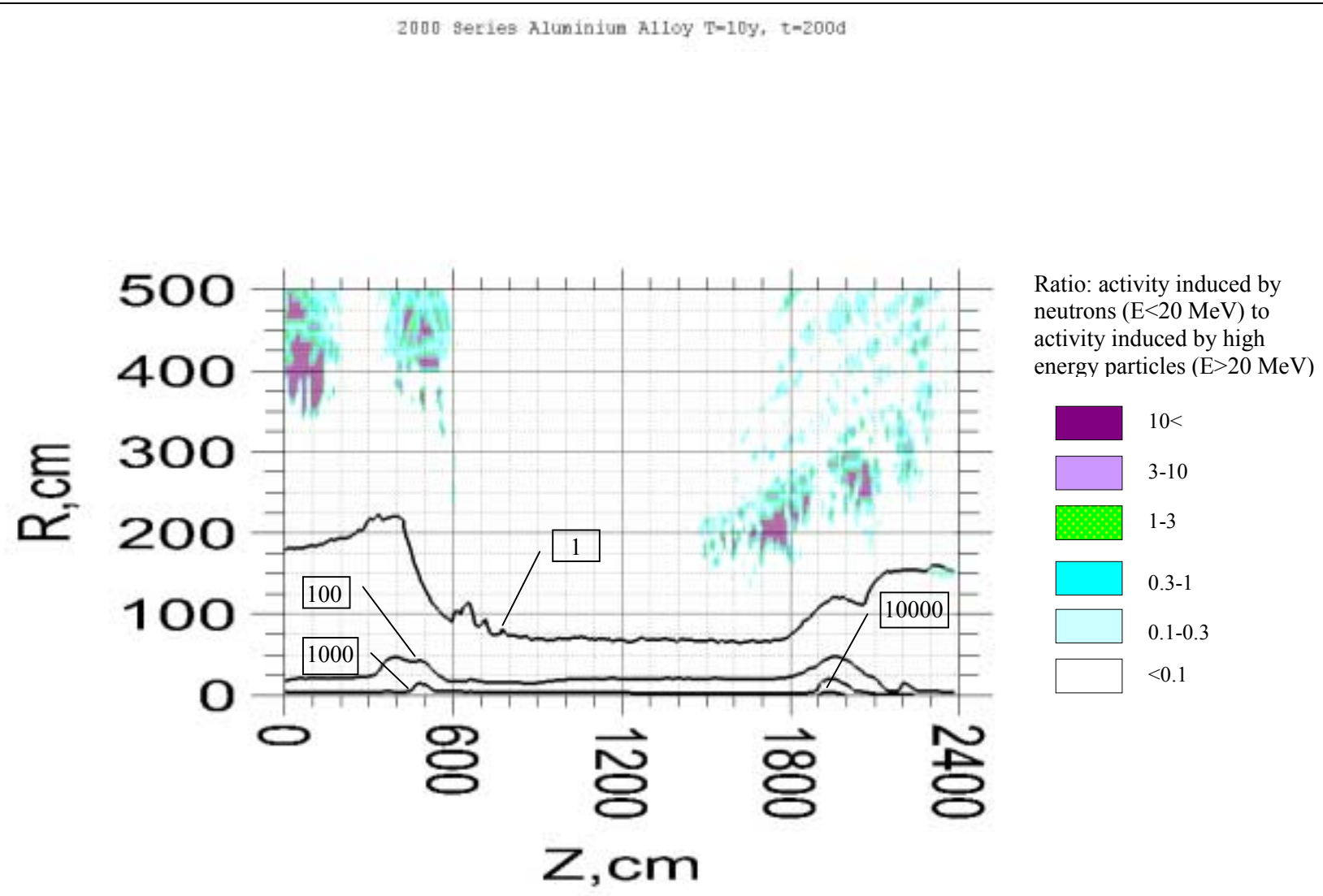

Fig .24. Distribution of induced radioactivity in 2000 Series Aluminum Alloy calculated at T=10y, t=200d. The levels show contact dose rate in μSv/h.

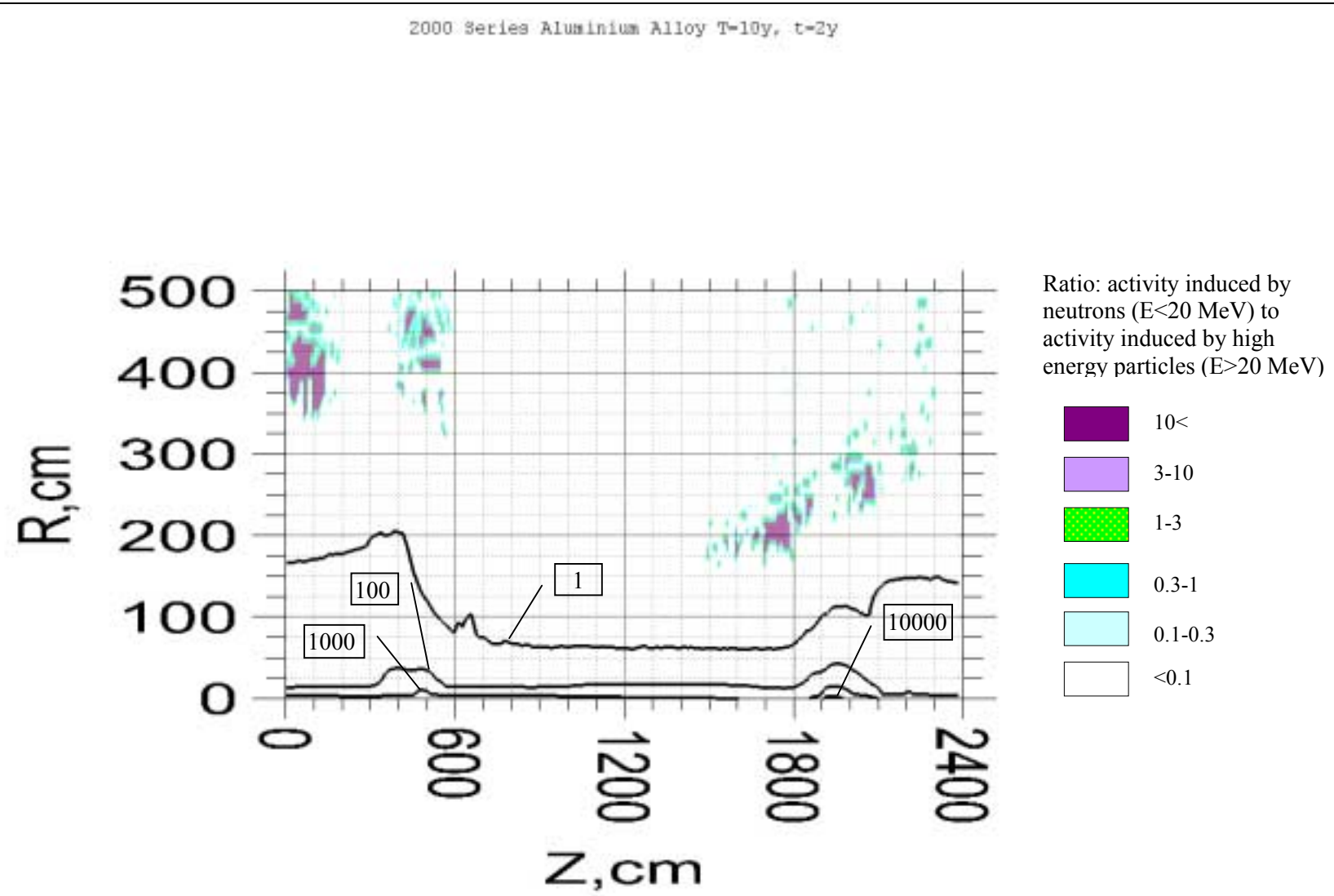

Fig .25. Distribution of induced radioactivity in 2000 Series Aluminum Alloy calculated at T=10y, t=2y. The levels show contact dose rate in μSv/h.

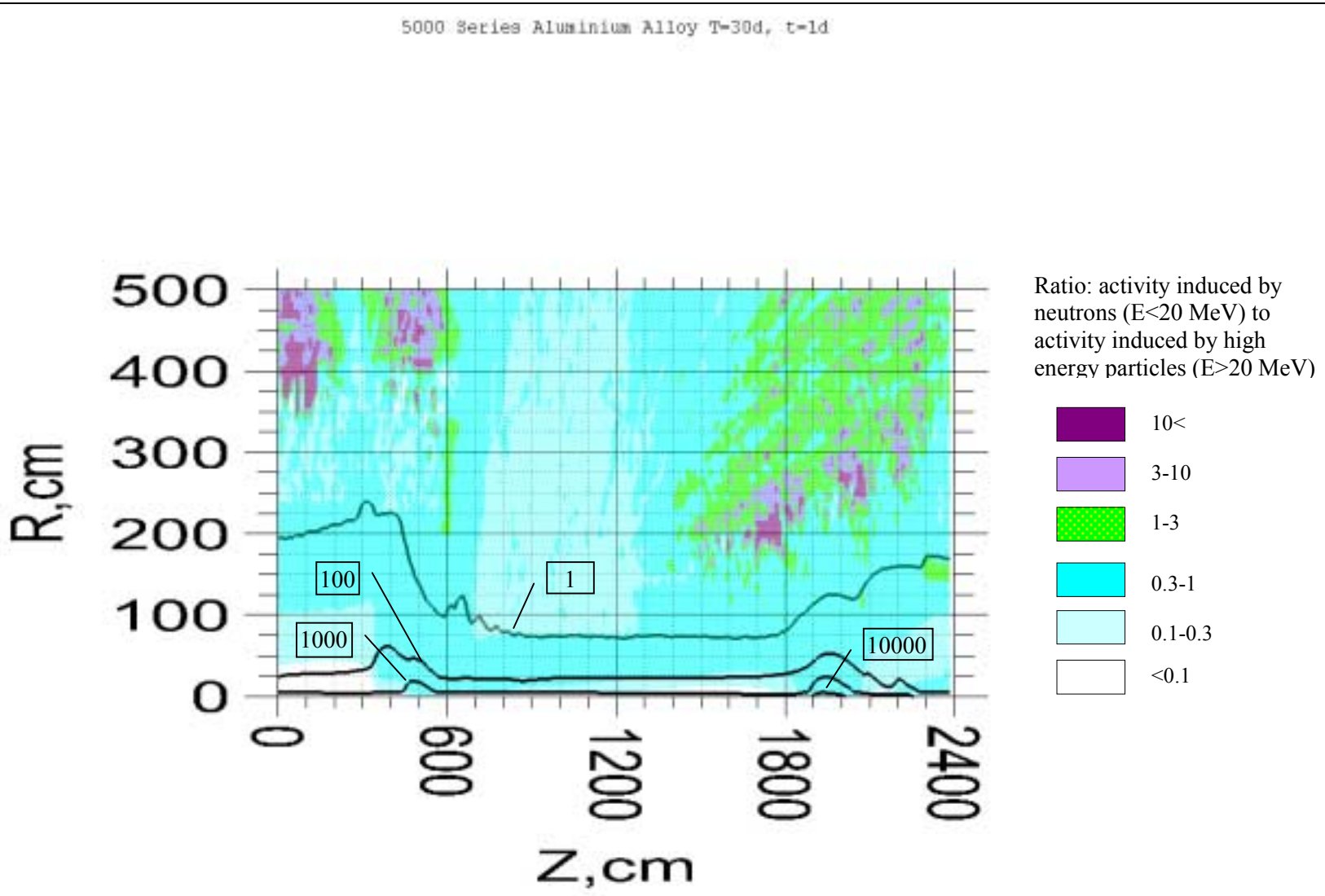

Fig .26. Distribution of induced radioactivity in 5000 Series Aluminum Alloy calculated at T=30d, t=1d. The levels show contact dose rate in μSv/h.

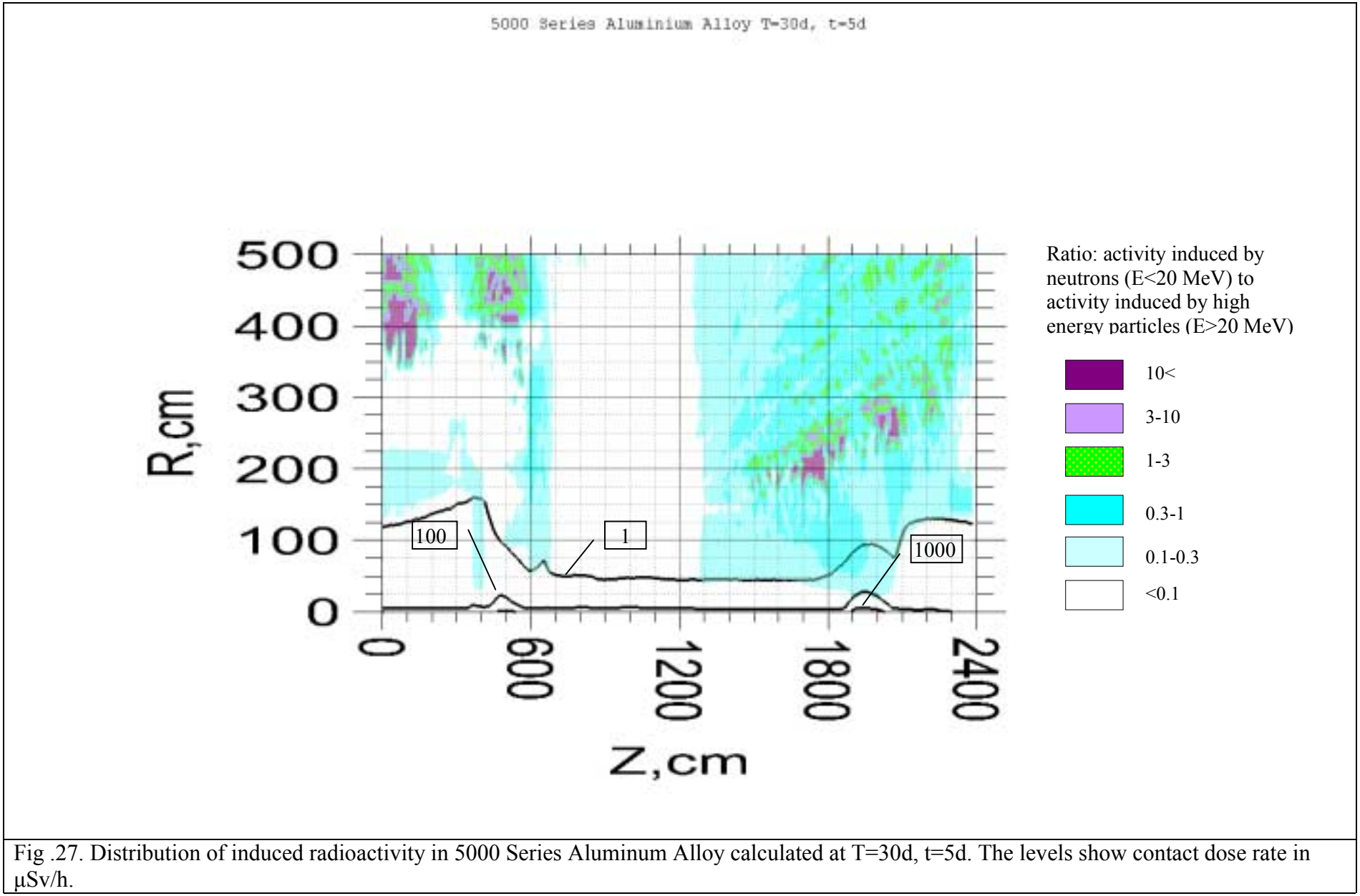

Fig .27. Distribution of induced radioactivity in 5000 Series Aluminum Alloy calculated at T=30d, t=5d. The levels show contact dose rate in μSv/h.

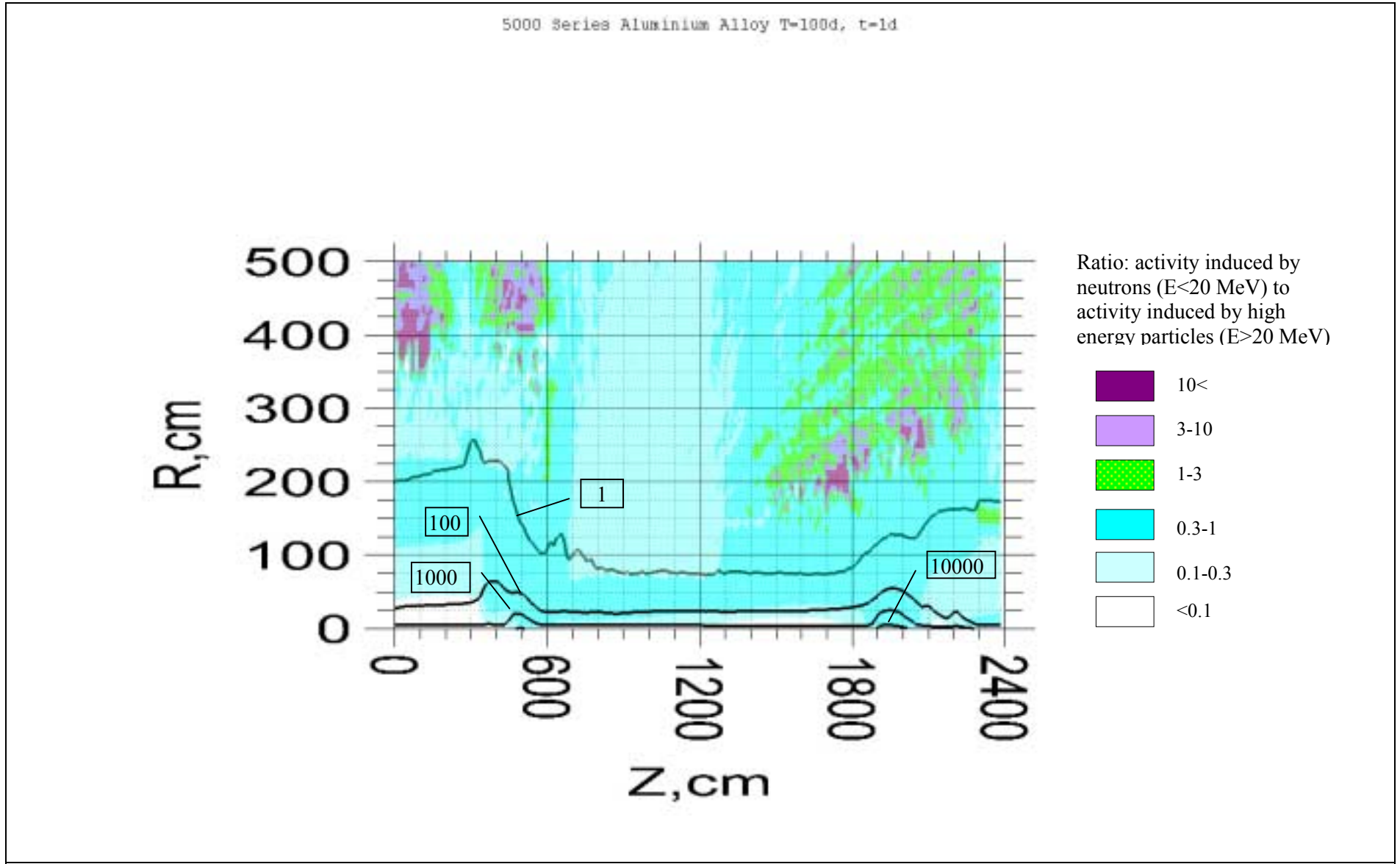

Fig .28. Distribution of induced radioactivity in 5000 Series Aluminum Alloy calculated at T=100d, t=1d. The levels show contact dose rate in μSv/h.

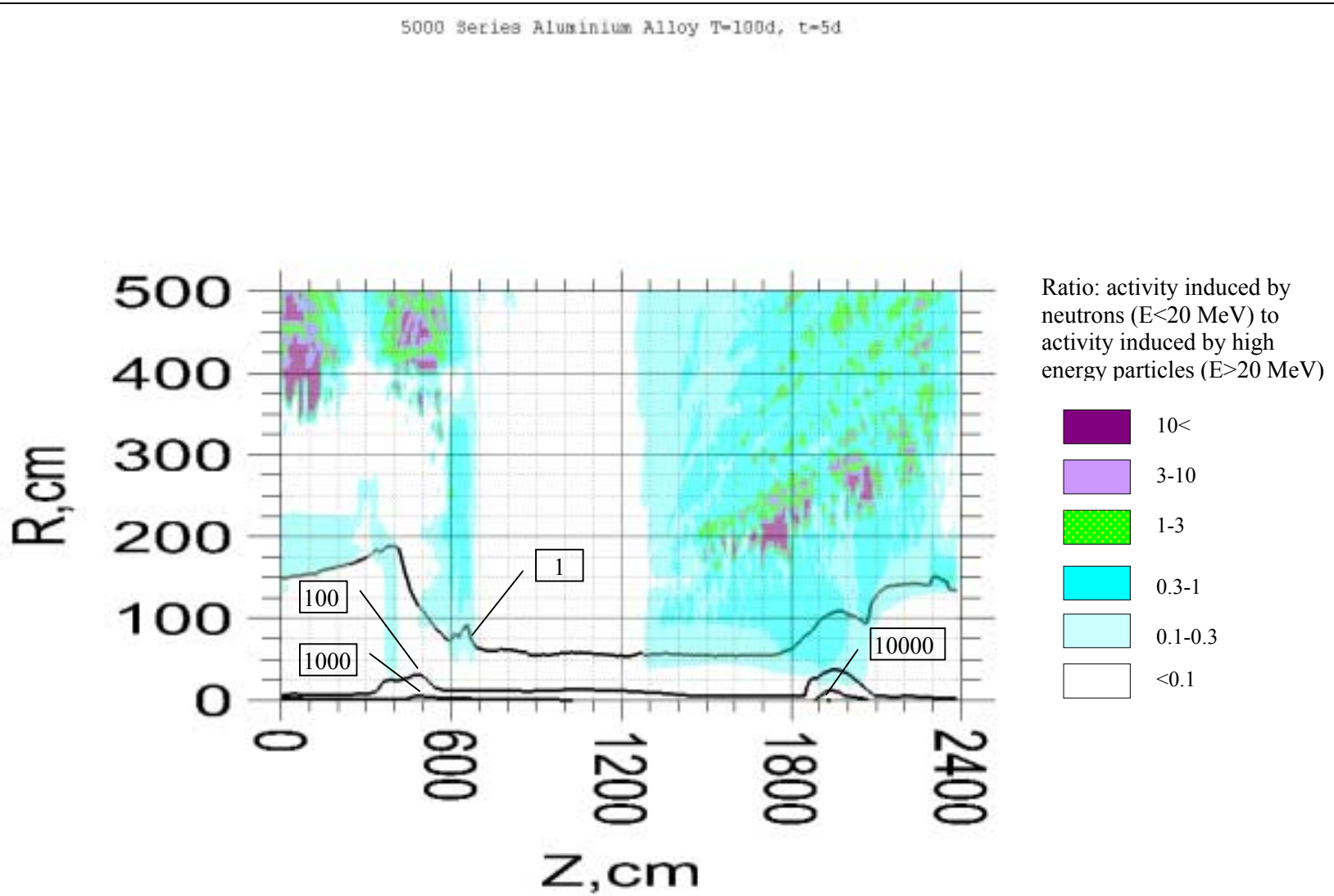

Fig .29. Distribution of induced radioactivity in 5000 Series Aluminum Alloy calculated at T=100d, t=5d. The levels show contact dose rate in μSv/h.

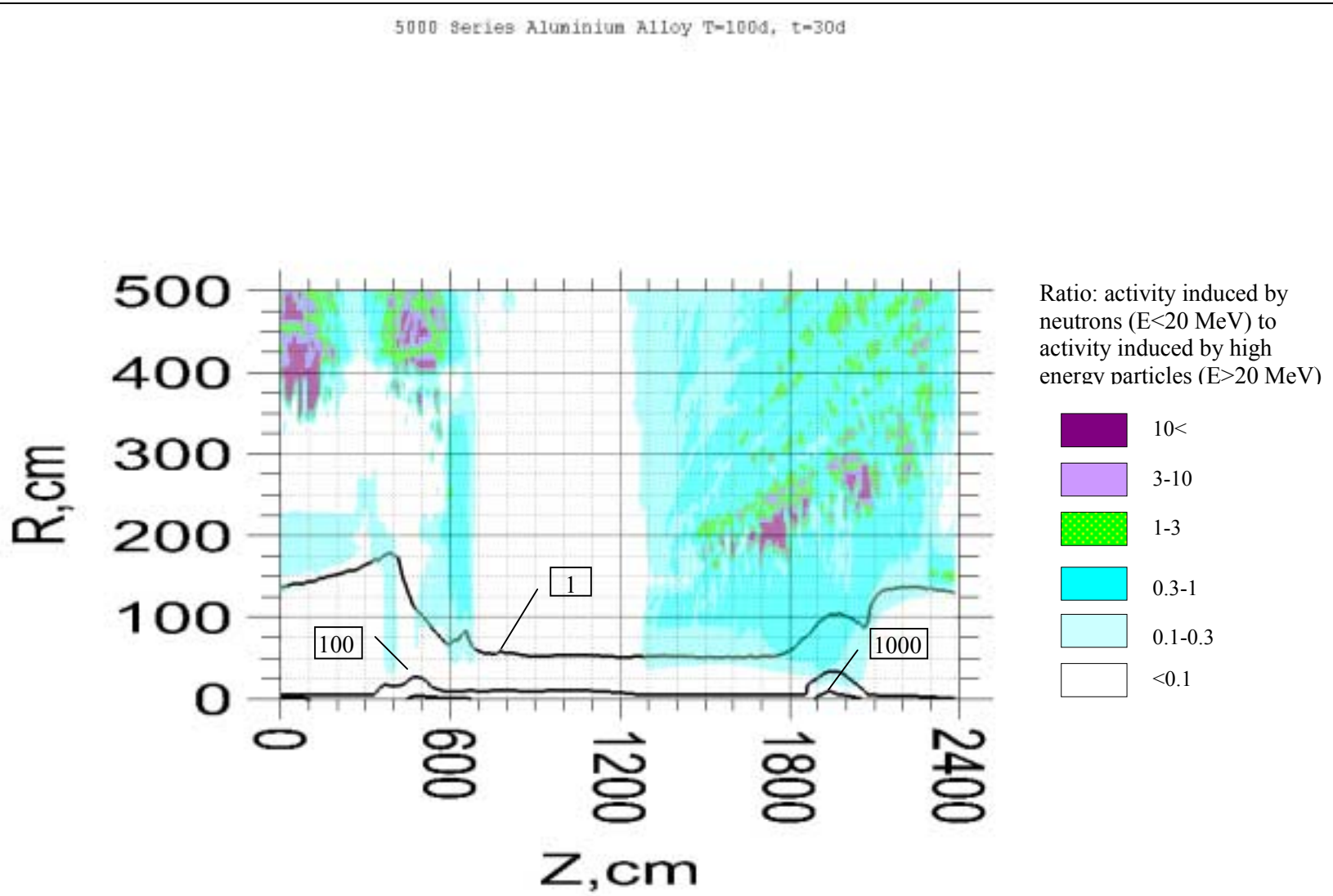

Fig .30. Distribution of induced radioactivity in 5000 Series Aluminum Alloy calculated at T=100d, t=30d. The levels show contact dose rate in μSv/h.

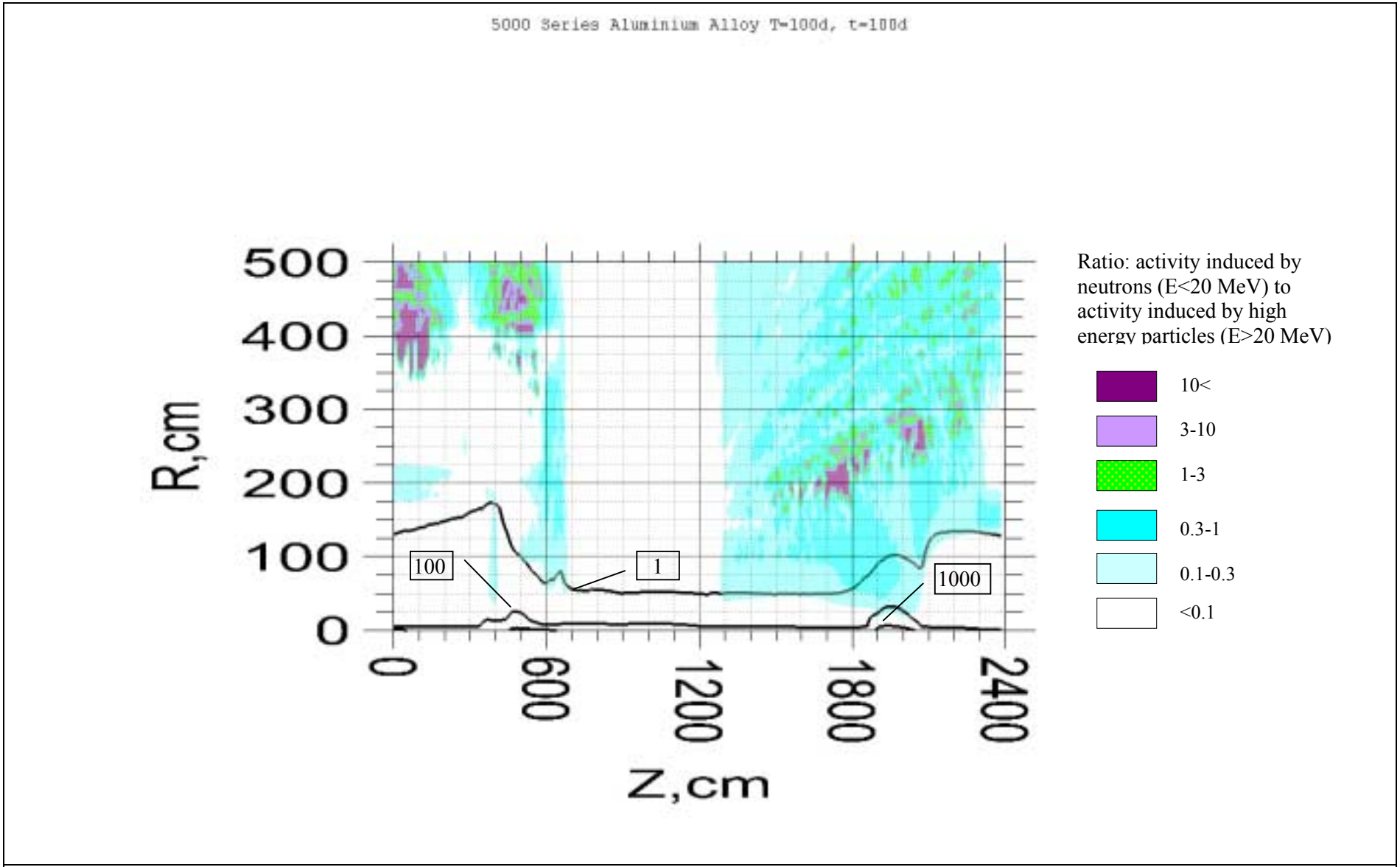

Fig .31. Distribution of induced radioactivity in 5000 Series Aluminum Alloy calculated at T=100d, t=100d. The levels show contact dose rate in μSv/h.

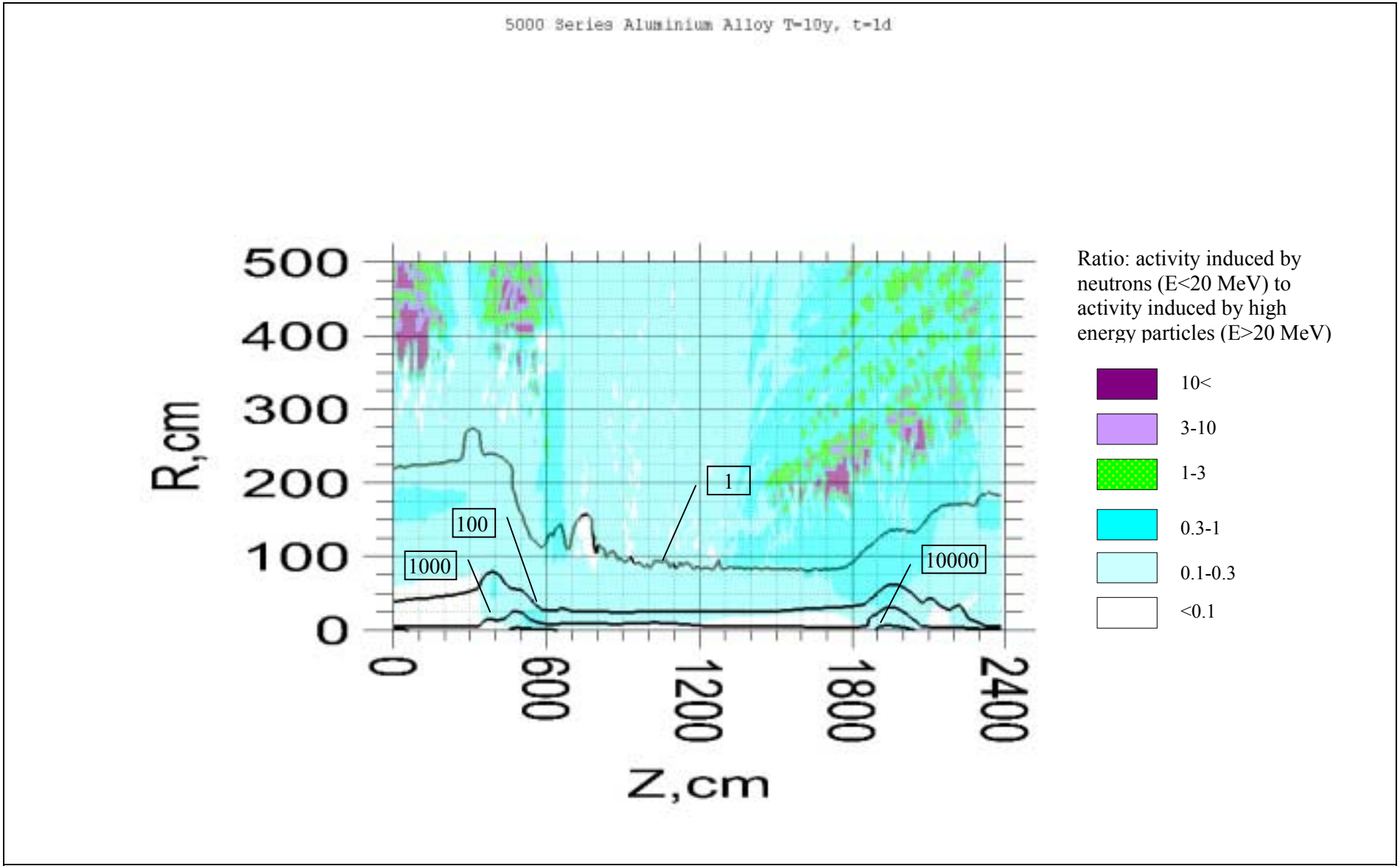

Fig .32. Distribution of induced radioactivity in 5000 Series Aluminum Alloy calculated at T=10y, t=1d. The levels show contact dose rate in μSv/h.

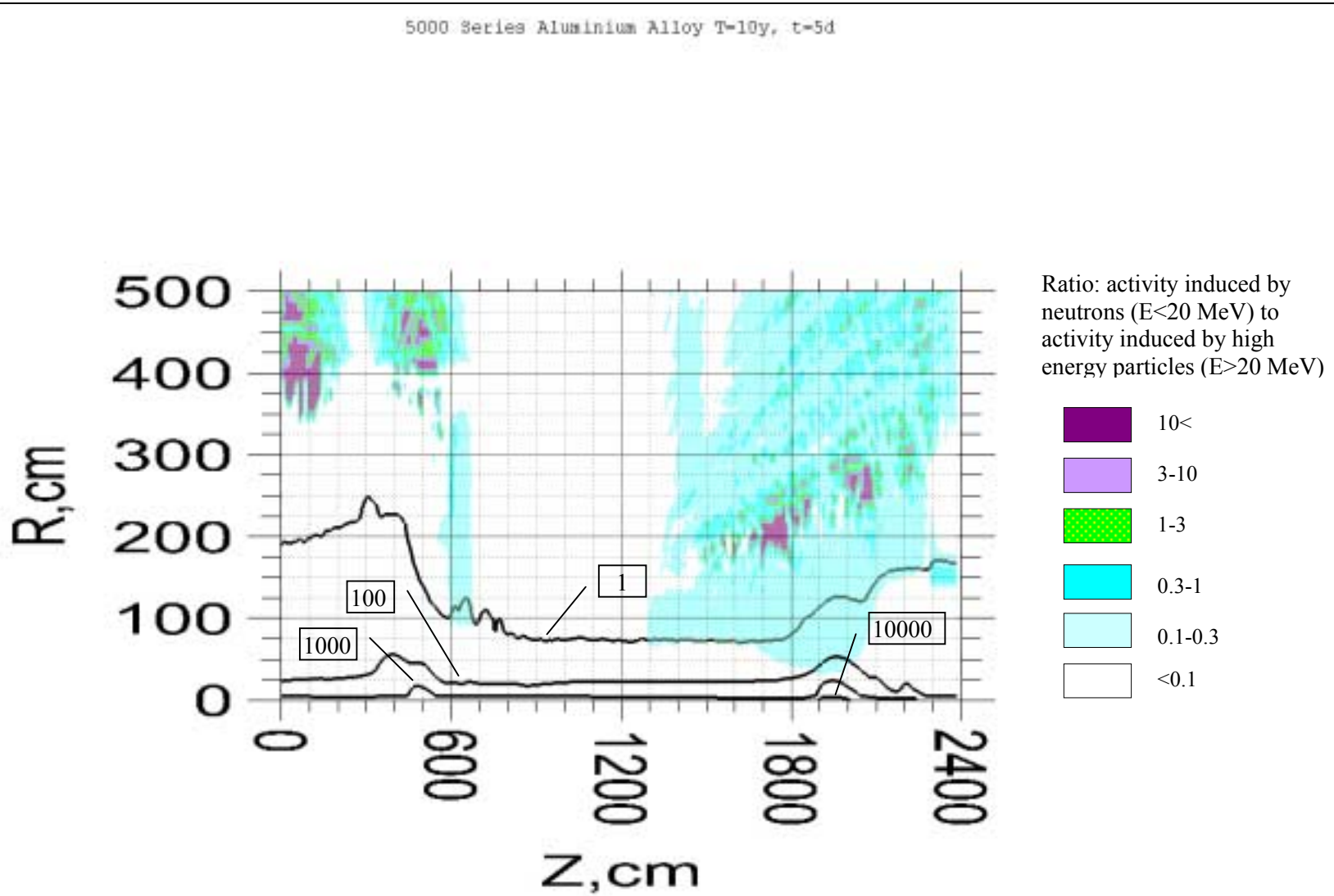

Fig .33. Distribution of induced radioactivity in 5000 Series Aluminum Alloy calculated at T=10y, t=5d. The levels show contact dose rate in μSv/h.

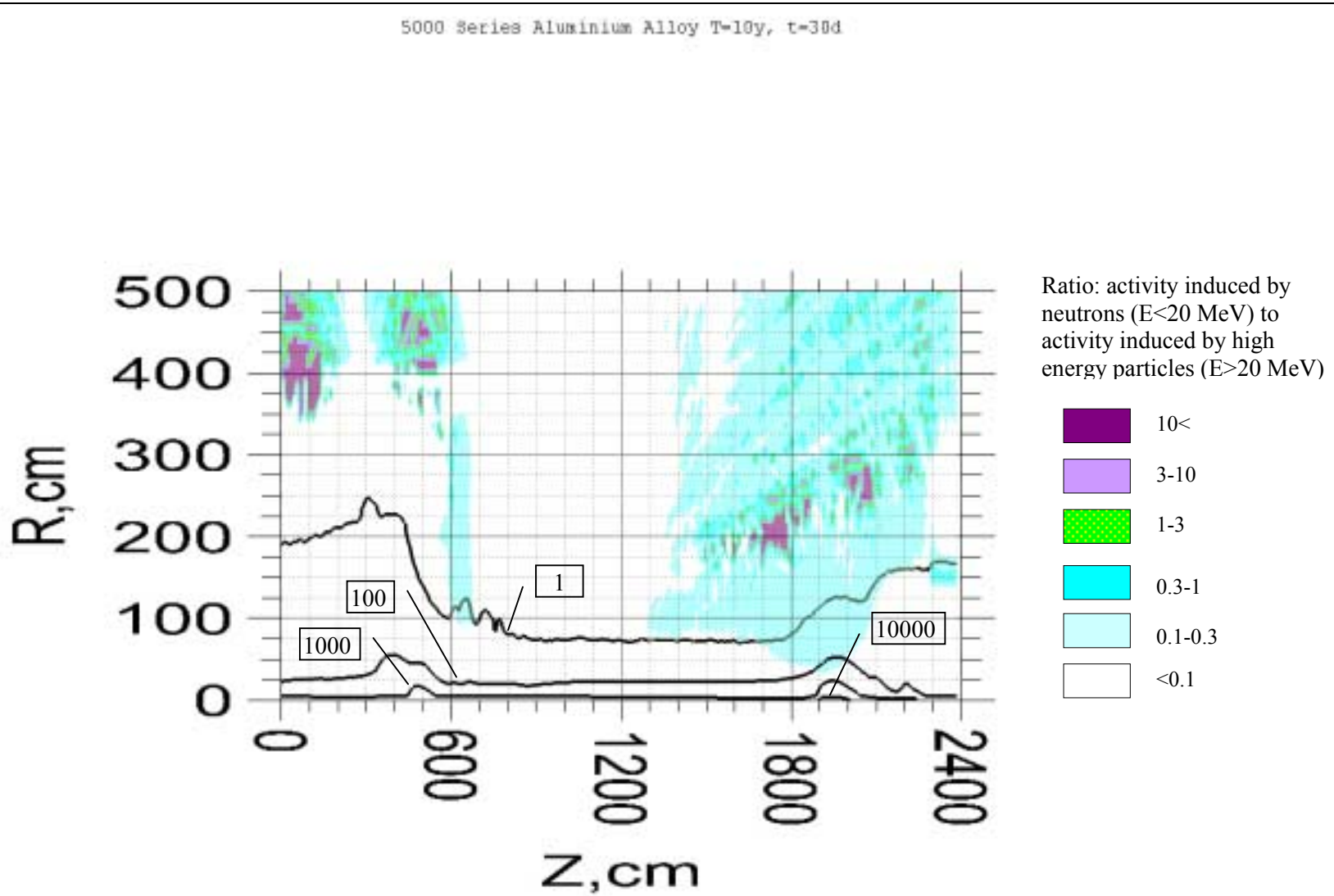

Fig .34. Distribution of induced radioactivity in 5000 Series Aluminum Alloy calculated at T=10y, t=30d. The levels show contact dose rate in μSv/h.

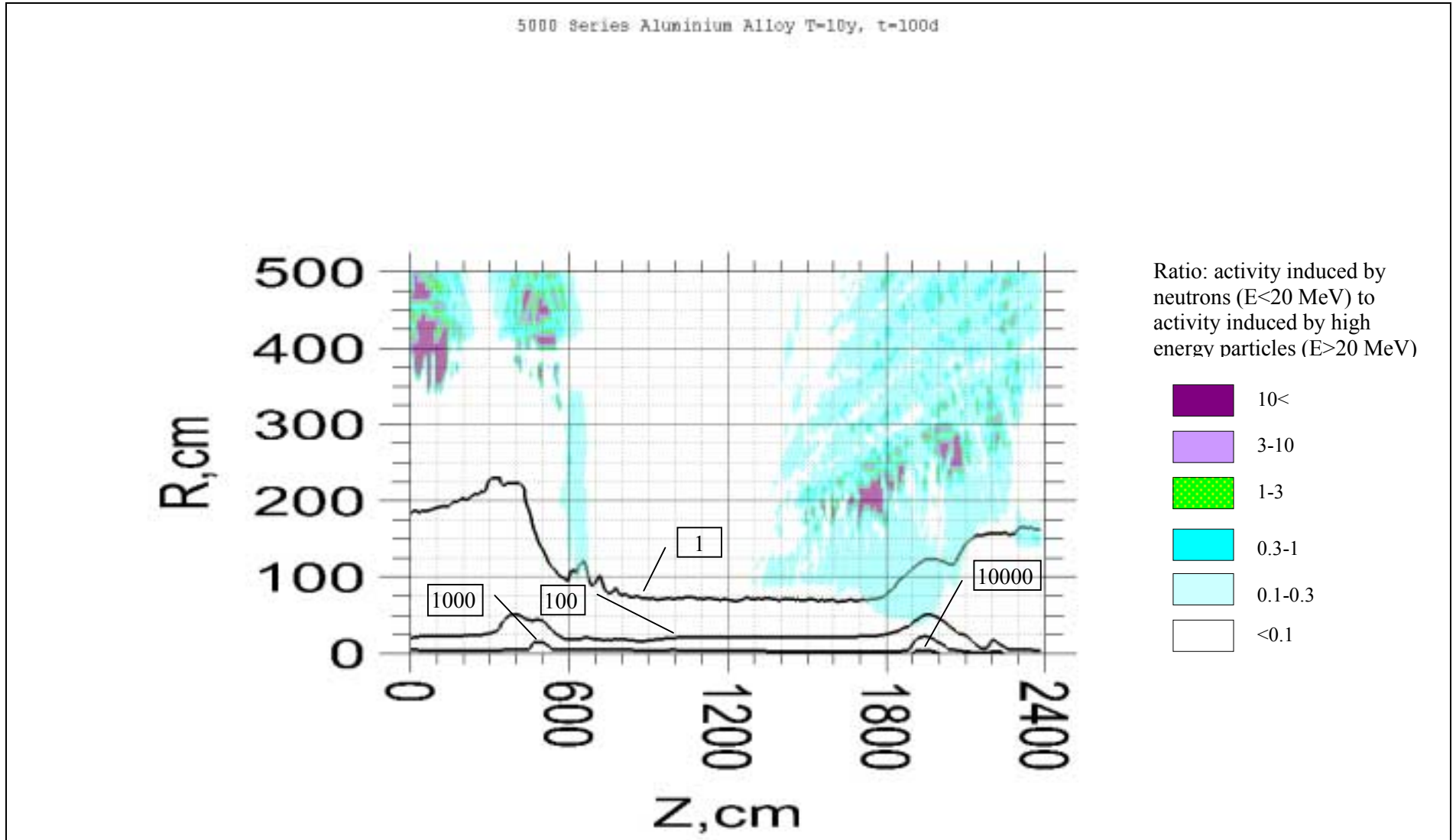

Fig .35. Distribution of induced radioactivity in 5000 Series Aluminum Alloy calculated at T=10y, t=100d. The levels show contact dose rate in μSv/h.

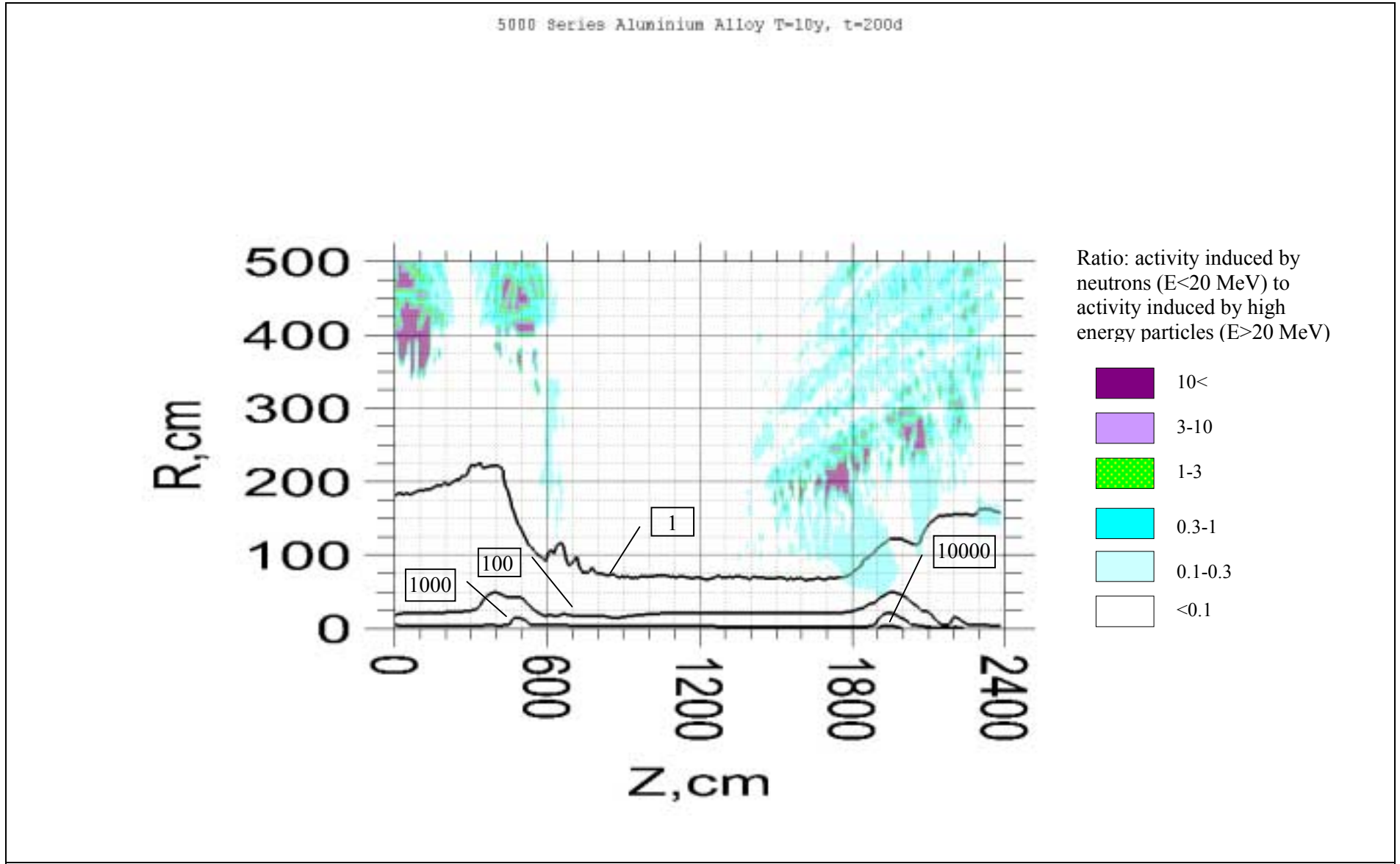

Fig .36. Distribution of induced radioactivity in 5000 Series Aluminum Alloy calculated at T=10y, t=200d. The levels show contact dose rate in μSv/h.

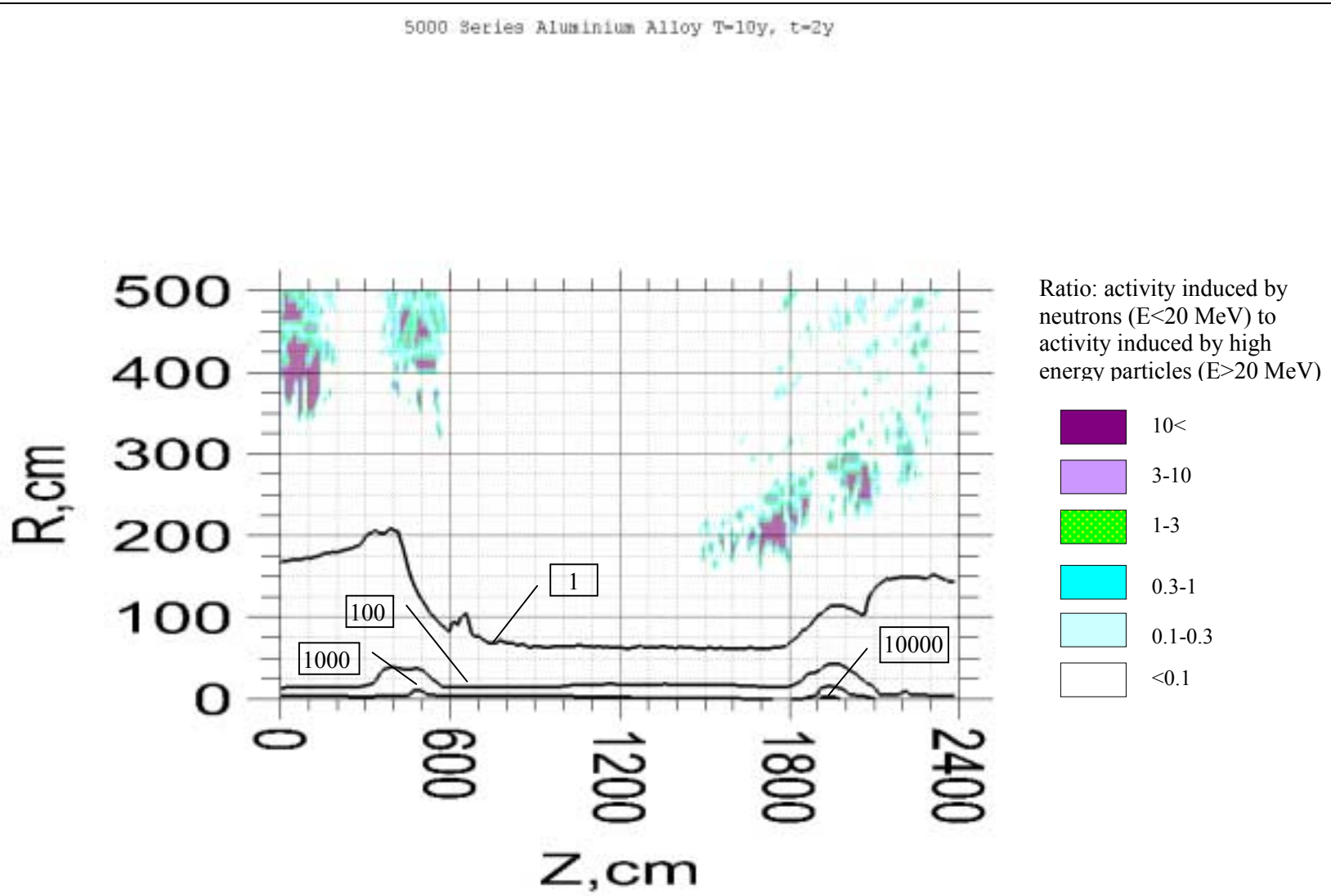

Fig .37. Distribution of induced radioactivity in 5000 Series Aluminum Alloy calculated at T=10y, t=2y. The levels show contact dose rate in μSv/h.

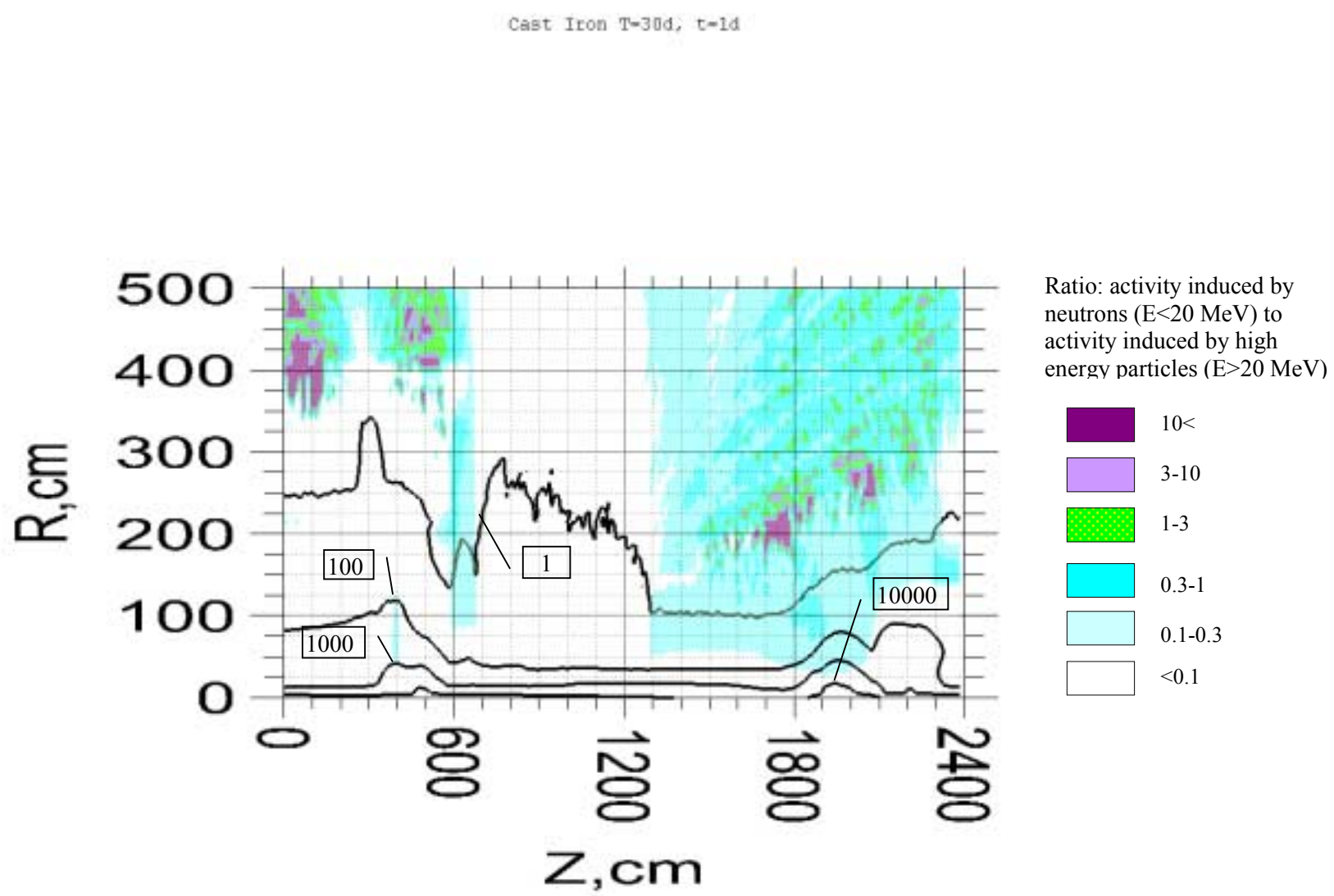

Fig .38. Distribution of induced radioactivity in Cast Iron calculated at T=30d, t=1d. The levels show contact dose rate in μSv/h.

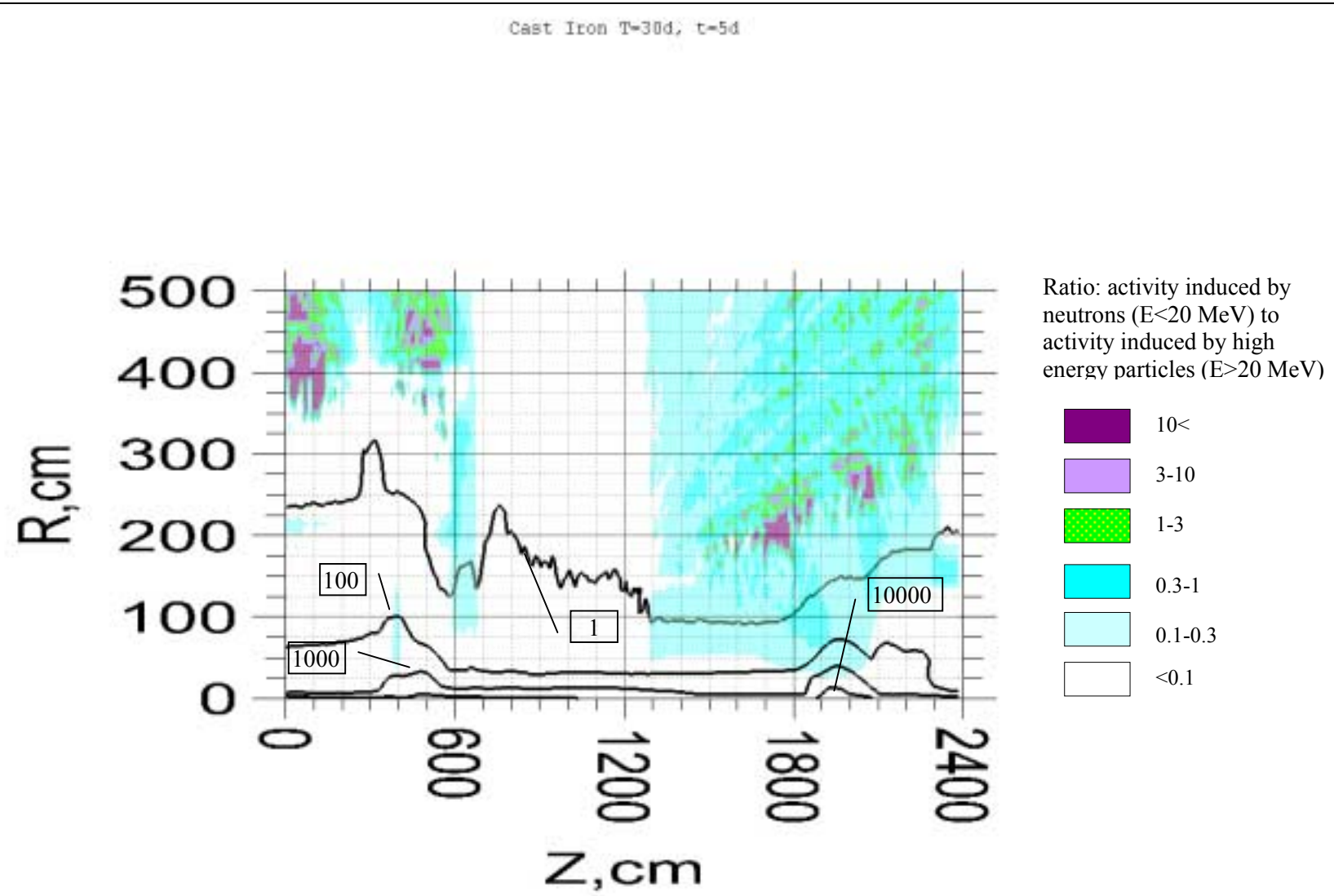

Fig .39. Distribution of induced radioactivity in Cast Iron calculated at T=30d, t=5d. The levels show contact dose rate in μSv/h.

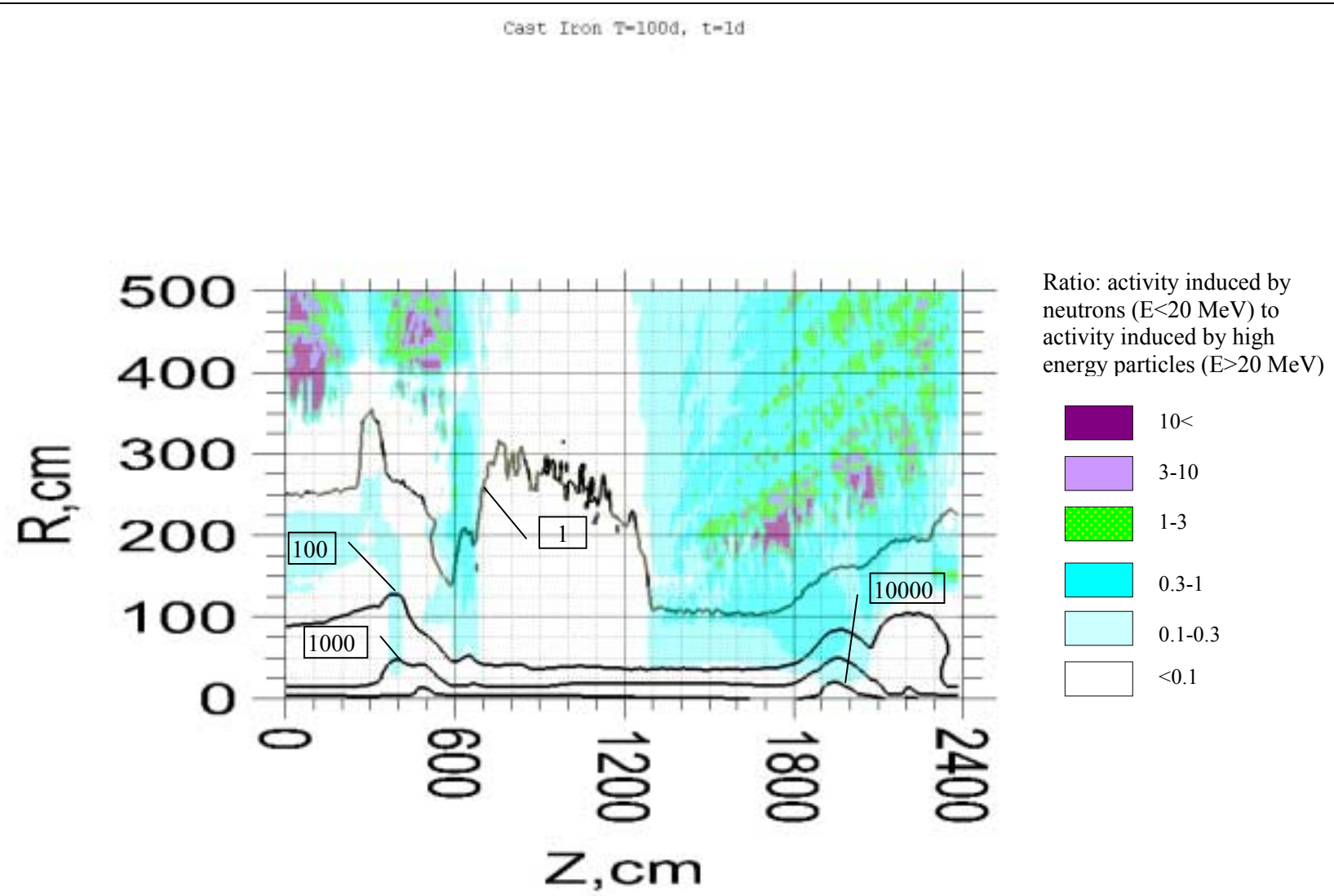

Fig .40. Distribution of induced radioactivity in Cast Iron calculated at T=100d, t=1d. The levels show contact dose rate in μSv/h.

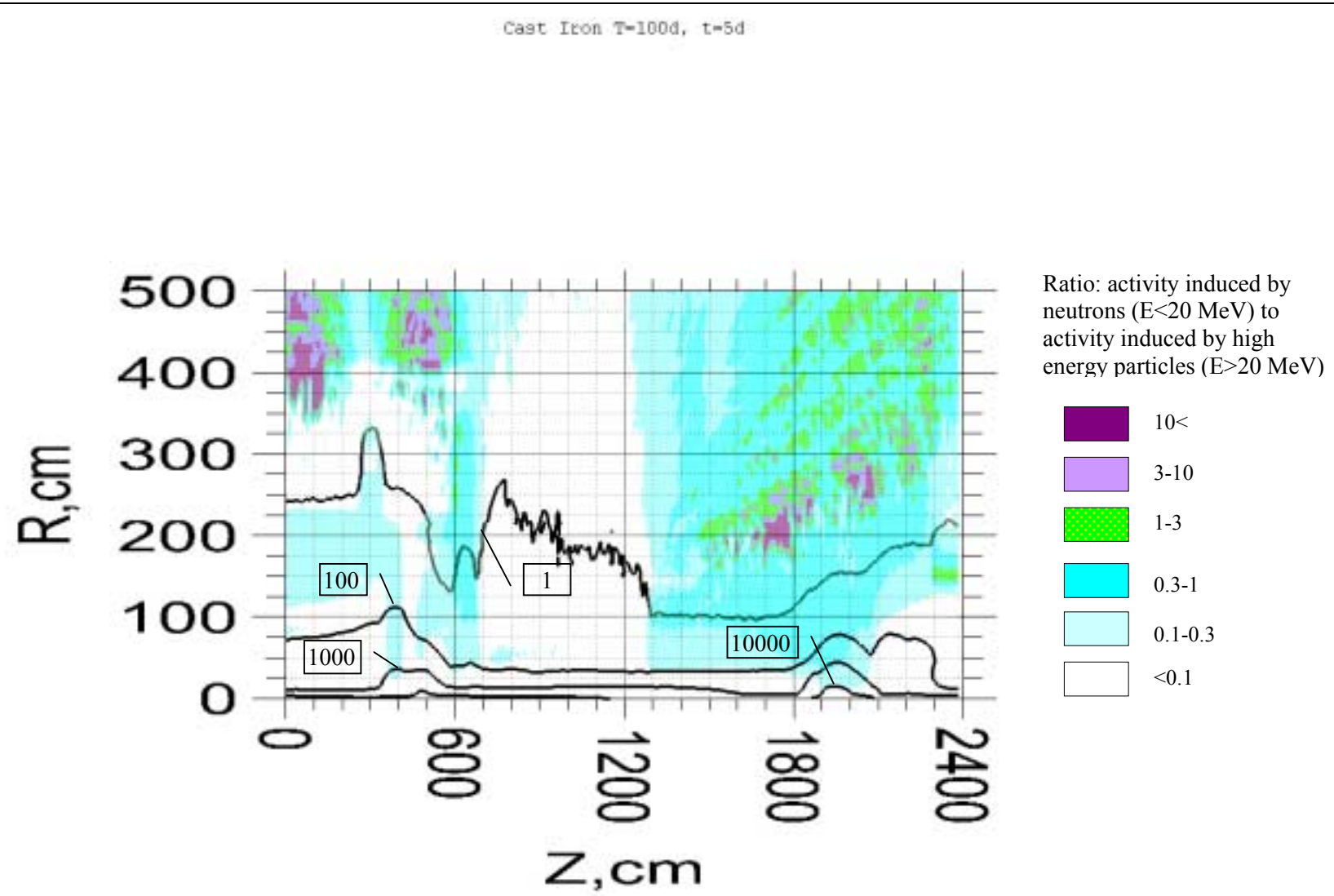

Fig .41. Distribution of induced radioactivity in Cast Iron calculated at T=100d, t=5d. The levels show contact dose rate in μSv/h.

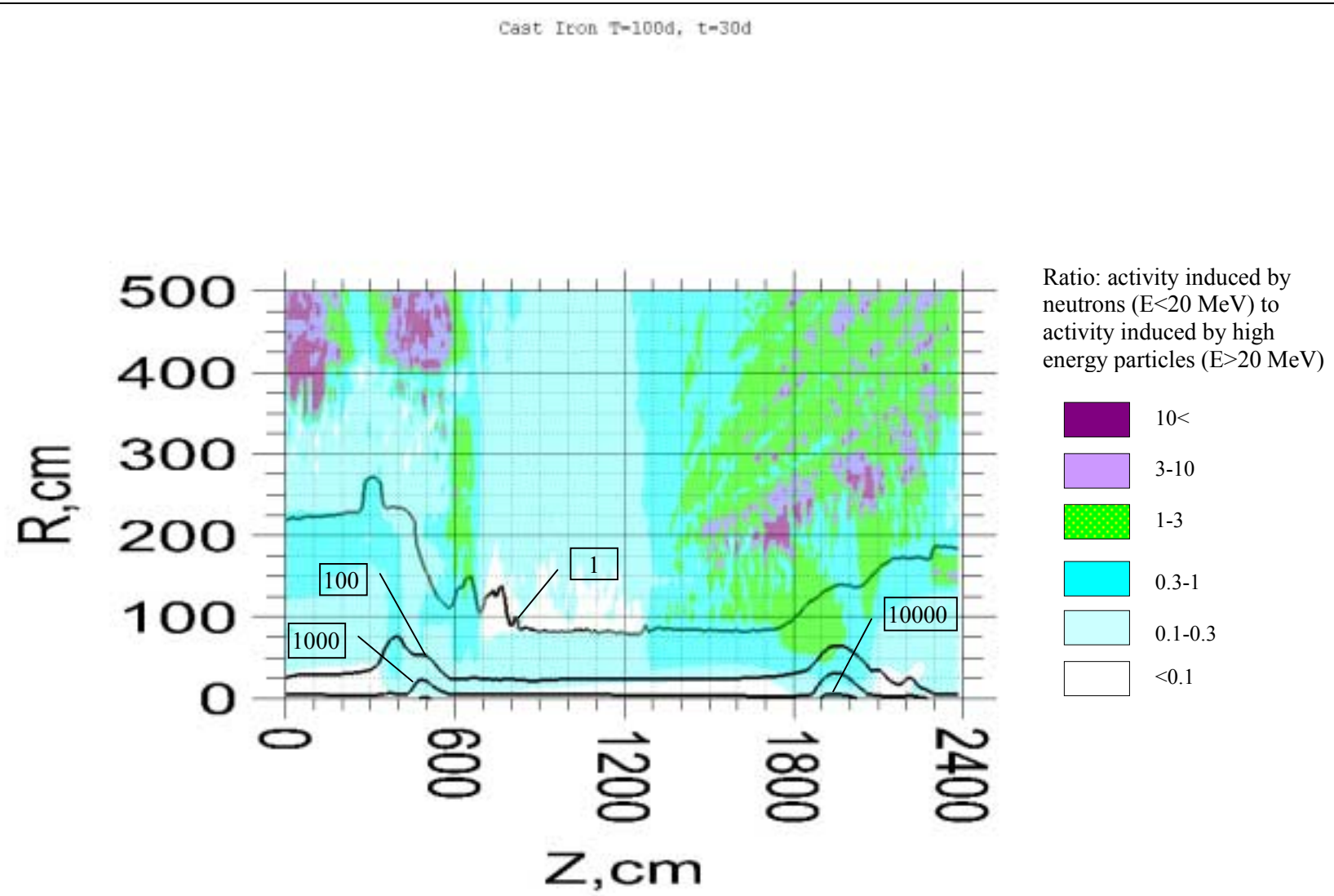

Fig .42. Distribution of induced radioactivity in Cast Iron calculated at T=100d, t=30d. The levels show contact dose rate in μSv/h.

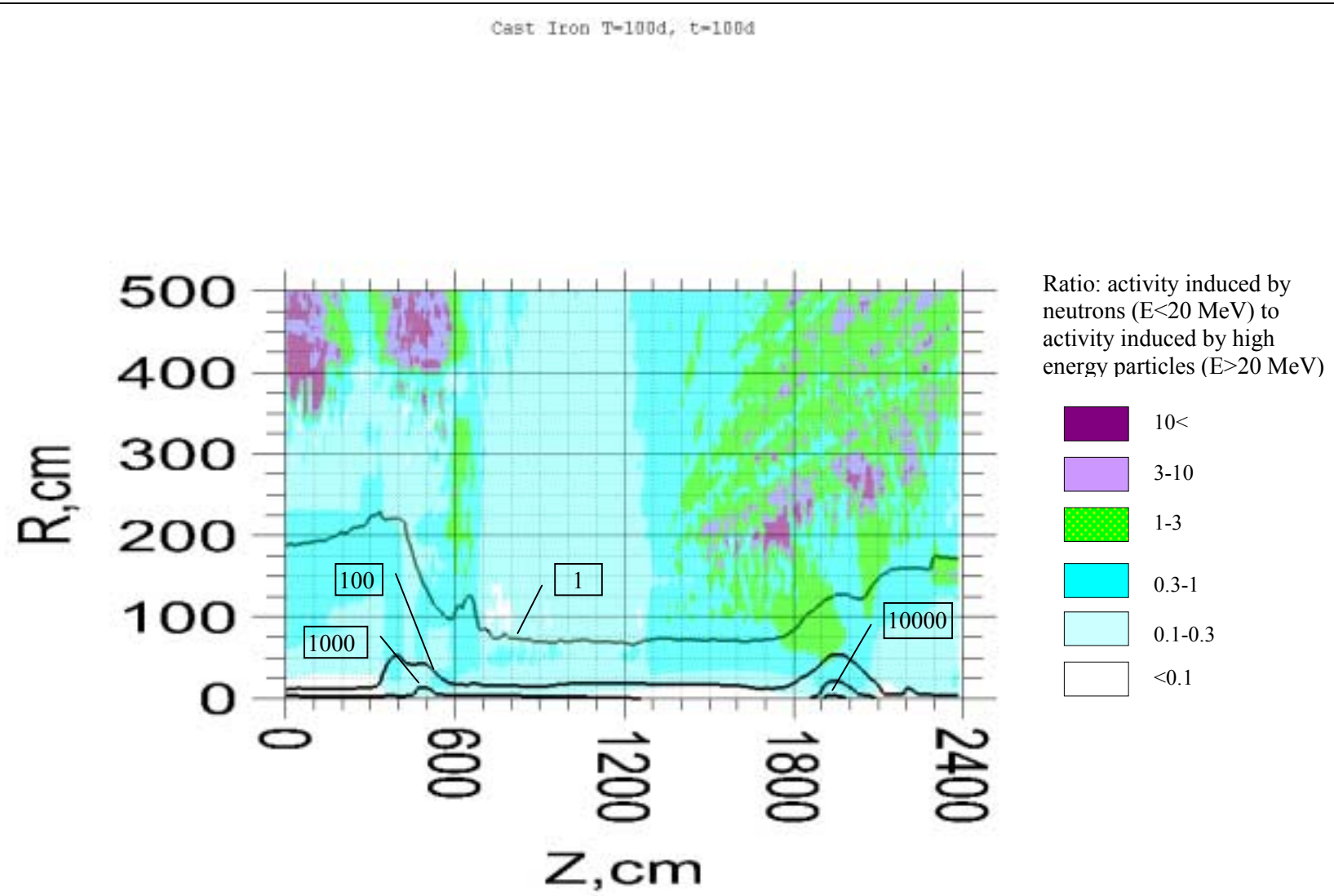

Fig .43. Distribution of induced radioactivity in Cast Iron calculated at T=100d, t=100d. The levels show contact dose rate in μSv/h.

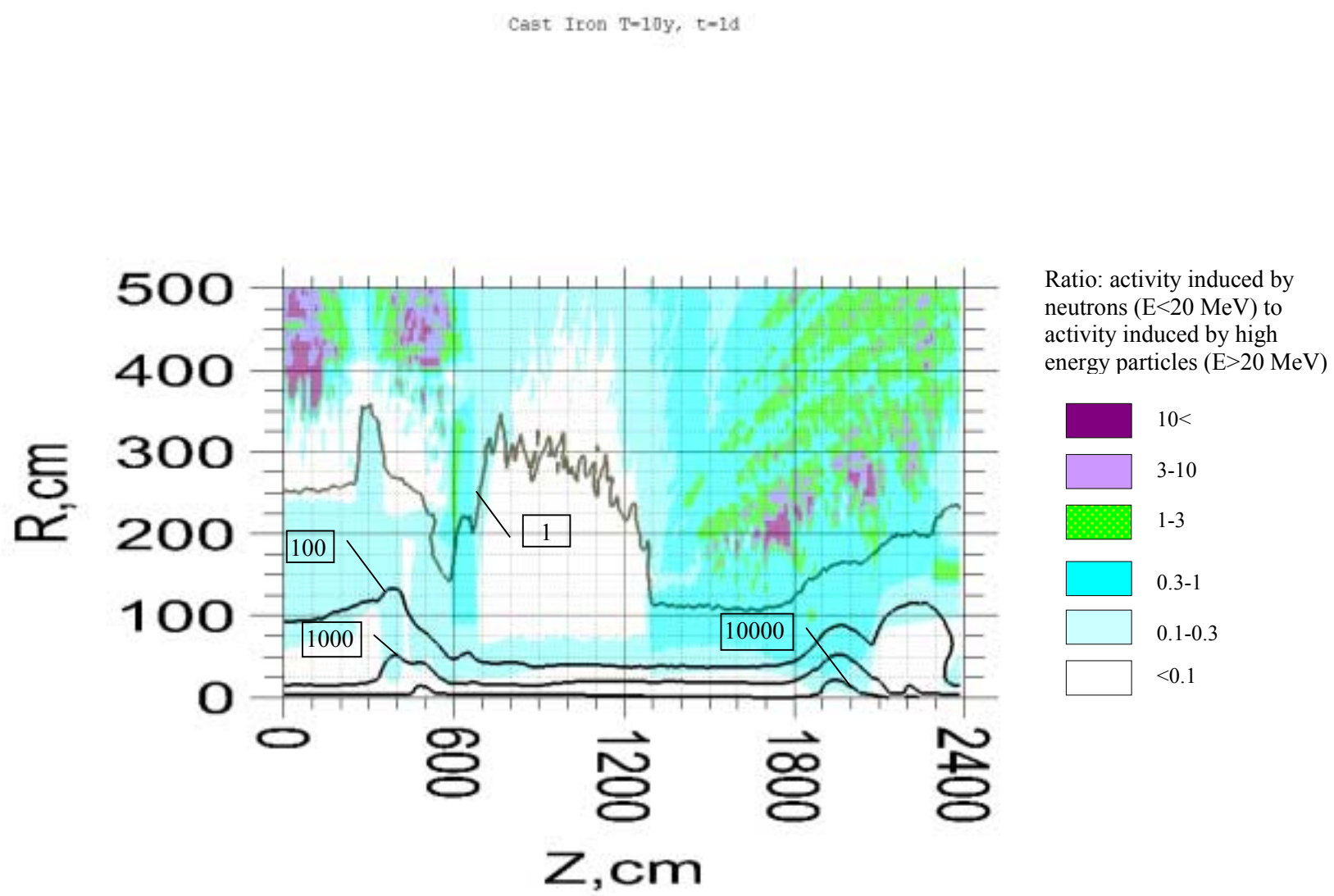

Fig .44. Distribution of induced radioactivity in Cast Iron calculated at T=10y, t=1d. The levels show contact dose rate in μSv/h.

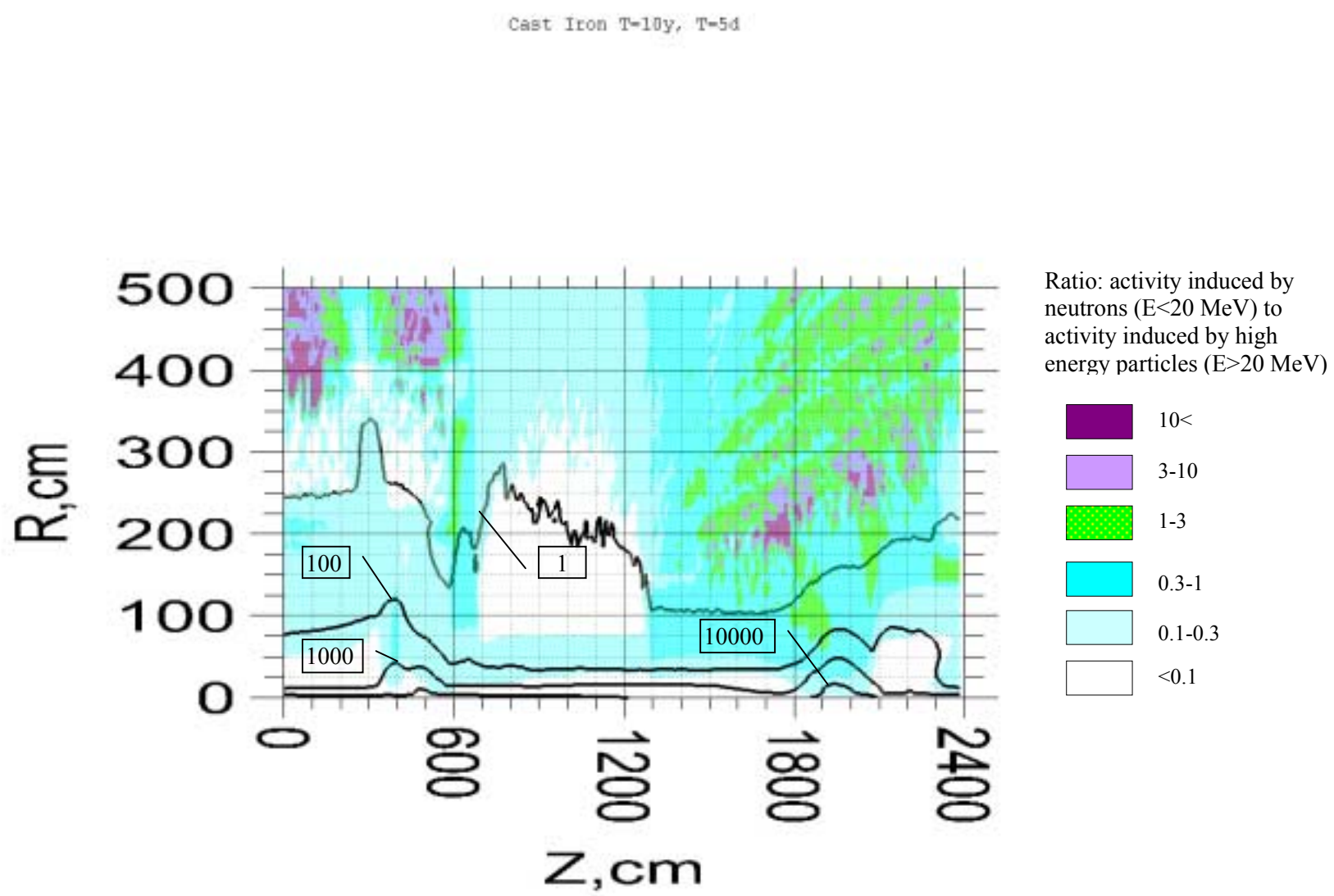

Fig .45. Distribution of induced radioactivity in Cast Iron calculated at T=10y, t=5d. The levels show contact dose rate in μSv/h.

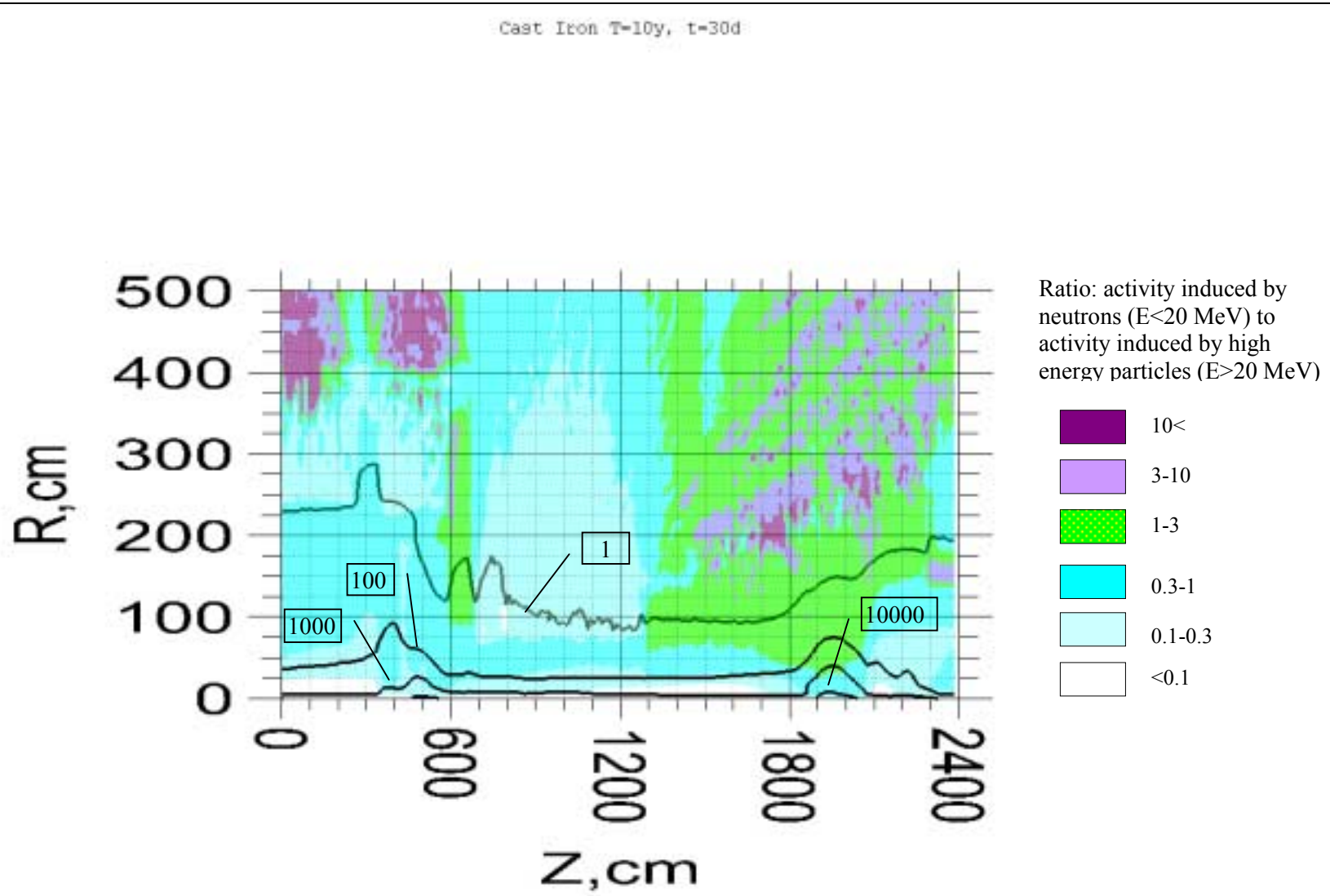

Fig .46. Distribution of induced radioactivity in Cast Iron calculated at T=10y, t=30d. The levels show contact dose rate in μSv/h.

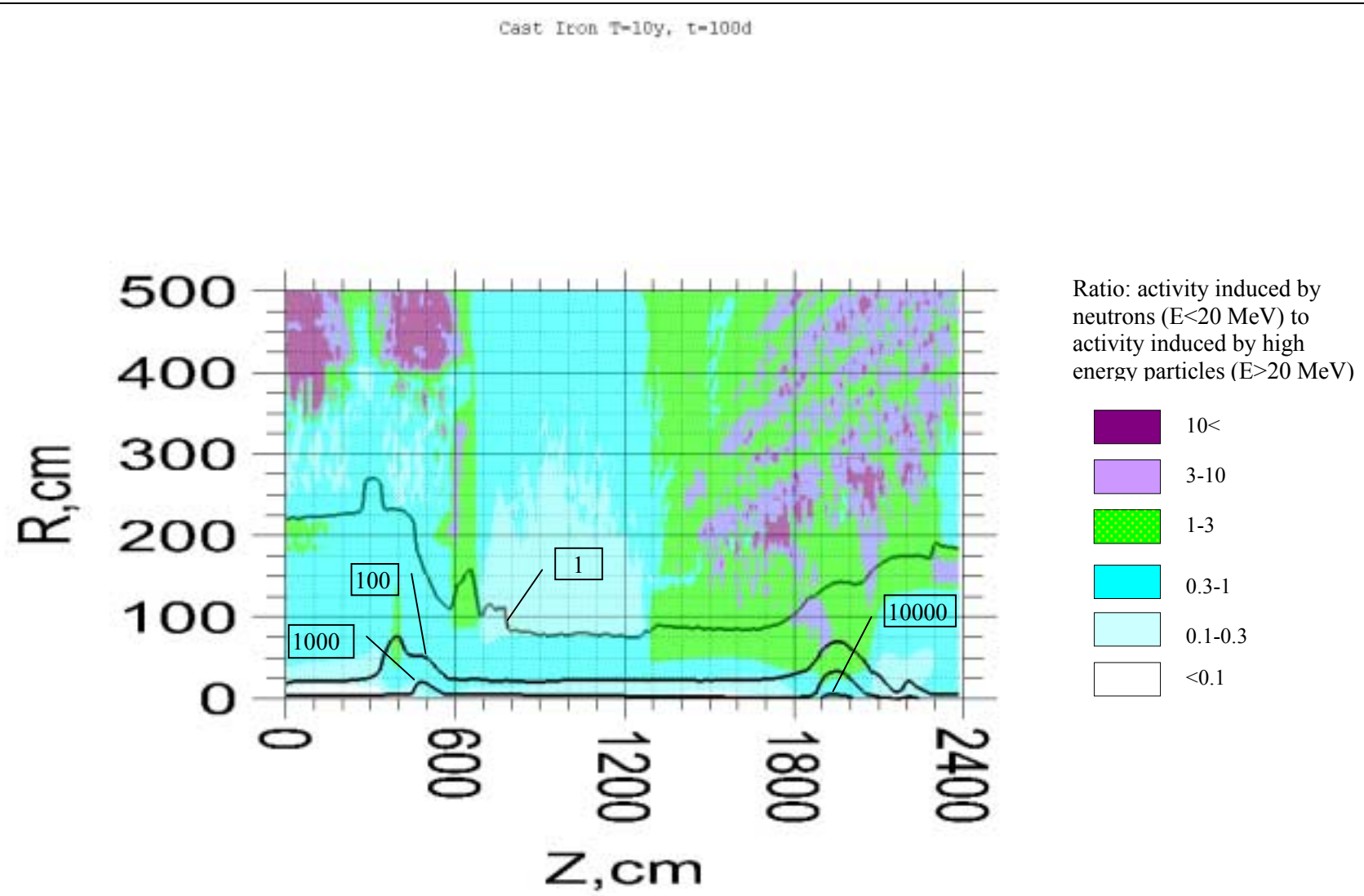

Fig .47. Distribution of induced radioactivity in Cast Iron calculated at T=10y, t=100d. The levels show contact dose rate in μSv/h.

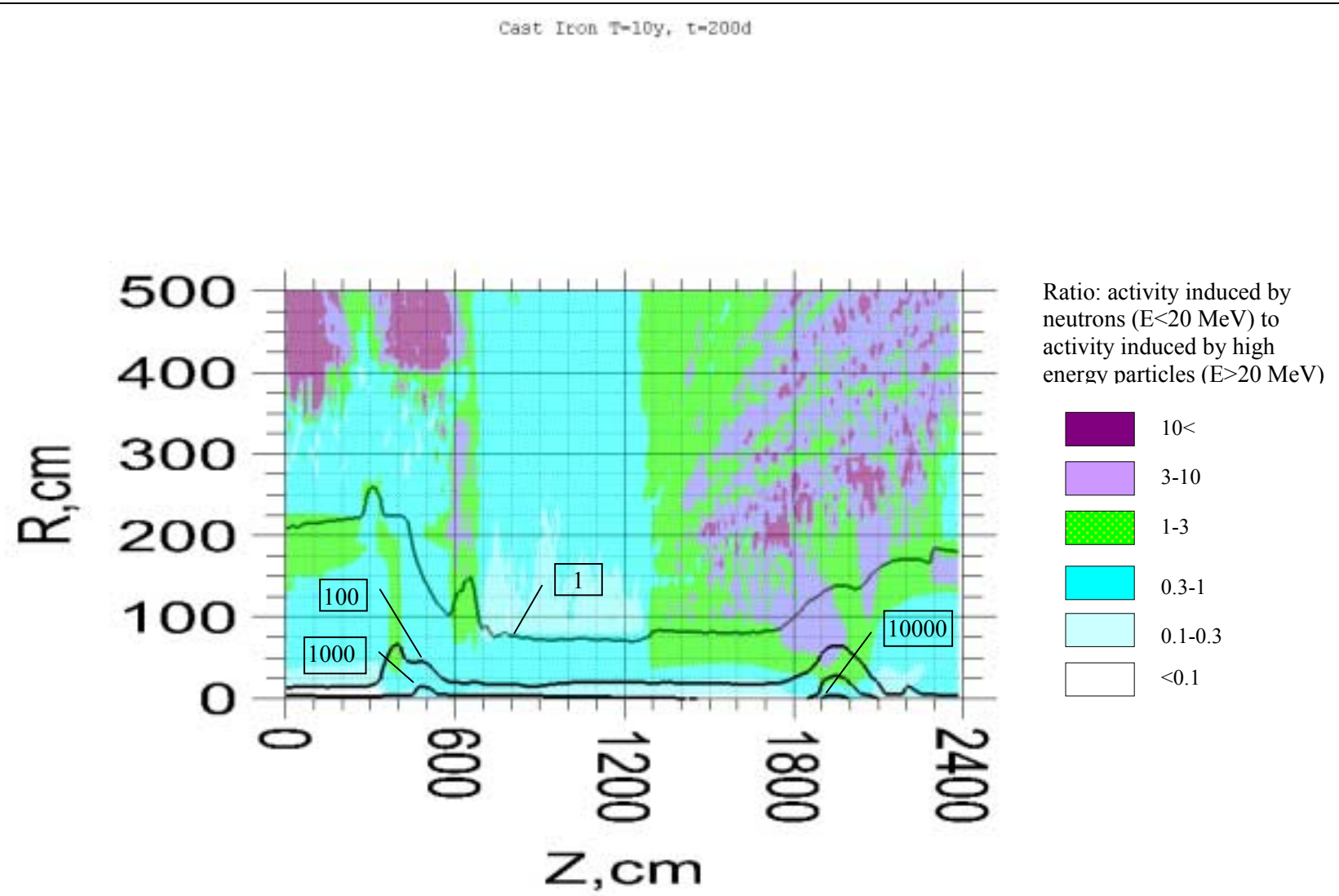

Fig .48. Distribution of induced radioactivity in Cast Iron calculated at T=10y, t=200d. The levels show contact dose rate in μSv/h.

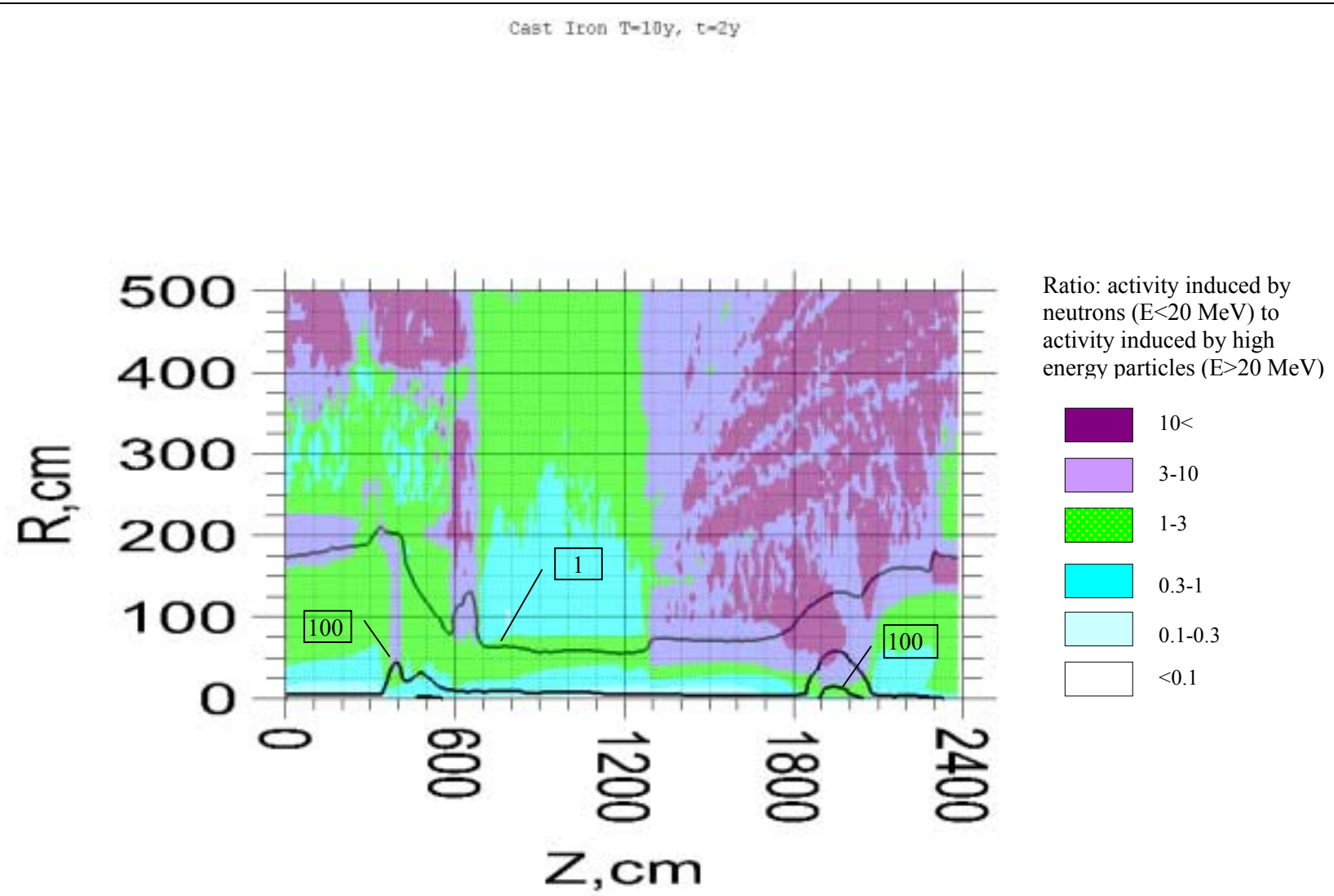

Fig .49. Distribution of induced radioactivity in Cast Iron calculated at T=10y, t=2y. The levels show contact dose rate in μSv/h.

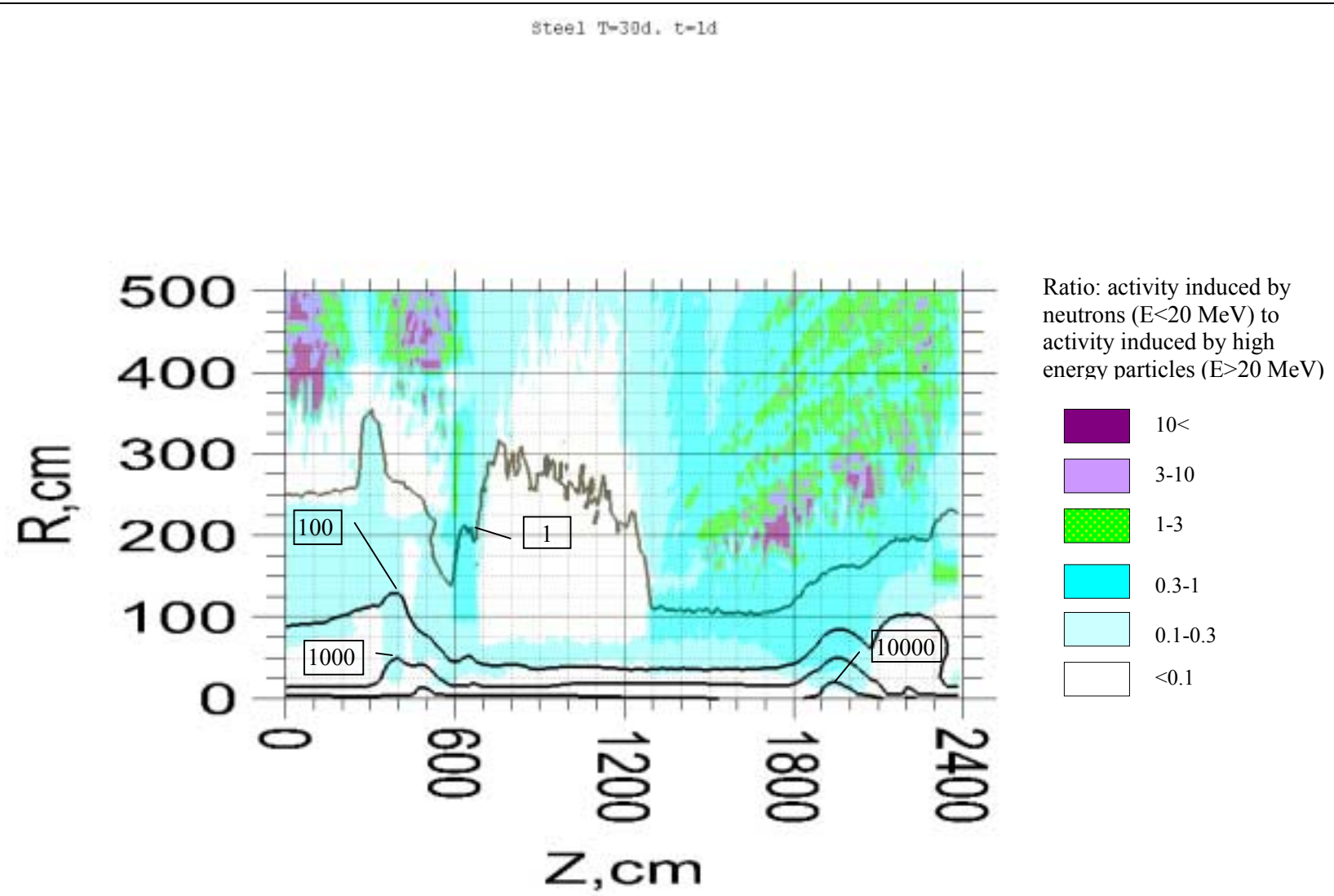

Fig .50. Distribution of induced radioactivity in Stainless Steel calculated at T=30d, t=1d. The levels show contact dose rate in μSv/h.

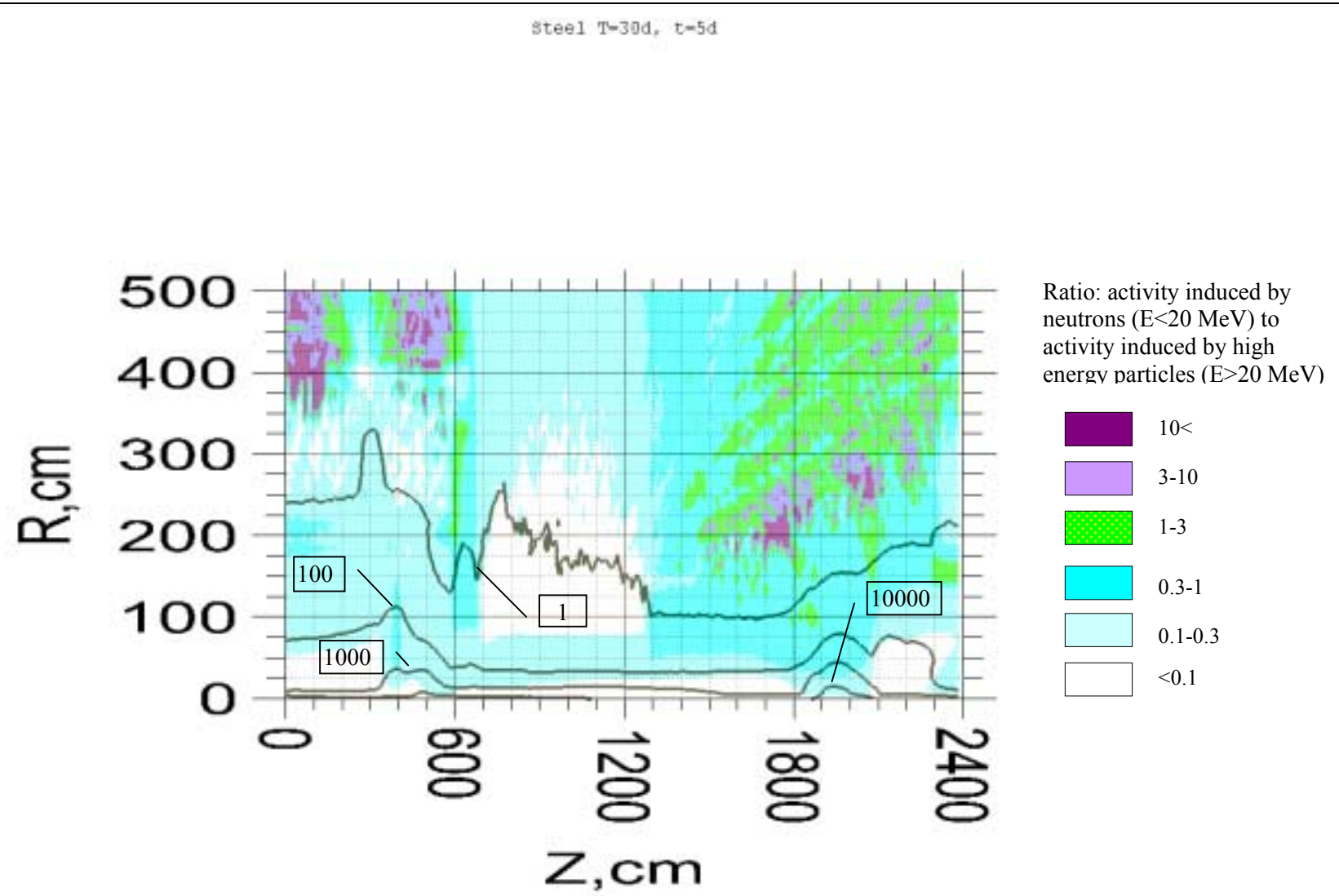

Fig .51. Distribution of induced radioactivity in Stainless Steel calculated at T=30d, t=5d. The levels show contact dose rate in μSv/h.

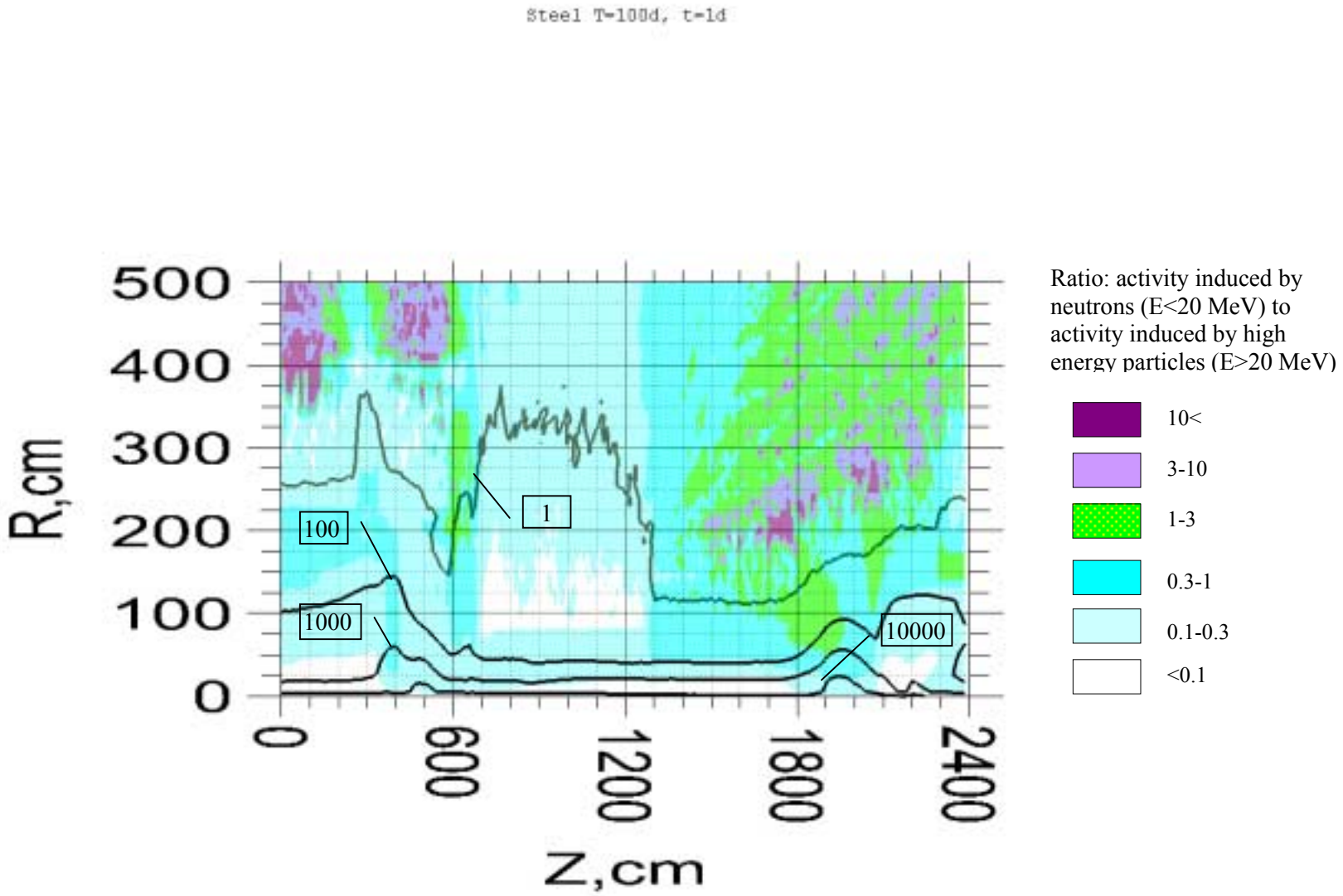

Fig .52. Distribution of induced radioactivity in Stainless Steel calculated at T=100d, t=1d. The levels show contact dose rate in μSv/h.

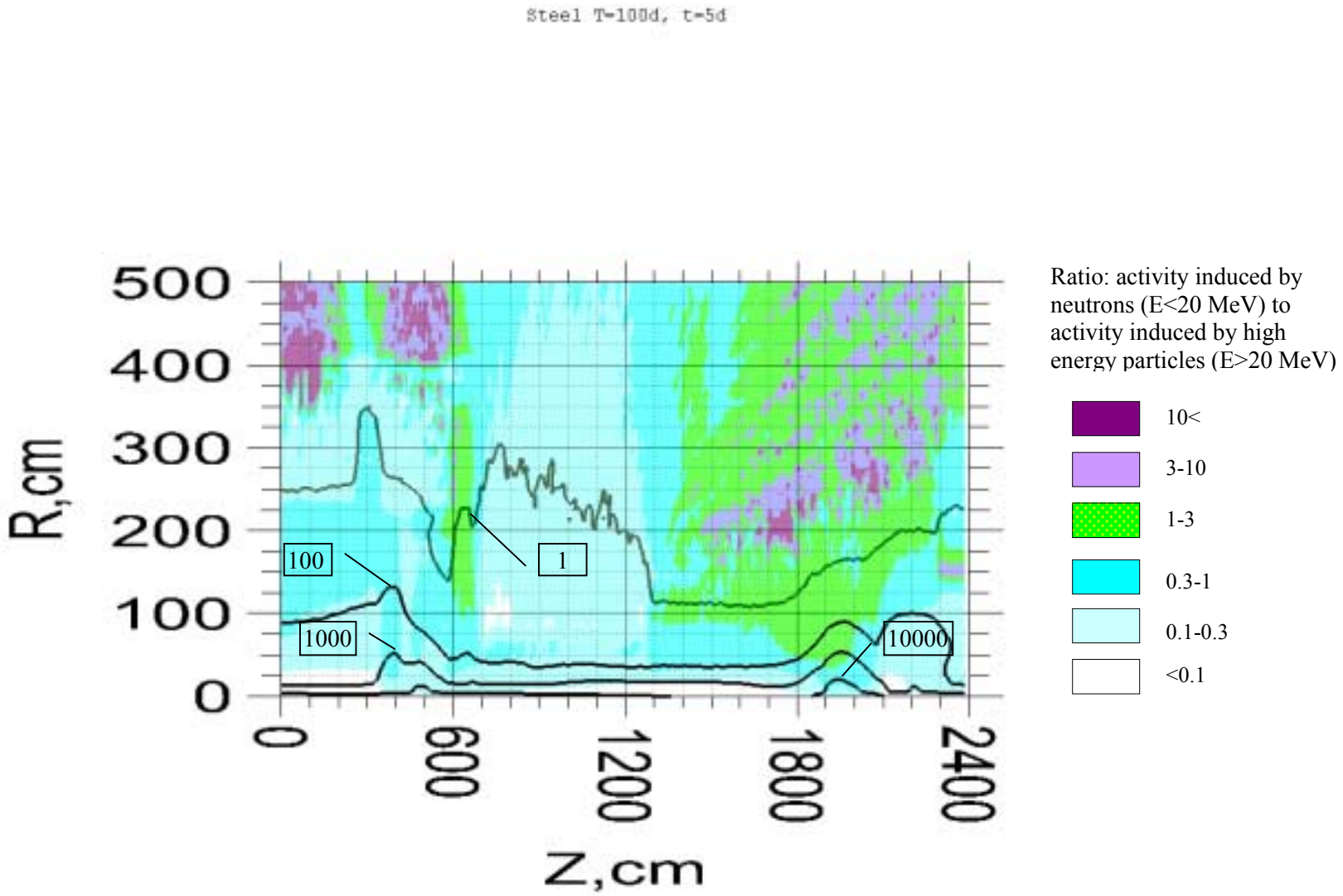

Fig .53. Distribution of induced radioactivity in Stainless Steel calculated at T=100d, t=5d. The levels show contact dose rate in μSv/h.

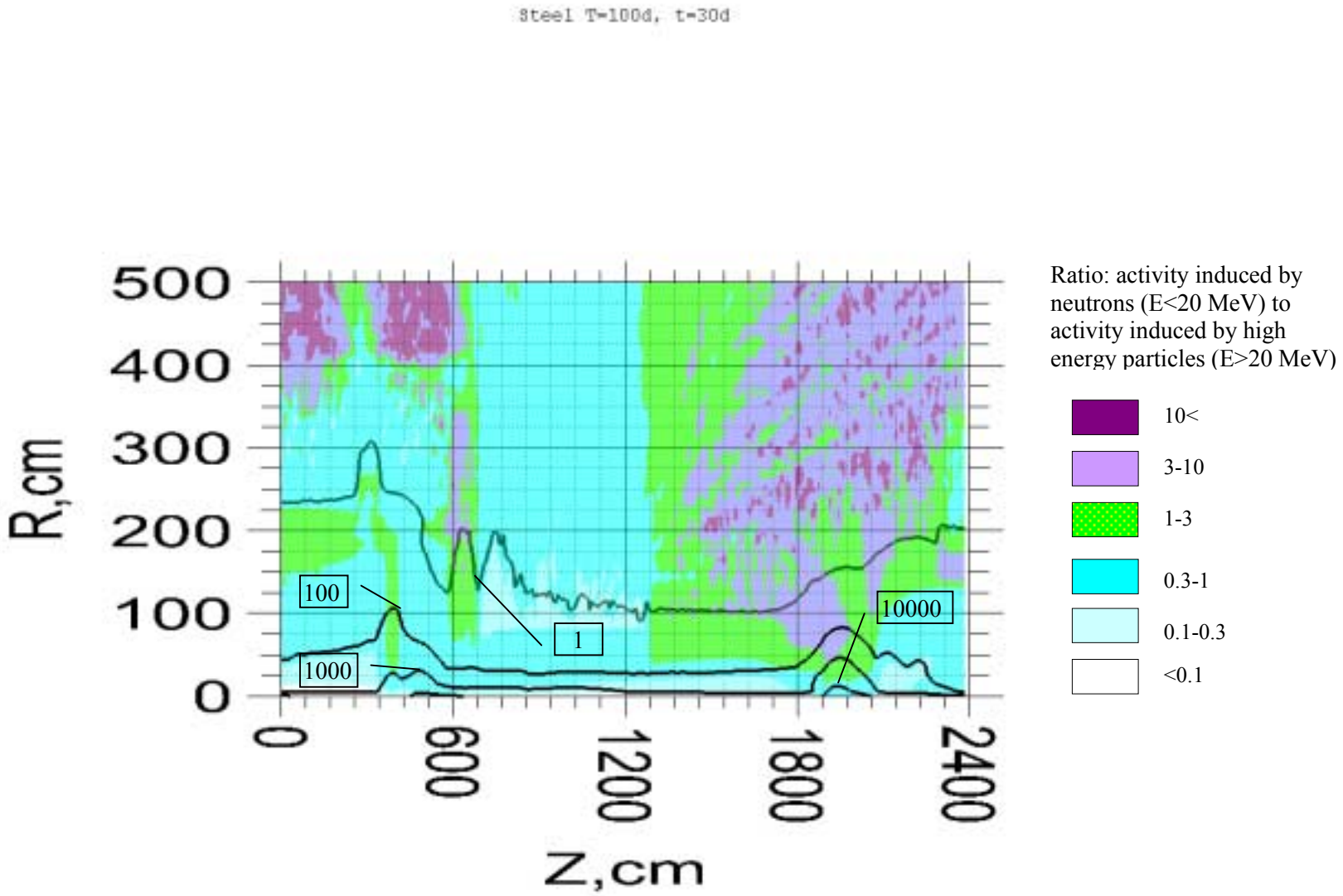

Fig .54. Distribution of induced radioactivity in Stainless Steel calculated at T=100d, t=30d. The levels show contact dose rate in μSv/h.

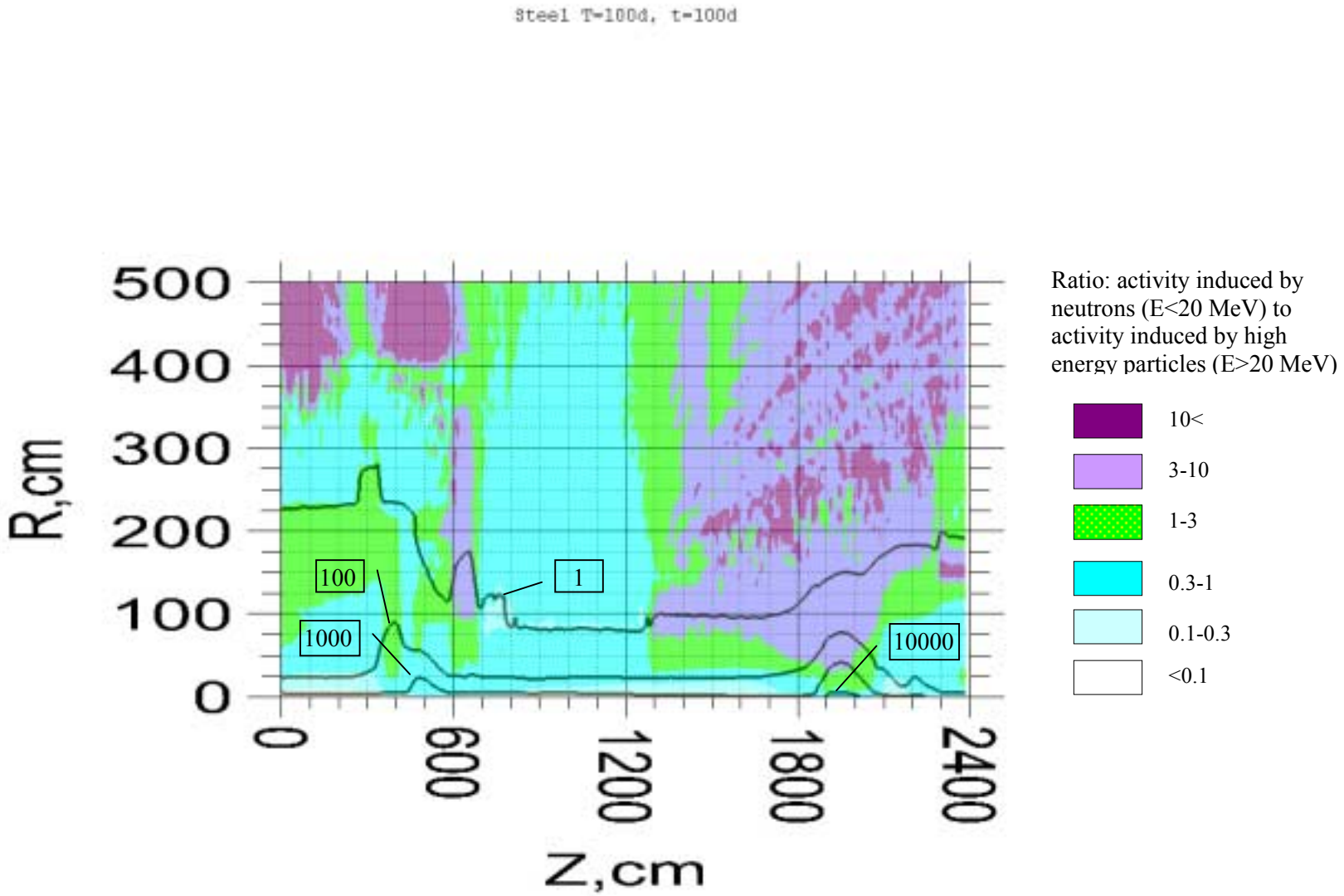

Fig .55. Distribution of induced radioactivity in Stainless Steel calculated at T=100d, t=100d. The levels show contact dose rate in μSv/h.

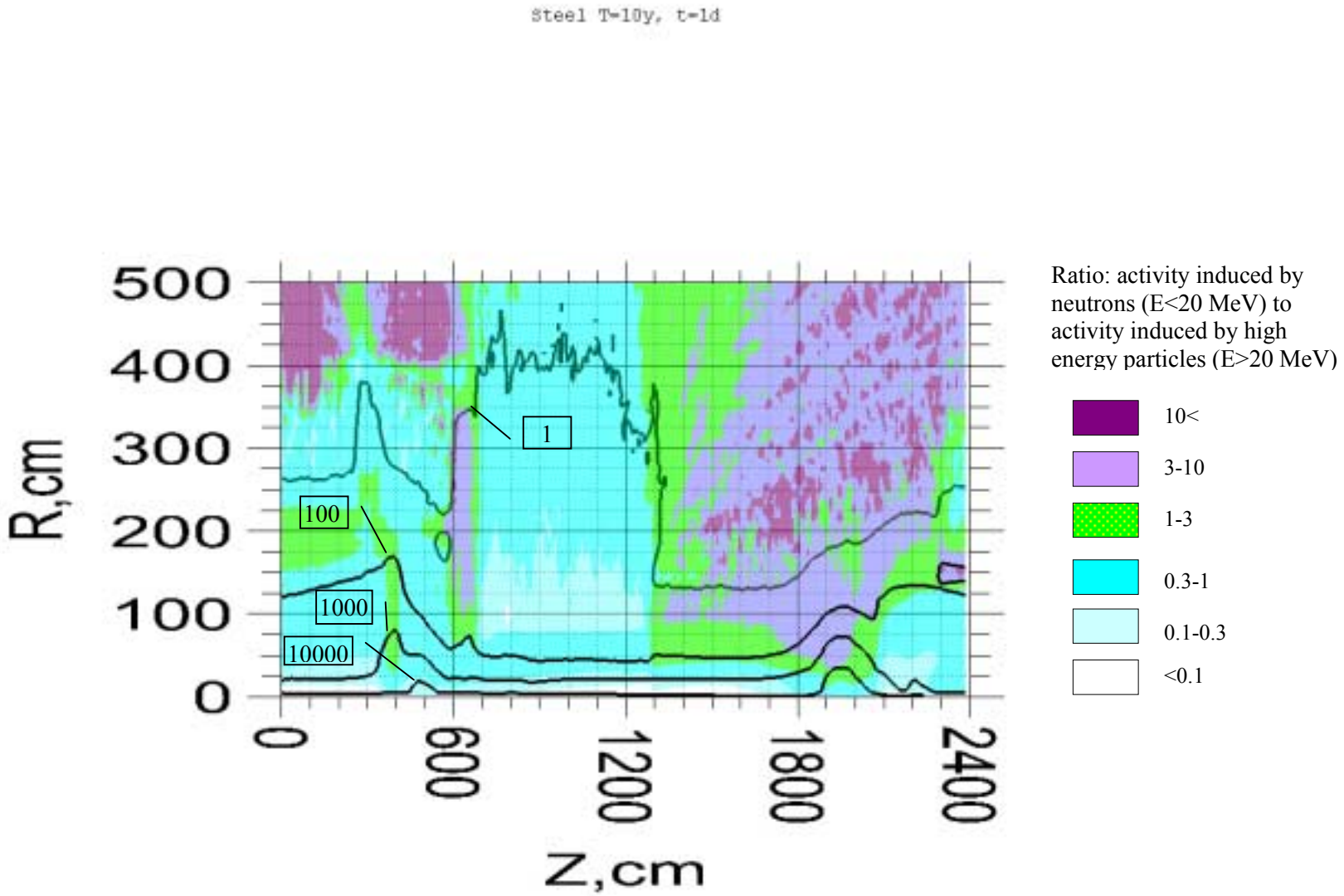

Fig .56. Distribution of induced radioactivity in Stainless Steel calculated at T=10y, t=1d. The levels show contact dose rate in μSv/h.

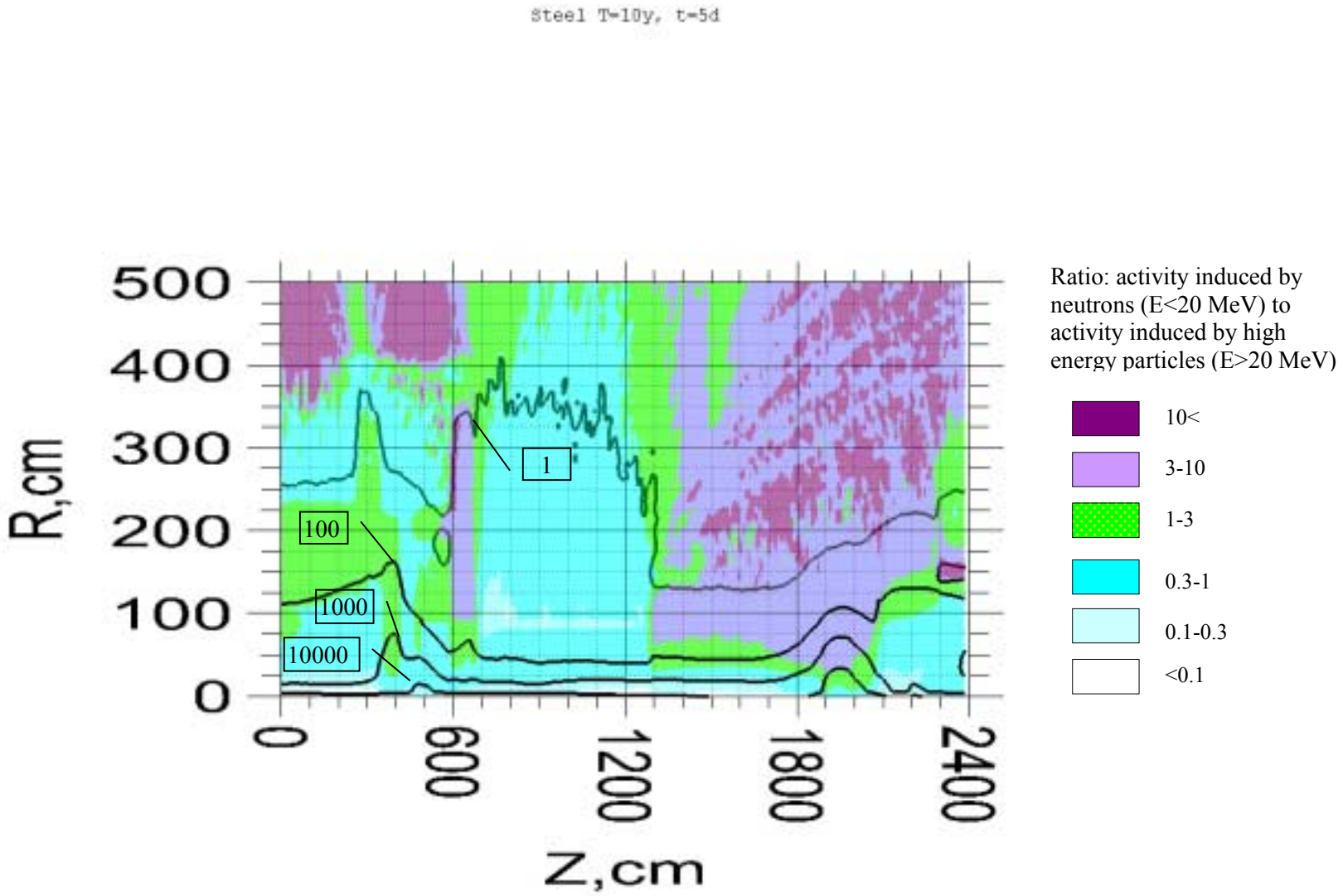

Fig .57. Distribution of induced radioactivity in Stainless Steel calculated at T=10y, t=5d. The levels show contact dose rate in μSv/h.

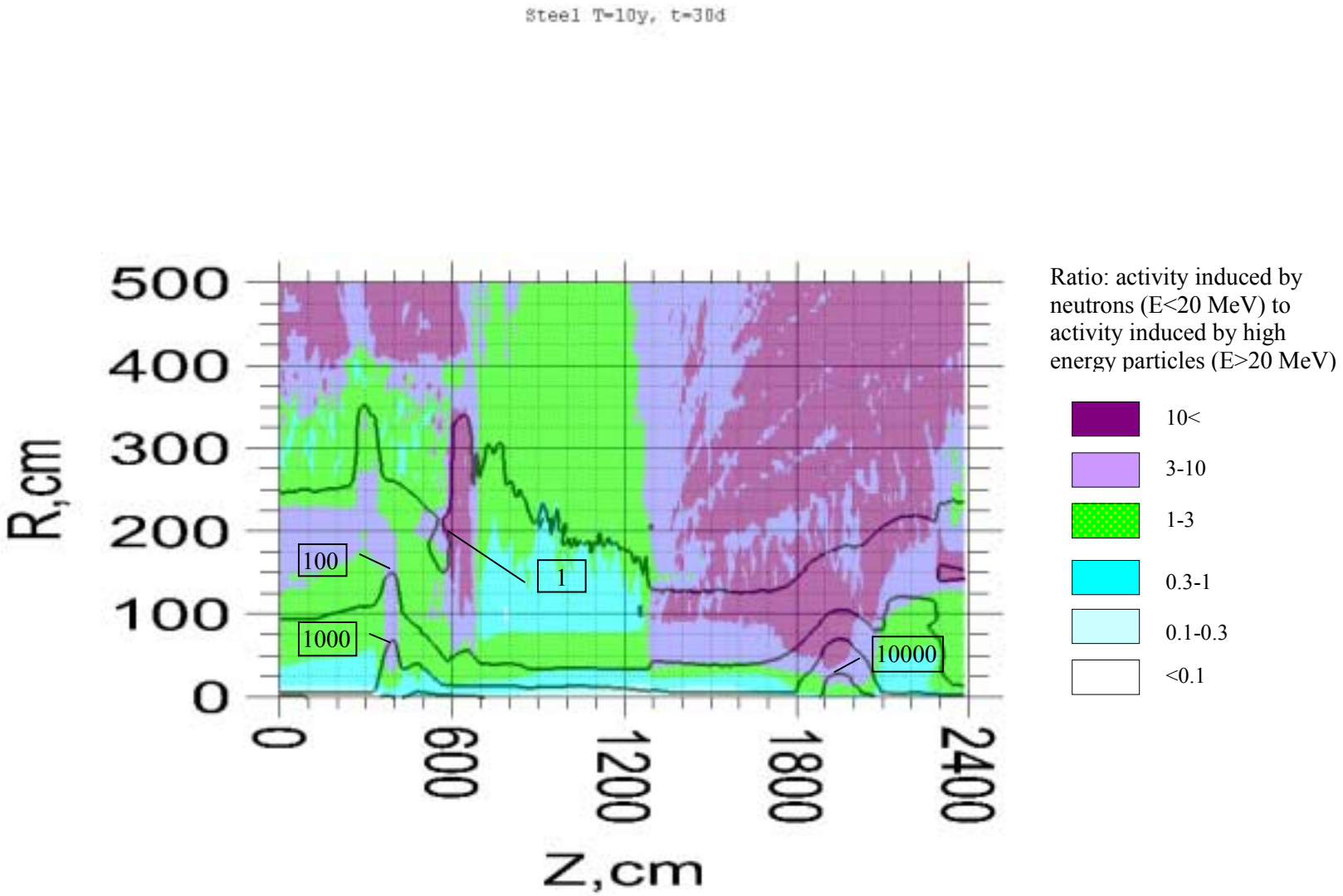

Fig .58. Distribution of induced radioactivity in Stainless Steel calculated at T=10y, t=30d. The levels show contact dose rate in μSv/h.

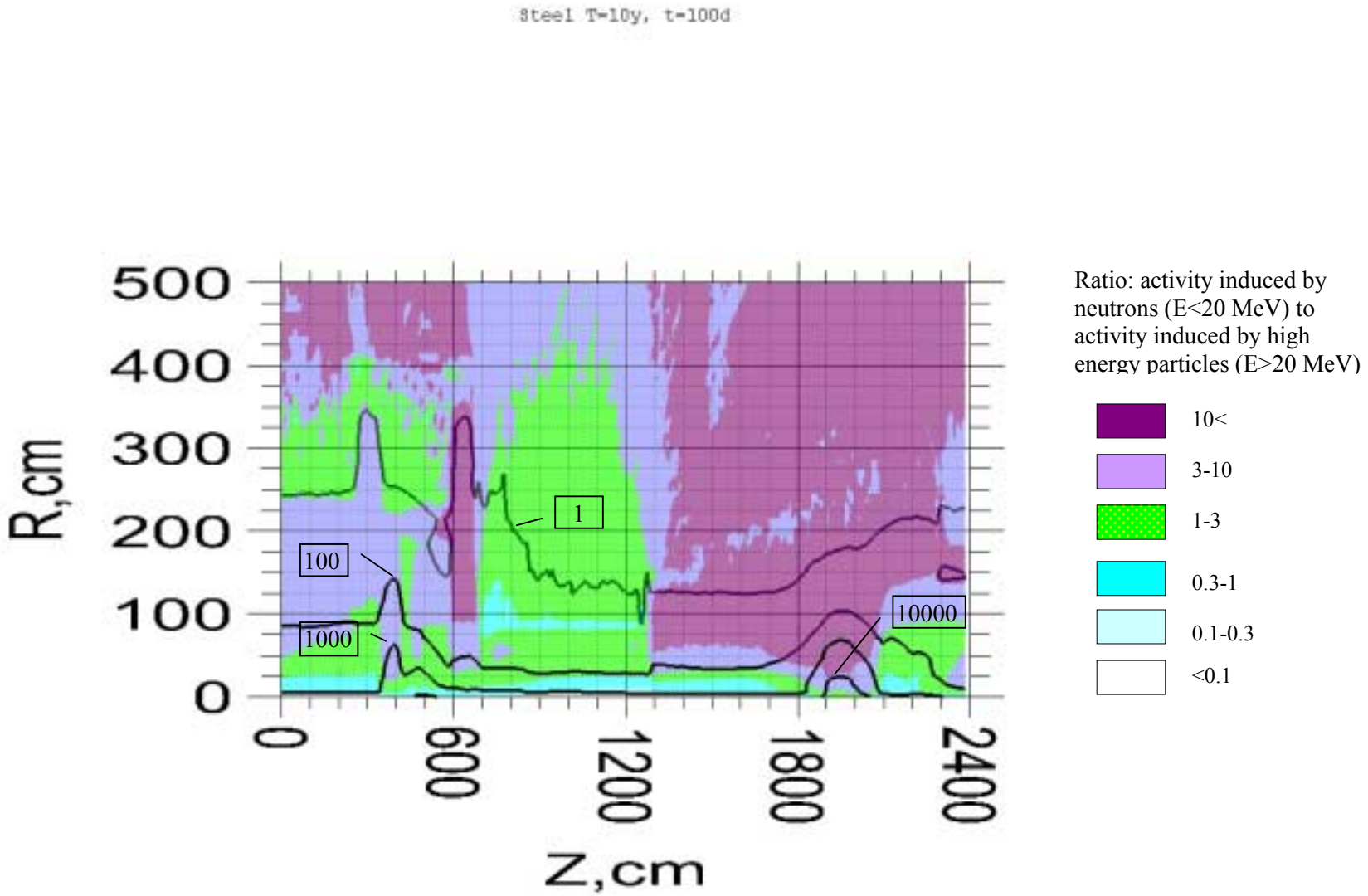

Fig .59. Distribution of induced radioactivity in Stainless Steel calculated at T=10y, t=100d. The levels show contact dose rate in μSv/h.

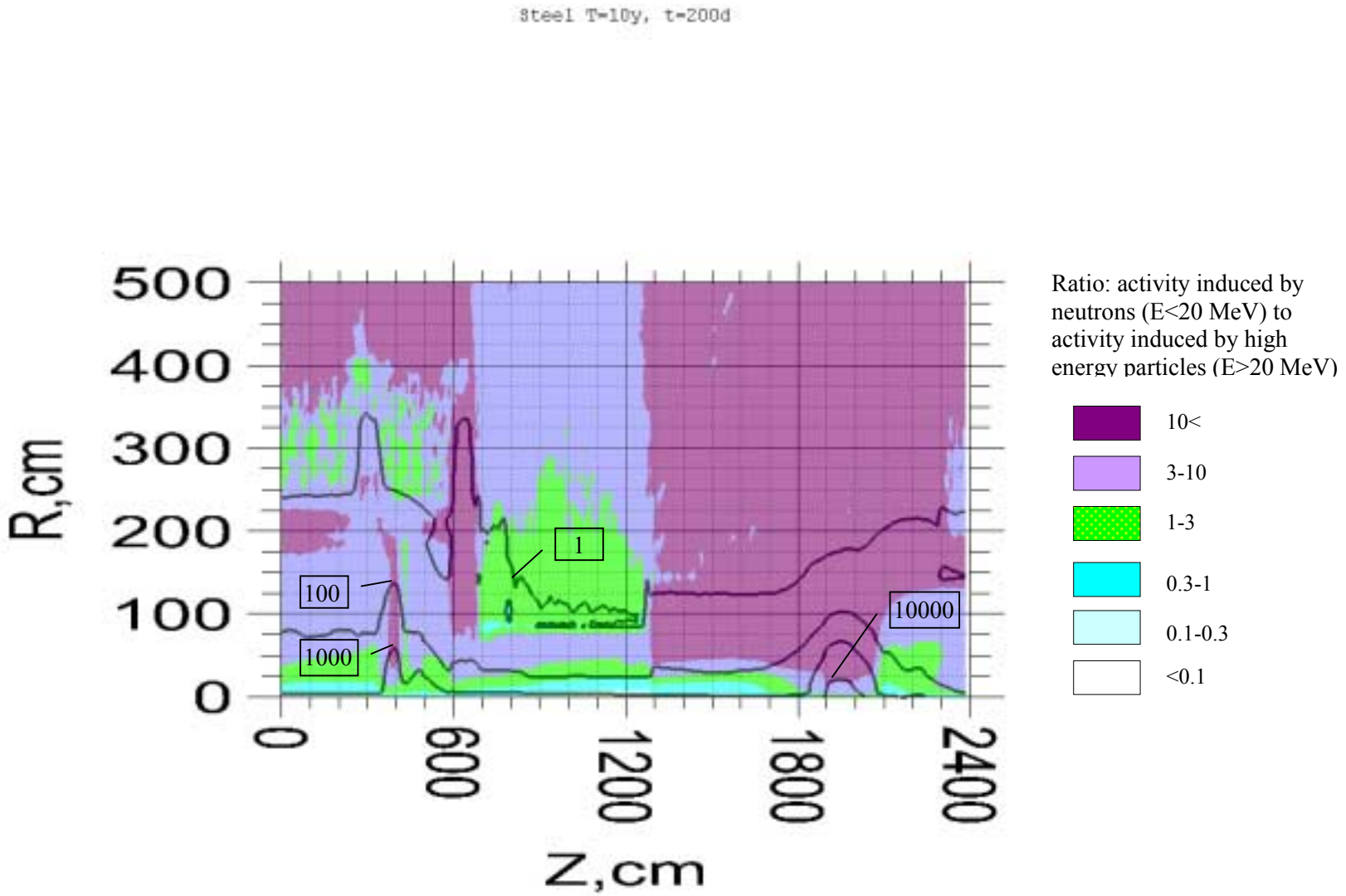

Fig .60. Distribution of induced radioactivity in Stainless Steel calculated at T=10y, t=200d. The levels show contact dose rate in μSv/h.

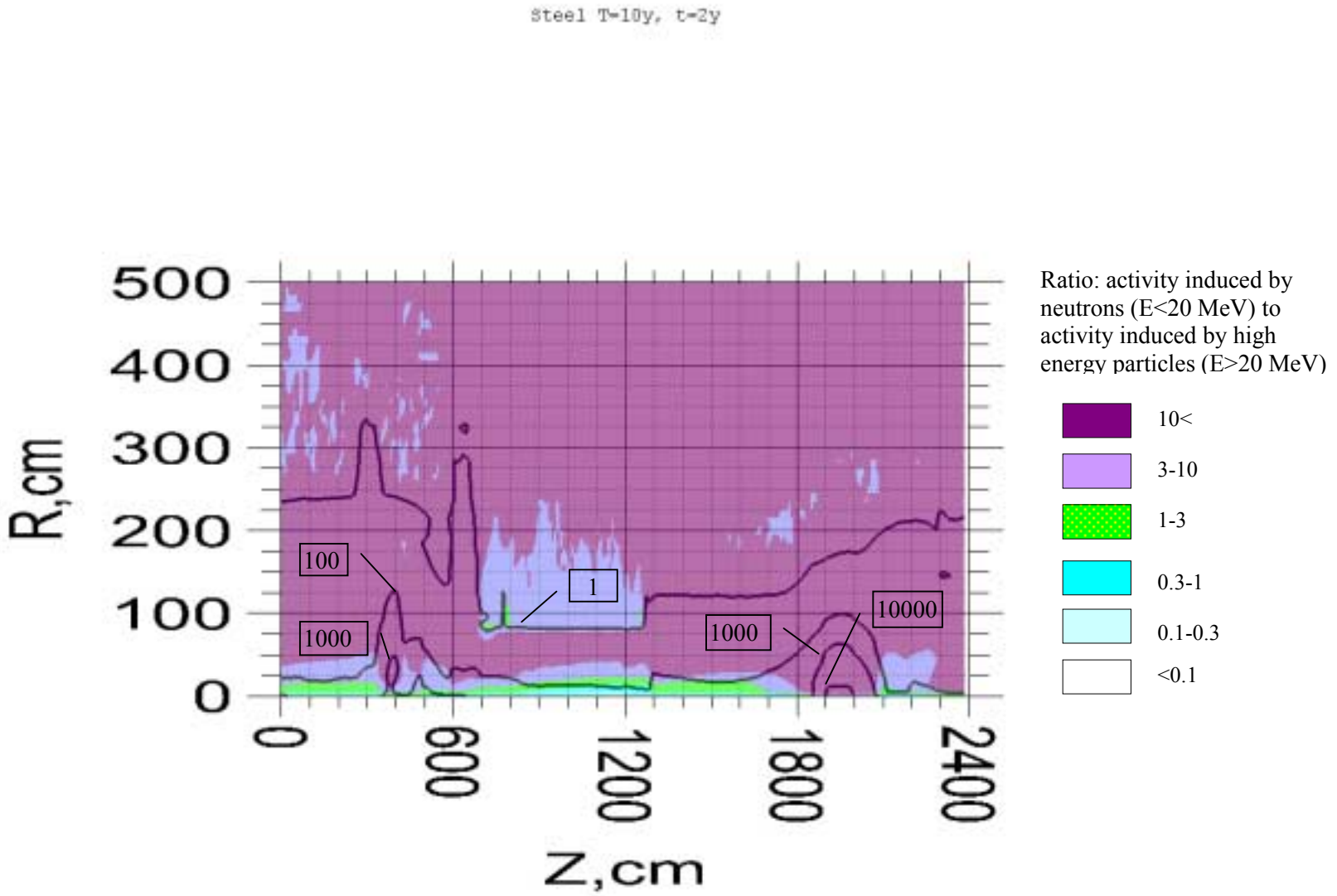

Fig .61. Distribution of induced radioactivity in Stainless Steel calculated at T=10y, t=2y. The levels show contact dose rate in μSv/h.

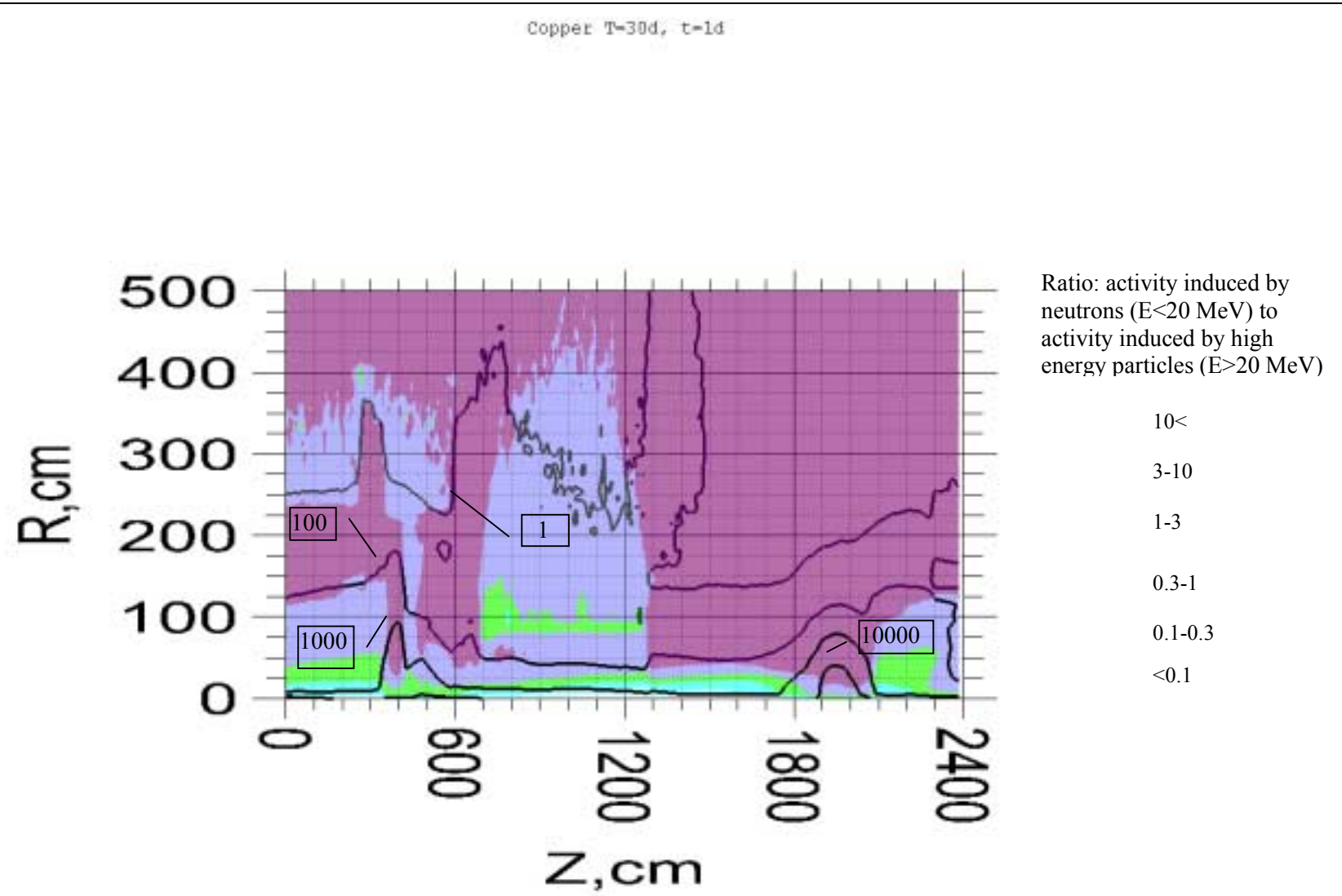

Fig .62. Distribution of induced radioactivity in Copper calculated at T=30d, t=1d The levels show contact dose rate in μSv/h.

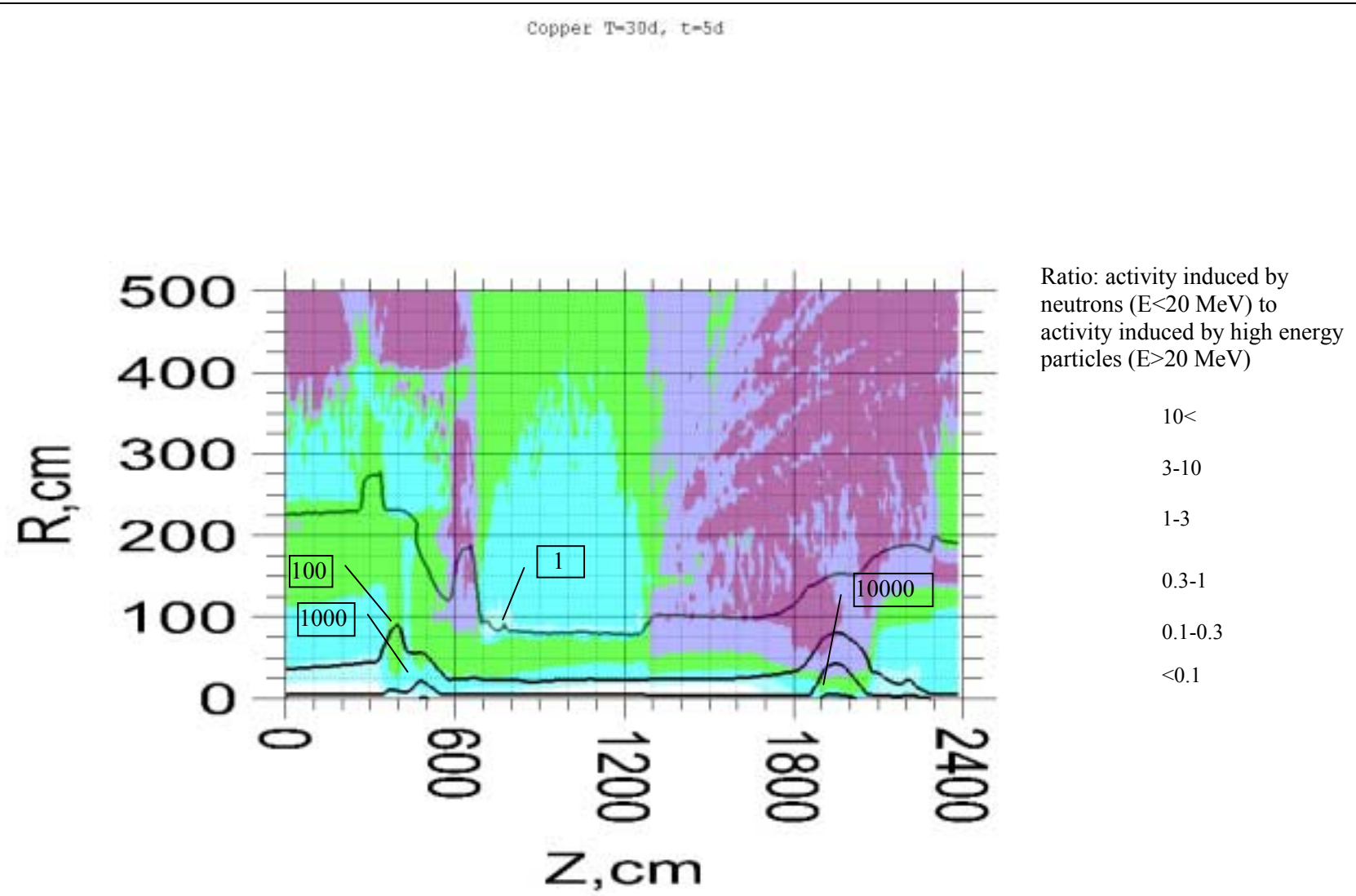

Fig .63. Distribution of induced radioactivity in Copper calculated at T=30d, t=5d The levels show contact dose rate in μSv/h.

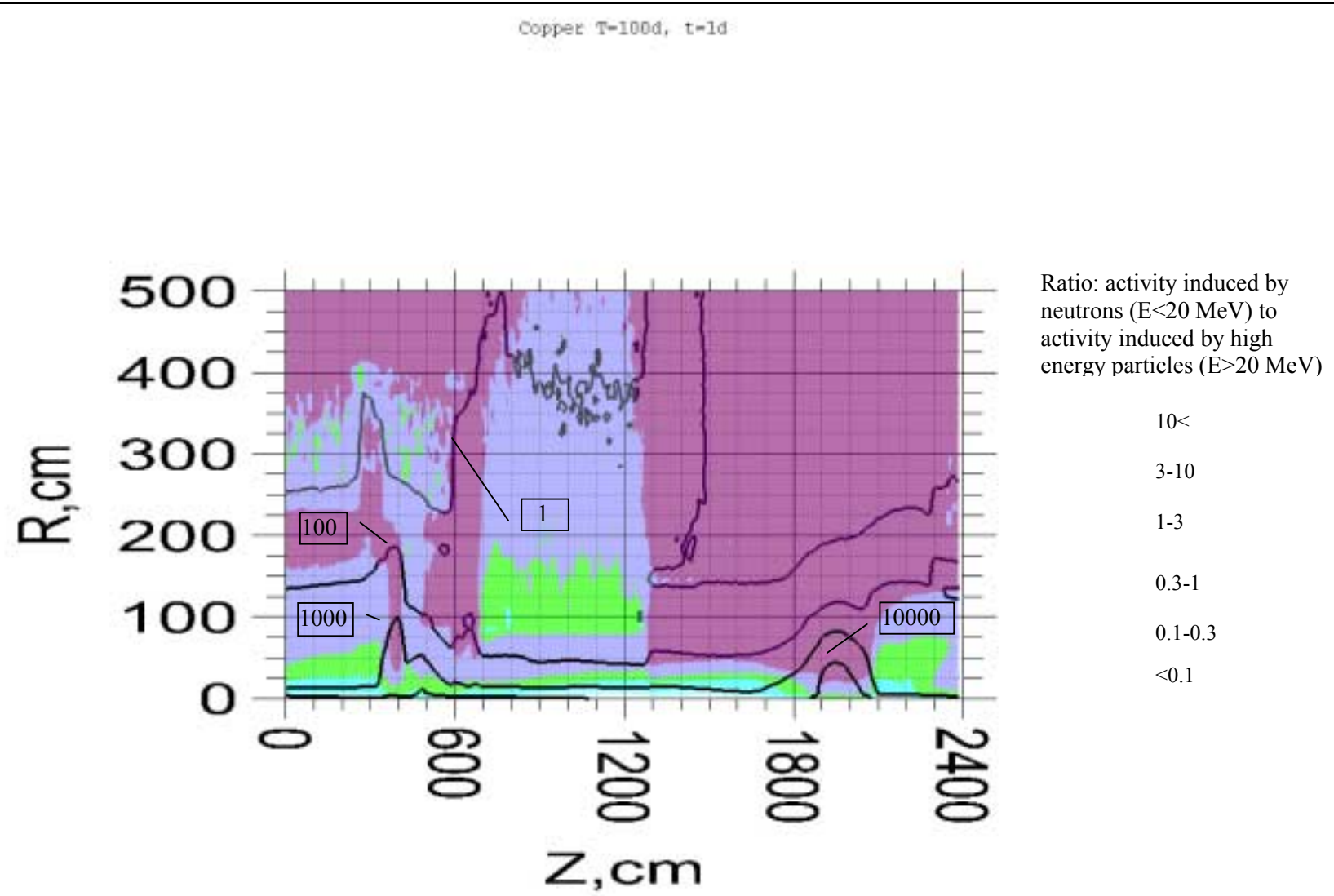

Fig .64. Distribution of induced radioactivity in Copper calculated at T=100d, t=1d. The levels show contact dose rate in μSv/h.

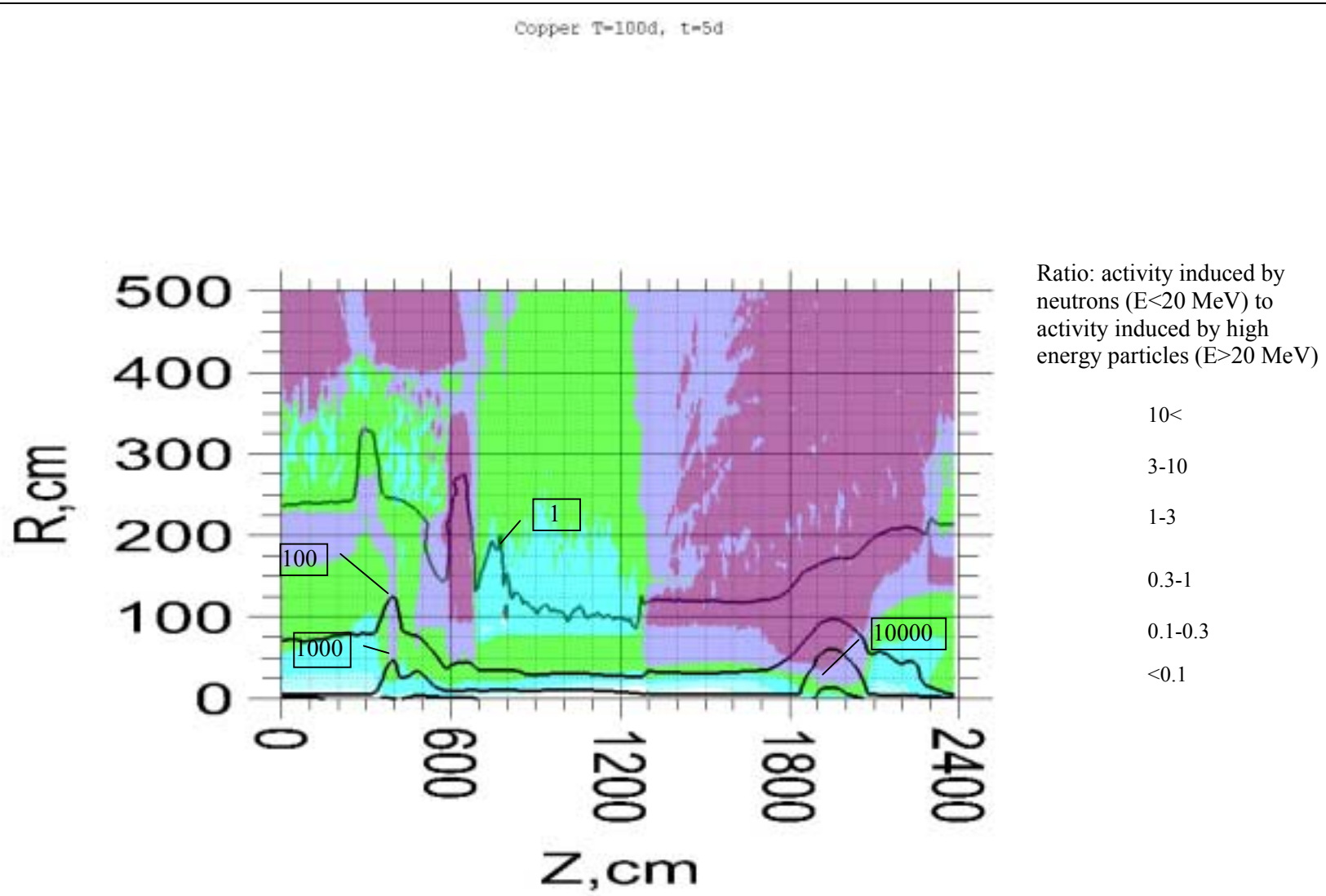

Fig .65. Distribution of induced radioactivity in Copper calculated at T=100d, t=5d. The levels show contact dose rate in μSv/h.

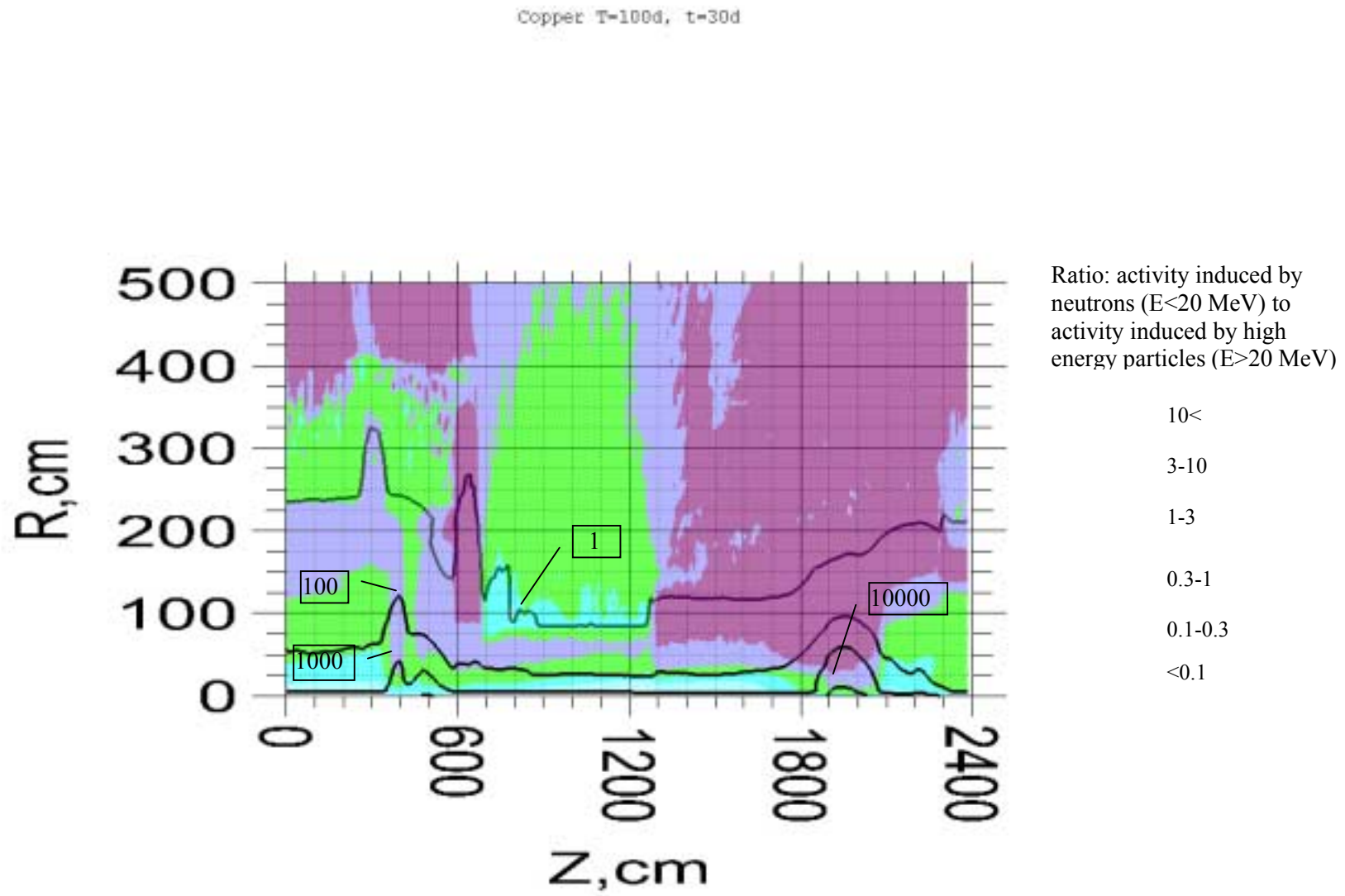

Fig .66. Distribution of induced radioactivity in Copper calculated at T=100d, t=30d. The levels show contact dose rate in μSv/h.

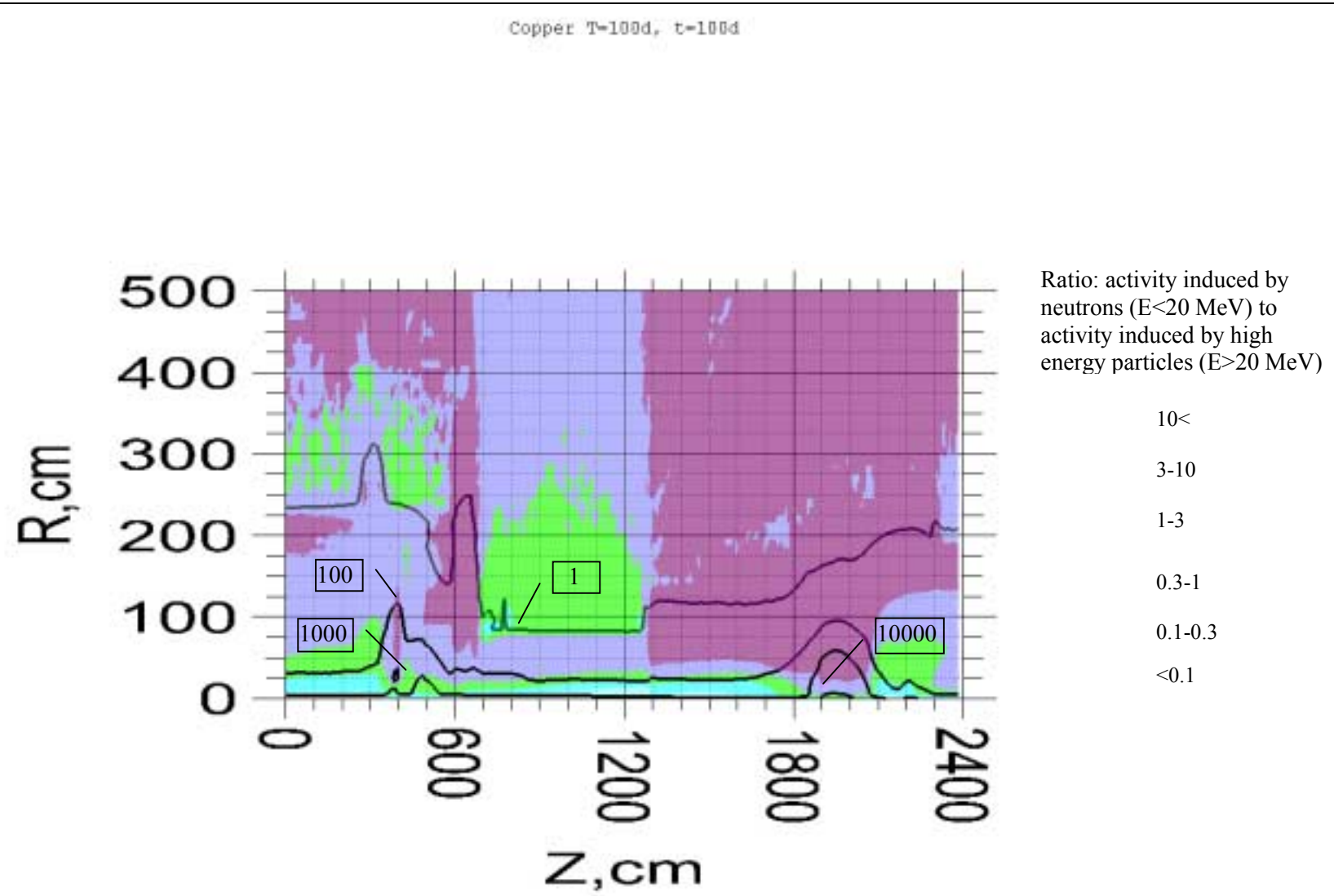

Fig .67. Distribution of induced radioactivity in Copper calculated at T=100d, t=100d. The levels show contact dose rate in μSv/h.

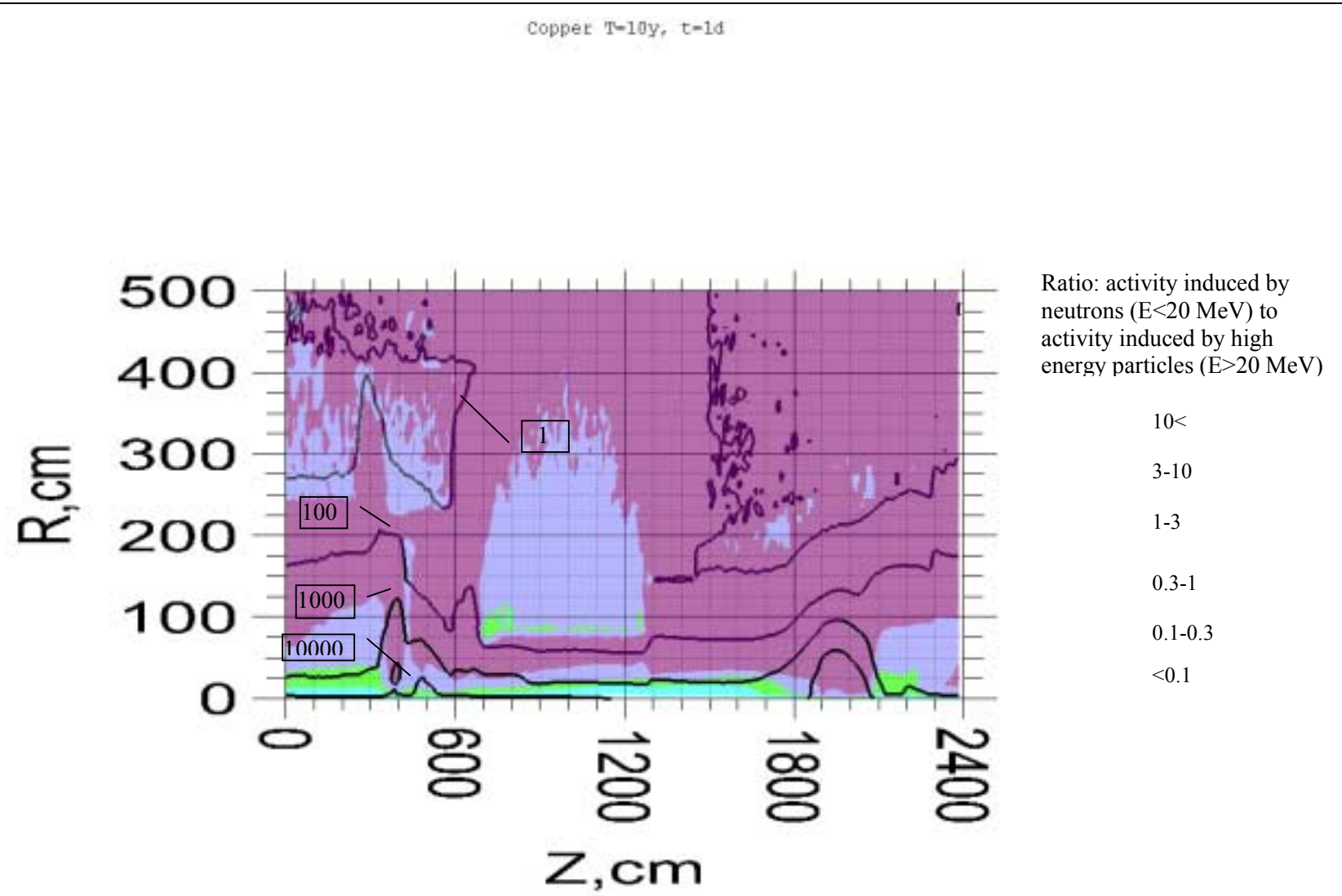

Fig .68. Distribution of induced radioactivity in Copper calculated at T=10y, t=1d. The levels show contact dose rate in μSv/h.

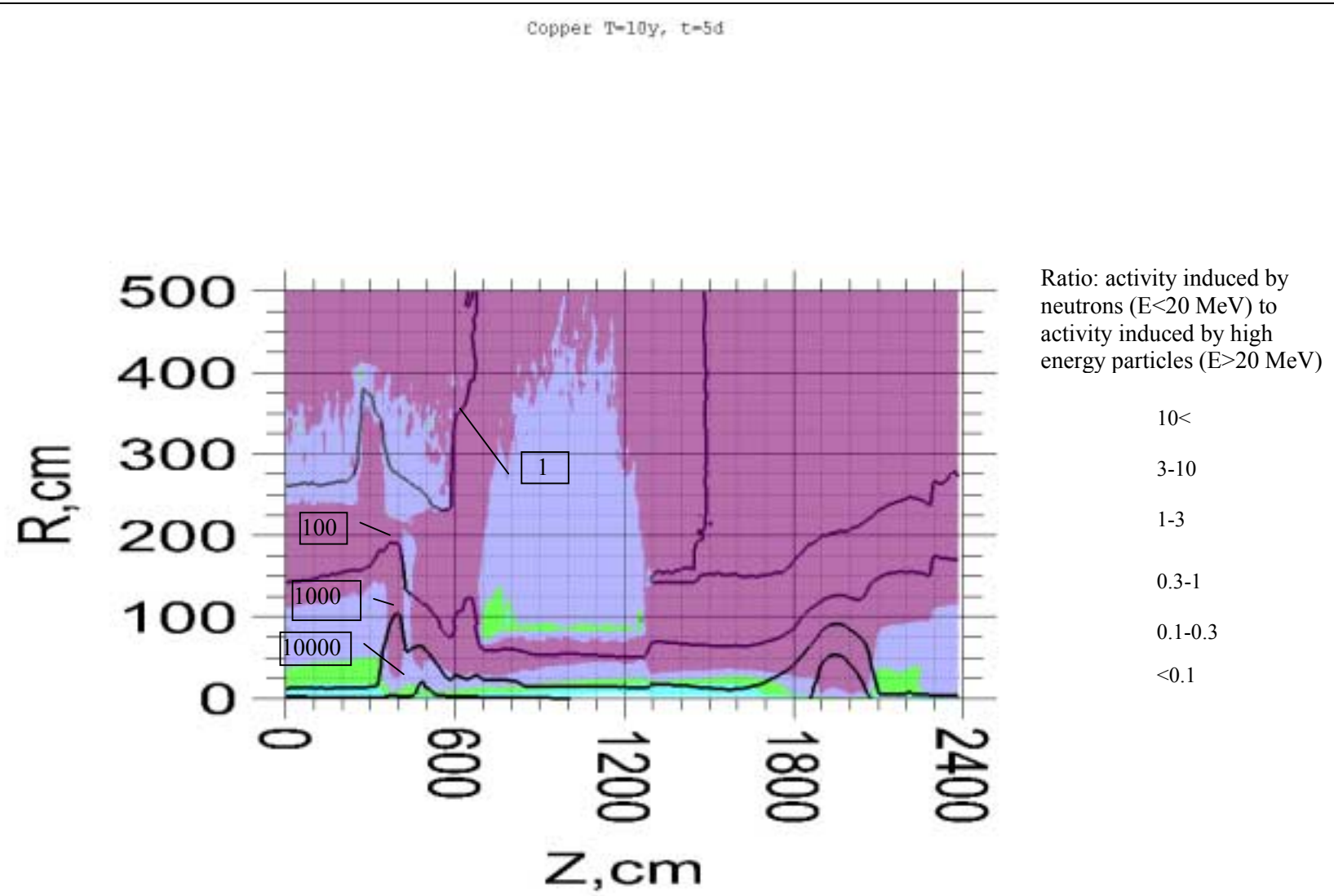

Fig .69. Distribution of induced radioactivity in Copper calculated at T=10y, t=5d. The levels show contact dose rate in μSv/h.

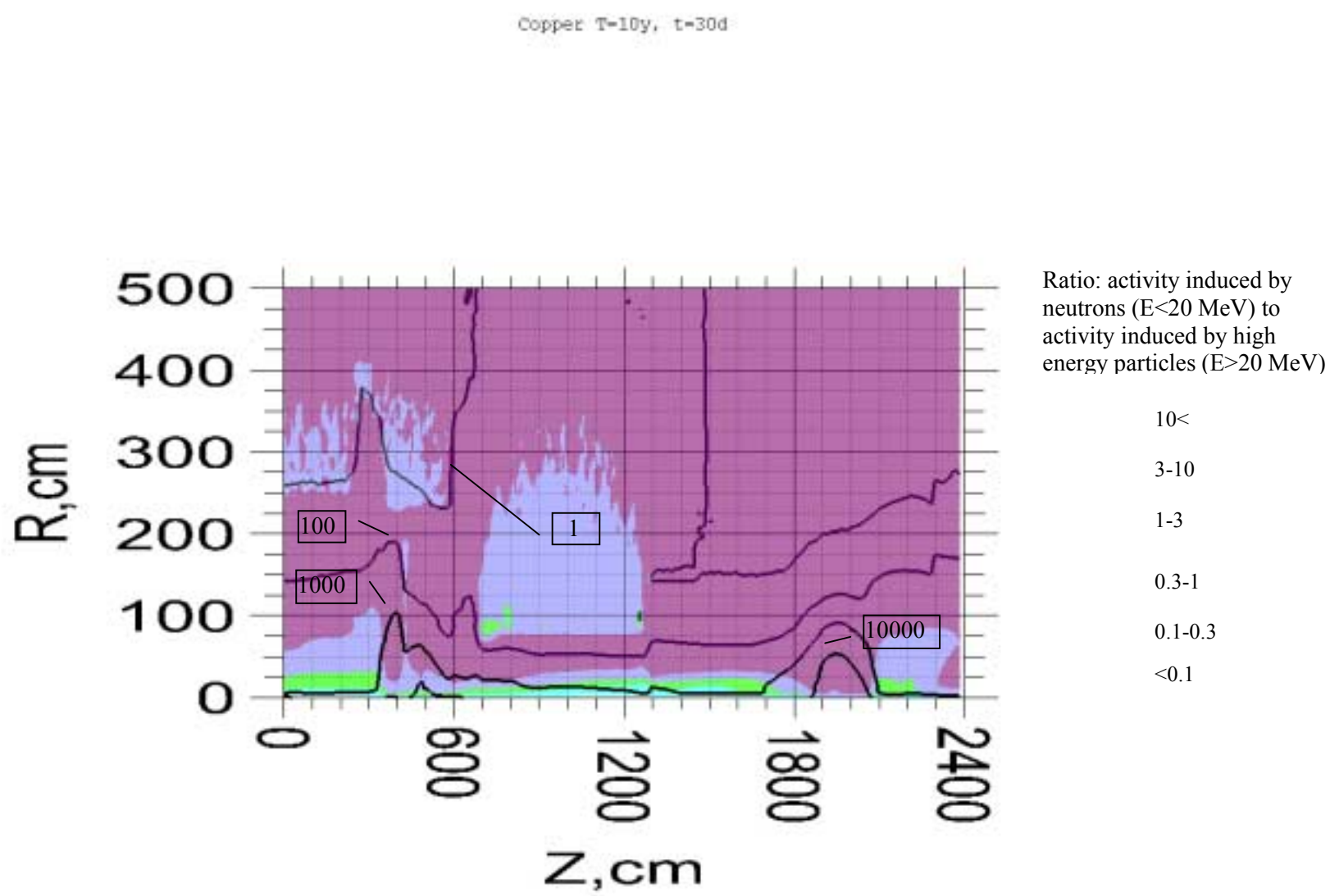

Fig .70. Distribution of induced radioactivity in Copper calculated at T=10y, t=30d. The levels show contact dose rate in μSv/h.

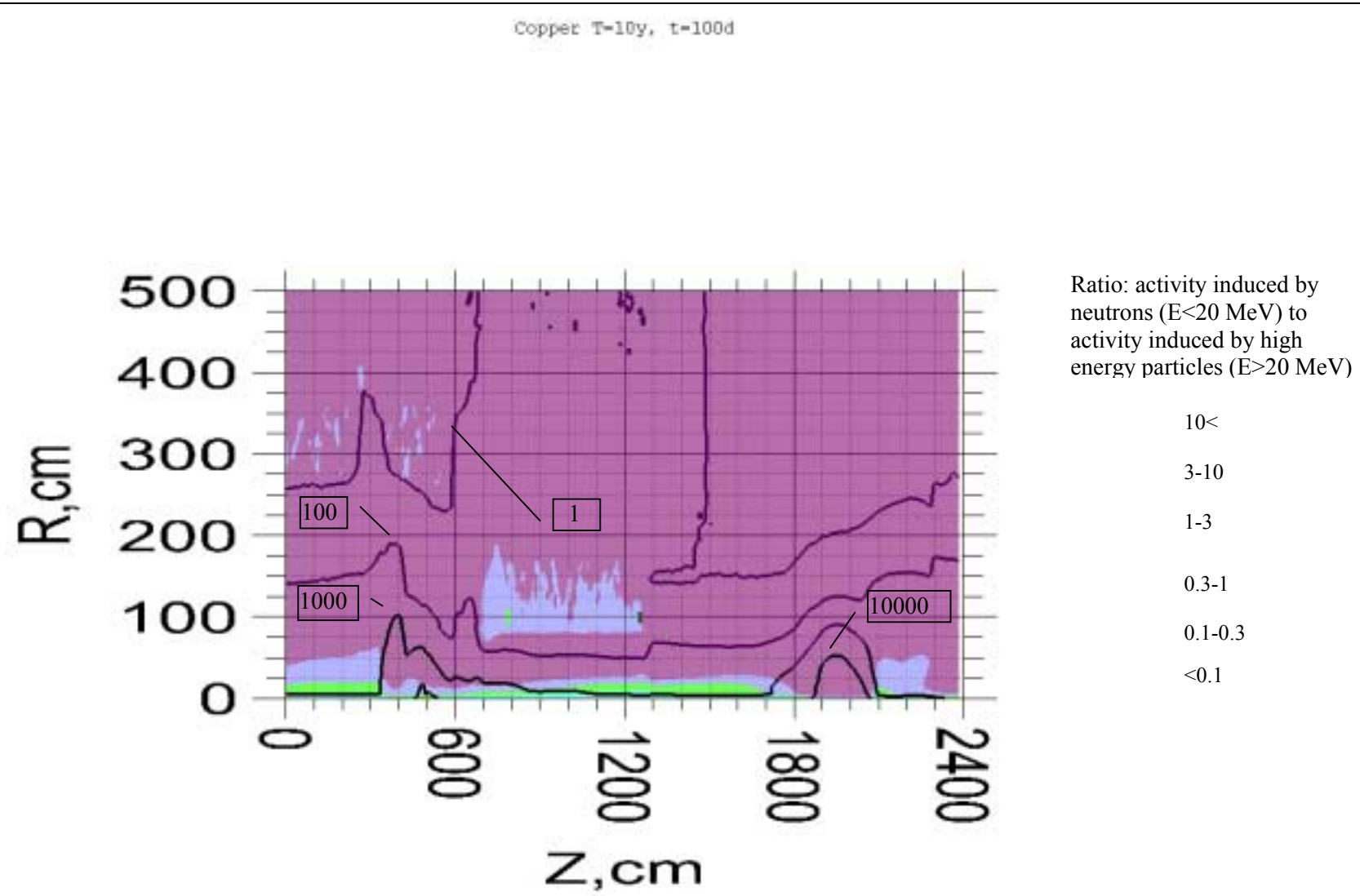

Fig .71. Distribution of induced radioactivity in Copper calculated at T=10y, t=100d. The levels show contact dose rate in μSv/h.

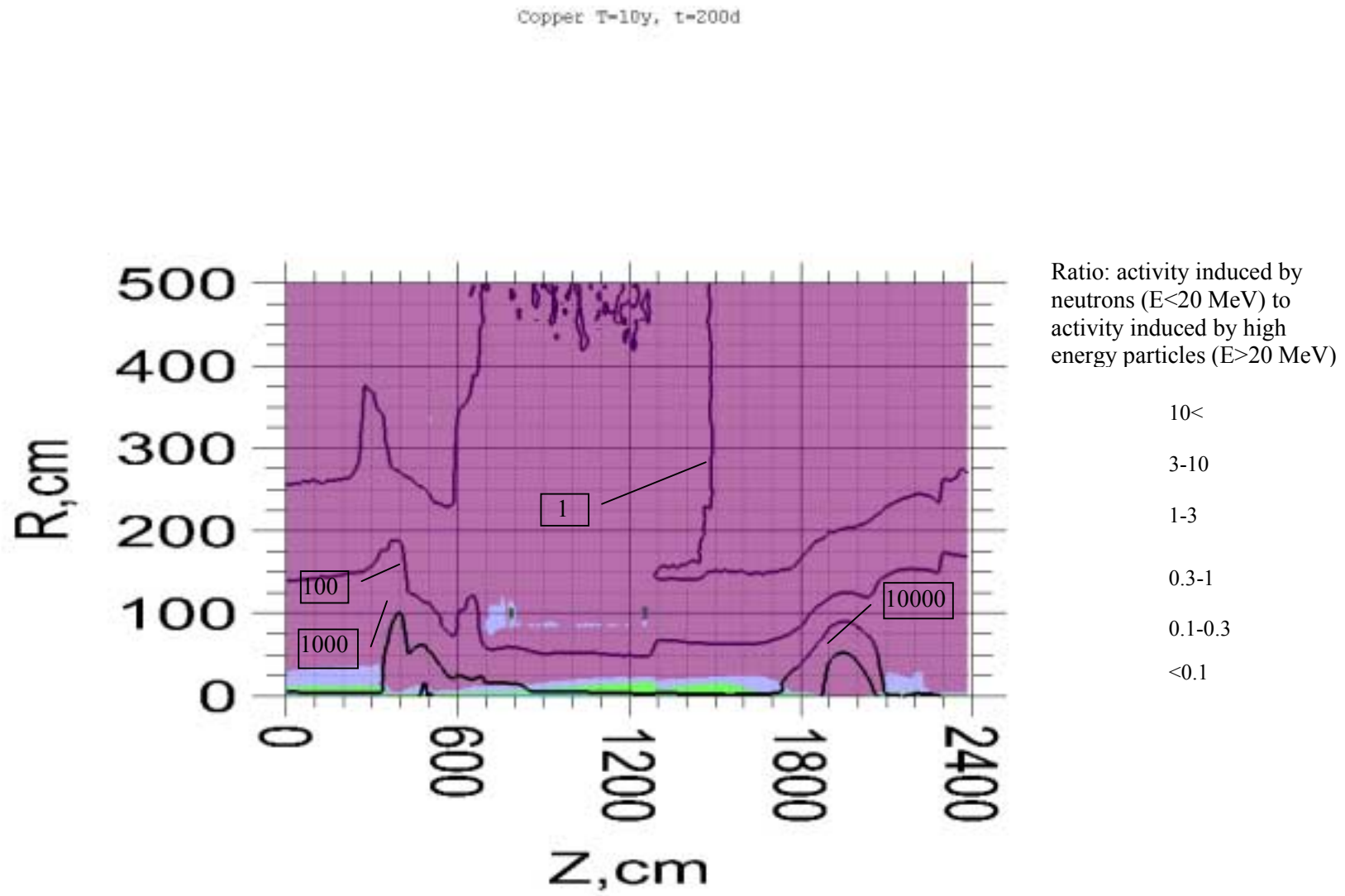

Fig .72. Distribution of induced radioactivity in Copper calculated at T=10y, t=200d. The levels show contact dose rate in μSv/h.

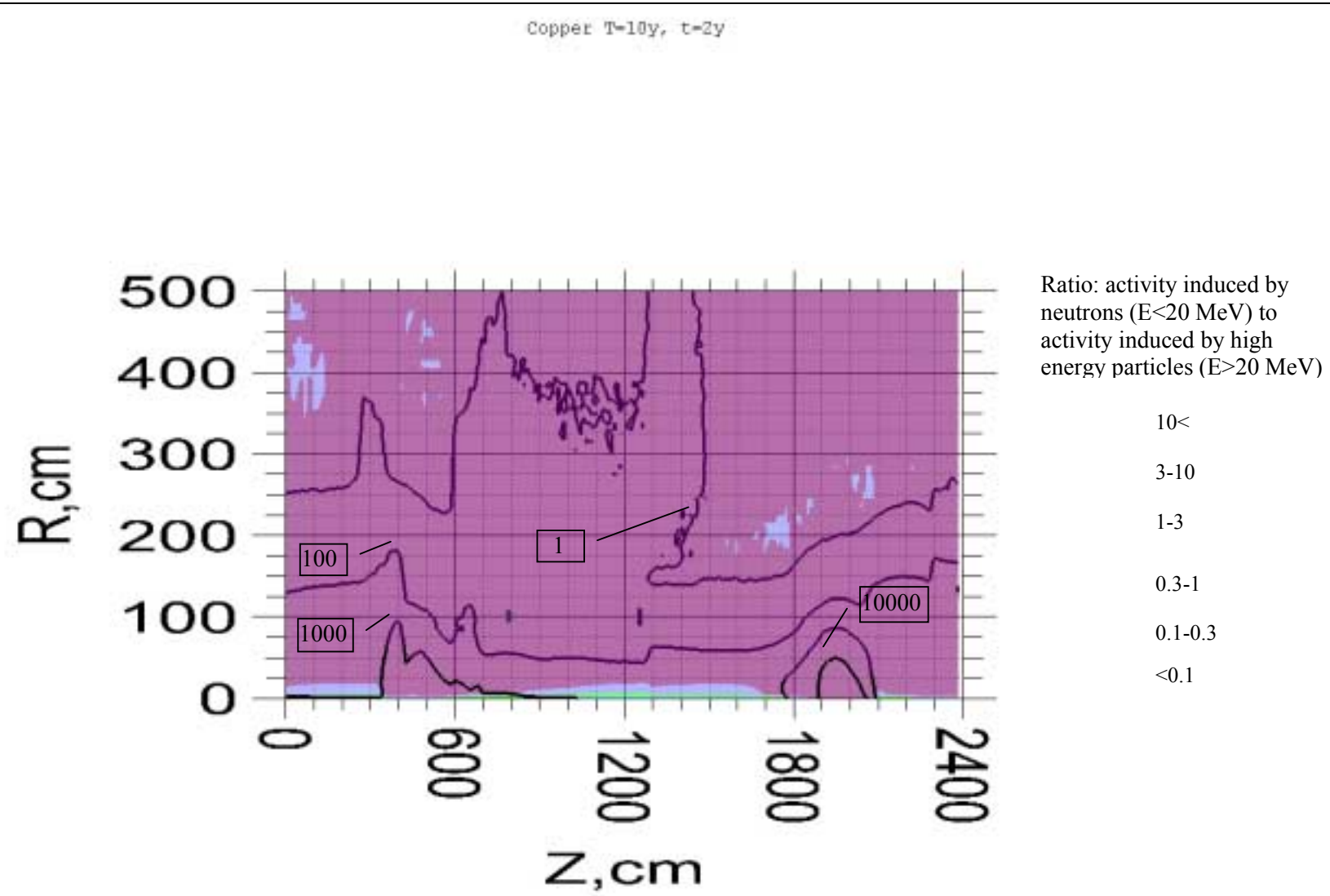

Fig .73. Distribution of induced radioactivity in Copper calculated at T=10y, t=2y. The levels show contact dose rate in μSv/h.

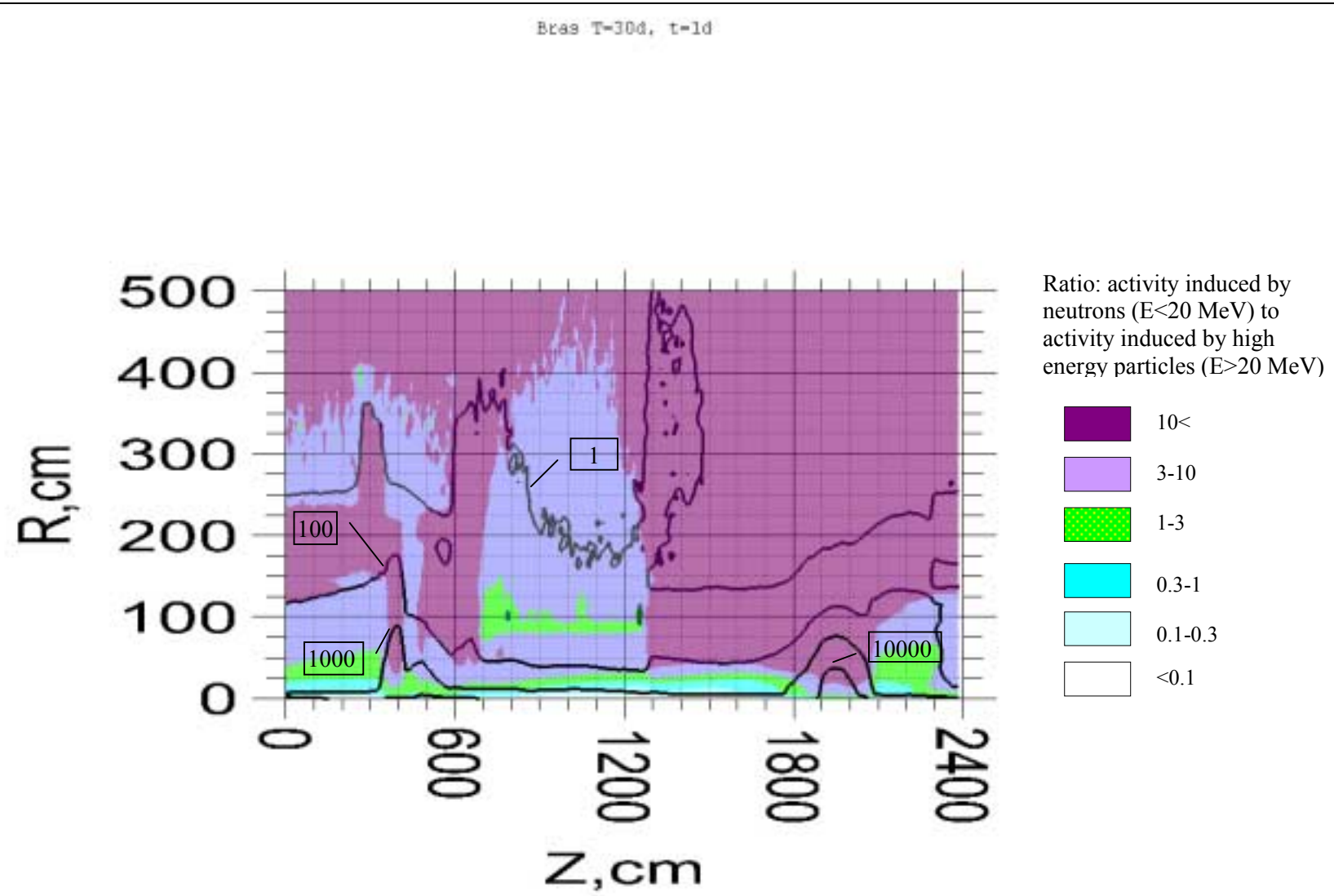

Fig .74. Distribution of induced radioactivity in Brass calculated at T=30d, t=1d. The levels show contact dose rate in μSv/h.

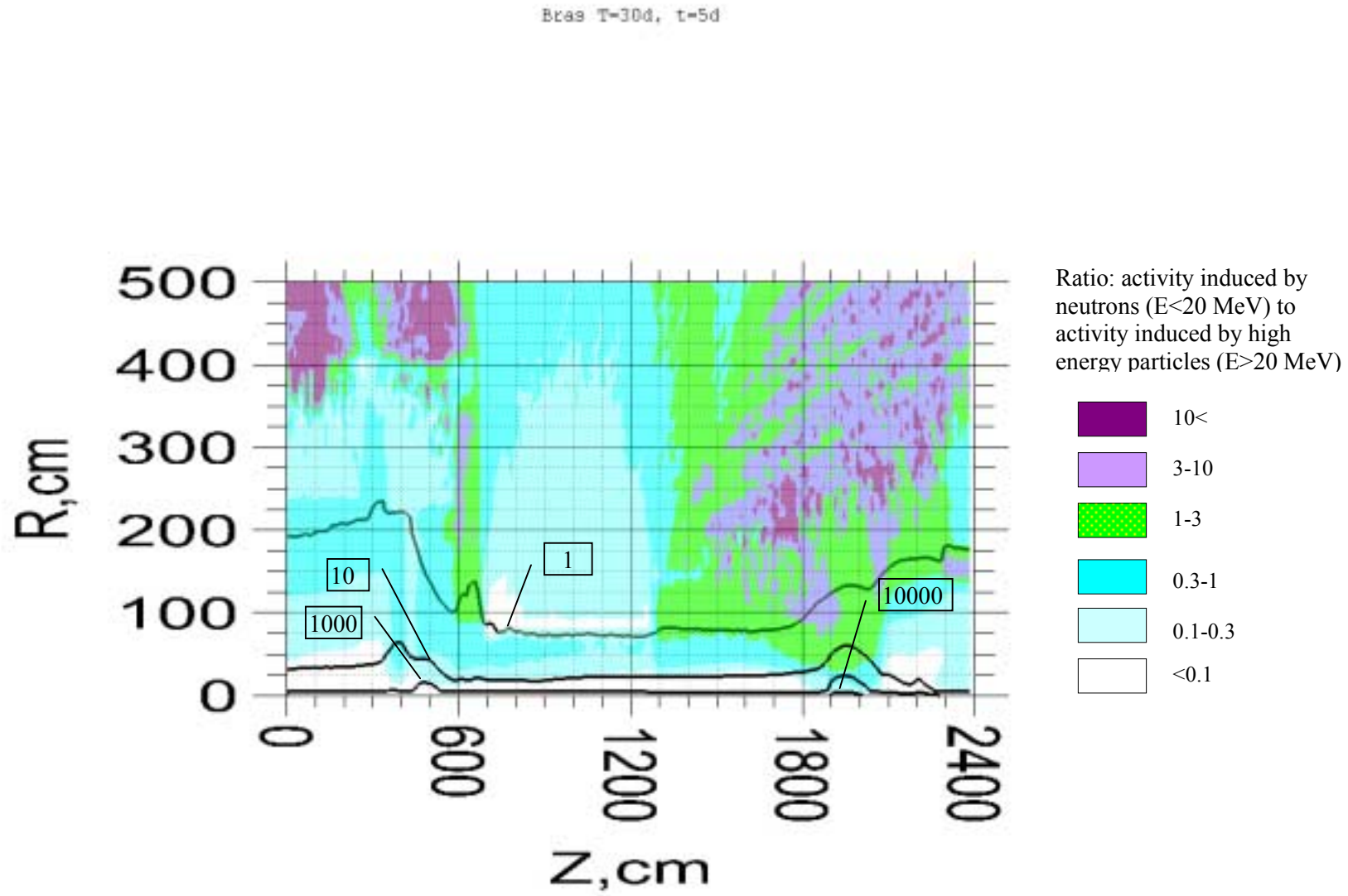

Fig .75. Distribution of induced radioactivity in Brass calculated at T=30d, t=5d. The levels show contact dose rate in μSv/h.

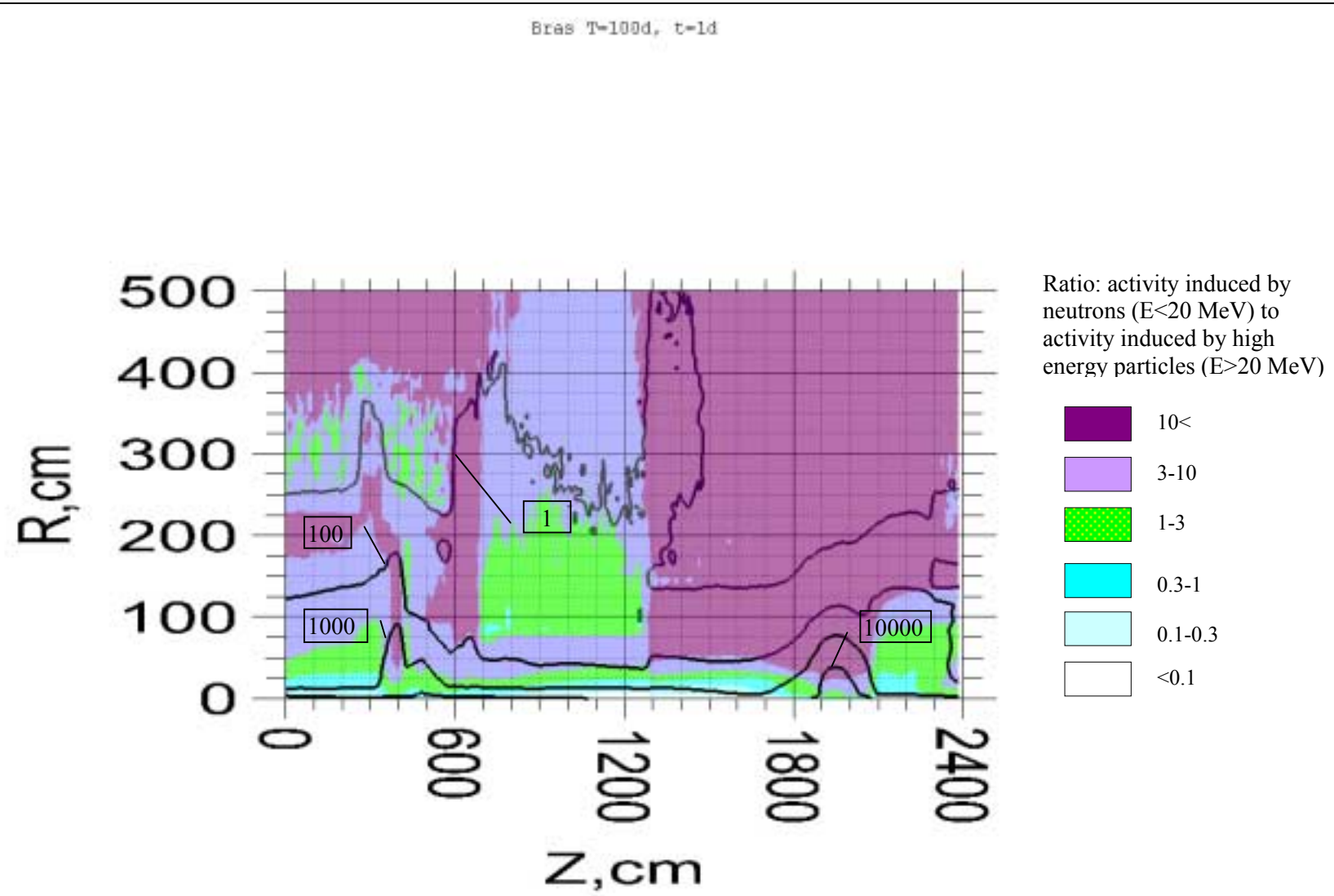

Fig .76. Distribution of induced radioactivity in Brass calculated at T=100d, t=1d. The levels show contact dose rate in μSv/h.

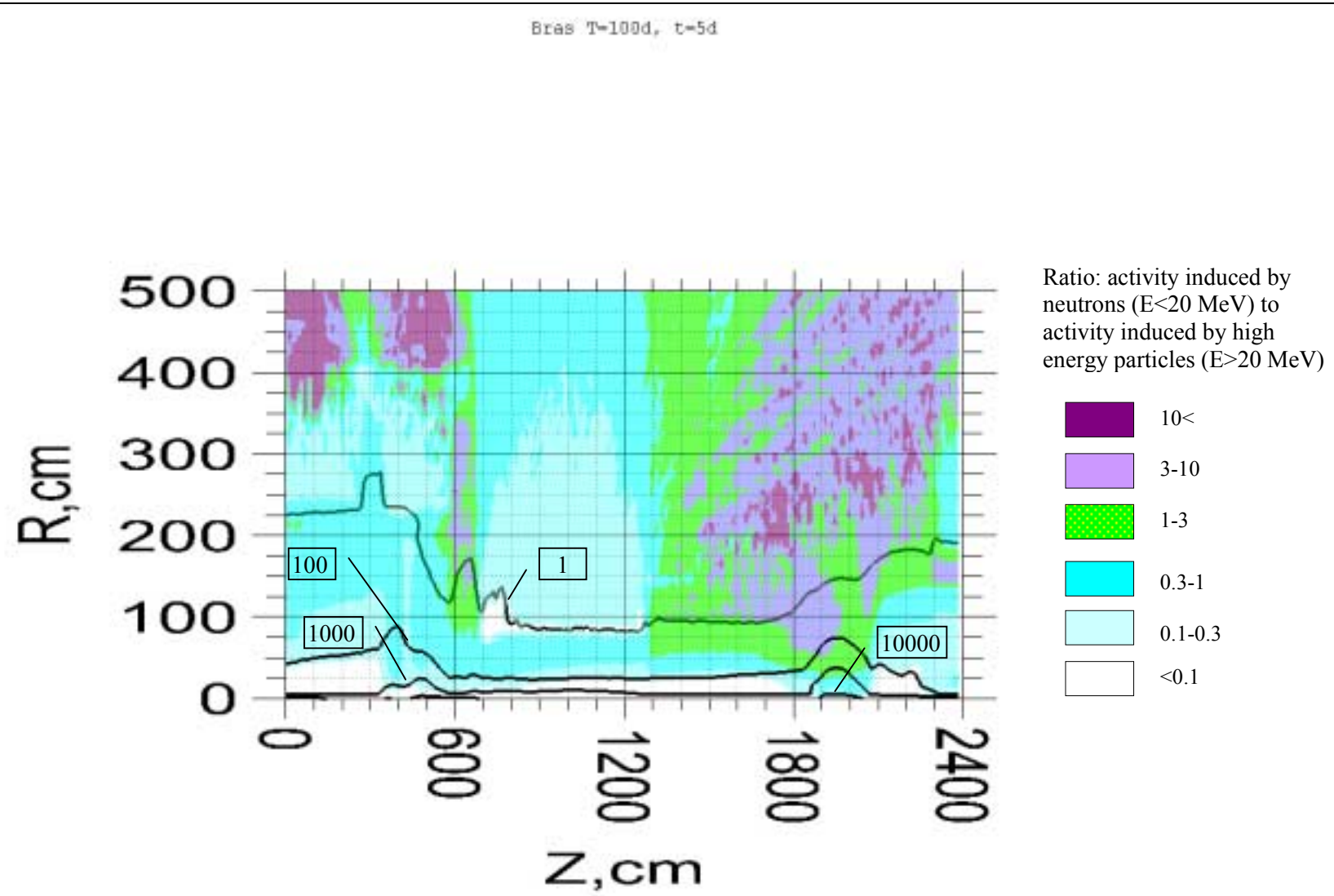

Fig .77. Distribution of induced radioactivity in Brass calculated at T=100d, t=5d. The levels show contact dose rate in μSv/h.

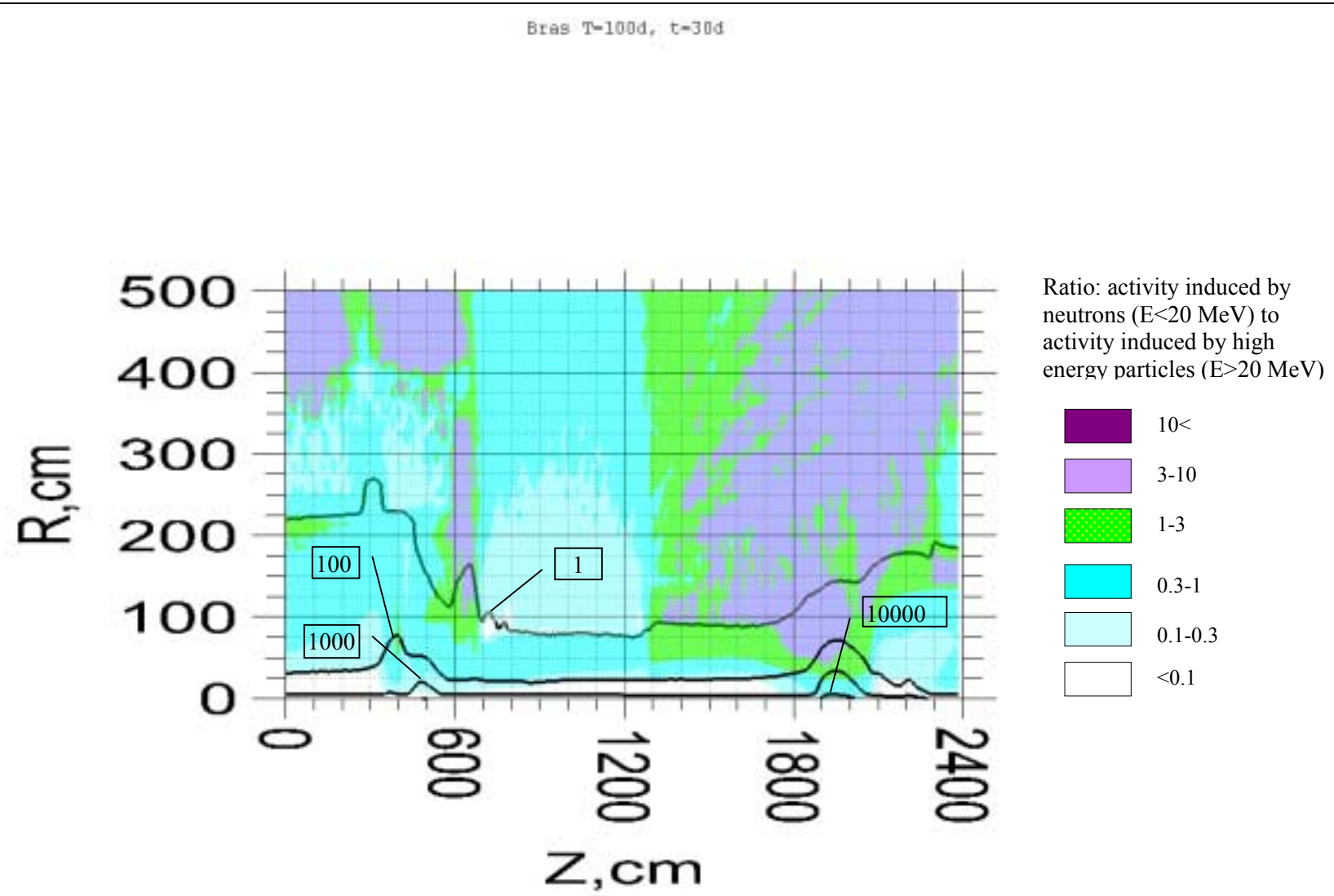

Fig .78. Distribution of induced radioactivity in Brass calculated at T=100d, t=30d. The levels show contact dose rate in μSv/h.

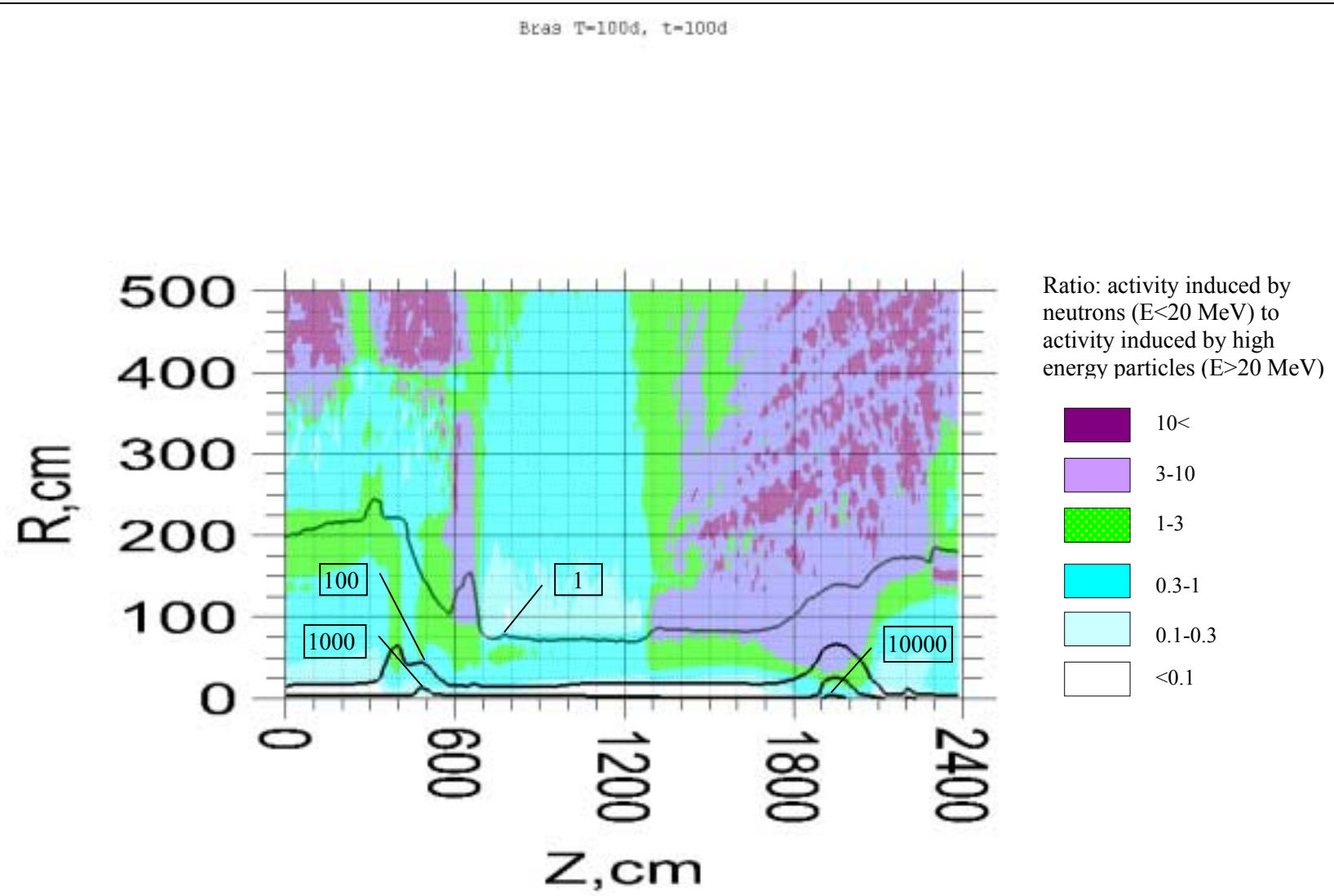

Fig .79. Distribution of induced radioactivity in Brass calculated at T=100d, t=100d. The levels show contact dose rate in μSv/h.

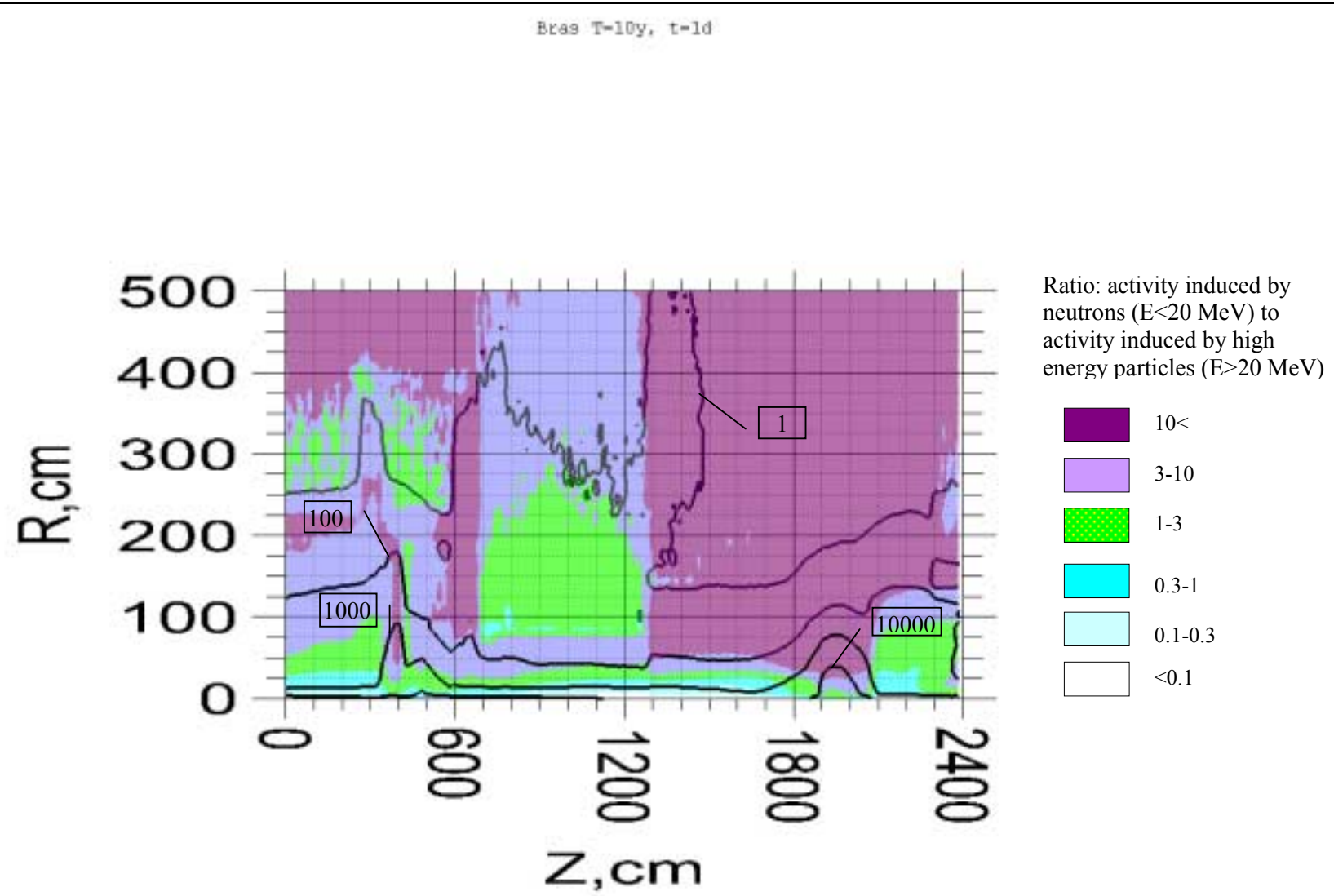

Fig .80. Distribution of induced radioactivity in Brass calculated at T=10y, t=1d. The levels show contact dose rate in μSv/h.

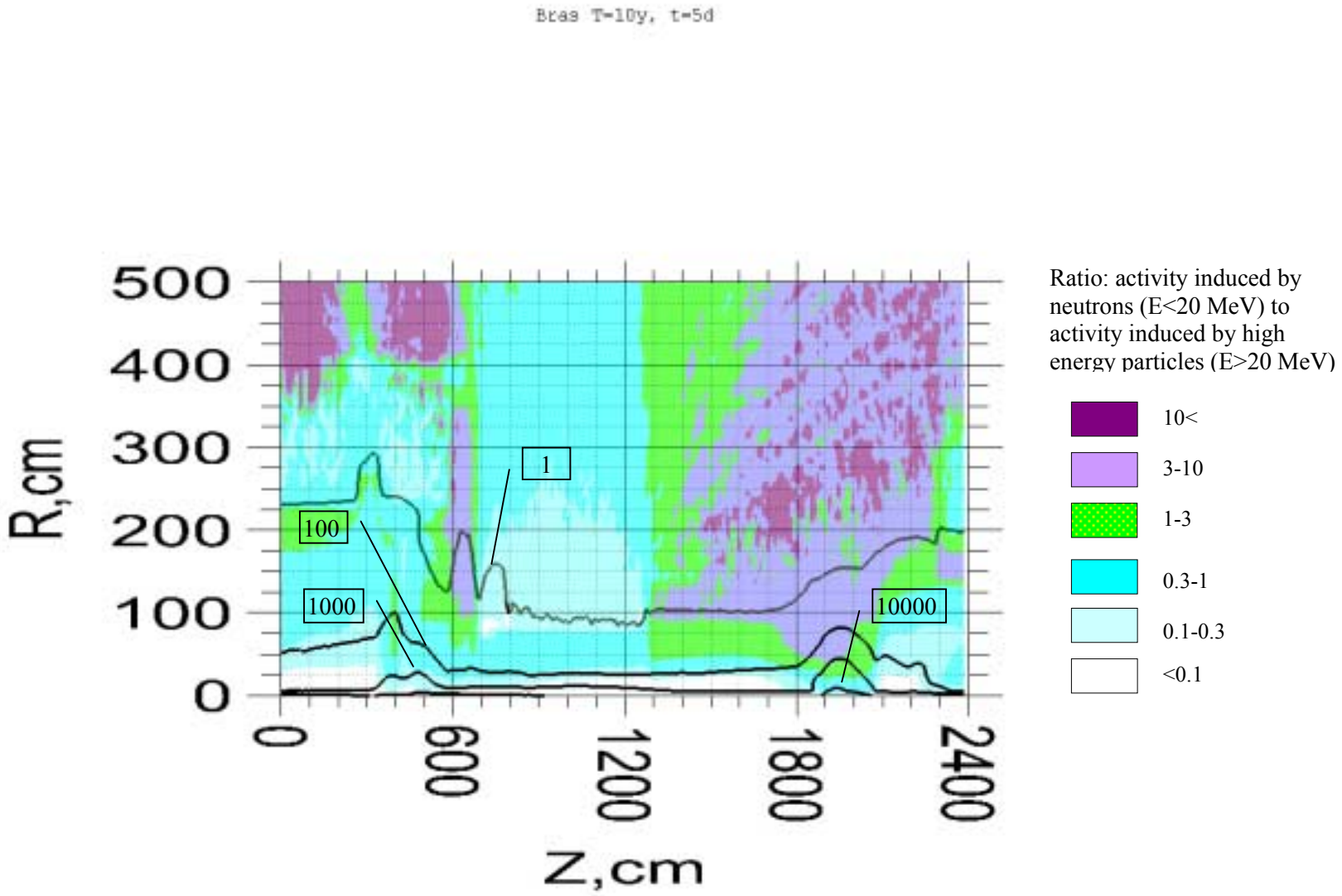

Fig .81. Distribution of induced radioactivity in Brass calculated at Bras T=10y, t=5d. The levels show contact dose rate in μSv/h.

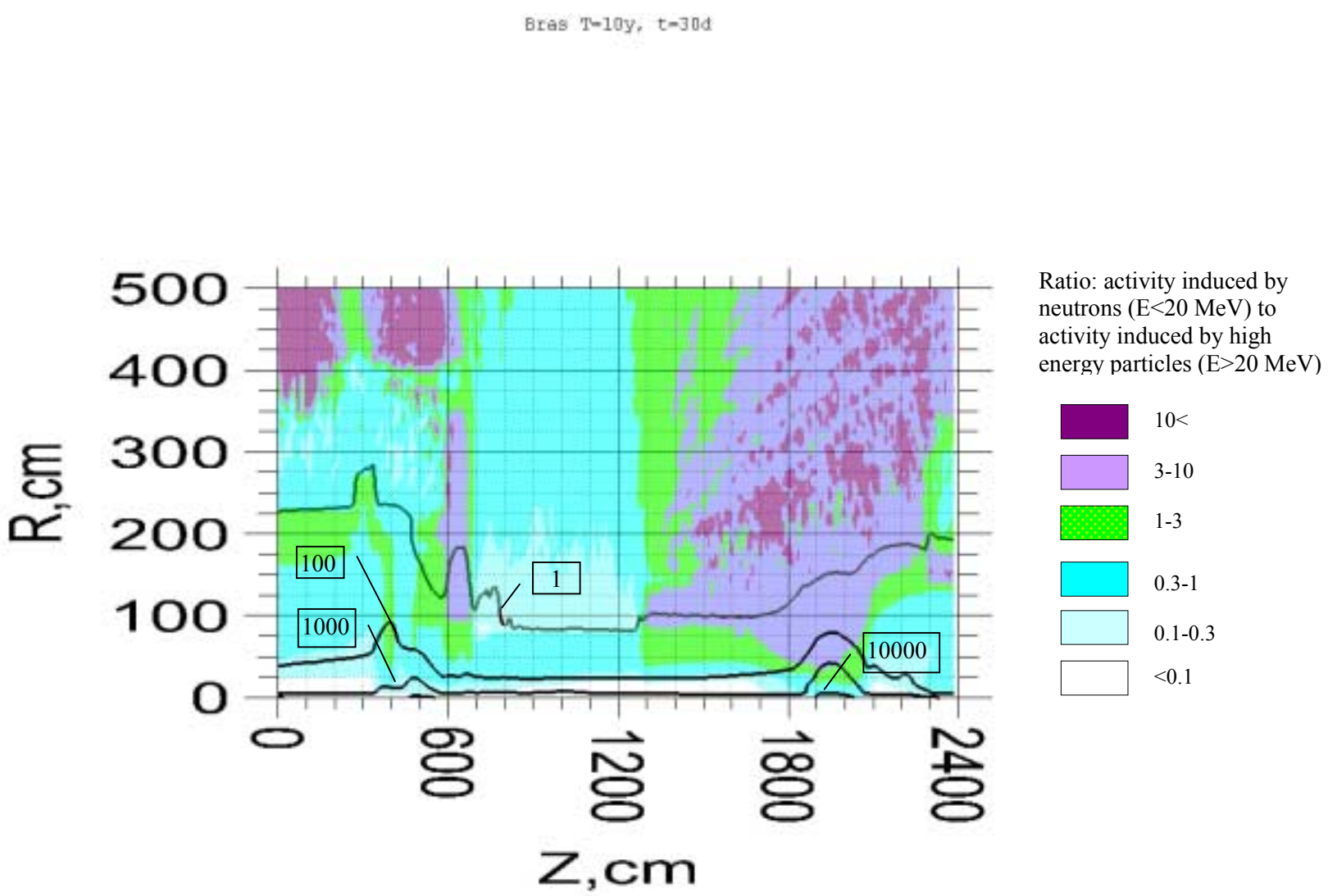

Fig .82. Distribution of induced radioactivity in Brass calculated at T=10y, t=30d. The levels show contact dose rate in μSv/h.

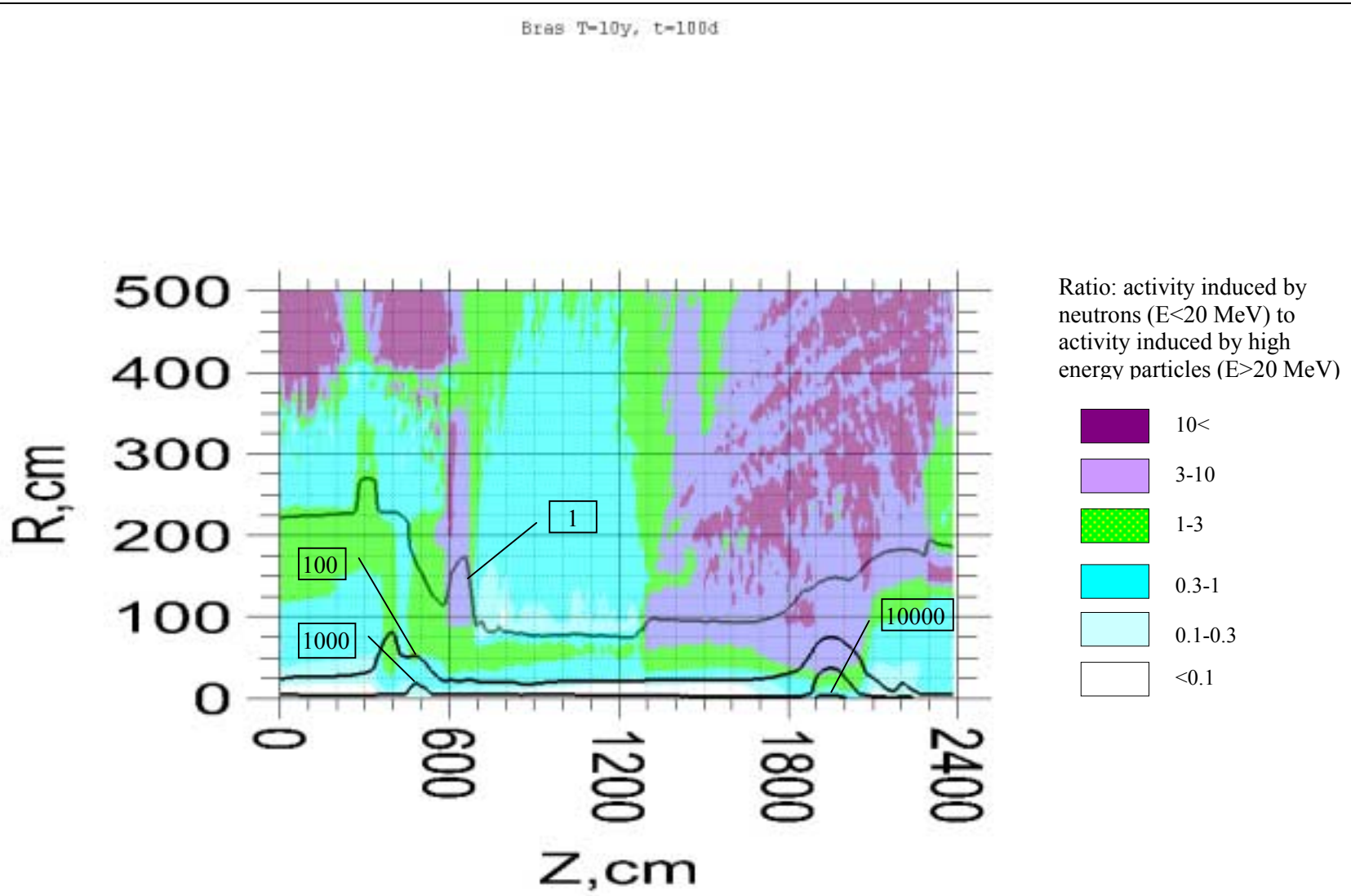

Fig .83. Distribution of induced radioactivity in Brass calculated at T=10y, t=100d. The levels show contact dose rate in μSv/h.

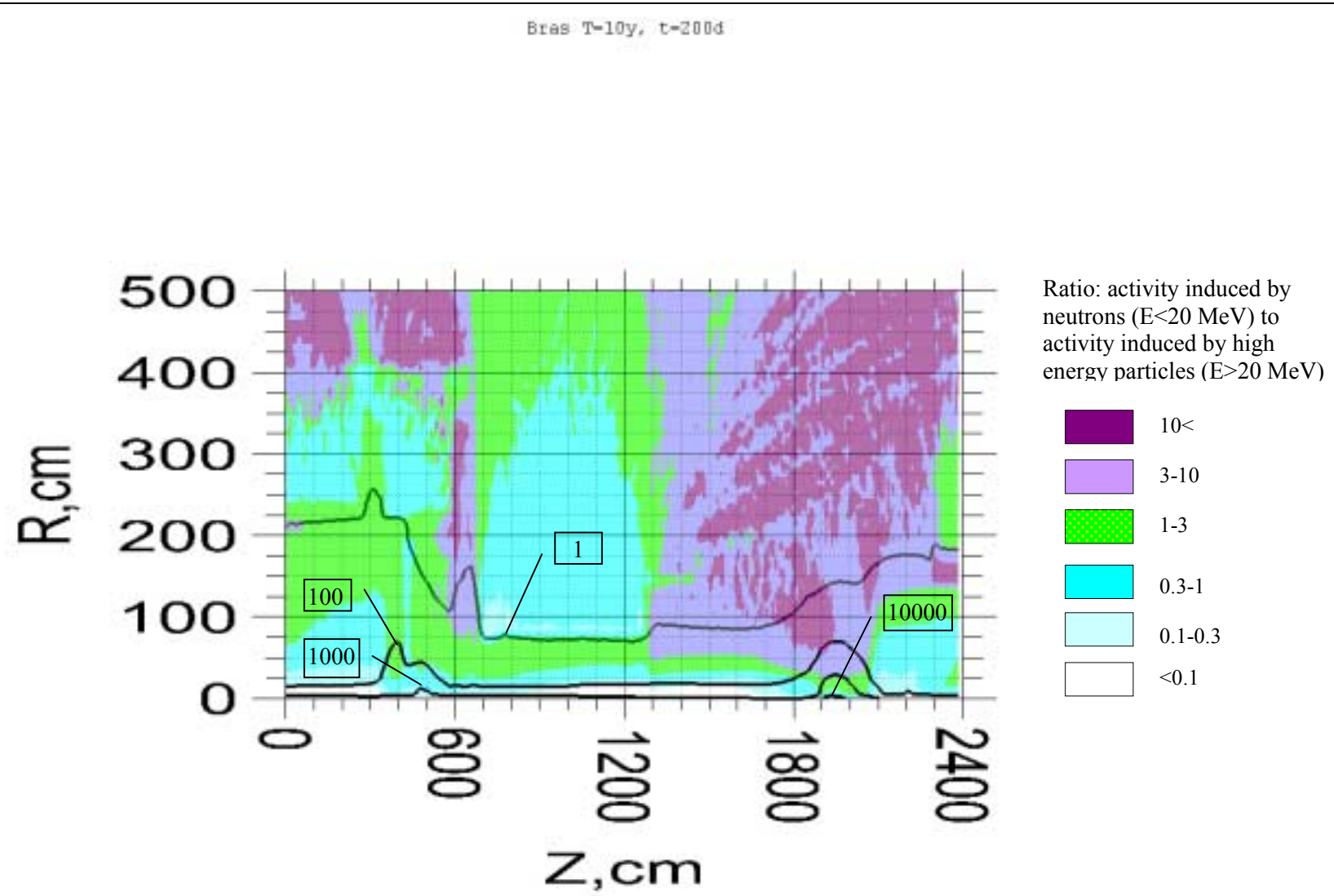

Fig .84. Distribution of induced radioactivity in Brass calculated at T=10y, t=200d. The levels show contact dose rate in μSv/h.

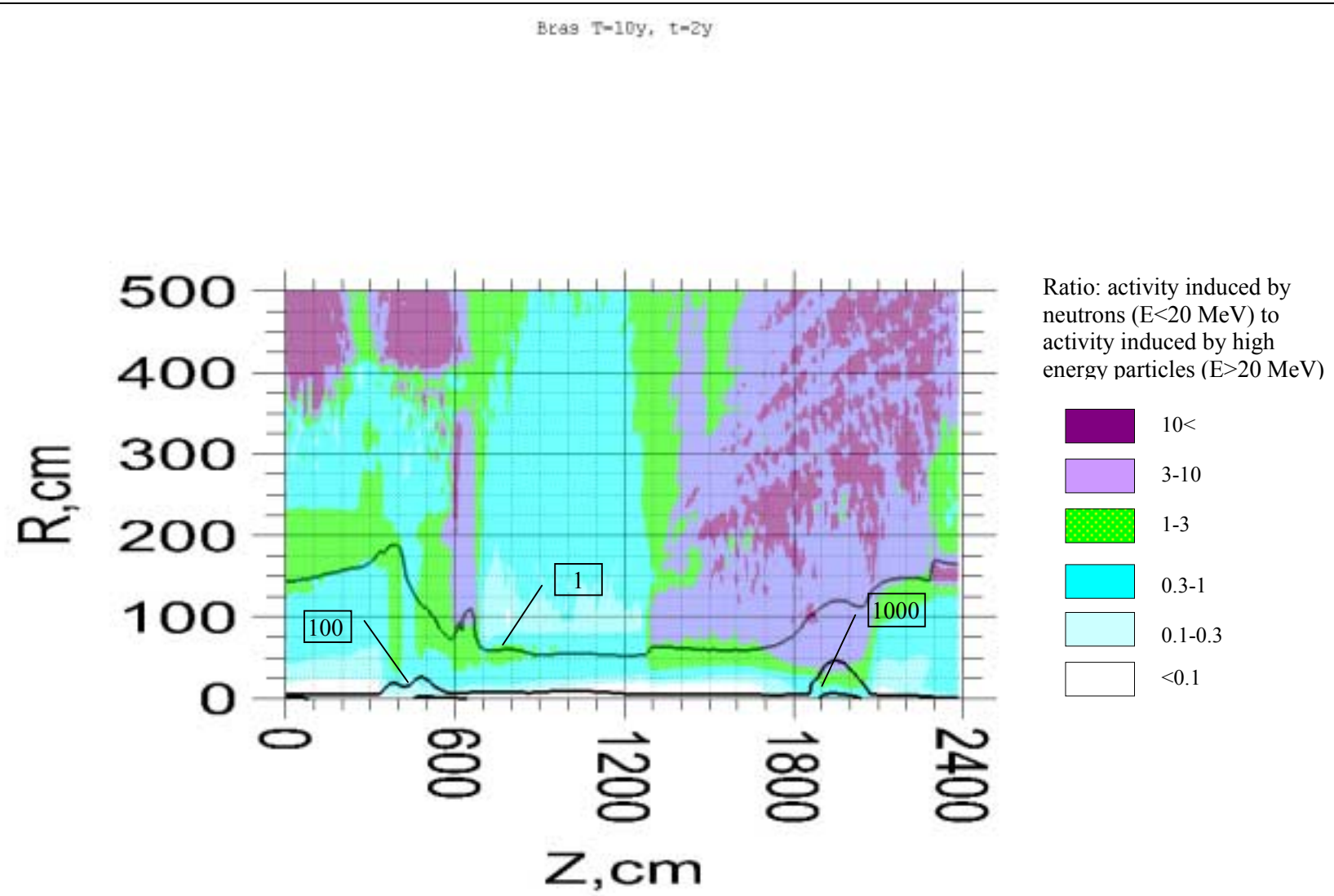

Fig .85. Distribution of induced radioactivity in Brass calculated at T=10y, t=2y. The levels show contact dose rate in μSv/h.

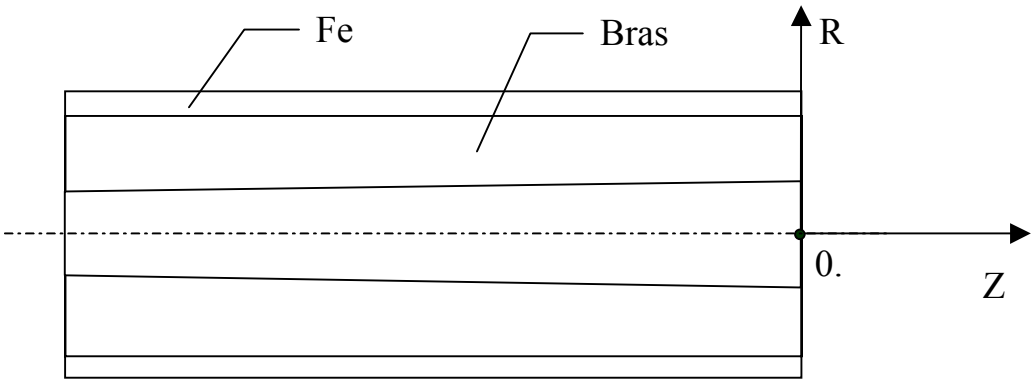

Table 2

Doze rate field in the copper plug region due to radioactivity induced by high energy hadrons, μSv/h

T=30d, t=1 d

Z, cm

R,cm	-(20 –10)	-(10 -0)	0.	0-10	10-20	20-30	30-40	40-50	50-60	60-70	70-80	80-90	90-100
5-10	1467.	1361.	980.	871.	478.	299.	206.	148.	107.	79.	57.	41.	30.
10-20			1154.	832.	365.	239.	156.	106.	82.	67.	56.	45.	35.
20-30			286.	271.	216.	162.	141.	107.	78.	61.	50.	43.	38.
30-40			201.	150.	119.	86.	78.	73.	60.	51.	47.	43.	40.
40-50			82.	74.	87.	56.	61.	56.	46.	33.	25.	25.	28.
50-60			59.	56.	71.	46.	36.	51.	48.	40.	27.	17.	13.
70-80			50.	47.	55.	50.	25.	29.	43.	41.	35.	24.	16.
80-90			44.	41.	44.	49.	27.	19.	25.	37.	36.	30.	21.

T = 30 d, t = 5 d

Z, cm

R,cm	-(20 –10)	-(10 -0)	0.	0-10	10-20	20-30	30-40	40-50	50-60	60-70	70-80	80-90	90-100
5-10	943.	871.	629.	557.	306.	191.	132.	94.	69.	51.	36.	26.	19.
10-20			730.	529.	233.	153.	100.	68.	53.	43.	36.	29.	22.
20-30			187.	174.	138.	104.	90.	68.	50.	39.	32.	28.	24.
30-40			126.	94.	76.	55.	50.	46.	39.	33.	30.	28.	25.
40-50			51.	46.	55.	35.	39.	36.	30.	21.	16.	16.	18.
50-60			37.	35.	45.	29.	23.	32.	31.	25.	17.	11.	8.
70-80			31.	29.	34.	31.	15.	19.	27.	26.	22.	15.	10.
80-90			27.	25.	27.	31.	17.	12.	16.	24.	23.	19.	14.

T=100d, t=1 d

Z, cm

R,cm	-(20 –10)	-(10 -0)	0.	0-10	10-20	20-30	30-40	40-50	50-60	60-70	70-80	80-90	90-100
5-10	1772.	1650.	1206.	1062	579.	363.	246.	178.	131.	96.	69.	49.	35.
10-20			1408.	1012	442.	288.	189.	128.	98.	80.	66.	53.	41.
20-30			360.	335.	259.	194.	169.	127.	92.	73.	60.	52.	45.
30-40			201.	158.	140.	103.	94.	88.	73.	61.	56.	52.	48.
40-50			80.	74.	98.	63.	71.	66.	55.	39.	30.	30.	33.
50-60			57.	54.	78.	50.	40.	58.	55.	45.	30.	19.	15.
70-80			47.	44.	58.	54.	25.	32.	49.	47.	39.	27.	17.
80-90			42.	39.	45.	53.	28.	19.	28.	42.	41.	34.	23.

T = 100 d, t = 5 d

Z, cm

R,cm	-(20 –10)	-(10 -0)	0.	0-10	10-20	20-30	30-40	40-50	50-60	60-70	70-80	80-90	90-100
5-10	1698.	1576.	1123.	1006	551.	346.	233.	169.	125.	92.	66.	47.	33.
10-20			1316.	958.	421.	274.	180.	122.	93.	75.	62.	50.	38.
20-30			349.	320.	245.	184.	159.	120.	87.	69.	57.	49.	43.
30-40			174.	141.	131.	97.	90.	83.	69.	58.	53.	49.	45.
40-50			68.	64.	90.	57.	66.	62.	52.	37.	29.	29.	32.
50-60			48.	46.	70.	45.	36.	54.	51.	42.	28.	17.	14.
70-80			40.	38.	52.	49.	22.	29.	46.	44.	36.	24.	15.
80-90			36.	33.	39.	48.	24.	16.	25.	39.	38.	31.	21.

T = 5 y, t = 1 d

Z, cm

R,cm	-(20 –10)	-(10 -0)	0.	0-10	10-20	20-30	30-40	40-50	50-60	60-70	70-80	80-90	90-100
5-10	3113.	2887.	2060.	1840.	1009.	630.	425.	307.	227.	167.	119.	85.	61.
10-20			2415.	1746.	764.	500.	328.	221.	170.	138.	115.	91.	70.
20-30			632.	580.	445.	336.	290.	220.	160.	126.	104.	90.	78.
30-40			340.	267.	239.	176.	163.	152.	125.	106.	97.	90.	83.
40-50			131.	122.	166.	106.	121.	114.	95.	68.	52.	52.	57.
50-60			93.	88.	130.	83.	67.	99.	94.	78.	52.	32.	26.
70-80			78.	73.	97.	90.	42.	54.	84.	80.	67.	45.	28.
80-90			69.	63.	74.	89.	46.	31.	46.	72.	70.	58.	39.

T = 5 y, t = 5 d

Z, cm

R,cm	-(20 –10)	-(10 -0)	0.	0-10	10-20	20-30	30-40	40-50	50-60	60-70	70-80	80-90	90-100
5-10	2420.	2257.	1617.	1441.	782.	490.	329.	238.	177.	131.	93.	66.	47.
10-20			1882.	1358.	595.	388.	255.	172.	131.	106.	88.	70.	54.
20-30			505.	455.	345.	260.	225.	169.	123.	97.	81.	70.	61.
30-40			242.	196.	184.	136.	127.	118.	97.	82.	75.	70.	65.
40-50			92.	87.	125.	79.	92.	88.	74.	53.	41.	41.	45.
50-60			65.	62.	97.	62.	50.	75.	72.	59.	39.	24.	20.
70-80			54.	51.	71.	67.	30.	41.	64.	61.	51.	34.	21.
80-90			48.	44.	53.	67.	33.	22.	35.	55.	53.	44.	29.

T = 10 y, t = 1 d

Z, cm

R,cm	-(20 –10)	-(10 -0)	0.	0-10	10-20	20-30	30-40	40-50	50-60	60-70	70-80	80-90	90-100
5-10	3158.	2927.	2120.	1869.	1018.	639.	430.	312.	230.	170.	122.	86.	62.
10-20			2447.	1766.	776.	507.	333.	224.	172.	140.	116.	93.	71.
20-30			641.	587.	451.	340.	295.	222.	162.	128.	106.	92.	80.
30-40			342.	269.	242.	178.	166.	154.	127.	107.	98.	91.	84.
40-50			131.	122.	167.	106.	122.	115.	96.	69.	53.	53.	58.
50-60			93.	88.	131.	84.	68.	100.	95.	79.	52.	33.	26.
70-80			78.	73.	97.	91.	42.	55.	85.	82.	68.	45.	28.
80-90			69.	63.	74.	90.	46.	31.	47.	73.	71.	59.	40.

T = 10 y, t = 5 d

Z, cm

R,cm	-(20 -10)	-(10 -0)	0.	0-10	10-20	20-30	30-40	40-50	50-60	60-70	70-80	80-90	90-100
5-10	2505.	2320.	1658.	1477.	805.	506.	339.	246.	183.	135.	96.	68.	48.
10-20			1924.	1401.	615.	401.	264.	177.	135.	110.	90.	73.	56.
20-30			518.	469.	355.	267.	232.	174.	127.	100.	83.	72.	63.
30-40			244.	199.	189.	140.	132.	122.	100.	84.	77.	72.	66.
40-50			92.	87.	128.	81.	94.	90.	76.	54.	42.	42.	46.
50-60			65.	62.	99.	63.	51.	77.	74.	61.	40.	25.	20.
70-80			54.	51.	73.	68.	30.	41.	65.	63.	52.	34.	21.
80-90			48.	44.	54.	68.	33.	22.	36.	56.	54.	45.	30.

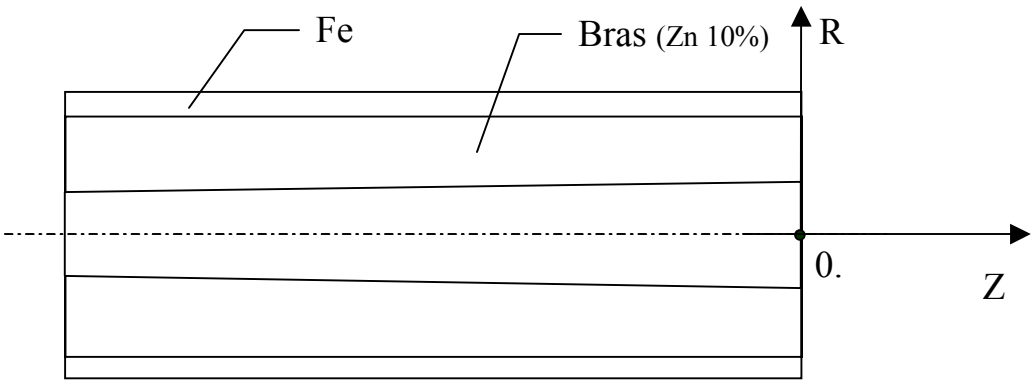

Table 3

Doze rate field in the copper plug region due to radioactivity induced by low energy neutrons, μSv/h

T=30d, t=1 d

Z, cm

R,cm	-(20 –10)	-(10 -0)	0.	0-10	10-20	20-30	30-40	40-50	50-60	60-70	70-80	80-90	90-100
5-10	763	688	489	445	260	190	125	82	69	62	55	46	36
10-20			553	433	233	154	119	88	62	47	37	29	24
20-30			541	360	172	112	88	68	50	37	30	26	23
30-40			136	113	97	72	63	55	46	37	29	26	23
40-50			9	18	49	37	36	39	38	33	27	22	20
50-60			7	8	30	25	21	24	24	22	20	17	15
70-80			5	4	20	19	12	17	20	19	16	12	9
80-90			5	3	12	20	7	8	14	17	17	14	10

T = 30 d, t = 5 d

Z, cm

R,cm	-(20 –10)	-(10 -0)	0.	0-10	10-20	20-30	30-40	40-50	50-60	60-70	70-80	80-90	90-100
5-10	43	39	28	25	15	11	7	5	4	4	3	3	2
10-20			31	25	14	9	7	5	4	3	2	2	1
20-30			30	21	10	7	5	4	3	2	2	2	1
30-40			10	8	6	4	4	3	3	2	2	2	1
40-50			2	2	3	3	2	2	2	2	2	1	1
50-60			2	1	2	2	2	2	2	1	1	1	1
70-80			1	1	2	2	1	1	1	1	1	1	1
80-90			1	1	1	2	1	1	1	1	1	1	1

T=100d, t=1 d

Z, cm

R,cm	-(20 –10)	-(10 -0)	0.	0-10	10-20	20-30	30-40	40-50	50-60	60-70	70-80	80-90	90-100
5-10	821	739	528	479	280	204	134	88	74	67	59	50	39
10-20			594	465	252	166	128	95	67	51	40	32	26
20-30			580	387	186	121	95	74	55	40	32	28	25
30-40			150	124	105	77	68	60	50	40	32	28	25
40-50			12	21	54	41	40	42	41	36	30	24	22
50-60			9	10	33	28	23	26	26	24	21	19	16
70-80			7	6	23	21	13	18	22	21	18	14	10
80-90			6	5	14	22	8	9	16	19	18	15	11

T = 100 d, t = 5 d

Z, cm

R,cm	-(20 –10)	-(10 -0)	0.	0-10	10-20	20-30	30-40	40-50	50-60	60-70	70-80	80-90	90-100
5-10	100	89	64	59	35	25	17	11	9	8	8	6	5
10-20			71	57	31	21	16	12	9	7	5	4	3
20-30			69	48	24	16	12	10	7	5	4	4	3
30-40			23	19	14	10	9	8	6	5	4	4	3
40-50			5	5	8	6	6	6	5	5	4	3	3
50-60			4	3	6	4	4	4	4	3	3	3	2
70-80			3	3	4	4	2	3	3	3	3	2	2
80-90			3	2	3	4	2	2	3	3	3	2	2

T = 5 y, t = 1 d

Z, cm

R,cm	-(20 –10)	-(10 -0)	0.	0-10	10-20	20-30	30-40	40-50	50-60	60-70	70-80	80-90	90-100
5-10	864	782	559	506	296	216	143	93	78	71	63	53	42
10-20			627	492	266	176	135	101	71	54	43	34	27
20-30			611	409	196	128	101	78	58	42	34	30	26
30-40			162	133	112	82	72	63	53	42	34	30	27
40-50			15	24	58	44	42	45	43	38	31	25	23
50-60			12	12	36	30	25	28	28	26	23	20	17
70-80			9	8	25	23	15	20	24	22	19	15	11
80-90			8	6	16	24	9	10	17	20	19	16	12

T = 5 y, t = 5 d

Z, cm

R,cm	-(20 –10)	-(10 -0)	0.	0-10	10-20	20-30	30-40	40-50	50-60	60-70	70-80	80-90	90-100
5-10	147	131	94	86	51	37	25	16	14	12	11	9	8
10-20			103	83	46	31	24	18	13	10	8	6	5
20-30			102	70	35	23	18	14	10	8	6	5	5
30-40			36	28	21	15	13	11	9	8	6	5	5
40-50			8	8	12	9	8	8	8	7	6	5	4
50-60			6	6	8	7	5	6	6	5	5	4	3
70-80			5	5	7	6	4	4	5	5	4	3	2
80-90			4	4	5	6	3	3	4	4	4	3	3

T = 10 y, t = 1 d

Z, cm

R,cm	-(20 –10)	-(10 -0)	0.	0-10	10-20	20-30	30-40	40-50	50-60	60-70	70-80	80-90	90-100
5-10	865	782	559	507	297	217	143	94	78	71	63	53	42
10-20			628	492	267	176	136	101	71	54	43	34	27
20-30			611	410	197	128	101	78	58	42	34	30	26
30-40			164	135	113	83	72	64	53	42	34	30	27
40-50			16	25	59	44	43	45	43	38	32	26	23
50-60			13	13	37	31	25	29	28	26	23	20	17
70-80			10	9	26	24	15	20	24	23	19	15	11
80-90			9	7	17	24	9	11	17	21	20	16	12

T = 10 y, t = 5 d

Z, cm

R,cm	-(20 -10)	-(10 -0)	0.	0-10	10-20	20-30	30-40	40-50	50-60	60-70	70-80	80-90	90-100
5-10	148	132	96	87	52	38	26	17	14	12	11	10	8
10-20			104	84	47	31	24	18	13	10	8	6	5
20-30			102	71	36	23	18	14	11	8	6	5	5
30-40			39	30	21	15	13	11	10	8	6	5	5
40-50			9	9	13	9	8	9	8	7	6	5	4
50-60			7	7	9	7	6	6	6	5	5	4	3
70-80			6	5	7	6	4	5	5	5	4	3	3
80-90			5	5	6	6	3	3	4	5	4	4	3

Table 4

Doze rate field in the copper plug region due to radioactivity induced by high energy hadrons, μSv/h

T = 30 d, t = 1 d

Z, cm

R,cm	0-10	10-20	20-30	30-40	40-50	50-60	60-70	70-80	80-90	90-100
5-10	9.8E+2	8.1E+2	3.4E+2	1.6E+2	9.4E+1	7.0E+1	5.7E+1	4.7E+1	4.1E+1	3.5E+1
10-20	5.5E+2	4.4E+2	2.8E+2	1.5E+2	9.7E+1	7.1E+1	5.7E+1	4.6E+1	3.9E+1	3.5E+1
20-30	3.2E+2	2.8E+2	2.0E+2	1.4E+2	9.3E+1	6.9E+1	5.4E+1	4.5E+1	3.8E+1	3.3E+1
30-40	2.0E+2	1.8E+2	1.5E+2	1.1E+2	8.5E+1	6.5E+1	5.1E+1	4.3E+1	3.6E+1	3.2E+1
40-50	1.4E+2	1.2E+2	1.1E+2	9.4E+1	7.2E+1	6.0E+1	4.8E+1	4.0E+1	3.5E+1	2.9E+1
50-60	1.0E+2	9.3E+1	8.4E+1	7.3E+1	6.3E+1	5.2E+1	4.5E+1	3.7E+1	3.2E+1	2.8E+1
70-80	7.8E+1	7.1E+1	6.4E+1	5.9E+1	5.2E+1	4.5E+1	4.0E+1	3.4E+1	3.0E+1	2.6E+1
80-90	6.0E+1	5.5E+1	5.2E+1	4.8E+1	4.3E+1	4.0E+1	3.5E+1	3.2E+1	2.7E+1	2.5E+1

Calculations of activation doses from JF bridge

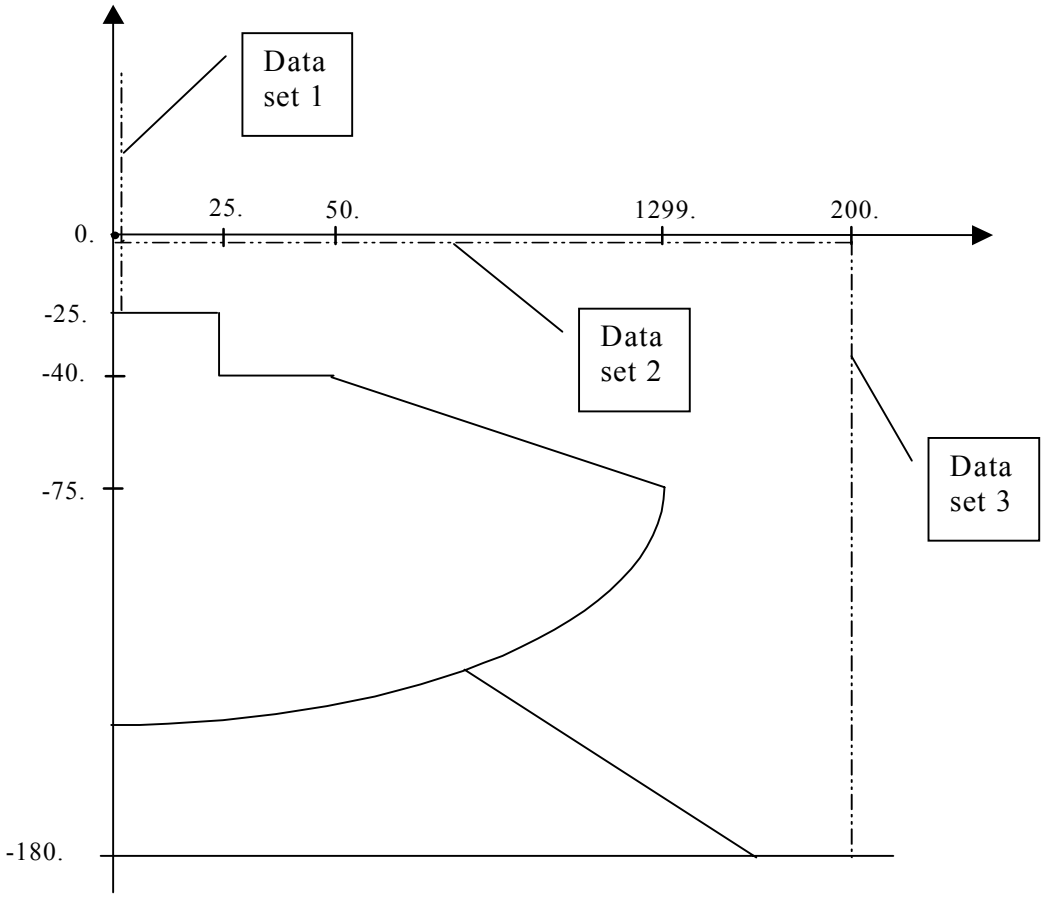

Table 5

Dose due to activity induced by high energy hadrons, μSv/h

T=30 d, t=1 d

Data set 1 (X=0.)

Y \ Z, cm	0.	60.	120.	180.	240.	300.	360.
-25.	455.	850.	900.	900.	900.	750.	430.
-15.	261.	669.	695.	679.	661.	602.	189.
0.	175.	388.	414.	408.	396.	357.	147.
25.	106.	202.	226.	226.	218.	188.	95.
75.	57.	89.	105.	108.	102.	85.	53.
125.	38.	52.	61.	63.	60.	50.	36.
175.	27.	35.	40.	41.	39.	34.	26.
225.	20.	25.	28.	29.	28.	24.	20.
275.	16.	19.	21.	21.	20.	18.	16.
375.	10.	12.	12.	13.	12.	12.	10.
475.	7.	8.	8.	8.	8.	8.	7.

Data set 2 (Y=0.)

X \ Z, cm	0.	60.	120.	180.	240.	300.	360.
0.	175.	388.	414.	408.	396.	357.	147.
25.	119.	250.	270.	267.	260.	235.	105.
50.	58.	110.	122.	123.	120.	107.	55.
75.	31.	54.	62.	63.	61.	53.	30.
100.	19.	31.	36.	37.	35.	30.	19.
125.	13.	19.	23.	23.	22.	19.	13.
150.	9.	13.	15.	16.	15.	13.	9.
175.	7.	9.	11.	11.	11.	9.	7.
200.	5.	7.	8.	8.	8.	7.	5.

Data set 3 (X= 200.)

Y \ Z, cm	0.	60.	120.	180.	240.	300.	360.
0.	5.4	7.0	8.1	8.5	8.1	7.0	5.4
-30.	2.0	2.7	3.2	3.4	3.3	2.9	2.2
-60.	1.7	2.3	2.7	2.8	2.8	2.4	1.9
-120.	0.02	0.04	0.04	0.04	0.04	0.03	0.02
-150.	0.03	0.04	0.04	0.04	0.04	0.03	0.02
-200.	0.03	0.04	0.04	0.04	0.04	0.03	0.02

T=30 d, t=5 d

Data set 1 (X=0.)

Y \ Z, cm	0.	60.	120.	180.	240.	300.	360.
-25.	280.	500.	550.	550.	550.	475.	265.
-15.	162.	413.	428.	421.	408.	372.	117.
0.	109.	240.	255.	252.	244.	220.	91.
25.	66.	125.	139.	140.	134.	116.	59.
75.	35.	55.	65.	67.	63.	52.	33.
125.	23.	32.	38.	39.	37.	31.	22.
175.	17.	21.	25.	26.	24.	21.	16.
225.	13.	15.	17.	18.	17.	15.	12.
275.	10.	12.	13.	13.	13.	11.	10.
375.	6.	7.	8.	8.	8.	7.	6.
475.	4.	5.	5.	5.	5.	5.	4.

Data set 2 (Y=0.)

X \ Z, cm	0.	60.	120.	180.	240.	300.	360.
0.	109.	240.	255.	252.	244.	220.	91.
25.	74.	155.	166.	165.	161.	145.	65.
50.	36.	68.	76.	76.	74.	66.	34.
75.	19.	33.	38.	39.	38.	33.	19.
100.	12.	19.	22.	23.	22.	19.	12.
125.	8.	12.	14.	14.	14.	12.	8.
150.	6.	8.	9.	10.	9.	8.	6.
175.	4.	6.	7.	7.	7.	6.	4.
200.	3.	4.	5.	5.	5.	4.	3.

Data set 3 (X= 200.)

Y \ Z, cm	0.	60.	120.	180.	240.	300.	360.
0.	3.3	4.3	5.0	5.2	5.0	4.4	3.3
-30.	1.3	1.7	2.0	2.1	2.0	1.8	1.4
-60.	1.0	1.4	1.6	1.7	1.7	1.5	1.2
-120.	0.02	0.02	0.02	0.02	0.02	0.02	0.01
-150.	0.02	0.02	0.03	0.03	0.02	0.02	0.01
-200.	0.02	0.02	0.02	0.03	0.02	0.02	0.01

T=100 d, t=1 d

Data set 1 (X=0.)

Y \ Z, cm	0.	60.	120.	180.	240.	300.	360.
-25.	550.	1000.	1100.	1100.	1050.	900.	500.
-15.	312.	792.	816.	811.	789.	715.	226.
0.	208.	459.	487.	486.	472.	424.	176.
25.	126.	239.	267.	269.	259.	224.	114.
75.	68.	106.	124.	128.	121.	101.	64.
125.	45.	62.	72.	75.	71.	60.	42.
175.	32.	41.	47.	49.	47.	40.	31.
225.	24.	29.	33.	34.	33.	29.	23.
275.	19.	22.	25.	25.	24.	22.	19.
375.	12.	14.	15.	15.	15.	14.	12.
475.	9.	9.	10.	10.	10.	9.	9.

Data set 2 (Y=0.)

X \ Z, cm	0.	60.	120.	180.	240.	300.	360.
0.	208.	459.	487.	486.	472.	424.	176.
25.	142.	297.	318.	318.	310.	280.	125.
50.	69.	130.	145.	146.	143.	128.	65.
75.	37.	64.	73.	75.	73.	63.	36.
100.	23.	36.	42.	43.	42.	36.	22.
125.	15.	23.	27.	28.	27.	23.	15.
150.	11.	15.	18.	19.	18.	15.	11.
175.	8.	11.	13.	14.	13.	11.	8.
200.	6.	8.	10.	10.	10.	8.	6.

Data set 3 (X= 200.)

Y \ Z, cm	0.	60.	120.	180.	240.	300.	360.
0.	6.4	8.3	9.6	10.1	9.7	8.4	6.4
-30.	2.4	3.2	3.8	4.0	3.9	3.5	2.6
-60.	2.0	2.7	3.2	3.4	3.3	2.9	2.2
-120.	0.03	0.04	0.05	0.05	0.04	0.04	0.02
-150.	0.03	0.04	0.05	0.05	0.05	0.04	0.02
-200.	0.03	0.04	0.05	0.05	0.05	0.04	0.03

T=100 d, t=5 d

Data set 1 (X=0.)

Y \ Z, cm	0.	60.	120.	180.	240.	300.	360.
-25.	360.	650.	700.	700.	700.	600.	340.
-15.	207.	530.	547.	536.	523.	477.	150.
0.	138.	307.	326.	321.	313.	282.	117.
25.	84.	159.	178.	178.	172.	149.	75.
75.	45.	70.	83.	85.	80.	67.	42.
125.	30.	41.	48.	50.	47.	40.	28.
175.	21.	27.	31.	33.	31.	27.	20.
225.	16.	20.	22.	23.	22.	19.	16.
275.	13.	15.	16.	17.	16.	15.	12.
375.	8.	9.	10.	10.	10.	9.	8.
475.	6.	6.	7.	7.	7.	6.	6.

Data set 2 (Y=0.)

X \ Z, cm	0.	60.	120.	180.	240.	300.	360.
0.	138.	307.	326.	321.	313.	282.	117.
25.	94.	198.	213.	210.	206.	186.	83.
50.	46.	87.	96.	97.	95.	85.	43.
75.	25.	43.	49.	50.	48.	42.	24.
100.	15.	24.	28.	29.	28.	24.	15.
125.	10.	15.	18.	18.	18.	15.	10.
150.	7.	10.	12.	13.	12.	10.	7.
175.	5.	7.	9.	9.	9.	7.	5.
200.	4.	6.	6.	7.	6.	6.	4.

Data set 3 (X= 200.)

Y \ Z, cm	0.	60.	120.	180.	240.	300.	360.
0.	4.2	5.5	6.4	6.7	6.4	5.6	4.3
-30.	1.6	2.1	2.5	2.7	2.6	2.3	1.7
-60.	1.3	1.8	2.1	2.2	2.2	1.9	1.5
-120.	0.02	0.03	0.03	0.03	0.03	0.02	0.01
-150.	0.02	0.03	0.03	0.03	0.03	0.03	0.02
-200.	0.02	0.03	0.03	0.03	0.03	0.03	0.02

T=5 y, t=1 d

Data set 1 (X=0.)

Y \ Z, cm	0.	60.	120.	180.	240.	300.	360.
-25.	600.	1050.	1150.	1150.	1100.	950.	550.
-15.	331.	836.	865.	852.	823.	756.	237.
0.	221.	485.	516.	511.	494.	448.	185.
25.	134.	253.	282.	283.	272.	236.	119.
75.	72.	112.	131.	135.	127.	106.	67.
125.	47.	65.	76.	79.	75.	63.	45.
175.	34.	43.	50.	52.	49.	42.	32.
225.	25.	31.	35.	36.	34.	30.	25.
275.	20.	24.	26.	27.	26.	23.	19.
375.	13.	15.	16.	16.	16.	14.	13.
475.	9.	10.	10.	11.	10.	10.	9.

Data set 2 (Y=0.)

X \ Z, cm	0.	60.	120.	180.	240.	300.	360.
0.	221.	485.	516.	511.	494.	448.	185.
25.	150.	313.	337.	335.	325.	295.	131.
50.	73.	138.	153.	154.	150.	135.	69.
75.	39.	68.	77.	79.	76.	67.	38.
100.	24.	38.	45.	46.	44.	38.	24.
125.	16.	24.	28.	29.	28.	24.	16.
150.	12.	16.	19.	20.	19.	16.	12.
175.	9.	12.	14.	14.	14.	12.	9.
200.	7.	9.	10.	11.	10.	9.	7.

Data set 3 (X= 200.)

Y \ Z, cm	0.	60.	120.	180.	240.	300.	360.
0.	6.7	8.8	10.2	10.6	10.2	8.9	6.8
-30.	2.6	3.4	4.0	4.3	4.2	3.7	2.8
-60.	2.1	2.9	3.3	3.6	3.5	3.1	2.4
-120.	0.03	0.04	0.05	0.05	0.05	0.04	0.02
-150.	0.03	0.05	0.05	0.05	0.05	0.04	0.03
-200.	0.03	0.05	0.05	0.05	0.05	0.04	0.03

T=5 y, t=5 d

Data set 1 (X=0.)

Y \ Z, cm	0.	60.	120.	180.	240.	300.	360.
-25.	395.	700.	800.	800.	750.	650.	375.
-15.	228.	578.	597.	592.	572.	522.	165.
0.	152.	335.	356.	355.	343.	309.	128.
25.	92.	174.	195.	196.	189.	163.	83.
75.	50.	77.	91.	93.	88.	73.	46.
125.	33.	45.	53.	55.	52.	43.	31.
175.	23.	30.	34.	36.	34.	29.	22.
225.	18.	21.	24.	25.	24.	21.	17.
275.	14.	16.	18.	18.	18.	16.	13.
375.	9.	10.	11.	11.	11.	10.	9.
475.	6.	7.	7.	7.	7.	7.	6.

Data set 2 (Y=0.)

X \ Z, cm	0.	60.	120.	180.	240.	300.	360.
0.	152.	335.	356.	355.	343.	309.	128.
25.	104.	216.	233.	232.	226.	204.	91.
50.	50.	95.	106.	106.	104.	93.	48.
75.	27.	47.	54.	54.	53.	46.	26.
100.	17.	26.	31.	32.	31.	26.	16.
125.	11.	17.	20.	20.	19.	17.	11.
150.	8.	11.	13.	14.	13.	11.	8.
175.	6.	8.	9.	10.	9.	8.	6.
200.	5.	6.	7.	7.	7.	6.	5.

Data set 3 (X= 200.)

Y \ Z, cm	0.	60.	120.	180.	240.	300.	360.
0.	4.6	6.1	7.0	7.4	7.1	6.1	4.7
-30.	1.8	2.4	2.8	2.9	2.9	2.5	1.9
-60.	1.5	2.0	2.3	2.5	2.4	2.1	1.6
-120.	0.02	0.03	0.03	0.03	0.03	0.03	0.02
-150.	0.02	0.03	0.04	0.04	0.03	0.03	0.02
-200.	0.02	0.03	0.04	0.04	0.03	0.03	0.02

T=10 y, t=1 d

Data set 1 (X=0.)

Y \ Z, cm	0.	60.	120.	180.	240.	300.	360.
-25.	600.	1050.	1150.	1150.	1100.	950.	550.
-15.	331.	836.	866.	853.	824.	757.	237.
0.	221.	486.	516.	511.	494.	448.	185.
25.	134.	253.	282.	283.	272.	236.	119.
75.	72.	112.	131.	135.	128.	106.	67.
125.	47.	65.	76.	79.	75.	63.	45.
175.	34.	43.	50.	52.	49.	42.	32.
225.	25.	31.	35.	36.	34.	30.	25.
275.	20.	24.	26.	27.	26.	23.	20.
375.	13.	15.	16.	16.	16.	14.	13.
475.	9.	10.	10.	11.	10.	10.	9.

Data set 2 (Y=0.)

X \ Z, cm	0.	60.	120.	180.	240.	300.	360.
0.	221.	486.	516.	511.	494.	448.	185.
25.	150.	314.	337.	335.	325.	296.	131.
50.	73.	138.	153.	154.	150.	135.	69.
75.	39.	68.	77.	79.	76.	67.	38.
100.	24.	38.	45.	46.	44.	38.	24.
125.	16.	24.	28.	29.	28.	24.	16.
150.	12.	16.	19.	20.	19.	16.	12.
175.	9.	12.	14.	14.	14.	12.	9.
200.	7.	9.	10.	11.	10.	9.	7.

Data set 3 (X= 200.)

Y \ Z, cm	0.	60.	120.	180.	240.	300.	360.
0.	6.7	8.8	10.2	10.7	10.2	8.9	6.8
-30.	2.6	3.4	4.0	4.3	4.2	3.7	2.8
-60.	2.1	2.9	3.3	3.6	3.5	3.1	2.4
-120.	0.03	0.04	0.05	0.05	0.05	0.04	0.02
-150.	0.03	0.05	0.05	0.05	0.05	0.04	0.03
-200.	0.03	0.05	0.05	0.05	0.05	0.04	0.03

T=10 y, t=5 d

Data set 1 (X=0.)

Y \ Z, cm	0.	60.	120.	180.	240.	300.	360.
-25.	600.	1050.	1150.	1150.	1100.	950.	550.
-15.	331.	836.	866.	853.	824.	757.	237.
0.	221.	486.	516.	511.	494.	448.	185.
25.	134.	253.	282.	283.	272.	236.	119.
75.	72.	112.	131.	135.	128.	106.	67.
125.	47.	65.	76.	79.	75.	63.	45.
175.	34.	43.	50.	52.	49.	42.	32.
225.	25.	31.	35.	36.	34.	30.	25.
275.	20.	24.	26.	27.	26.	23.	20.
375.	13.	15.	16.	16.	16.	14.	13.
475.	9.	10.	10.	11.	10.	10.	9.

Data set 2 (Y=0.)

X \ Z, cm	0.	60.	120.	180.	240.	300.	360.
0.	221.	486.	516.	511.	494.	448.	185.
25.	150.	314.	337.	335.	325.	296.	131.
50.	73.	138.	153.	154.	150.	135.	69.
75.	39.	68.	77.	79.	76.	67.	38.
100.	24.	38.	45.	46.	44.	38.	24.
125.	16.	24.	28.	29.	28.	24.	16.
150.	12.	16.	19.	20.	19.	16.	12.
175.	9.	12.	14.	14.	14.	12.	9.
200.	7.	9.	10.	11.	10.	9.	7.

Data set 3 (X= 200.)

Y \ Z, cm	0.	60.	120.	180.	240.	300.	360.
0.	6.7	8.8	10.2	10.7	10.2	8.9	6.8
-30.	2.6	3.4	4.0	4.3	4.2	3.7	2.8
-60.	2.1	2.9	3.3	3.6	3.5	3.1	2.4
-120.	0.03	0.04	0.05	0.05	0.05	0.04	0.02
-150.	0.03	0.05	0.05	0.05	0.05	0.04	0.03
-200.	0.03	0.05	0.05	0.05	0.05	0.04	0.03

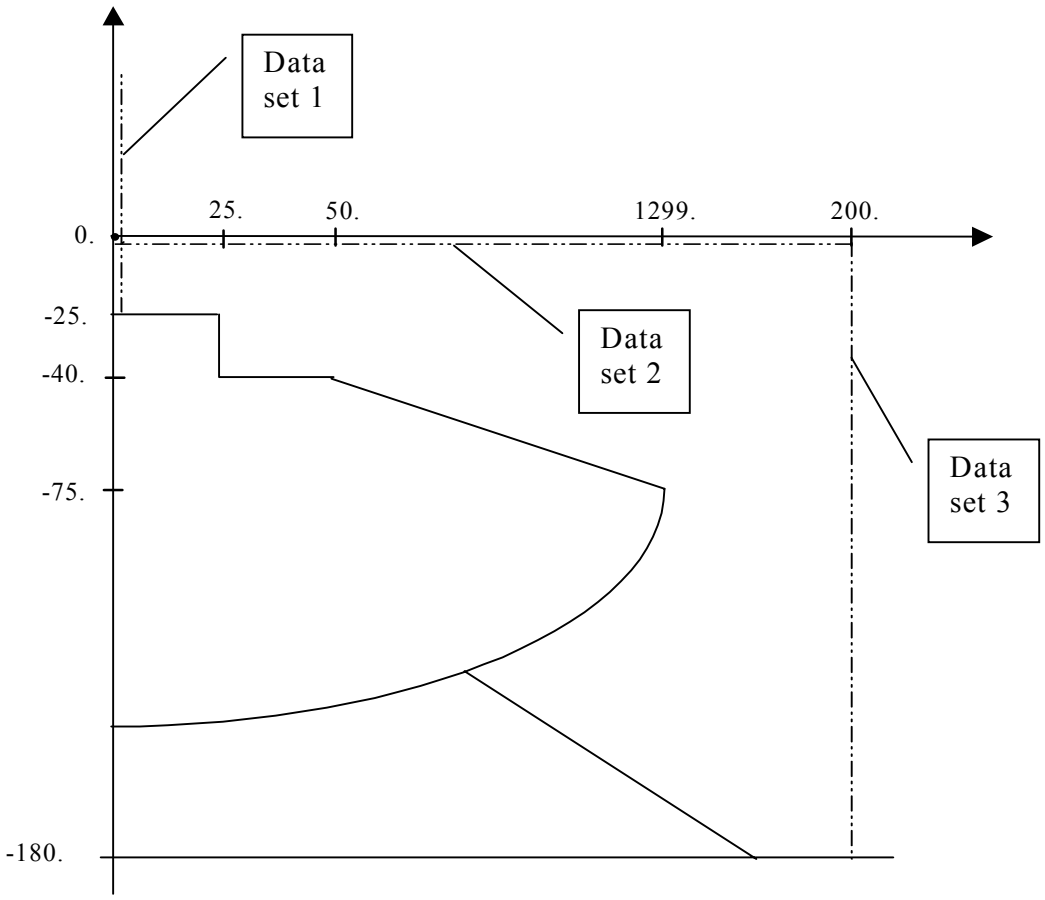
Data
set 1
25.
50.
1299.
200.
0.
-25.
-40.
-75.
-180.
Data
set 2
Data
set 3

Table 6

Dose due to activity induced by low energy neutrons, μSv/h

T=30 d, t=1 d

Data set 1 (X=0.)

Y \ Z, cm	0.	60.	120.	180.	240.	300.	360.
-25.	1.9	3.5	3.35	3	2.8	2.65	1.6
-15.	1.1	2.7	2.5	2.2	2.1	2.1	0.7
0.	0.9	1.8	1.8	1.6	1.5	1.4	0.7
25.	0.6	1.1	1.2	1.1	1.0	0.9	0.5
75.	0.4	0.6	0.6	0.6	0.6	0.5	0.3
125.	0.3	0.3	0.4	0.4	0.4	0.3	0.2
175.	0.2	0.2	0.3	0.3	0.2	0.2	0.2
225.	0.1	0.2	0.2	0.2	0.2	0.2	0.1
275.	0.1	0.1	0.1	0.1	0.1	0.1	0.1
375.	0.1	0.1	0.1	0.1	0.1	0.1	0.1
475.	0.1	0.1	0.1	0.1	0.1	0.1	0.0

Data set 2 (Y=0.)

X \ Z, cm	0.	60.	120.	180.	240.	300.	360.
0.	0.9	1.8	1.8	1.6	1.5	1.4	0.7
25.	0.8	1.6	1.5	1.4	1.3	1.2	0.6
50.	0.6	1.1	1.1	1.0	0.9	0.8	0.4
75.	0.4	0.7	0.7	0.7	0.6	0.5	0.3
100.	0.3	0.4	0.5	0.4	0.4	0.3	0.2
125.	0.2	0.3	0.3	0.3	0.3	0.2	0.1
150.	0.1	0.2	0.2	0.2	0.2	0.2	0.1
175.	0.1	0.1	0.1	0.1	0.1	0.1	0.1
200.	0.1	0.1	0.1	0.1	0.1	0.1	0.1

Data set 3 (X= 200.)

Y \ Z, cm	0.	60.	120.	180.	240.	300.	360.
0.	0.075	0.099	0.112	0.113	0.105	0.088	0.065
-30.	0.052	0.07	0.079	0.08	0.074	0.062	0.045
-60.	0.039	0.052	0.058	0.059	0.054	0.046	0.033
-120.	0.002	0.004	0.005	0.005	0.005	0.004	0.003
-150.	0.003	0.004	0.005	0.005	0.005	0.004	0.003
-200.	0.003	0.004	0.005	0.005	0.005	0.004	0.003

T=30 d, t=5 d

Data set 1 (X=0.)

Y \ Z, cm	0.	60.	120.	180.	240.	300.	360.
-25.	1.6	2.9	2.75	2.45	2.3	2.15	1.35
-15.	0.9	2.3	2.1	1.8	1.7	1.7	0.6
0.	0.7	1.5	1.5	1.3	1.2	1.2	0.5
25.	0.5	0.9	1.0	0.9	0.8	0.7	0.4
75.	0.3	0.5	0.5	0.5	0.5	0.4	0.3
125.	0.2	0.3	0.3	0.3	0.3	0.2	0.2
175.	0.2	0.2	0.2	0.2	0.2	0.2	0.1
225.	0.1	0.1	0.2	0.2	0.1	0.1	0.1
275.	0.1	0.1	0.1	0.1	0.1	0.1	0.1
375.	0.1	0.1	0.1	0.1	0.1	0.1	0.1
475.	0.0	0.0	0.0	0.0	0.0	0.0	0.0

Data set 2 (Y=0.)

X \ Z, cm	0.	60.	120.	180.	240.	300.	360.
0.	0.7	1.5	1.5	1.3	1.2	1.2	0.5
25.	0.7	1.3	1.2	1.1	1.0	1.0	0.5
50.	0.5	0.9	0.9	0.8	0.8	0.7	0.4
75.	0.3	0.6	0.6	0.6	0.5	0.5	0.3
100.	0.2	0.4	0.4	0.4	0.3	0.3	0.2
125.	0.2	0.2	0.3	0.2	0.2	0.2	0.1
150.	0.1	0.2	0.2	0.2	0.2	0.1	0.1
175.	0.1	0.1	0.1	0.1	0.1	0.1	0.1
200.	0.1	0.1	0.1	0.1	0.1	0.1	0.1

Data set 3 (X= 200.)

Y \ Z, cm	0.	60.	120.	180.	240.	300.	360.
0.	0.064	0.084	0.095	0.095	0.089	0.075	0.055
-30.	0.045	0.06	0.067	0.068	0.063	0.053	0.038
-60.	0.033	0.044	0.049	0.05	0.046	0.039	0.028
-120.	0.002	0.003	0.004	0.004	0.004	0.003	0.002
-150.	0.002	0.004	0.004	0.004	0.004	0.004	0.002
-200.	0.002	0.003	0.004	0.004	0.004	0.004	0.002

T=100 d, t=1 d

Data set 1 (X=0.)

Y \ Z, cm	0.	60.	120.	180.	240.	300.	360.
-25.	4	7.5	7	6	6	5.5	3.35
-15.	2.2	5.7	5.2	4.6	4.3	4.3	1.6
0.	1.8	3.8	3.7	3.3	3.1	3.0	1.4
25.	1.3	2.3	2.4	2.2	2.1	1.9	1.0
75.	0.8	1.2	1.3	1.3	1.2	1.0	0.7
125.	0.5	0.7	0.8	0.8	0.7	0.6	0.5
175.	0.4	0.5	0.5	0.5	0.5	0.4	0.3
225.	0.3	0.3	0.4	0.4	0.4	0.3	0.3
275.	0.2	0.3	0.3	0.3	0.3	0.3	0.2
375.	0.2	0.2	0.2	0.2	0.2	0.2	0.1
475.	0.1	0.1	0.1	0.1	0.1	0.1	0.1

Data set 2 (Y=0.)

X \ Z, cm	0.	60.	120.	180.	240.	300.	360.
0.	1.8	3.8	3.7	3.3	3.1	3.0	1.4
25.	1.6	3.2	3.1	2.8	2.6	2.5	1.2
50.	1.2	2.3	2.2	2.1	1.9	1.8	0.9
75.	0.8	1.4	1.5	1.4	1.3	1.1	0.6
100.	0.5	0.9	0.9	0.9	0.8	0.7	0.4
125.	0.4	0.6	0.6	0.6	0.6	0.5	0.3
150.	0.3	0.4	0.4	0.4	0.4	0.3	0.2
175.	0.2	0.3	0.3	0.3	0.3	0.2	0.2
200.	0.2	0.2	0.2	0.2	0.2	0.2	0.1

Data set 3 (X= 200.)

Y \ Z, cm	0.	60.	120.	180.	240.	300.	360.
0.	0.159	0.209	0.235	0.237	0.22	0.186	0.138
-30.	0.111	0.148	0.167	0.168	0.156	0.132	0.096
-60.	0.082	0.109	0.123	0.123	0.115	0.097	0.07
-120.	0.005	0.008	0.01	0.01	0.01	0.008	0.005
-150.	0.006	0.009	0.01	0.011	0.011	0.009	0.006
-200.	0.006	0.008	0.01	0.011	0.01	0.009	0.006

T=100 d, t=5 d

Data set 1 (X=0.)

Y \ Z, cm	0.	60.	120.	180.	240.	300.	360.
-25.	3.55	6.5	6	5.5	5	4.85	3
-15.	2.0	5.1	4.6	4.1	3.8	3.9	1.4
0.	1.6	3.4	3.3	2.9	2.7	2.6	1.2
25.	1.2	2.1	2.1	2.0	1.8	1.7	0.9
75.	0.7	1.1	1.2	1.1	1.1	0.9	0.6
125.	0.5	0.6	0.7	0.7	0.7	0.6	0.4
175.	0.3	0.4	0.5	0.5	0.5	0.4	0.3
225.	0.3	0.3	0.3	0.3	0.3	0.3	0.2
275.	0.2	0.2	0.3	0.3	0.3	0.2	0.2
375.	0.1	0.2	0.2	0.2	0.2	0.1	0.1
475.	0.1	0.1	0.1	0.1	0.1	0.1	0.1

Data set 2 (Y=0.)

X \ Z, cm	0.	60.	120.	180.	240.	300.	360.
0.	1.6	3.4	3.3	2.9	2.7	2.6	1.2
25.	1.5	2.9	2.8	2.5	2.3	2.2	1.1
50.	1.1	2.0	2.0	1.9	1.7	1.6	0.8
75.	0.7	1.3	1.3	1.2	1.2	1.0	0.6
100.	0.5	0.8	0.9	0.8	0.8	0.7	0.4
125.	0.3	0.5	0.6	0.6	0.5	0.4	0.3
150.	0.2	0.4	0.4	0.4	0.4	0.3	0.2
175.	0.2	0.3	0.3	0.3	0.3	0.2	0.2
200.	0.1	0.2	0.2	0.2	0.2	0.2	0.1

Data set 3 (X= 200.)

Y \ Z, cm	0.	60.	120.	180.	240.	300.	360.
0.	0.143	0.189	0.212	0.214	0.199	0.168	0.124
-30.	0.1	0.134	0.151	0.152	0.141	0.119	0.086
-60.	0.074	0.098	0.111	0.111	0.104	0.087	0.064
-120.	0.004	0.007	0.009	0.009	0.009	0.008	0.005
-150.	0.005	0.008	0.009	0.01	0.01	0.008	0.005
-200.	0.005	0.008	0.009	0.01	0.009	0.008	0.005

T=5 y, t=1 d

Data set 1 (X=0.)

Y \ Z, cm	0.	60.	120.	180.	240.	300.	360.
-25.	6.5	11.5	11	10	9.5	9	5.5
-15.	3.5	9.1	8.3	7.4	7.0	7.0	2.5
0.	2.9	6.2	5.9	5.3	5.0	4.7	2.2
25.	2.1	3.8	3.8	3.6	3.3	3.0	1.6
75.	1.3	1.9	2.1	2.1	1.9	1.6	1.1
125.	0.9	1.1	1.3	1.3	1.2	1.0	0.7
175.	0.6	0.8	0.9	0.9	0.8	0.7	0.5
225.	0.5	0.6	0.6	0.6	0.6	0.5	0.4
275.	0.4	0.4	0.5	0.5	0.5	0.4	0.3
375.	0.2	0.3	0.3	0.3	0.3	0.3	0.2
475.	0.2	0.2	0.2	0.2	0.2	0.2	0.2

Data set 2 (Y=0.)

X \ Z, cm	0.	60.	120.	180.	240.	300.	360.
0.	2.9	6.2	5.9	5.3	5.0	4.7	2.2
25.	2.6	5.2	5.0	4.5	4.2	4.0	2.0
50.	1.9	3.6	3.6	3.3	3.1	2.8	1.5
75.	1.3	2.3	2.3	2.2	2.0	1.8	1.0
100.	0.9	1.4	1.5	1.4	1.3	1.2	0.7
125.	0.6	0.9	1.0	1.0	0.9	0.8	0.5
150.	0.4	0.6	0.7	0.7	0.6	0.5	0.4
175.	0.3	0.4	0.5	0.5	0.5	0.4	0.3
200.	0.3	0.3	0.4	0.4	0.4	0.3	0.2

Data set 3 (X= 200.)

Y \ Z, cm	0.	60.	120.	180.	240.	300.	360.
0.	0.252	0.332	0.374	0.377	0.351	0.296	0.219
-30.	0.175	0.235	0.265	0.267	0.248	0.209	0.152
-60.	0.129	0.173	0.195	0.196	0.183	0.154	0.112
-120.	0.008	0.013	0.015	0.016	0.016	0.013	0.008
-150.	0.009	0.014	0.017	0.017	0.017	0.014	0.01
-200.	0.009	0.014	0.016	0.017	0.016	0.014	0.01

T=5 y, t=5 d

Data set 1 (X=0.)

Y \ Z, cm	0.	60.	120.	180.	240.	300.	360.
-25.	6	11	10.5	9.5	8.5	8	5
-15.	3.2	8.5	7.7	6.9	6.5	6.5	2.3
0.	2.7	5.7	5.4	4.9	4.6	4.4	2.1
25.	2.0	3.5	3.6	3.3	3.1	2.8	1.5
75.	1.2	1.8	2.0	1.9	1.8	1.5	1.0
125.	0.8	1.1	1.2	1.2	1.1	0.9	0.7
175.	0.6	0.7	0.8	0.8	0.8	0.6	0.5
225.	0.4	0.5	0.6	0.6	0.5	0.5	0.4
275.	0.3	0.4	0.4	0.4	0.4	0.4	0.3
375.	0.2	0.3	0.3	0.3	0.3	0.2	0.2
475.	0.2	0.2	0.2	0.2	0.2	0.2	0.2

Data set 2 (Y=0.)

X \ Z, cm	0.	60.	120.	180.	240.	300.	360.
0.	2.7	5.7	5.4	4.9	4.6	4.4	2.1
25.	2.4	4.8	4.6	4.2	4.0	3.7	1.8
50.	1.8	3.4	3.3	3.1	2.9	2.7	1.4
75.	1.2	2.1	2.2	2.0	1.9	1.7	1.0
100.	0.8	1.3	1.4	1.3	1.3	1.1	0.7
125.	0.6	0.8	0.9	0.9	0.8	0.7	0.5
150.	0.4	0.6	0.6	0.6	0.6	0.5	0.3
175.	0.3	0.4	0.5	0.5	0.4	0.4	0.3
200.	0.2	0.3	0.4	0.4	0.3	0.3	0.2

Data set 3 (X= 200.)

Y \ Z, cm	0.	60.	120.	180.	240.	300.	360.
0.	0.236	0.311	0.35	0.353	0.328	0.278	0.205
-30.	0.164	0.22	0.248	0.25	0.232	0.196	0.142
-60.	0.121	0.162	0.182	0.184	0.171	0.144	0.105
-120.	0.007	0.012	0.014	0.015	0.015	0.013	0.008
-150.	0.008	0.013	0.016	0.016	0.016	0.014	0.009
-200.	0.009	0.013	0.015	0.016	0.015	0.013	0.009

T=10 y, t=1 d

Data set 1 (X=0.)

Y \ Z, cm	0.	60.	120.	180.	240.	300.	360.
-25.	7.5	14.5	13.5	12	11.5	11	6.5
-15.	4.2	11.1	10.2	9.1	8.5	8.5	3.1
0.	3.5	7.5	7.2	6.4	6.0	5.8	2.7
25.	2.6	4.6	4.7	4.4	4.1	3.6	2.0
75.	1.6	2.3	2.6	2.5	2.3	1.9	1.3
125.	1.0	1.4	1.6	1.6	1.4	1.2	0.9
175.	0.7	0.9	1.0	1.1	1.0	0.8	0.7
225.	0.6	0.7	0.7	0.8	0.7	0.6	0.5
275.	0.5	0.5	0.6	0.6	0.6	0.5	0.4
375.	0.3	0.3	0.4	0.4	0.3	0.3	0.3
475.	0.2	0.2	0.2	0.2	0.2	0.2	0.2

Data set 2 (Y=0.)

X \ Z, cm	0.	60.	120.	180.	240.	300.	360.
0.	3.5	7.5	7.2	6.4	6.0	5.8	2.7
25.	3.1	6.3	6.1	5.5	5.2	4.9	2.4
50.	2.3	4.4	4.4	4.0	3.7	3.5	1.8
75.	1.6	2.8	2.8	2.7	2.5	2.2	1.3
100.	1.0	1.7	1.8	1.8	1.6	1.4	0.9
125.	0.7	1.1	1.2	1.2	1.1	0.9	0.6
150.	0.5	0.8	0.8	0.8	0.8	0.6	0.4
175.	0.4	0.5	0.6	0.6	0.6	0.5	0.3
200.	0.3	0.4	0.5	0.5	0.4	0.4	0.3

Data set 3 (X= 200.)

Y \ Z, cm	0.	60.	120.	180.	240.	300.	360.
0.	0.306	0.404	0.455	0.459	0.427	0.361	0.267
-30.	0.213	0.286	0.322	0.324	0.302	0.255	0.185
-60.	0.157	0.211	0.237	0.239	0.222	0.188	0.137
-120.	0.01	0.016	0.019	0.02	0.019	0.016	0.01
-150.	0.011	0.017	0.02	0.021	0.021	0.018	0.012
-200.	0.011	0.017	0.02	0.021	0.02	0.017	0.012

T=10 y, t=5 d

Data set 1 (X=0.)

Y \ Z, cm	0.	60.	120.	180.	240.	300.	360.
-25.	7.5	13.5	13	11.5	10.5	10	6
-15.	4.0	10.5	9.6	8.5	8.0	8.0	2.9
0.	3.3	7.1	6.7	6.1	5.7	5.5	2.6
25.	2.4	4.3	4.4	4.1	3.8	3.4	1.9
75.	1.5	2.2	2.4	2.4	2.2	1.8	1.2
125.	1.0	1.3	1.5	1.5	1.4	1.1	0.8
175.	0.7	0.9	1.0	1.0	0.9	0.8	0.6
225.	0.5	0.6	0.7	0.7	0.7	0.6	0.5
275.	0.4	0.5	0.5	0.5	0.5	0.5	0.4
375.	0.3	0.3	0.3	0.3	0.3	0.3	0.3
475.	0.2	0.2	0.2	0.2	0.2	0.2	0.2

Data set 2 (Y=0.)

X \ Z, cm	0.	60.	120.	180.	240.	300.	360.
0.	3.3	7.1	6.7	6.1	5.7	5.5	2.6
25.	3.0	6.0	5.8	5.2	4.9	4.6	2.3
50.	2.2	4.2	4.1	3.8	3.5	3.3	1.7
75.	1.5	2.6	2.7	2.5	2.3	2.1	1.2
100.	1.0	1.6	1.7	1.7	1.5	1.3	0.8
125.	0.7	1.0	1.2	1.1	1.0	0.9	0.6
150.	0.5	0.7	0.8	0.8	0.7	0.6	0.4
175.	0.4	0.5	0.6	0.6	0.5	0.4	0.3
200.	0.3	0.4	0.4	0.4	0.4	0.3	0.3

Data set 3 (X= 200.)

Y \ Z, cm	0.	60.	120.	180.	240.	300.	360.
0.	0.29	0.382	0.431	0.434	0.404	0.341	0.252
-30.	0.202	0.271	0.305	0.307	0.286	0.241	0.175
-60.	0.149	0.199	0.225	0.226	0.21	0.178	0.129
-120.	0.009	0.015	0.018	0.019	0.018	0.016	0.01
-150.	0.01	0.016	0.019	0.02	0.02	0.017	0.011
-200.	0.011	0.016	0.019	0.02	0.019	0.016	0.011

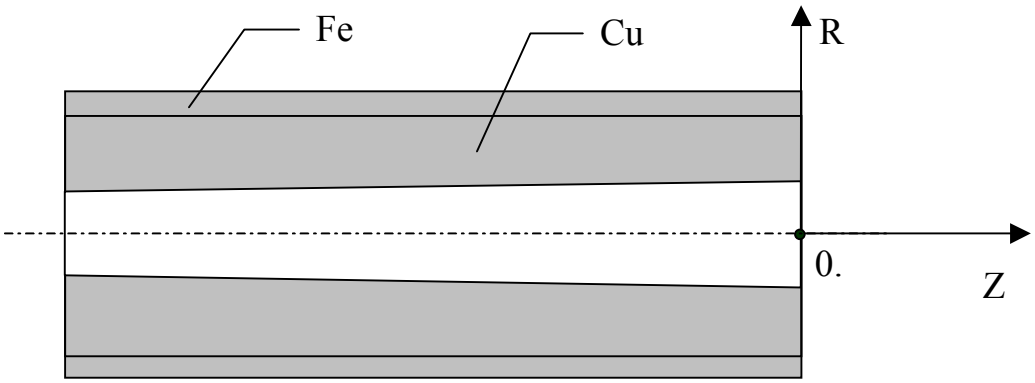

Doze rate field in the copper plug region due to radioactivity induced by low energy neutrons, μSv/h

T=30d, t=1 d

Z, cm

R,cm	-(20 –10)	-(10 -0)	0.	0-10	10-20	20-30	30-40	40-50	50-60	60-70	70-80	80-90	90-100
5-10	1351	1216	861	783	458	335	219	144	122	109	96	81	64
10-20			977	763	411	271	209	154	109	83	65	51	42
20-30			954	635	302	196	154	120	88	64	53	46	40
30-40			230	194	170	127	111	98	82	65	51	45	41
40-50			15	29	86	65	64	68	66	59	48	39	36
50-60			12	12	52	44	37	42	42	39	34	30	26
70-80			8	6	35	33	21	29	35	33	28	22	15
80-90			7	5	21	34	11	14	25	30	29	24	18

T = 30 d, t = 5 d

Z, cm

R,cm	-(20 –10)	-(10 -0)	0.	0-10	10-20	20-30	30-40	40-50	50-60	60-70	70-80	80-90	90-100
5-10	17	15	11	10	6	4	3	2	2	1	1	1	1
10-20			12	10	5	4	3	2	2	1	1	1	1
20-30			12	8	4	3	2	2	1	1	1	1	1
30-40			6	4	3	2	1	1	1	1	1	1	1
40-50			2	2	2	1	1	1	1	1	1	1	0
50-60			1	1	1	1	1	1	1	1	1	0	0
70-80			1	1	1	1	1	1	1	1	1	0	0
80-90			1	1	1	1	1	0	1	1	1	1	0

T=100d, t=1 d

Z, cm

R,cm	-(20 –10)	-(10 -0)	0.	0-10	10-20	20-30	30-40	40-50	50-60	60-70	70-80	80-90	90-100
5-10	1361	1219	867	788	461	336	221	145	123	110	97	82	64
10-20			982	767	415	273	210	156	110	84	66	52	42
20-30			956	638	305	198	155	120	89	65	53	46	41
30-40			235	197	173	127	112	98	82	65	52	46	41
40-50			17	31	87	66	64	69	66	59	49	39	36
50-60			13	13	54	45	37	43	43	39	35	30	26
70-80			9	8	36	34	21	30	36	34	29	22	16
80-90			9	6	22	35	12	14	26	31	29	24	18

T = 100 d, t = 5 d

Z, cm

R,cm	-(20 –10)	-(10 -0)	0.	0-10	10-20	20-30	30-40	40-50	50-60	60-70	70-80	80-90	90-100
5-10	25	23	16	15	9	6	5	3	2	2	2	2	1
10-20			18	14	8	5	4	3	2	2	2	1	1
20-30			17	12	6	4	3	3	2	1	1	1	1
30-40			10	7	4	3	2	2	2	1	1	1	1
40-50			3	3	3	2	2	2	1	1	1	1	1
50-60			3	2	2	2	1	1	1	1	1	1	1
70-80			2	2	2	2	1	1	1	1	1	1	1
80-90			2	2	2	2	1	1	1	1	1	1	1

T = 5 y, t = 1 d

Z, cm

R,cm	-(20 –10)	-(10 -0)	0.	0-10	10-20	20-30	30-40	40-50	50-60	60-70	70-80	80-90	90-100
5-10	1361	1221	867	788	461	336	221	145	122	109	97	82	64
10-20			982	767	415	273	210	156	110	84	66	52	42
20-30			955	636	305	198	156	120	89	65	53	46	40
30-40			238	199	173	128	112	98	82	65	52	46	41
40-50			18	32	88	66	65	69	67	59	49	39	36
50-60			14	14	54	45	38	43	43	39	35	30	27
70-80			10	8	37	34	22	30	36	34	29	22	16
80-90			9	7	23	35	12	15	26	31	30	25	18

T = 5 y, t = 5 d

Z, cm

R,cm	-(20 –10)	-(10 -0)	0.	0-10	10-20	20-30	30-40	40-50	50-60	60-70	70-80	80-90	90-100
5-10	27	24	17	16	10	7	5	3	3	2	2	2	2
10-20			19	15	9	6	5	4	3	2	2	1	1
20-30			18	13	7	5	4	3	2	2	1	1	1
30-40			13	9	5	3	3	2	2	2	1	1	1
40-50			5	4	4	3	2	2	2	1	1	1	1
50-60			4	3	3	2	2	2	2	1	1	1	1
70-80			3	3	3	2	2	1	1	1	1	1	1
80-90			3	3	2	2	2	1	1	1	1	1	1

T = 10 y, t = 1 d

Z, cm

R,cm	-(20 –10)	-(10 -0)	0.	0-10	10-20	20-30	30-40	40-50	50-60	60-70	70-80	80-90	90-100
5-10	1361	1221	868	788	461	336	222	145	122	109	97	82	64
10-20			982	768	415	273	210	156	110	84	66	52	42
20-30			956	637	305	198	156	121	89	65	53	46	41
30-40			238	199	173	128	112	98	82	66	52	46	41
40-50			19	33	88	66	65	69	67	59	49	39	36
50-60			15	15	54	45	38	43	43	39	35	30	27
70-80			10	9	37	35	22	30	36	34	29	22	16
80-90			10	7	23	36	12	15	26	31	30	25	18

T = 10 y, t = 5 d

Z, cm

R,cm	-(20 -10)	-(10 -0)	0.	0-10	10-20	20-30	30-40	40-50	50-60	60-70	70-80	80-90	90-100
5-10	27	25	18	16	10	7	5	3	3	2	2	2	2
10-20			19	16	9	6	5	4	3	2	2	1	1
20-30			19	13	7	5	4	3	2	2	1	1	1
30-40			14	10	5	3	3	2	2	2	1	1	1
40-50			5	5	4	3	2	2	2	1	1	1	1
50-60			4	4	3	3	2	2	2	2	1	1	1
70-80			4	3	3	2	2	2	2	2	1	1	1
80-90			3	3	3	2	2	1	1	1	1	1	1

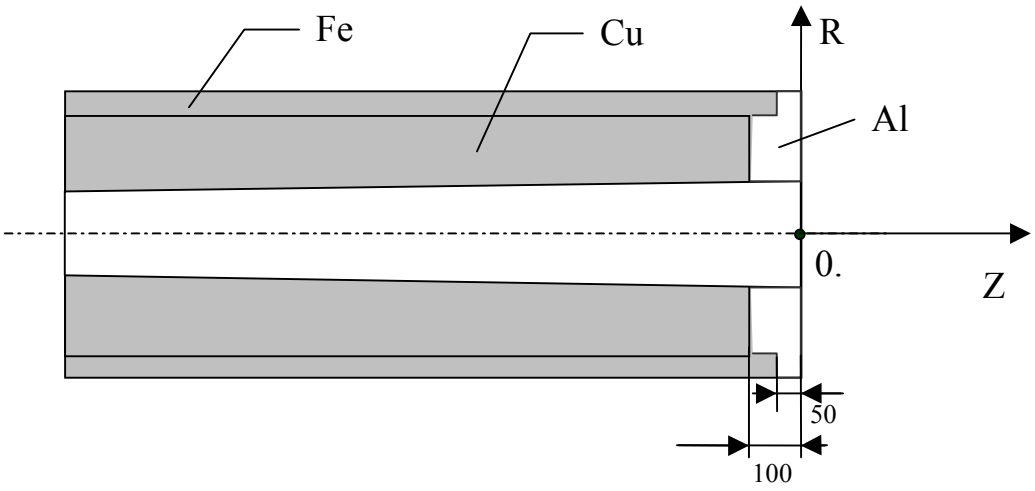

Doze rate field in the copper plug region due to radioactivity induced by low energy neutrons, μSv/h

T = 30 d, t = 1 d

Z, cm

R,cm	-(20 -10)	-(10 -0)	0.	0-10	10-20	20-30	30-40	40-50	50-60	60-70	70-80	80-90	90-100
5-10	1175	849	533	458	266	162	110	79	58	41	29	20	14
10-20			347	296	193	130	87	65	51	41	32	24	17
20-30			108	97	93	86	69	54	46	40	35	30	25
30-40			34	32	36	50	47	34	26	26	28	29	28
40-50			10	9	16	16	33	32	22	14	12	13	16
50-60			6	6	11	8	11	25	23	15	8	7	7
70-80			5	4	8	6	5	10	21	19	11	5	3
80-90			5	4	6	6	3	4	8	18	17	10	4

T = 30 d, t = 5 d

Z, cm

R,cm	-(20 -10)	-(10 -0)	0.	0-10	10-20	20-30	30-40	40-50	50-60	60-70	70-80	80-90	90-100
5-10	15	11	7	6	4	2	2	1	1	1	0	0	0
10-20			5	4	3	2	1	1	1	1	1	0	0
20-30			2	2	1	1	1	1	1	1	1	0	0
30-40			1	1	1	1	1	1	0	0	0	0	0
40-50			1	1	1	1	1	1	0	0	0	0	0
50-60			1	1	1	0	0	1	1	0	0	0	0
70-80			1	1	1	1	0	0	1	0	0	0	0
80-90			1	1	1	1	0	0	0	0	0	0	0

T = 100 d, t = 1 d

Z, cm

R,cm	-(20 -10)	-(10 -0)	0.	0-10	10-20	20-30	30-40	40-50	50-60	60-70	70-80	80-90	90-100
5-10	1176	856	536	461	267	163	111	80	58	42	29	20	14
10-20			350	298	194	131	87	66	52	41	32	24	17
20-30			109	98	94	87	70	55	47	41	35	30	26
30-40			35	33	36	50	47	35	27	26	28	29	28
40-50			11	10	17	17	34	32	22	14	12	13	16
50-60			8	7	12	8	12	26	24	15	9	7	7
70-80			6	6	9	7	5	10	21	20	12	6	4
80-90			6	5	7	7	3	4	9	19	17	10	5

T = 100 d, t = 5 d

Z, cm

R,cm	-(20 -10)	-(10 -0)	0.	0-10	10-20	20-30	30-40	40-50	50-60	60-70	70-80	80-90	90-100
5-10	22	16	10	9	5	4	3	2	1	1	1	1	1
10-20			7	6	4	3	2	2	1	1	1	1	0
20-30			3	3	2	2	2	1	1	1	1	1	1
30-40			2	2	1	1	1	1	1	1	1	1	1
40-50			2	2	1	1	1	1	1	0	0	0	0
50-60			2	2	1	1	1	1	1	1	0	0	0
70-80			2	2	1	1	1	1	1	1	1	1	0
80-90			2	2	1	1	1	1	1	1	1	1	1

T = 5 y, t = 1 d

Z, cm

R,cm	-(20 -10)	-(10 -0)	0.	0-10	10-20	20-30	30-40	40-50	50-60	60-70	70-80	80-90	90-100
5-10	1176	856	536	461	267	163	111	80	58	41	29	20	14
10-20			350	298	194	130	87	66	52	41	32	24	17
20-30			109	98	94	87	70	55	47	41	35	30	26
30-40			35	33	36	50	47	35	27	26	28	29	28
40-50			12	11	17	17	34	32	22	14	12	13	16
50-60			8	7	12	8	12	26	24	15	9	7	7
70-80			7	6	10	7	5	10	22	20	12	6	4
80-90			7	6	7	7	3	4	9	19	17	10	5

T = 5 y, t = 5 d

Z, cm

R,cm	-(20 -10)	-(10 -0)	0.	0-10	10-20	20-30	30-40	40-50	50-60	60-70	70-80	80-90	90-100
5-10	23	17	11	10	6	4	3	2	1	1	1	1	1
10-20			8	7	5	3	2	2	2	1	1	1	1
20-30			4	3	3	2	2	2	1	1	1	1	1
30-40			3	2	2	1	1	1	1	1	1	1	1
40-50			3	3	2	1	1	1	1	1	0	0	0
50-60			3	3	2	1	1	1	1	1	1	0	0
70-80			3	3	2	2	1	1	1	1	1	1	1
80-90			3	2	2	2	1	1	1	1	1	1	1

T = 10 y, t = 1 d

Z, cm

R,cm	-(20 -10)	-(10 -0)	0.	0-10	10-20	20-30	30-40	40-50	50-60	60-70	70-80	80-90	90-100
5-10	1176	856	536	461	267	163	112	80	58	41	29	20	14
10-20			350	298	194	130	87	66	52	41	32	24	17
20-30			109	98	94	87	70	55	47	41	35	30	26
30-40			35	33	36	50	47	35	27	26	28	29	28
40-50			12	11	17	17	34	33	22	14	12	13	16
50-60			9	8	13	9	12	26	24	15	9	7	7
70-80			8	7	10	7	6	10	22	20	12	6	4
80-90			7	6	7	8	4	5	9	19	17	10	5

T = 10 y, t = 5 d

Z, cm

R,cm	-(20 -10)	-(10 -0)	0.	0-10	10-20	20-30	30-40	40-50	50-60	60-70	70-80	80-90	90-100
5-10	24	18	12	10	6	4	3	2	1	1	1	1	1
10-20			8	7	5	3	2	2	2	1	1	1	1
20-30			4	3	3	3	2	2	1	1	1	1	1
30-40			3	3	2	1	1	1	1	1	1	1	1
40-50			4	3	2	1	1	1	1	1	0	0	0
50-60			4	3	2	1	1	1	1	1	1	0	0
70-80			3	3	2	2	1	1	1	1	1	1	1
80-90			3	3	2	2	1	1	1	1	1	1	1

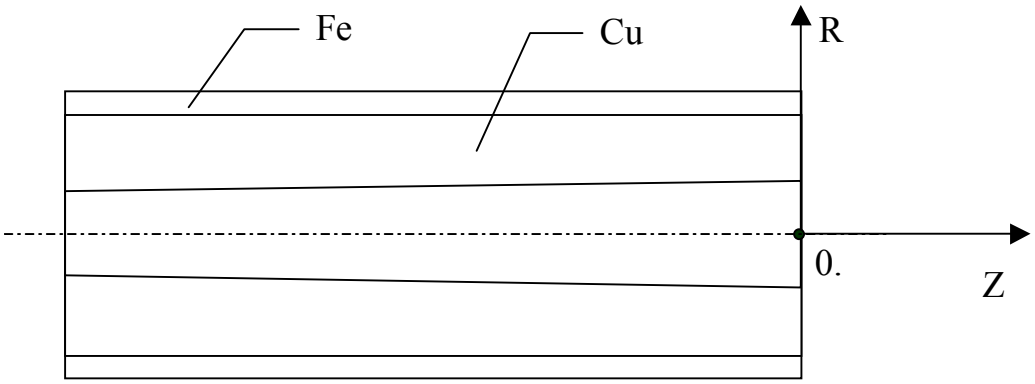

Doze rate field in the copper plug region due to radioactivity induced by high energy hadrons, μSv/h

T=30d, t=1 d

Z, cm

R,cm	-(20 –10)	-(10 -0)	0.	0-10	10-20	20-30	30-40	40-50	50-60	60-70	70-80	80-90	90-100
5-10	1467.	1361.	980.	871.	478.	299.	206.	148.	107.	79.	57.	41.	30.
10-20			1154.	832.	365.	239.	156.	106.	82.	67.	56.	45.	35.
20-30			286.	271.	216.	162.	141.	107.	78.	61.	50.	43.	38.
30-40			201.	150.	119.	86.	78.	73.	60.	51.	47.	43.	40.
40-50			82.	74.	87.	56.	61.	56.	46.	33.	25.	25.	28.
50-60			59.	56.	71.	46.	36.	51.	48.	40.	27.	17.	13.
70-80			50.	47.	55.	50.	25.	29.	43.	41.	35.	24.	16.
80-90			44.	41.	44.	49.	27.	19.	25.	37.	36.	30.	21.

T = 30 d, t = 5 d

Z, cm

R,cm	-(20 –10)	-(10 -0)	0.	0-10	10-20	20-30	30-40	40-50	50-60	60-70	70-80	80-90	90-100
5-10	943.	871.	629.	557.	306.	191.	132.	94.	69.	51.	36.	26.	19.
10-20			730.	529.	233.	153.	100.	68.	53.	43.	36.	29.	22.
20-30			187.	174.	138.	104.	90.	68.	50.	39.	32.	28.	24.
30-40			126.	94.	76.	55.	50.	46.	39.	33.	30.	28.	25.
40-50			51.	46.	55.	35.	39.	36.	30.	21.	16.	16.	18.
50-60			37.	35.	45.	29.	23.	32.	31.	25.	17.	11.	8.
70-80			31.	29.	34.	31.	15.	19.	27.	26.	22.	15.	10.
80-90			27.	25.	27.	31.	17.	12.	16.	24.	23.	19.	14.

T=100d, t=1 d

Z, cm

R,cm	-(20 –10)	-(10 -0)	0.	0-10	10-20	20-30	30-40	40-50	50-60	60-70	70-80	80-90	90-100
5-10	1772.	1650.	1206.	1062	579.	363.	246.	178.	131.	96.	69.	49.	35.
10-20			1408.	1012	442.	288.	189.	128.	98.	80.	66.	53.	41.
20-30			360.	335.	259.	194.	169.	127.	92.	73.	60.	52.	45.
30-40			201.	158.	140.	103.	94.	88.	73.	61.	56.	52.	48.
40-50			80.	74.	98.	63.	71.	66.	55.	39.	30.	30.	33.
50-60			57.	54.	78.	50.	40.	58.	55.	45.	30.	19.	15.
70-80			47.	44.	58.	54.	25.	32.	49.	47.	39.	27.	17.
80-90			42.	39.	45.	53.	28.	19.	28.	42.	41.	34.	23.

T = 100 d, t = 5 d

Z, cm

R,cm	-(20 –10)	-(10 -0)	0.	0-10	10-20	20-30	30-40	40-50	50-60	60-70	70-80	80-90	90-100
5-10	1698.	1576.	1123.	1006	551.	346.	233.	169.	125.	92.	66.	47.	33.
10-20			1316.	958.	421.	274.	180.	122.	93.	75.	62.	50.	38.
20-30			349.	320.	245.	184.	159.	120.	87.	69.	57.	49.	43.
30-40			174.	141.	131.	97.	90.	83.	69.	58.	53.	49.	45.
40-50			68.	64.	90.	57.	66.	62.	52.	37.	29.	29.	32.
50-60			48.	46.	70.	45.	36.	54.	51.	42.	28.	17.	14.
70-80			40.	38.	52.	49.	22.	29.	46.	44.	36.	24.	15.
80-90			36.	33.	39.	48.	24.	16.	25.	39.	38.	31.	21.

T = 5 y, t = 1 d

Z, cm

R,cm	-(20 –10)	-(10 -0)	0.	0-10	10-20	20-30	30-40	40-50	50-60	60-70	70-80	80-90	90-100
5-10	3113.	2887.	2060.	1840.	1009.	630.	425.	307.	227.	167.	119.	85.	61.
10-20			2415.	1746.	764.	500.	328.	221.	170.	138.	115.	91.	70.
20-30			632.	580.	445.	336.	290.	220.	160.	126.	104.	90.	78.
30-40			340.	267.	239.	176.	163.	152.	125.	106.	97.	90.	83.
40-50			131.	122.	166.	106.	121.	114.	95.	68.	52.	52.	57.
50-60			93.	88.	130.	83.	67.	99.	94.	78.	52.	32.	26.
70-80			78.	73.	97.	90.	42.	54.	84.	80.	67.	45.	28.
80-90			69.	63.	74.	89.	46.	31.	46.	72.	70.	58.	39.

T = 5 y, t = 5 d

Z, cm

R,cm	-(20 –10)	-(10 -0)	0.	0-10	10-20	20-30	30-40	40-50	50-60	60-70	70-80	80-90	90-100
5-10	2420.	2257.	1617.	1441.	782.	490.	329.	238.	177.	131.	93.	66.	47.
10-20			1882.	1358.	595.	388.	255.	172.	131.	106.	88.	70.	54.
20-30			505.	455.	345.	260.	225.	169.	123.	97.	81.	70.	61.
30-40			242.	196.	184.	136.	127.	118.	97.	82.	75.	70.	65.
40-50			92.	87.	125.	79.	92.	88.	74.	53.	41.	41.	45.
50-60			65.	62.	97.	62.	50.	75.	72.	59.	39.	24.	20.
70-80			54.	51.	71.	67.	30.	41.	64.	61.	51.	34.	21.
80-90			48.	44.	53.	67.	33.	22.	35.	55.	53.	44.	29.

T = 10 y, t = 1 d

Z, cm

R,cm	-(20 –10)	-(10 -0)	0.	0-10	10-20	20-30	30-40	40-50	50-60	60-70	70-80	80-90	90-100
5-10	3158.	2927.	2120.	1869.	1018.	639.	430.	312.	230.	170.	122.	86.	62.
10-20			2447.	1766.	776.	507.	333.	224.	172.	140.	116.	93.	71.
20-30			641.	587.	451.	340.	295.	222.	162.	128.	106.	92.	80.
30-40			342.	269.	242.	178.	166.	154.	127.	107.	98.	91.	84.
40-50			131.	122.	167.	106.	122.	115.	96.	69.	53.	53.	58.
50-60			93.	88.	131.	84.	68.	100.	95.	79.	52.	33.	26.
70-80			78.	73.	97.	91.	42.	55.	85.	82.	68.	45.	28.
80-90			69.	63.	74.	90.	46.	31.	47.	73.	71.	59.	40.

T = 10 y, t = 5 d

Z, cm

R,cm	-(20 -10)	-(10 -0)	0.	0-10	10-20	20-30	30-40	40-50	50-60	60-70	70-80	80-90	90-100
5-10	2505.	2320.	1658.	1477.	805.	506.	339.	246.	183.	135.	96.	68.	48.
10-20			1924.	1401.	615.	401.	264.	177.	135.	110.	90.	73.	56.
20-30			518.	469.	355.	267.	232.	174.	127.	100.	83.	72.	63.
30-40			244.	199.	189.	140.	132.	122.	100.	84.	77.	72.	66.
40-50			92.	87.	128.	81.	94.	90.	76.	54.	42.	42.	46.
50-60			65.	62.	99.	63.	51.	77.	74.	61.	40.	25.	20.
70-80			54.	51.	73.	68.	30.	41.	65.	63.	52.	34.	21.
80-90			48.	44.	54.	68.	33.	22.	36.	56.	54.	45.	30.

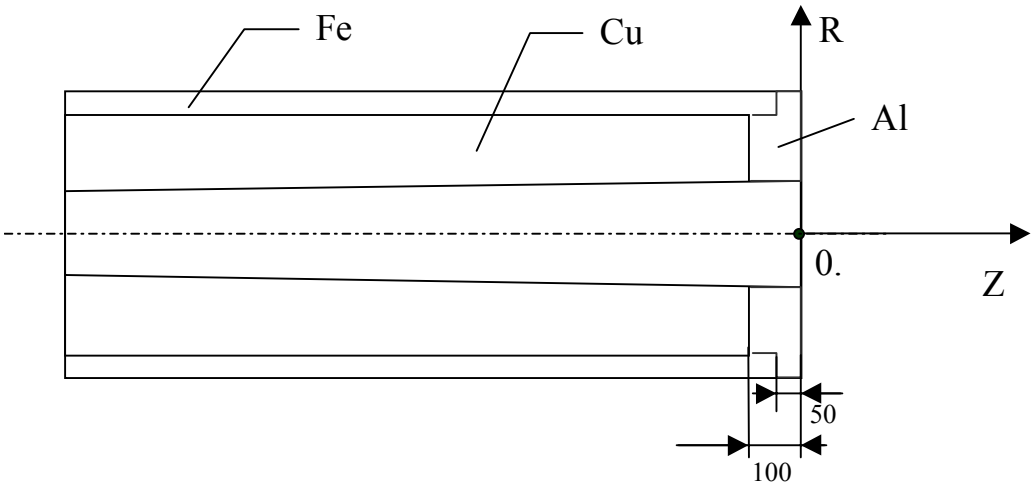

Doze rate field in the copper plug region due to radioactivity induced by high energy hadrons, μSv/h

T = 30 d, t = 1 d

Z, cm

R,cm	-(20 -10)	-(10 -0)	0.	0-10	10-20	20-30	30-40	40-50	50-60	60-70	70-80	80-90	90-100
5-10	1617.	1256.	829.	728.	420.	273.	192.	135.	97.	68.	48.	34.	25.
10-20			705.	567.	322.	209.	139.	103.	82.	67.	54.	41.	30.
20-30			258.	230.	182.	154.	125.	95.	76.	62.	53.	46.	39.
30-40			107.	98.	87.	83.	78.	64.	52.	48.	47.	45.	43.
40-50			79.	70.	64.	51.	61.	54.	39.	27.	23.	25.	28.
50-60			68.	60.	59.	38.	42.	54.	48.	33.	20.	14.	12.
70-80			59.	53.	51.	39.	25.	35.	47.	43.	31.	20.	14.
80-90			53.	48.	44.	40.	26.	21.	30.	40.	37.	28.	19.

T = 30 d, t = 5 d

Z, cm

R,cm	-(20 -10)	-(10 -0)	0.	0-10	10-20	20-30	30-40	40-50	50-60	60-70	70-80	80-90	90-100
5-10	998.	737.	463.	403.	234.	149.	106.	73.	50.	33.	22.	15.	11.
10-20			316.	267.	173.	112.	74.	57.	46.	38.	30.	22.	16.
20-30			96.	88.	87.	82.	65.	51.	43.	36.	31.	27.	23.
30-40			48.	41.	36.	44.	41.	30.	24.	25.	26.	26.	25.
40-50			45.	37.	28.	25.	34.	30.	19.	12.	11.	12.	14.
50-60			41.	34.	29.	19.	22.	31.	27.	17.	10.	7.	6.
70-80			36.	31.	26.	20.	14.	18.	27.	25.	17.	11.	8.
80-90			32.	29.	23.	20.	15.	11.	16.	23.	22.	15.	10.

T = 100 d, t = 1 d

Z, cm

R,cm	-(20 -10)	-(10 -0)	0.	0-10	10-20	20-30	30-40	40-50	50-60	60-70	70-80	80-90	90-100
5-10	2467.	1892.	1246.	1081	625.	402.	282.	199.	142.	98.	67.	47.	33.
10-20			1000.	812.	474.	307.	202.	151.	121.	98.	78.	60.	43.
20-30			347.	312.	257.	224.	180.	137.	111.	93.	80.	69.	59.
30-40			137.	128.	117.	121.	113.	91.	74.	70.	69.	68.	64.
40-50			97.	86.	82.	69.	88.	78.	55.	37.	33.	35.	41.
50-60			82.	73.	74.	47.	55.	76.	68.	45.	27.	19.	16.
70-80			71.	64.	64.	49.	32.	46.	66.	60.	42.	26.	18.
80-90			64.	58.	54.	50.	32.	26.	40.	57.	52.	37.	24.

T = 100 d, t = 5 d

Z, cm

R,cm	-(20 -10)	-(10 -0)	0.	0-10	10-20	20-30	30-40	40-50	50-60	60-70	70-80	80-90	90-100
5-10	1795.	1348.	846.	736.	427.	271.	192.	134.	92.	62.	41.	28.	20.
10-20			597.	499.	316.	204.	134.	102.	82.	67.	53.	40.	28.
20-30			183.	167.	159.	147.	118.	90.	76.	65.	56.	49.	41.
30-40			77.	69.	65.	79.	75.	56.	45.	45.	47.	47.	45.
40-50			62.	52.	45.	41.	59.	53.	34.	21.	20.	22.	26.
50-60			54.	46.	43.	28.	34.	52.	46.	29.	16.	11.	10.
70-80			47.	42.	37.	29.	20.	29.	44.	41.	27.	16.	11.
80-90			42.	38.	33.	29.	20.	16.	25.	38.	35.	24.	15.

T = 5 y, t = 1 d

Z, cm

R,cm	-(20 -10)	-(10 -0)	0.	0-10	10-20	20-30	30-40	40-50	50-60	60-70	70-80	80-90	90-100
5-10	2755.	2173.	1447.	1268.	728.	471.	330.	234.	170.	121.	85.	59.	42.
10-20			1252.	1003.	560.	364.	243.	178.	140.	114.	91.	70.	52.
20-30			464.	410.	317.	266.	215.	163.	128.	106.	91.	79.	67.
30-40			171.	162.	152.	145.	135.	112.	91.	84.	81.	78.	73.
40-50			108.	99.	102.	84.	101.	92.	67.	47.	41.	43.	49.
50-60			89.	80.	89.	57.	65.	87.	78.	54.	33.	23.	20.
70-80			77.	69.	74.	58.	37.	54.	75.	68.	49.	31.	21.
80-90			68.	62.	62.	59.	35.	29.	47.	64.	59.	43.	28.

T = 5 y, t = 5 d

Z, cm

R,cm	-(20 -10)	-(10 -0)	0.	0-10	10-20	20-30	30-40	40-50	50-60	60-70	70-80	80-90	90-100
5-10	2109.	1624.	1078.	930.	538.	344.	241.	171.	122.	86.	59.	41.	29.
10-20			858.	698.	408.	265.	175.	130.	103.	84.	67.	51.	37.
20-30			301.	268.	221.	192.	155.	117.	95.	80.	68.	59.	50.
30-40			112.	105.	100.	104.	98.	78.	63.	60.	59.	58.	55.
40-50			73.	65.	66.	57.	74.	67.	47.	32.	28.	30.	35.
50-60			61.	54.	58.	38.	45.	63.	56.	38.	22.	16.	14.
70-80			53.	47.	49.	38.	25.	37.	54.	49.	34.	21.	14.
80-90			47.	43.	41.	39.	24.	20.	32.	47.	43.	30.	19.

T = 10 y, t = 1 d

Z, cm

R,cm	-(20 -10)	-(10 -0)	0.	0-10	10-20	20-30	30-40	40-50	50-60	60-70	70-80	80-90	90-100
5-10	2810.	2243.	1489.	1309.	755.	489.	341.	244.	178.	128.	89.	63.	45.
10-20			1341.	1063.	584.	379.	253.	184.	144.	118.	94.	73.	54.
20-30			500.	441.	333.	277.	225.	169.	133.	109.	93.	81.	69.
30-40			180.	172.	162.	151.	141.	118.	96.	88.	84.	80.	75.
40-50			109.	101.	108.	88.	105.	95.	71.	50.	44.	46.	51.
50-60			90.	81.	93.	60.	67.	89.	80.	56.	35.	24.	22.
70-80			77.	70.	77.	60.	38.	56.	77.	70.	51.	32.	21.
80-90			68.	62.	63.	61.	36.	30.	48.	66.	61.	45.	29.

T = 10 y, t = 5 d

Z, cm

R,cm	-(20 -10)	-(10 -0)	0.	0-10	10-20	20-30	30-40	40-50	50-60	60-70	70-80	80-90	90-100
5-10	2196.	1713.	1122.	984.	570.	365.	256.	182.	131.	92.	64.	44.	31.
10-20			938.	759.	434.	282.	187.	138.	109.	88.	71.	54.	40.
20-30			337.	298.	239.	204.	165.	125.	100.	83.	72.	62.	53.
30-40			121.	115.	111.	111.	104.	85.	69.	64.	63.	61.	58.
40-50			75.	68.	72.	61.	78.	71.	51.	35.	31.	33.	38.
50-60			62.	55.	62.	40.	47.	66.	59.	41.	24.	17.	15.
70-80			53.	48.	52.	40.	26.	39.	56.	52.	36.	22.	15.
80-90			47.	43.	42.	41.	25.	21.	34.	49.	45.	32.	20.

Induced Activity in Lead Based Materials

Here are given results of routine induced activity simulations in the ATLAS detector materials. Two lead based materials were studied—chemical pure lead and hard lead (PB-Sb alloy). Elementary composition is given in the table below.

Fig. 1-12 present contact dose rate for chemical lead.
Fig. 13-24 present contact dose rate for hard lead.

Table

Concentration of elements in materials, %

Element	Chemical Lead, UNS L51120	Hard Lead, UNS L52901
Fe	<0.002	
Cu	0.04 - 0.08	
Zn	<0.001	
As	<0.002	
Ag	0.002 - 0.02	
Sn	<0.002	
Sb	<0.002	3
Pb	99.9	97
Bi	<0.005	

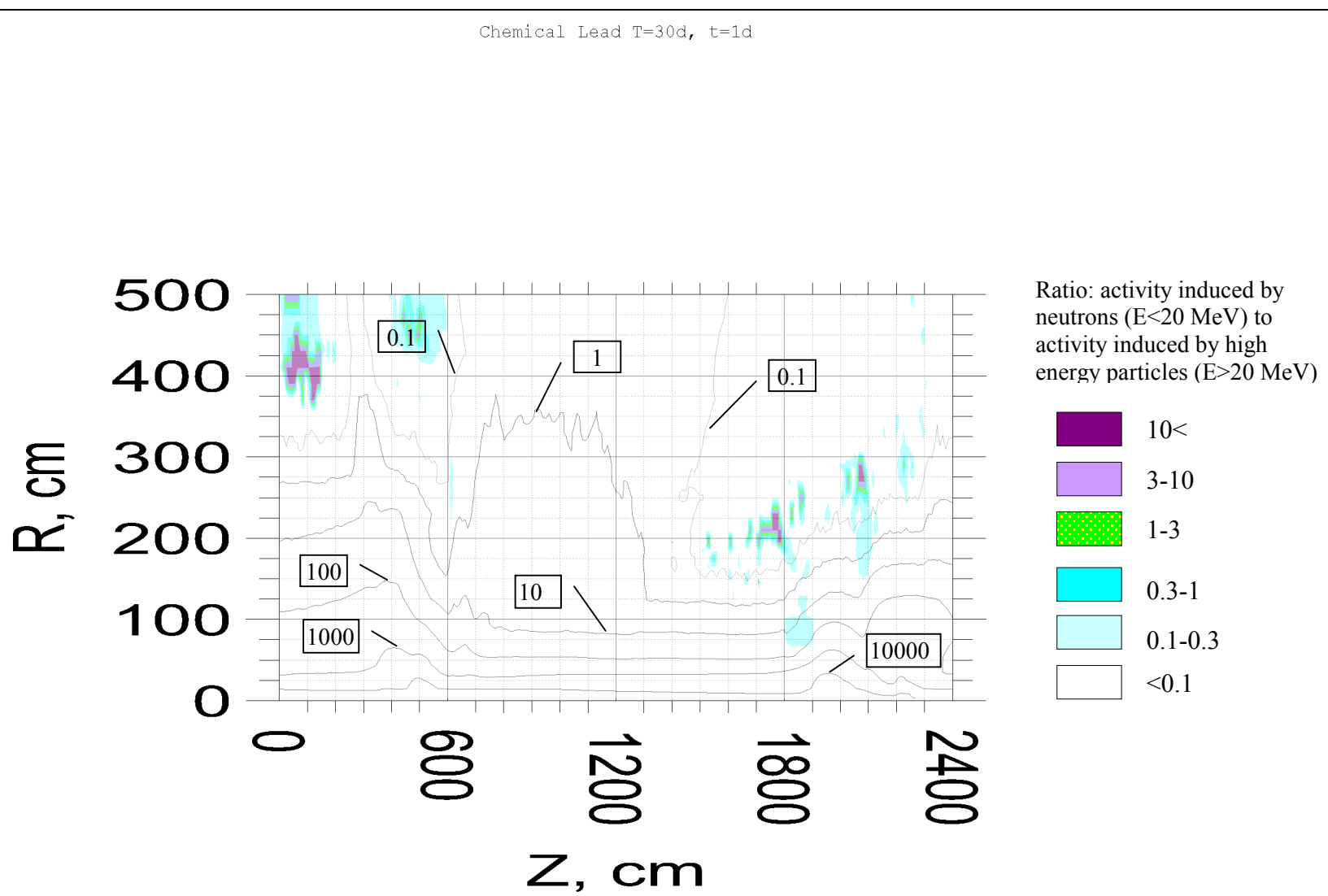

Fig .1. Distribution of induced radioactivity in Chemical Lead calculated at T=30d, t=1d The levels show contact dose rate in μSv/h.

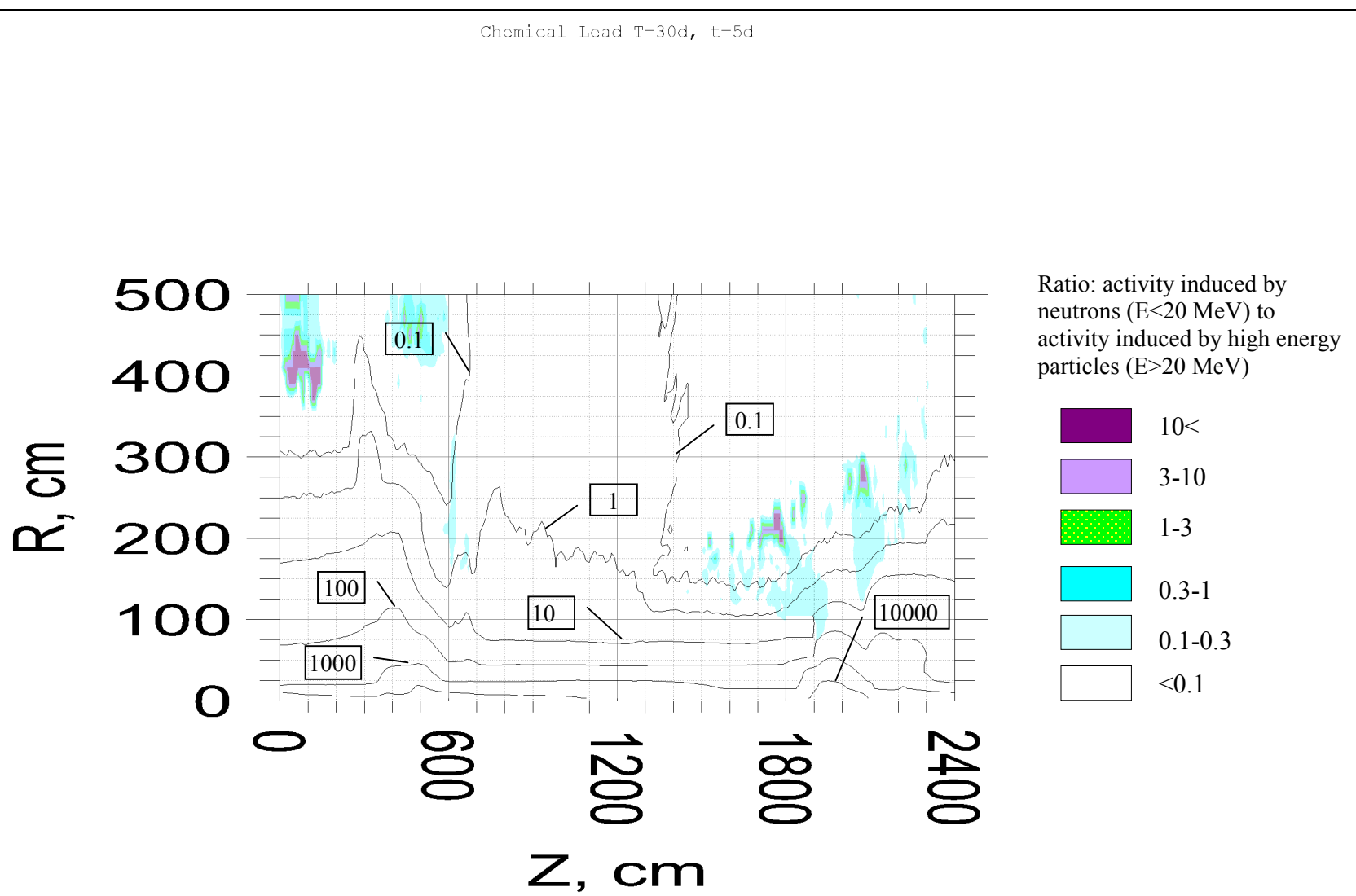

Fig .2. Distribution of induced radioactivity in Chemical Lead calculated at T=30d, t=5d The levels show contact dose rate in μSv/h.

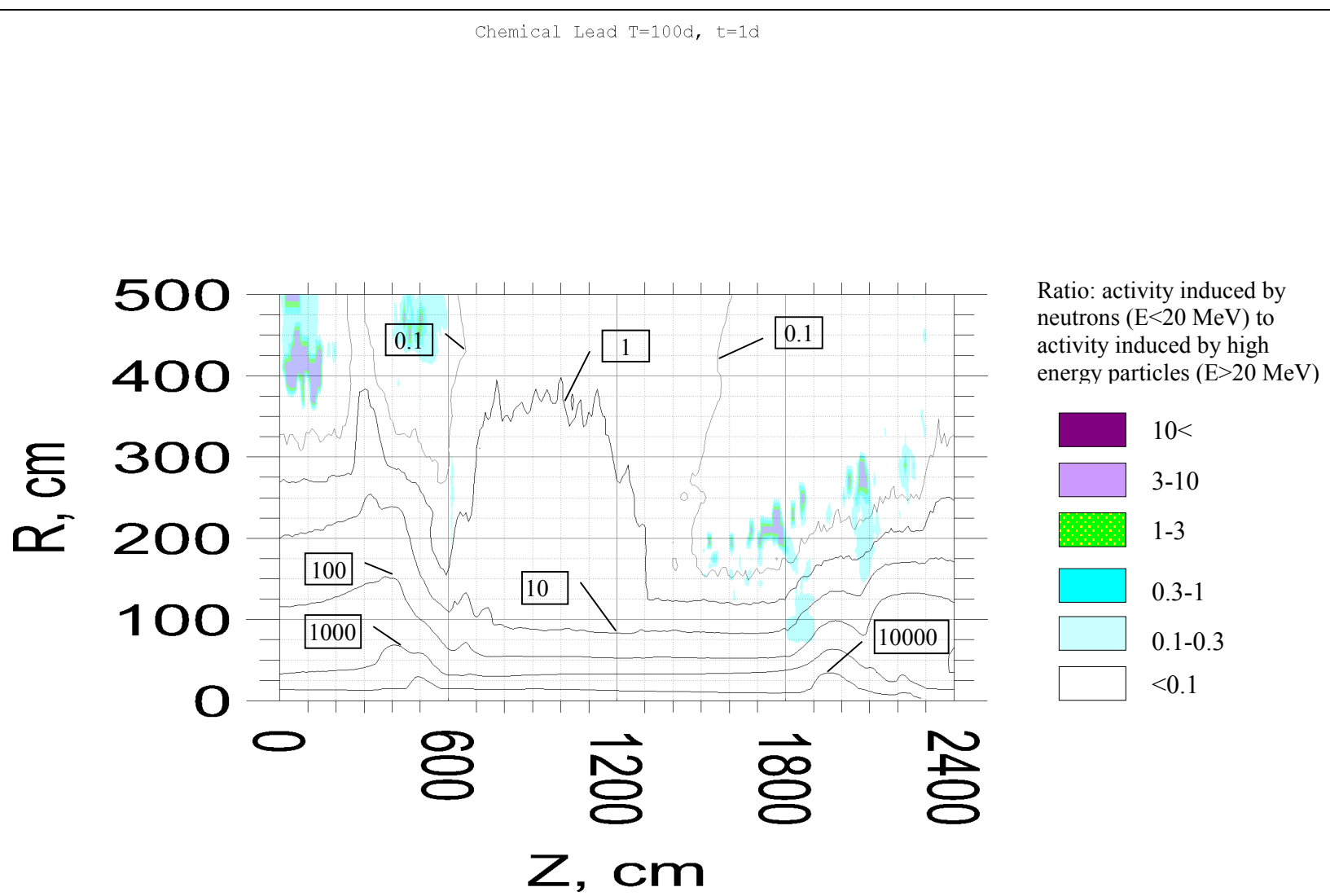

Fig .3. Distribution of induced radioactivity in Chemical Lead calculated at T=100d, t=1d. The levels show contact dose rate in μSv/h.

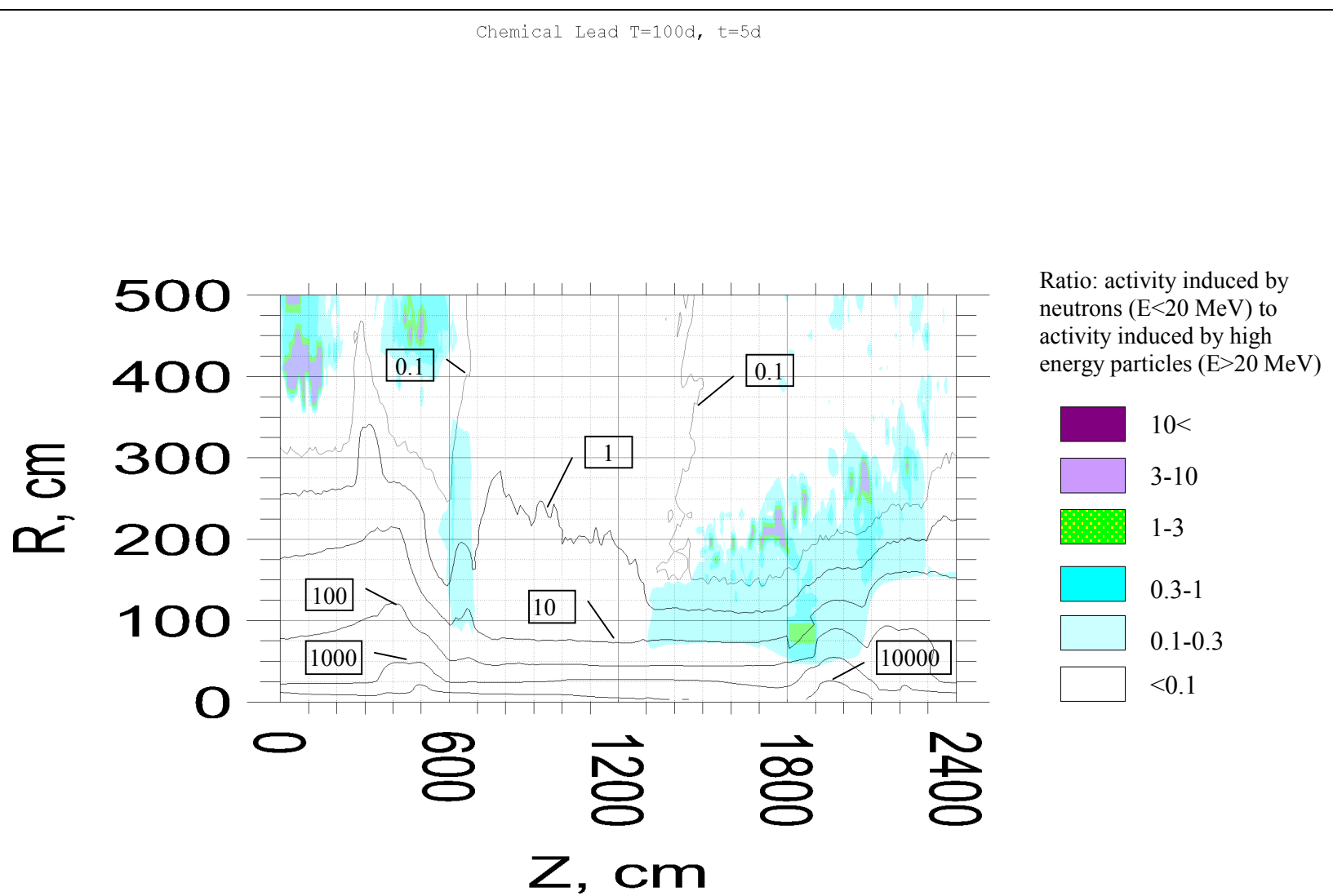

Fig .4. Distribution of induced radioactivity in Chemical Lead calculated at T=100d, t=5d. The levels show contact dose rate in μSv/h.

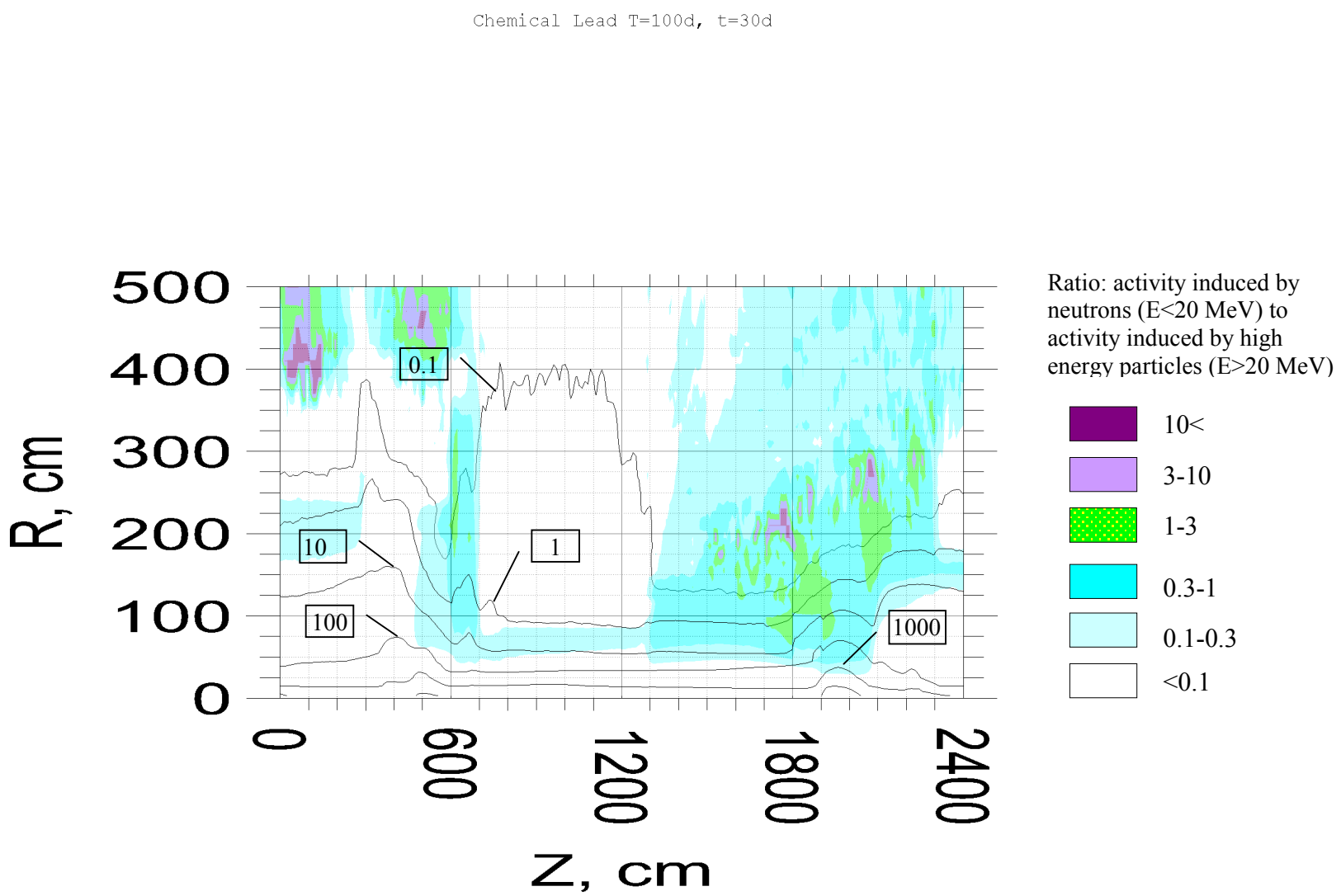

Fig .5. Distribution of induced radioactivity in Chemical Lead calculated at T=100d, t=30d. The levels show contact dose rate in μSv/h.

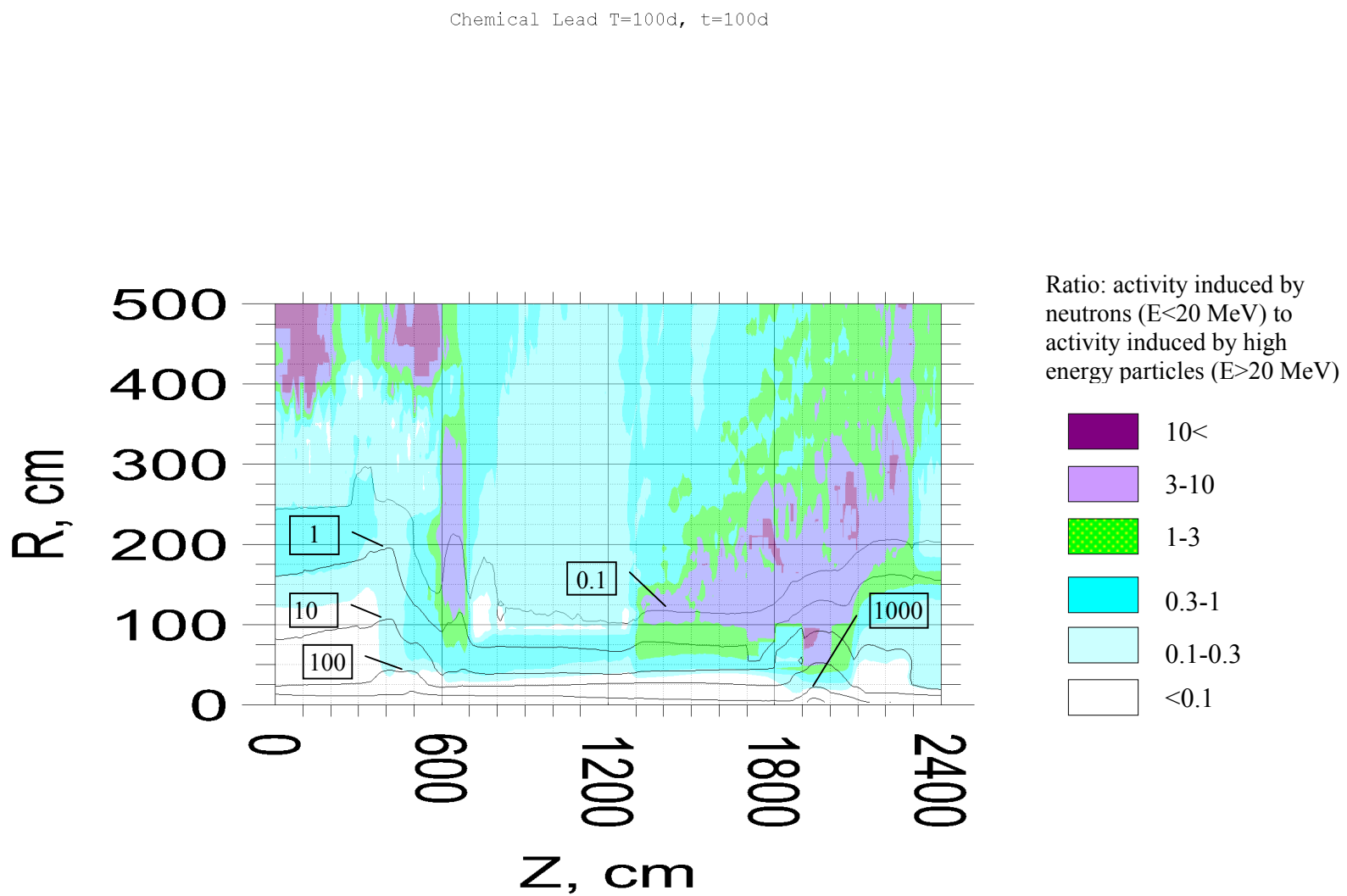

Fig .6. Distribution of induced radioactivity in Chemical Lead calculated at T=100d, t=100d. The levels show contact dose rate in μSv/h.

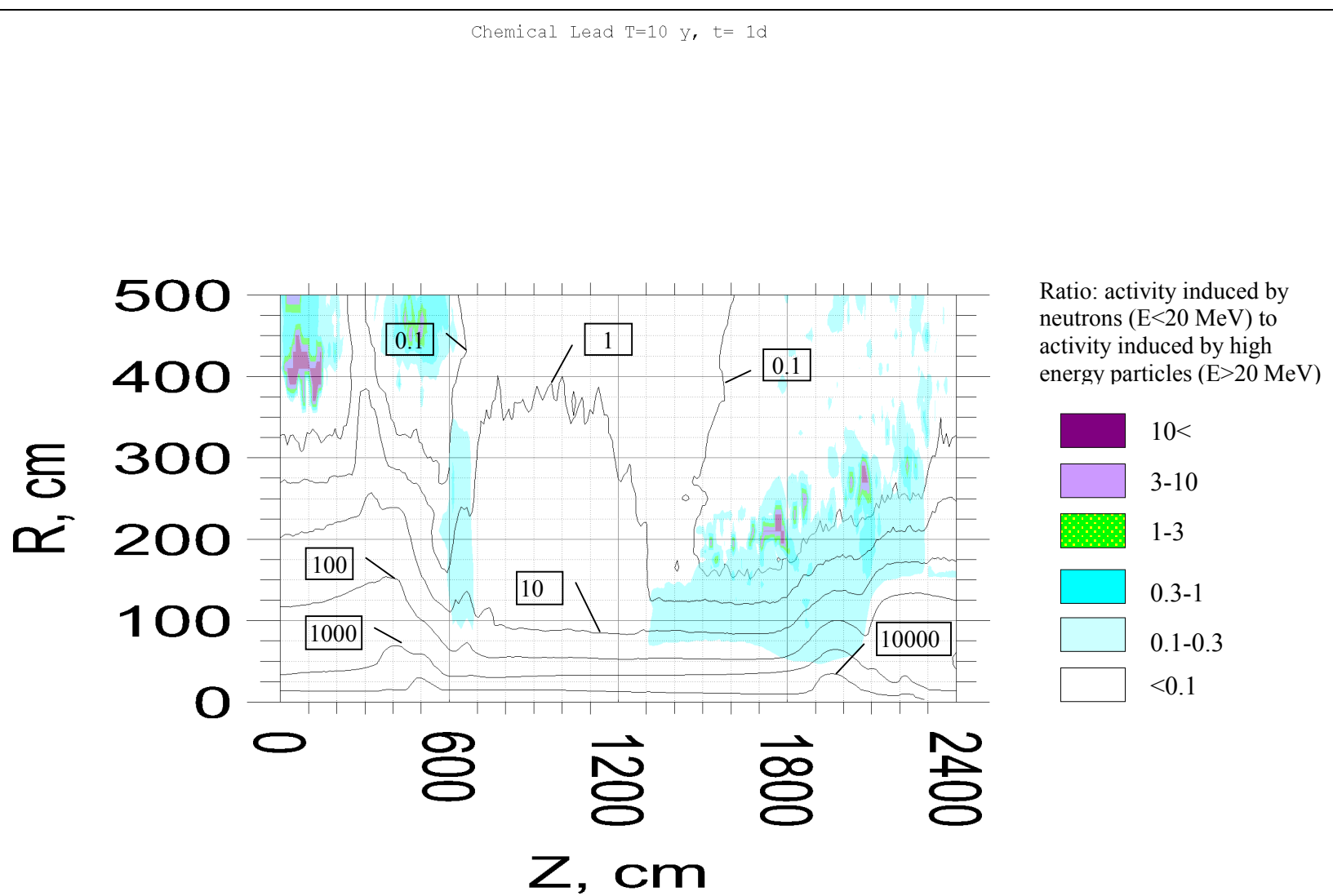

Fig .7. Distribution of induced radioactivity in Chemical Lead calculated at T=10y, t=1d. The levels show contact dose rate in μSv/h.

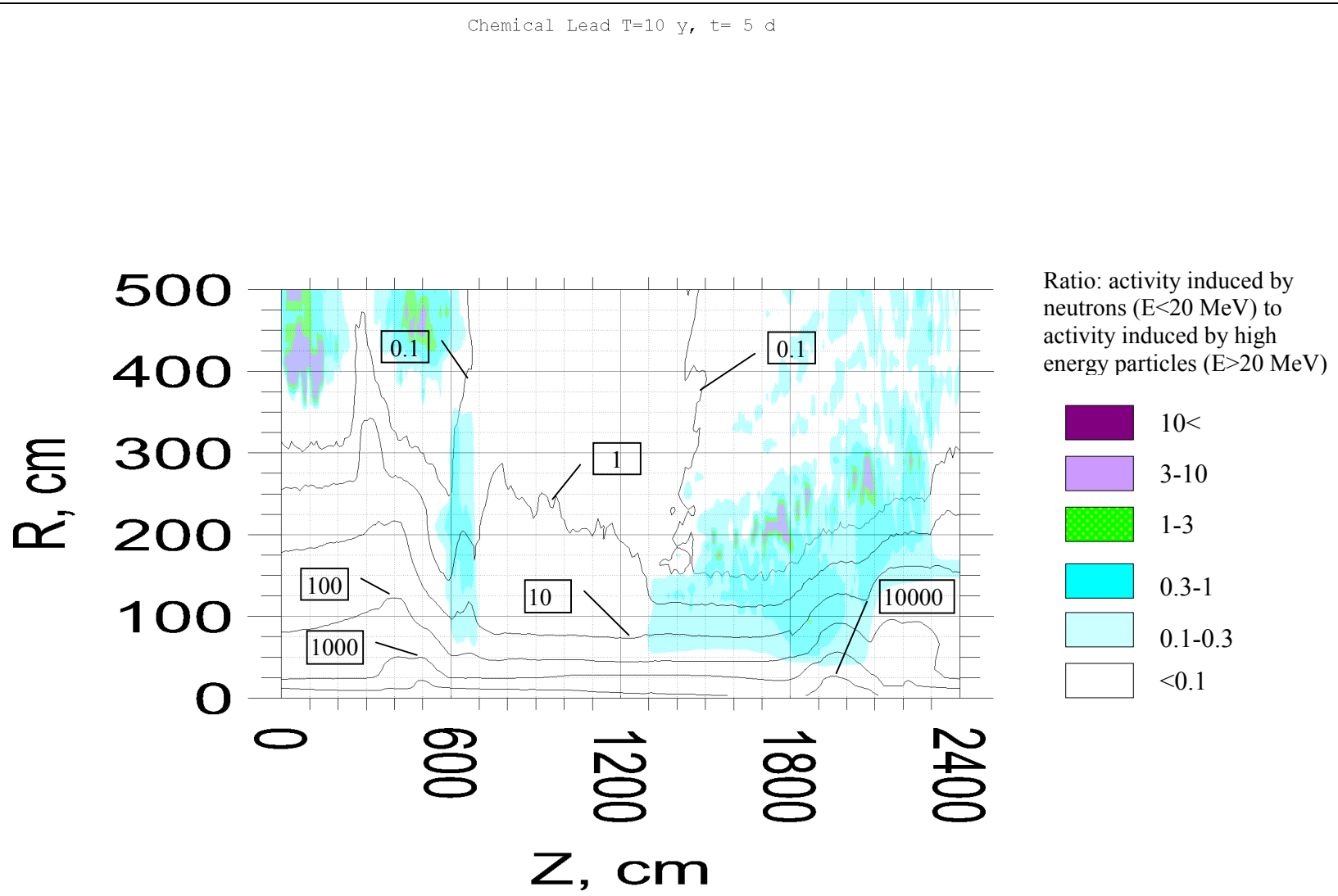

Fig .8. Distribution of induced radioactivity in Chemical Lead calculated at T=10y, t=5d. The levels show contact dose rate in μSv/h.

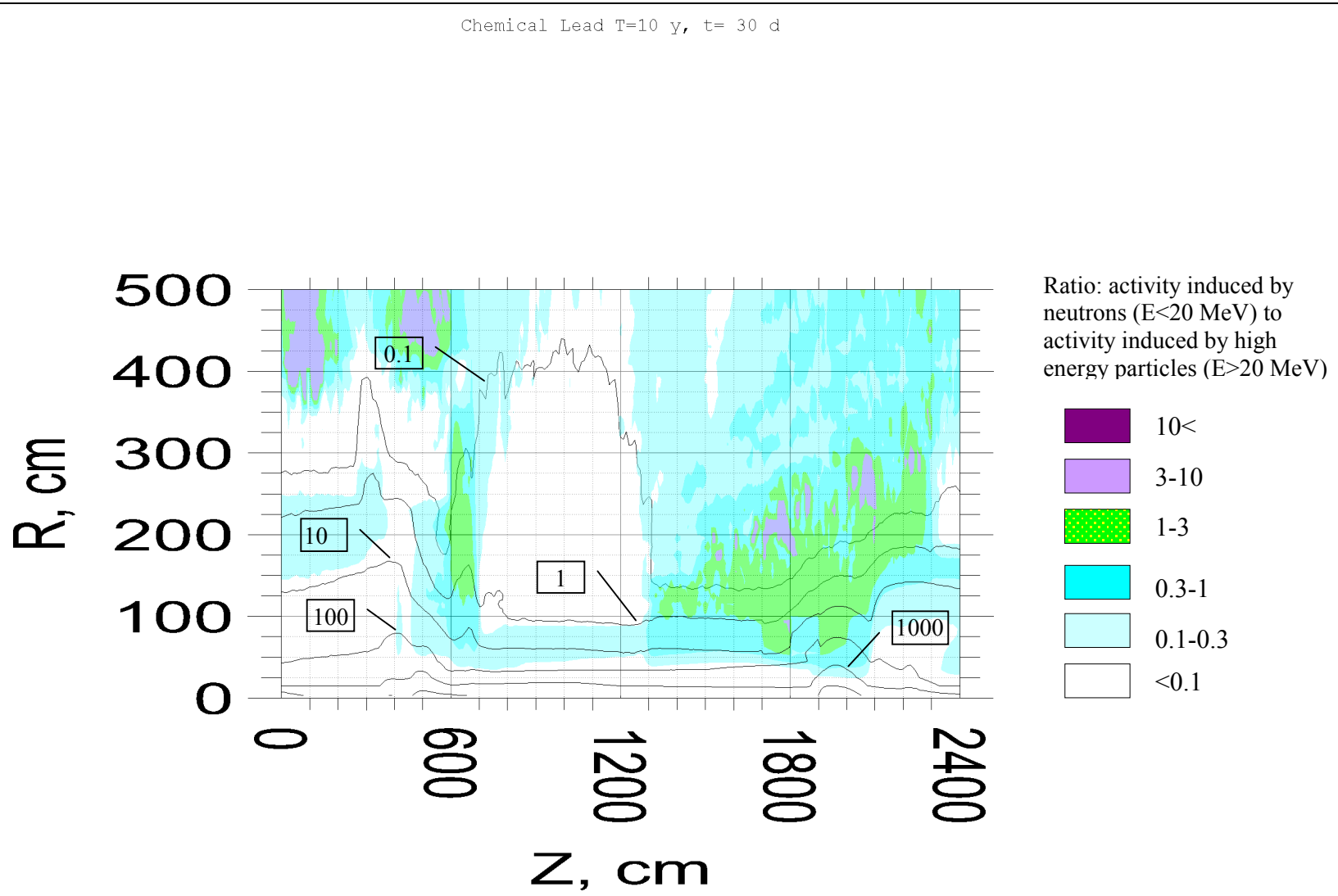

Fig .9. Distribution of induced radioactivity in Chemical Lead calculated at T=10y, t=30d. The levels show contact dose rate in μSv/h.

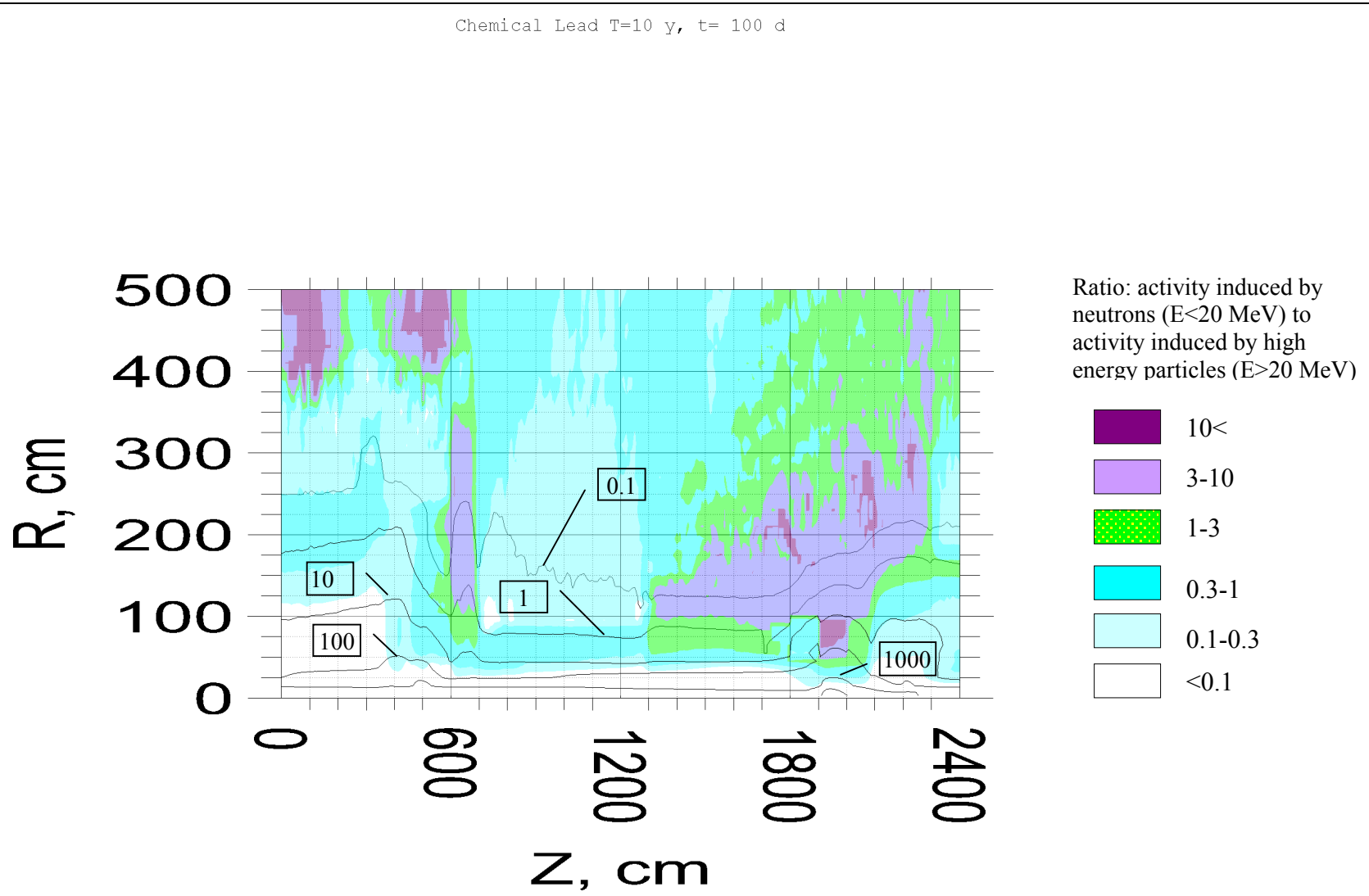

Fig .10. Distribution of induced radioactivity in Chemical Lead calculated at T=10y, t=100d. The levels show contact dose rate in μSv/h.

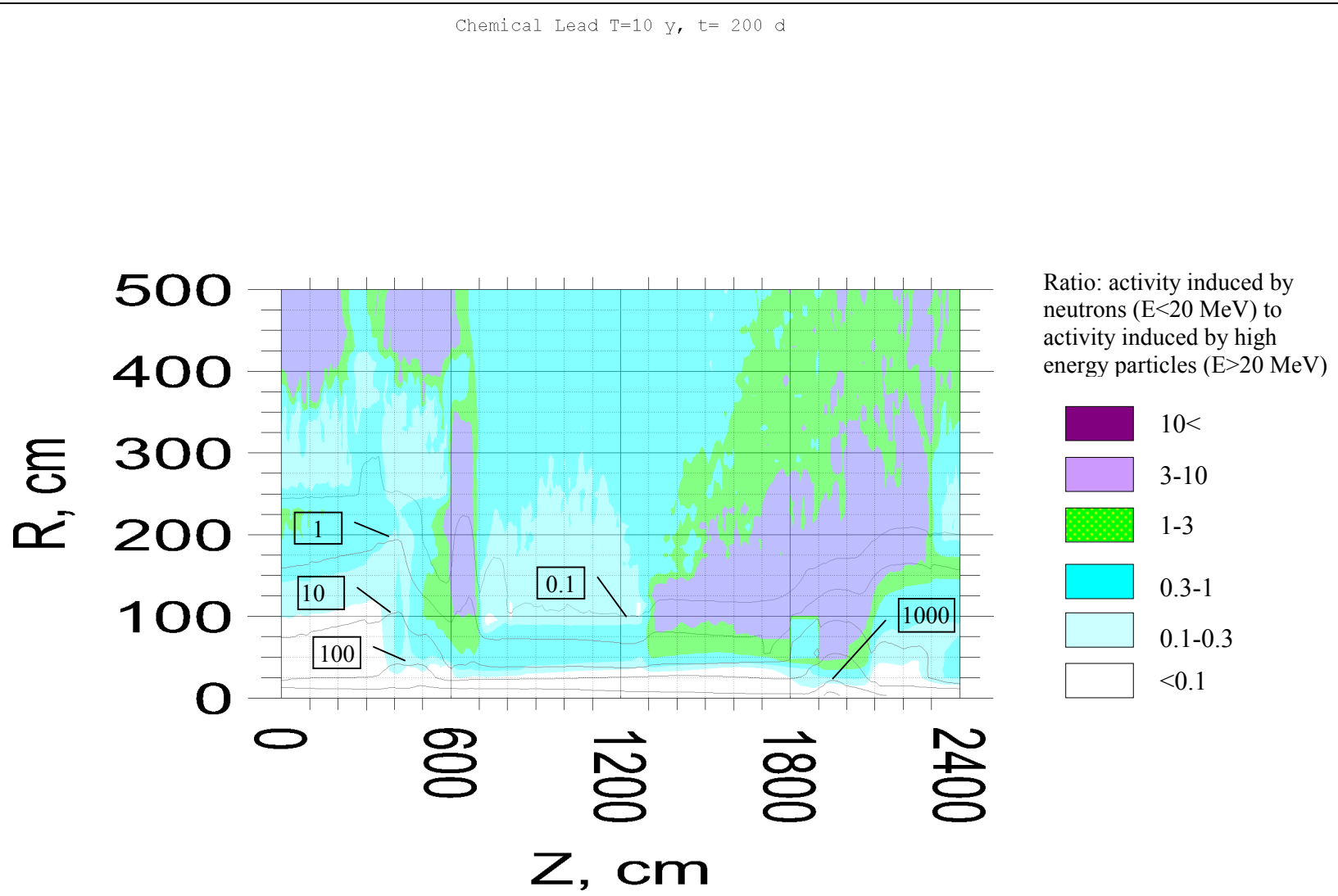

Fig .11. Distribution of induced radioactivity in Chemical Lead calculated at T=10y, t=200d. The levels show contact dose rate in μSv/h.

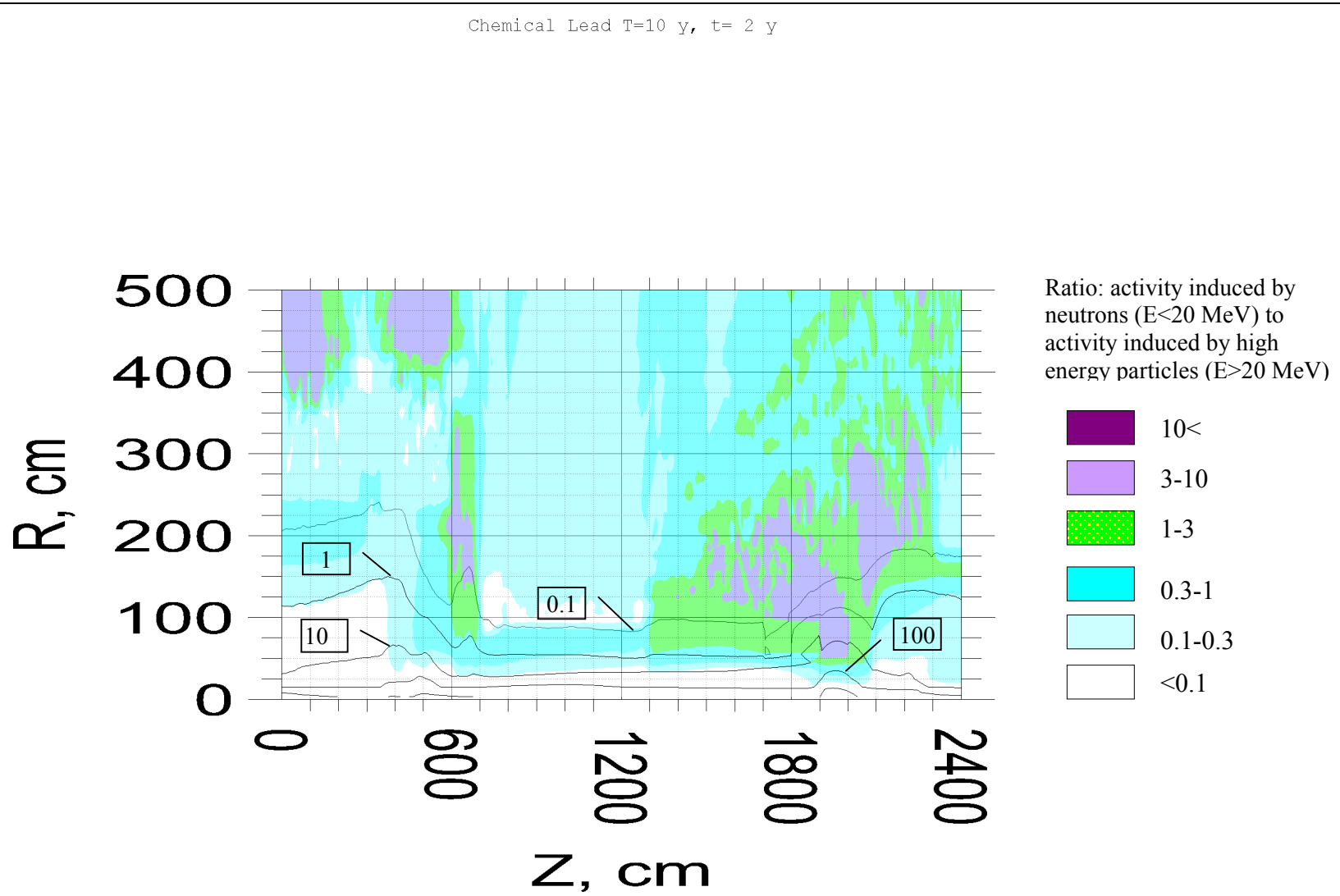

Fig .12. Distribution of induced radioactivity in Chemical Lead calculated at T=10y, t=2y. The levels show contact dose rate in μSv/h.

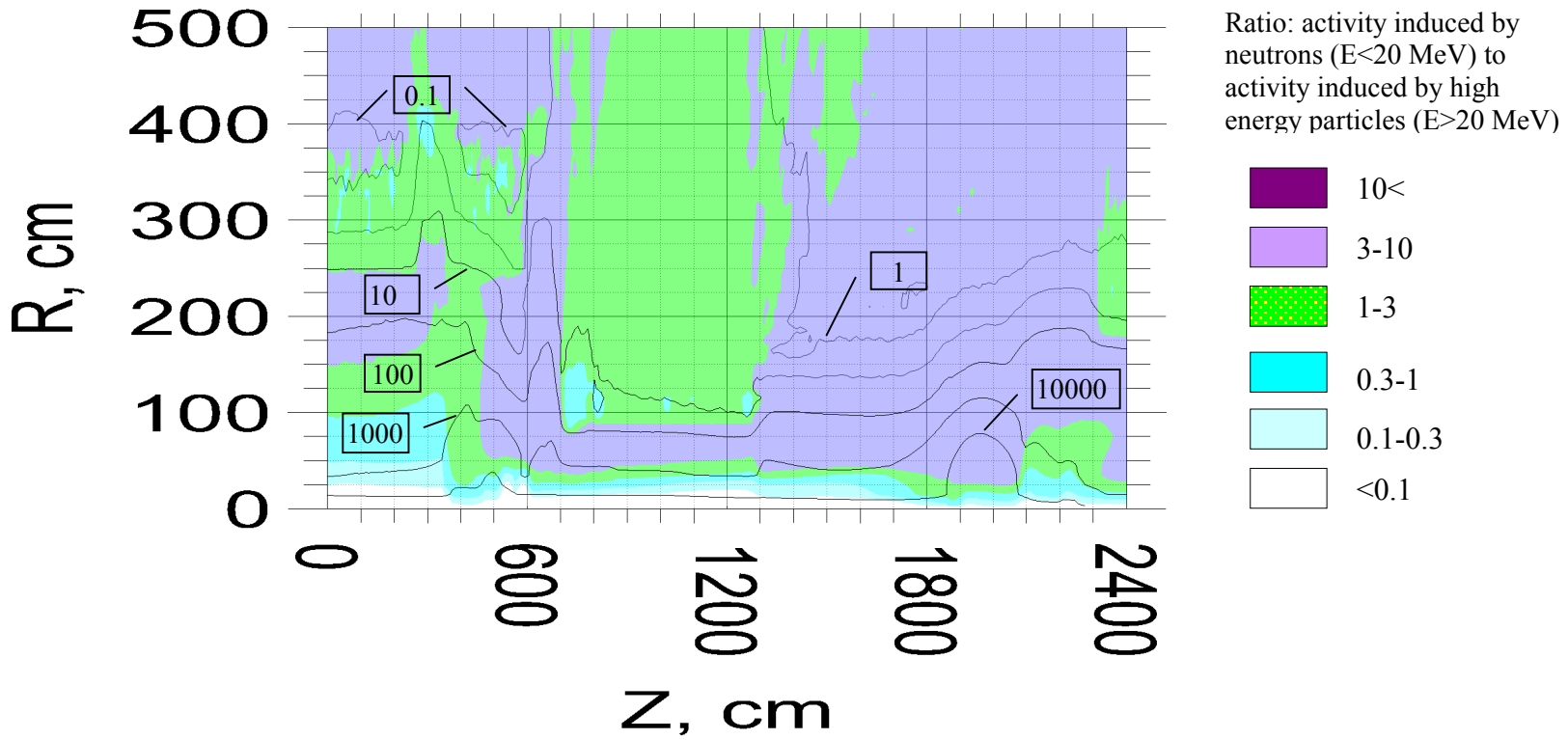

Fig .13. Distribution of induced radioactivity in Hard Lead calculated at T=30d, t=1d The levels show contact dose rate in μSv/h.

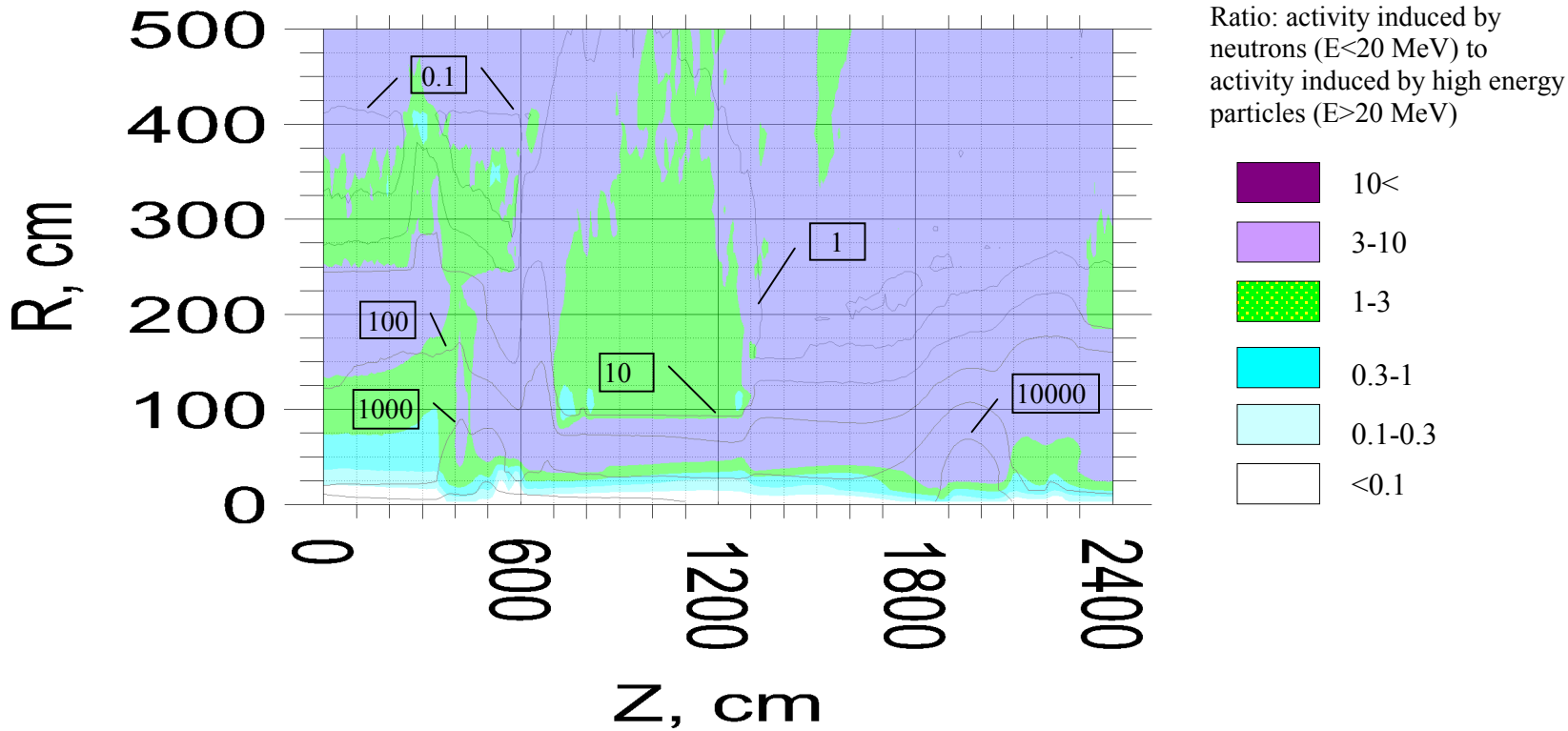

Fig .14. Distribution of induced radioactivity in Hard Lead calculated at T=30d, t=5d The levels show contact dose rate in μSv/h.

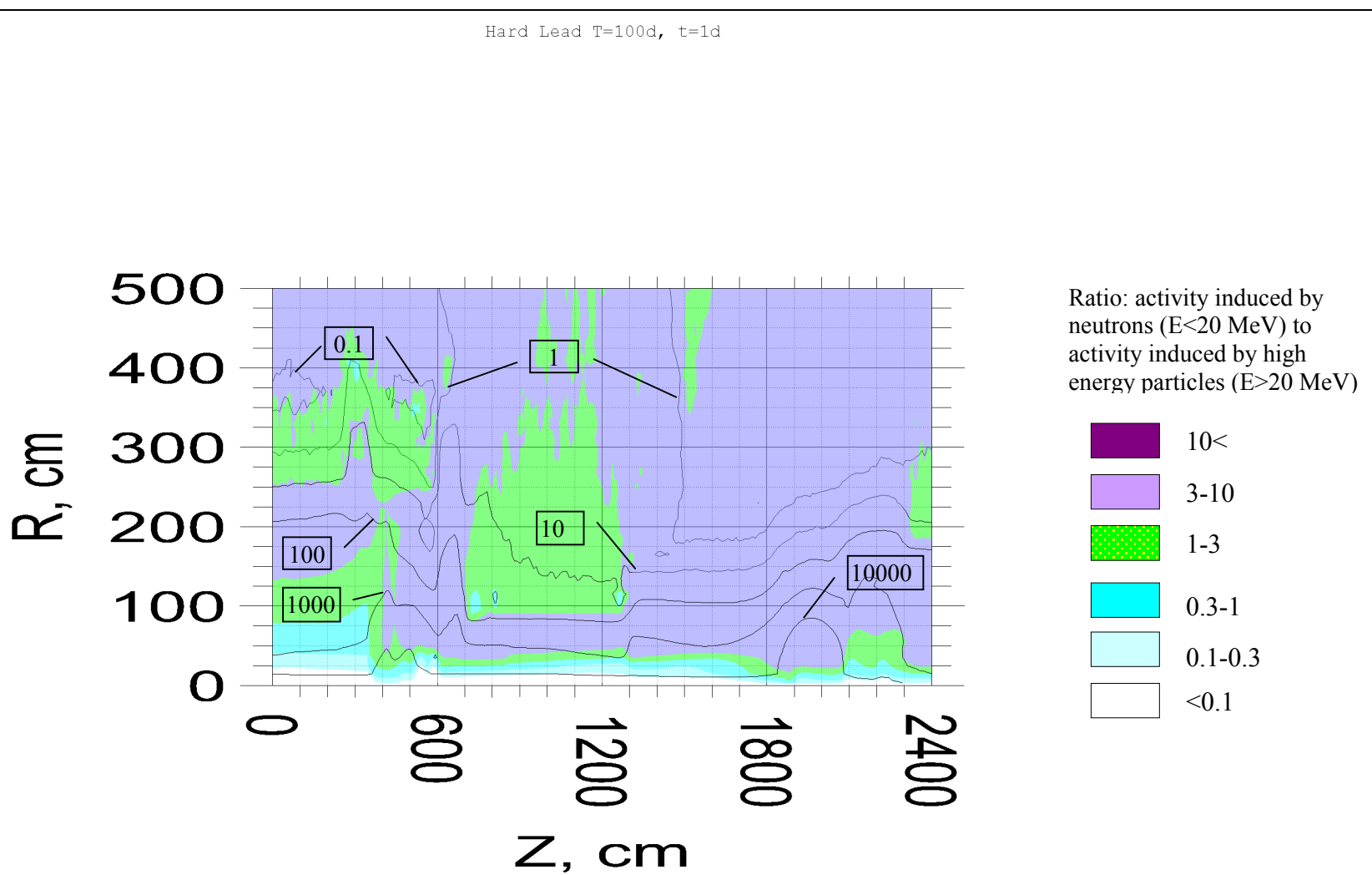

Fig .15. Distribution of induced radioactivity in Hard Lead calculated at T=100d, t=1d. The levels show contact dose rate in μSv/h.

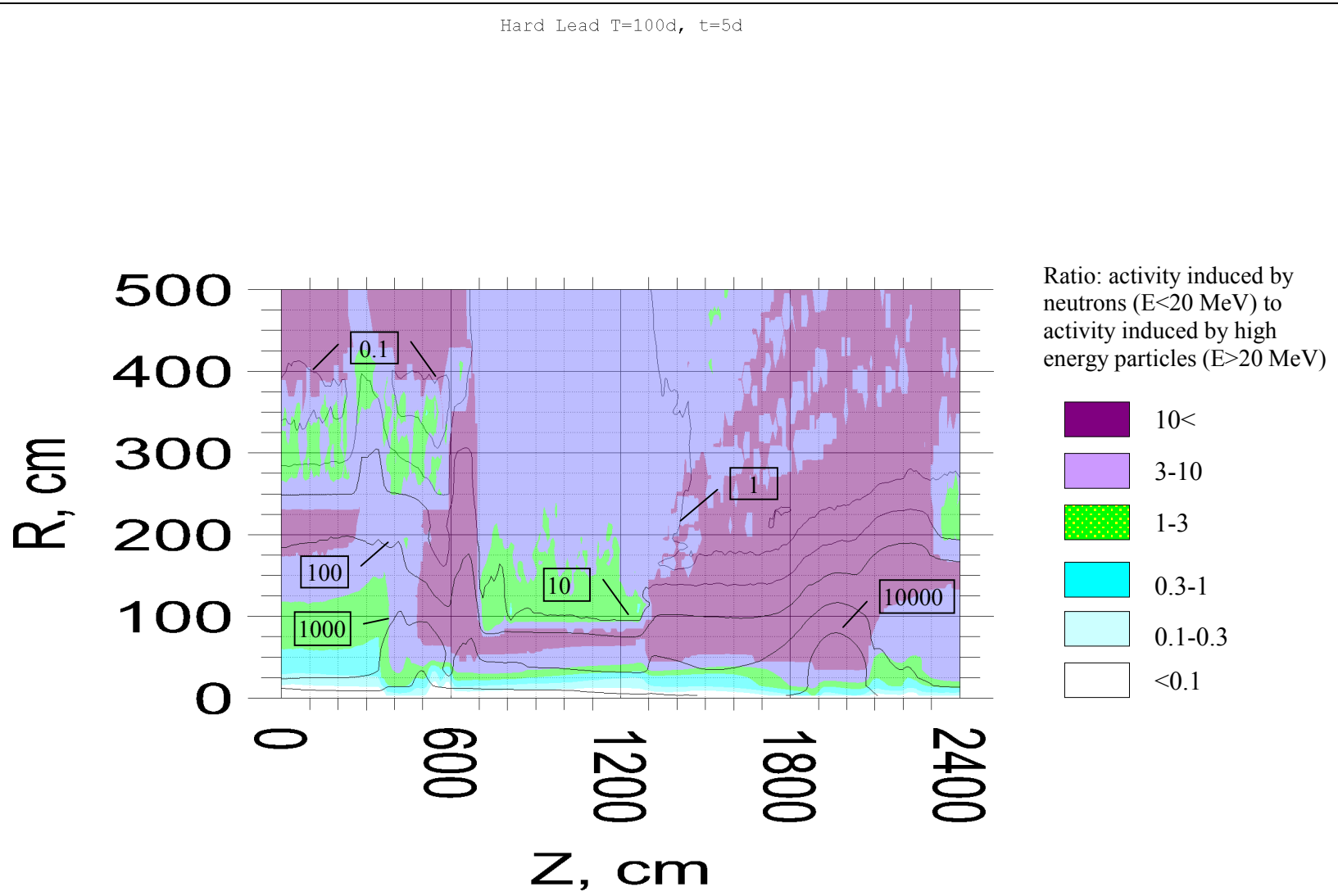

Fig .16. Distribution of induced radioactivity in Hard Lead calculated at T=100d, t=5d. The levels show contact dose rate in μSv/h.

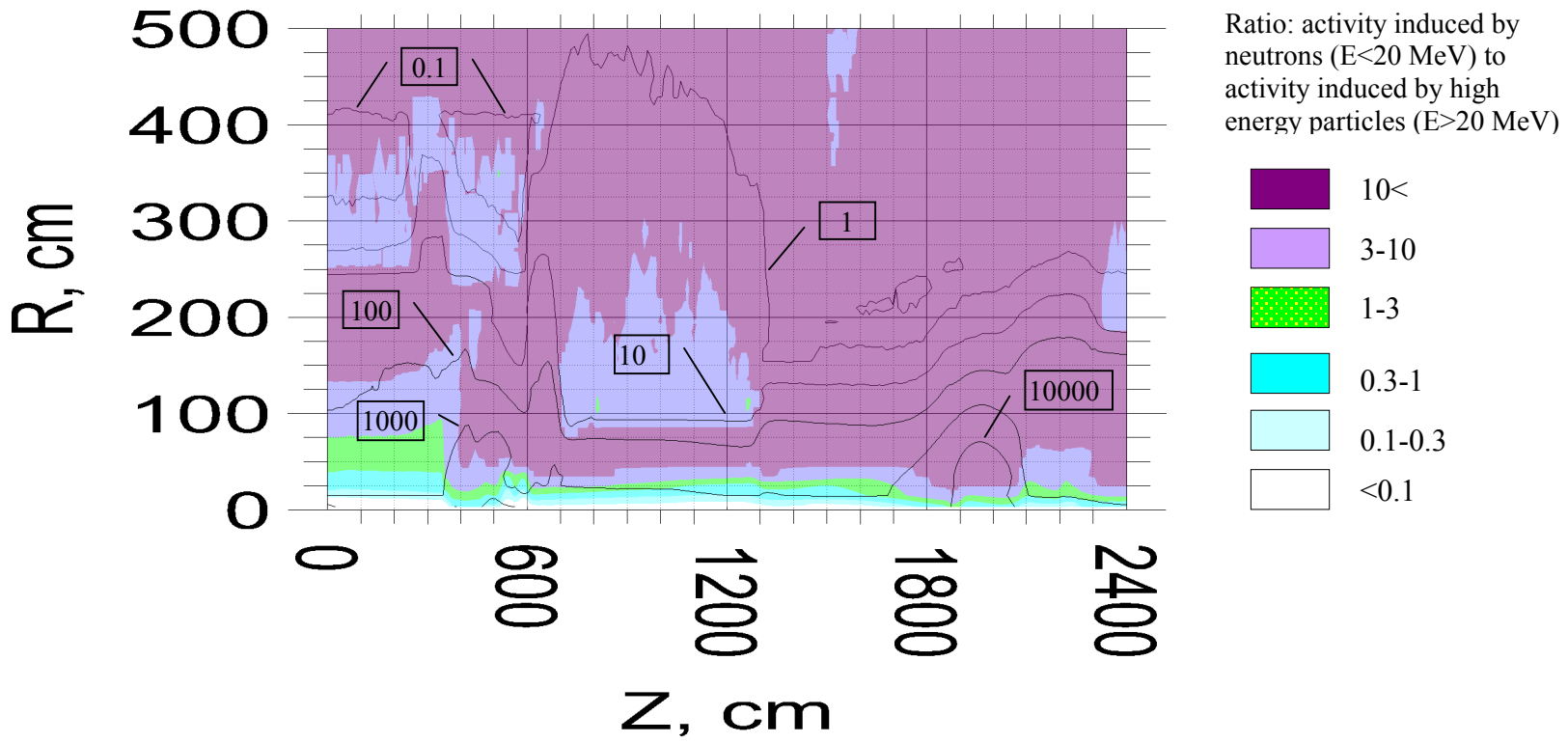

Fig .17. Distribution of induced radioactivity in Hard Lead calculated at T=100d, t=30d. The levels show contact dose rate in μSv/h.

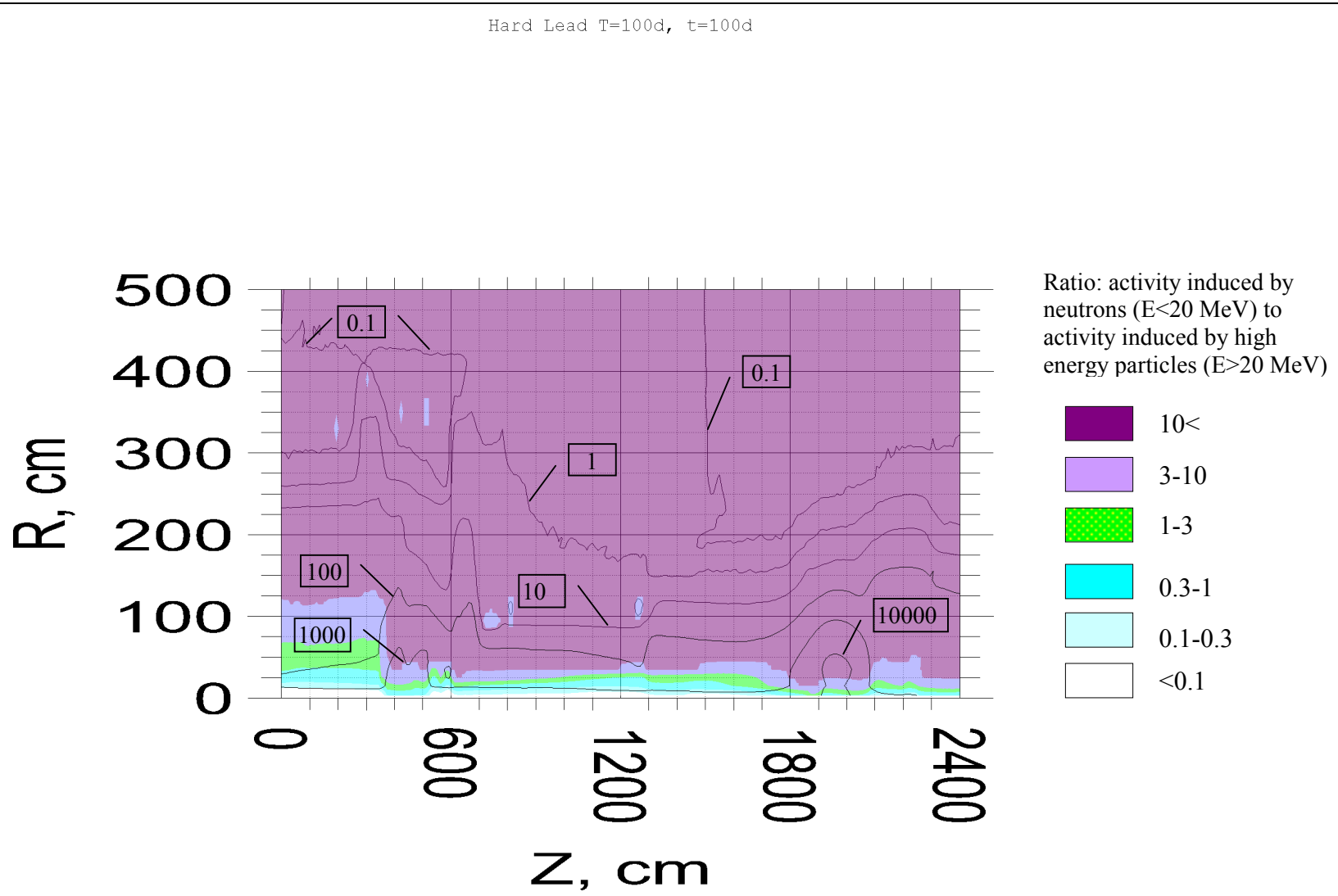

Fig .18. Distribution of induced radioactivity in Hard Lead calculated at T=100d, t=100d. The levels show contact dose rate in μSv/h.

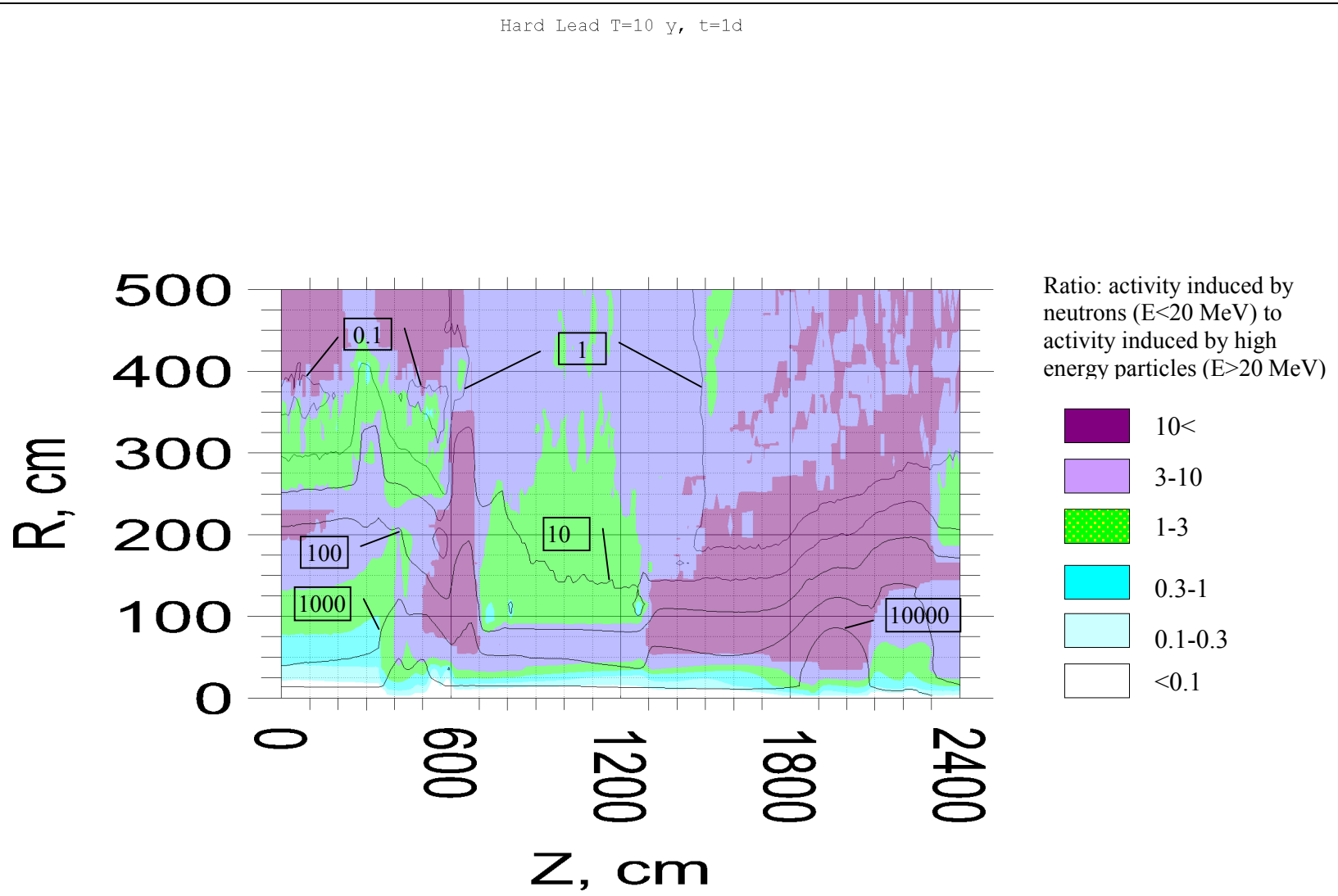

Fig .19. Distribution of induced radioactivity in Hard Lead calculated at T=10y, t=1d. The levels show contact dose rate in μSv/h.

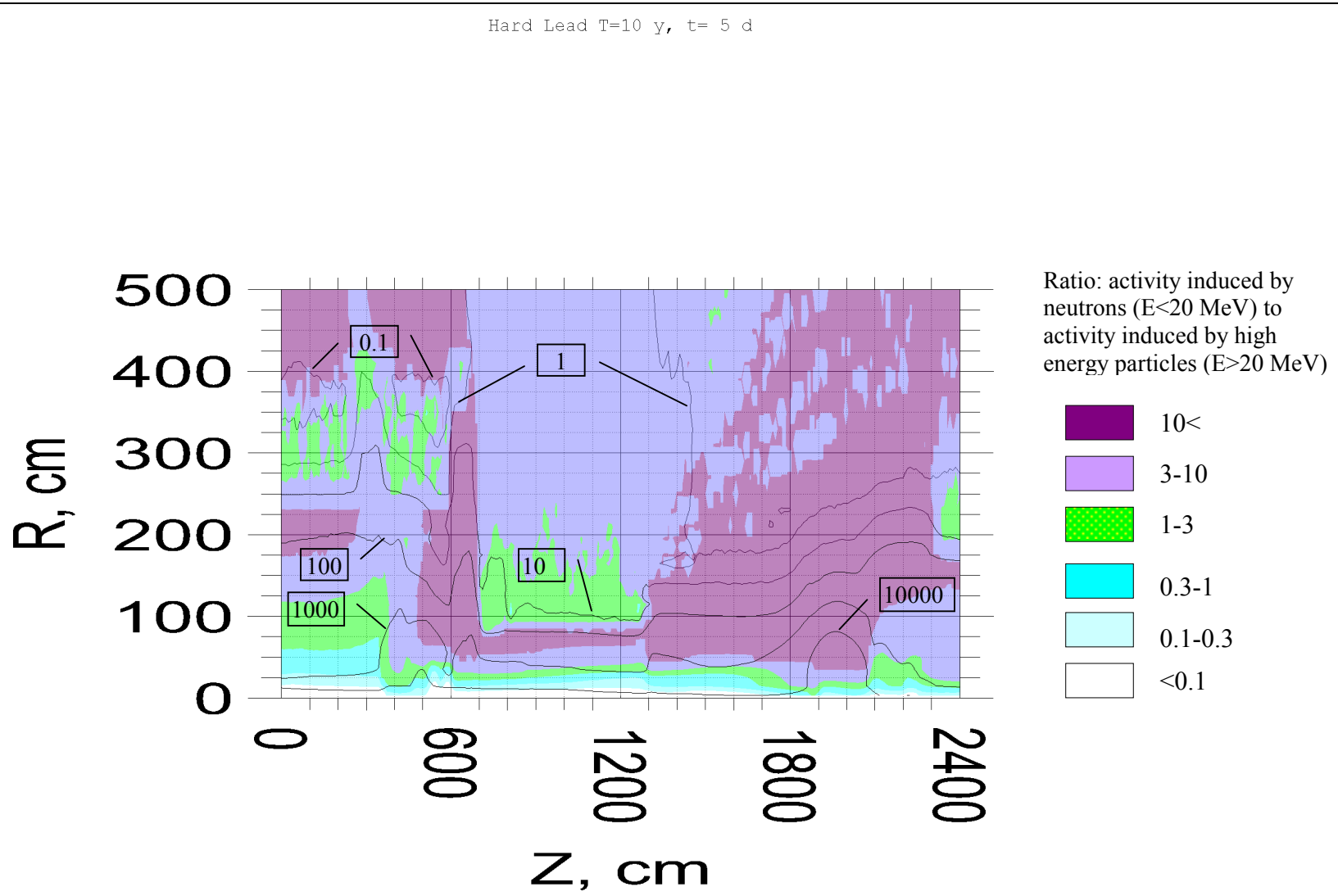

Fig .20. Distribution of induced radioactivity in Hard Lead calculated at T=10y, t=5d. The levels show contact dose rate in μSv/h.

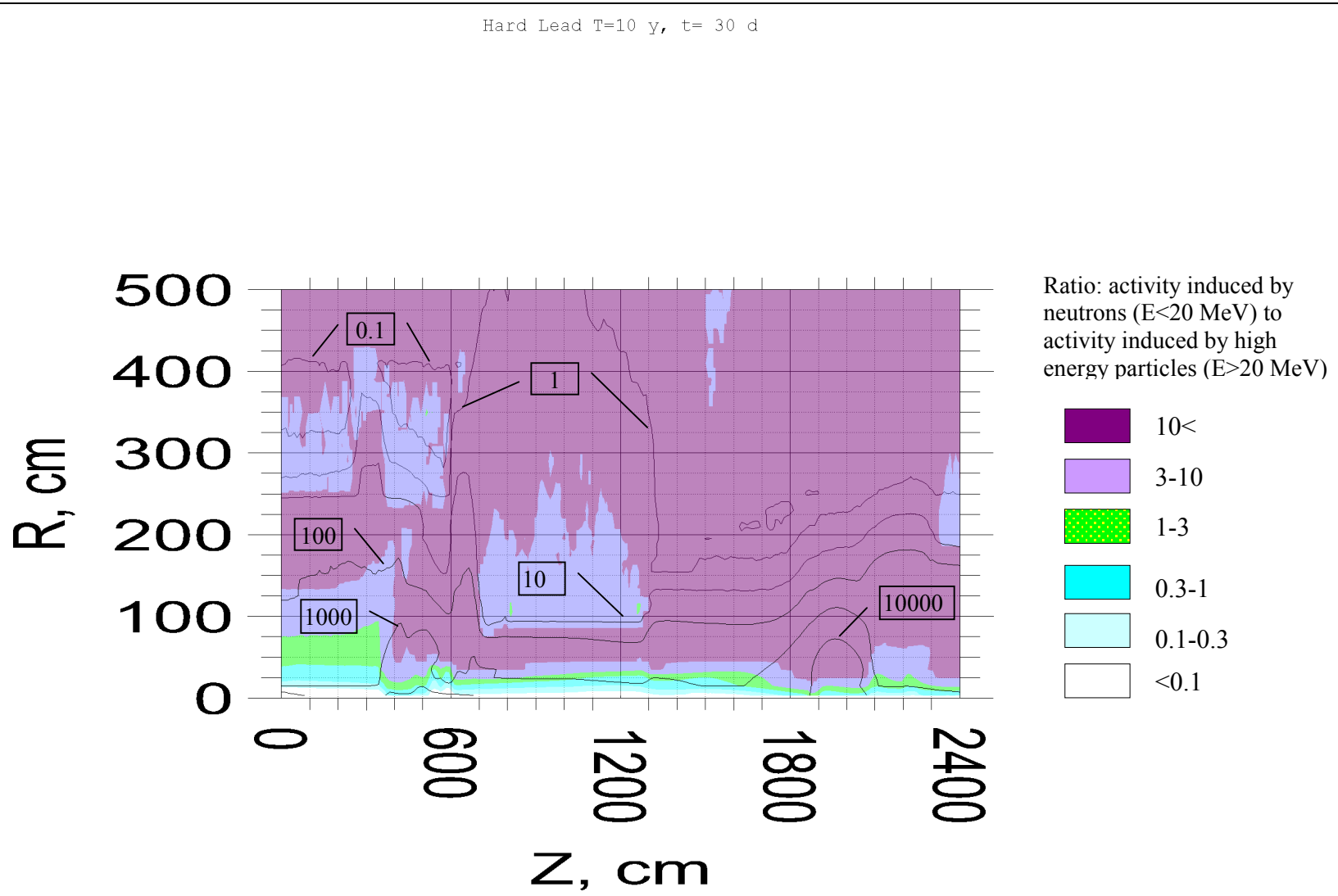

Fig .21. Distribution of induced radioactivity in Hard Lead calculated at T=10y, t=30d. The levels show contact dose rate in μSv/h.

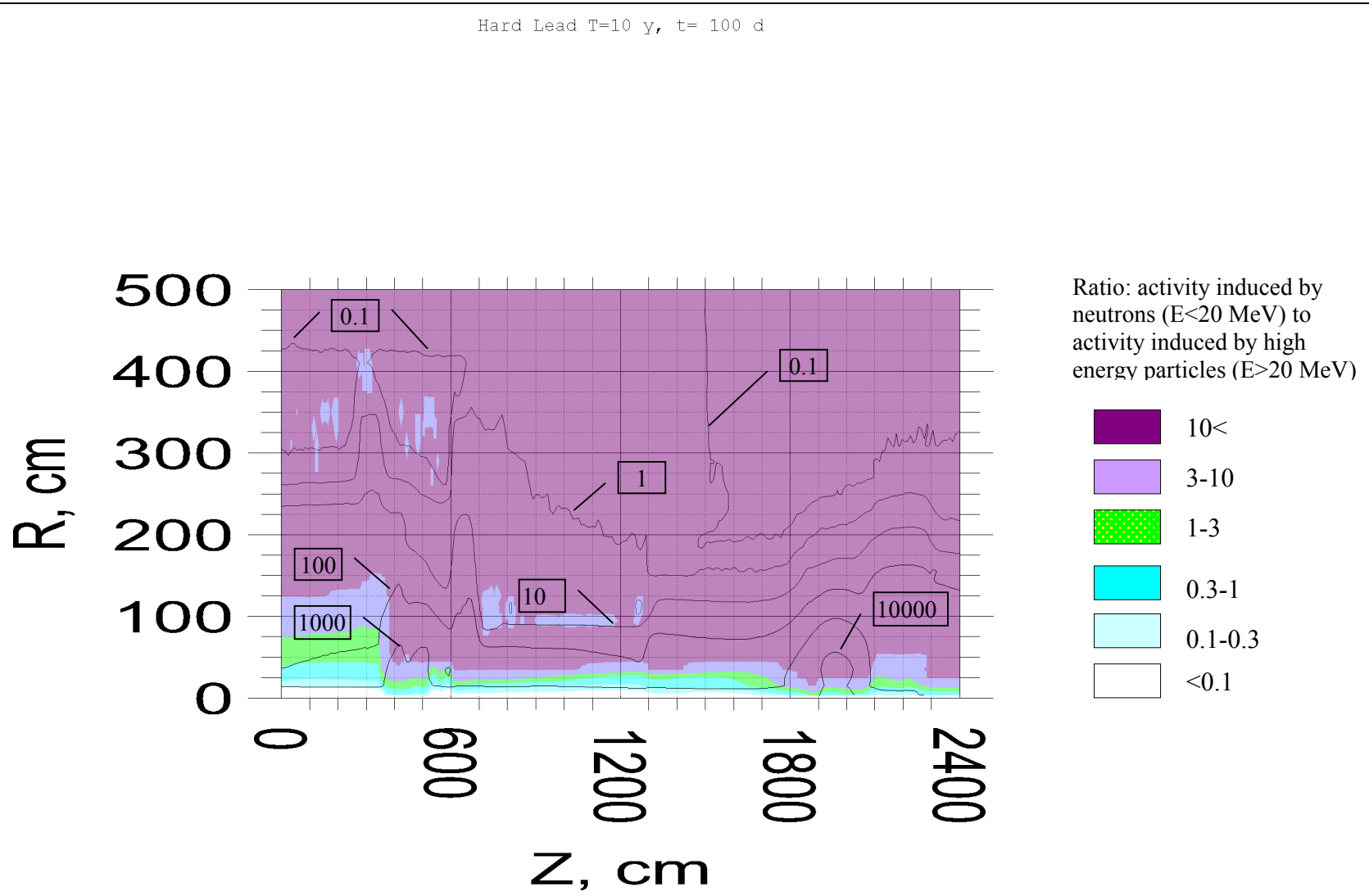

Fig .22. Distribution of induced radioactivity in Hard Lead calculated at T=10y, t=100d. The levels show contact dose rate in μSv/h.

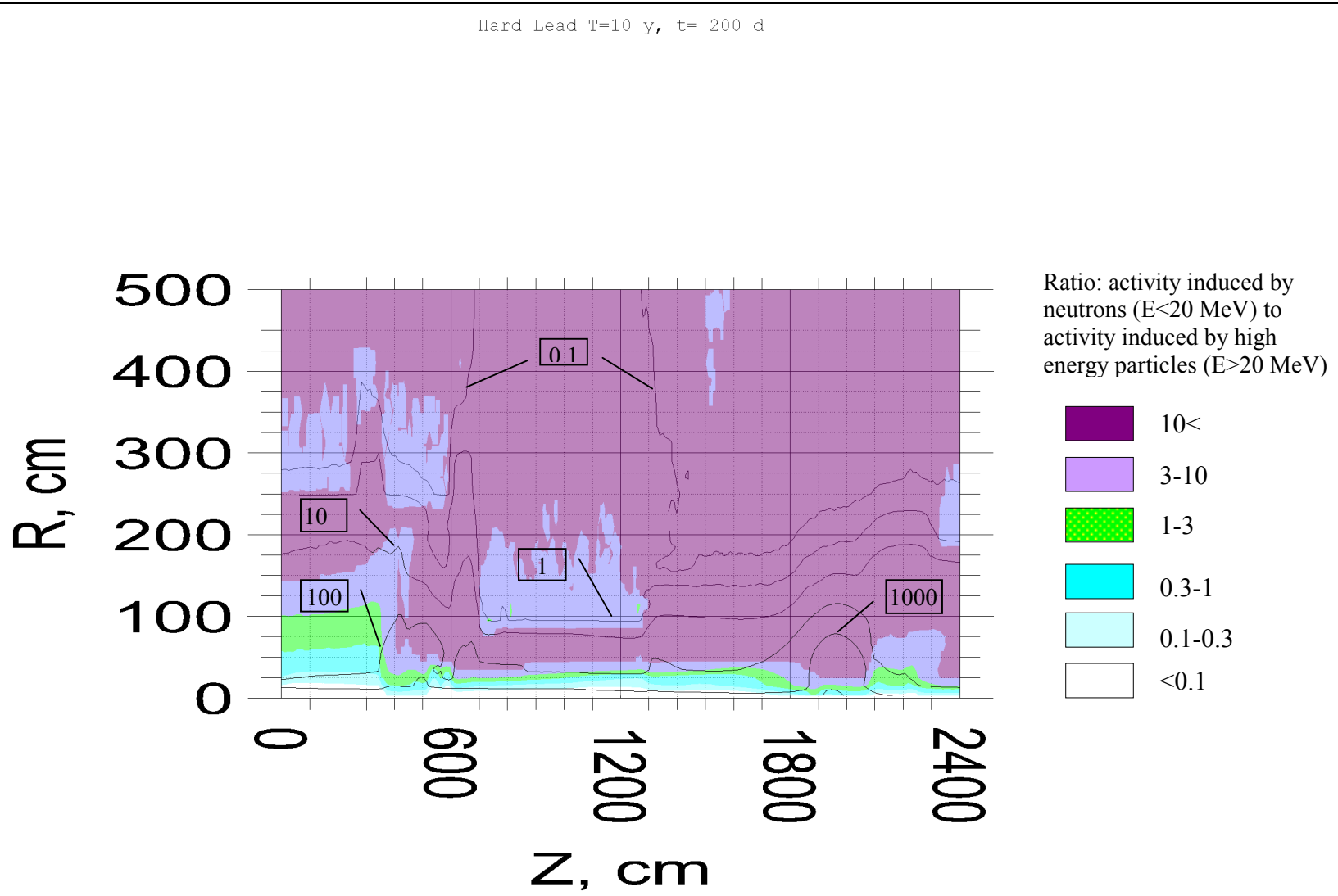

Fig .23. Distribution of induced radioactivity in Hard Lead calculated at T=10y, t=200d. The levels show contact dose rate in μSv/h.

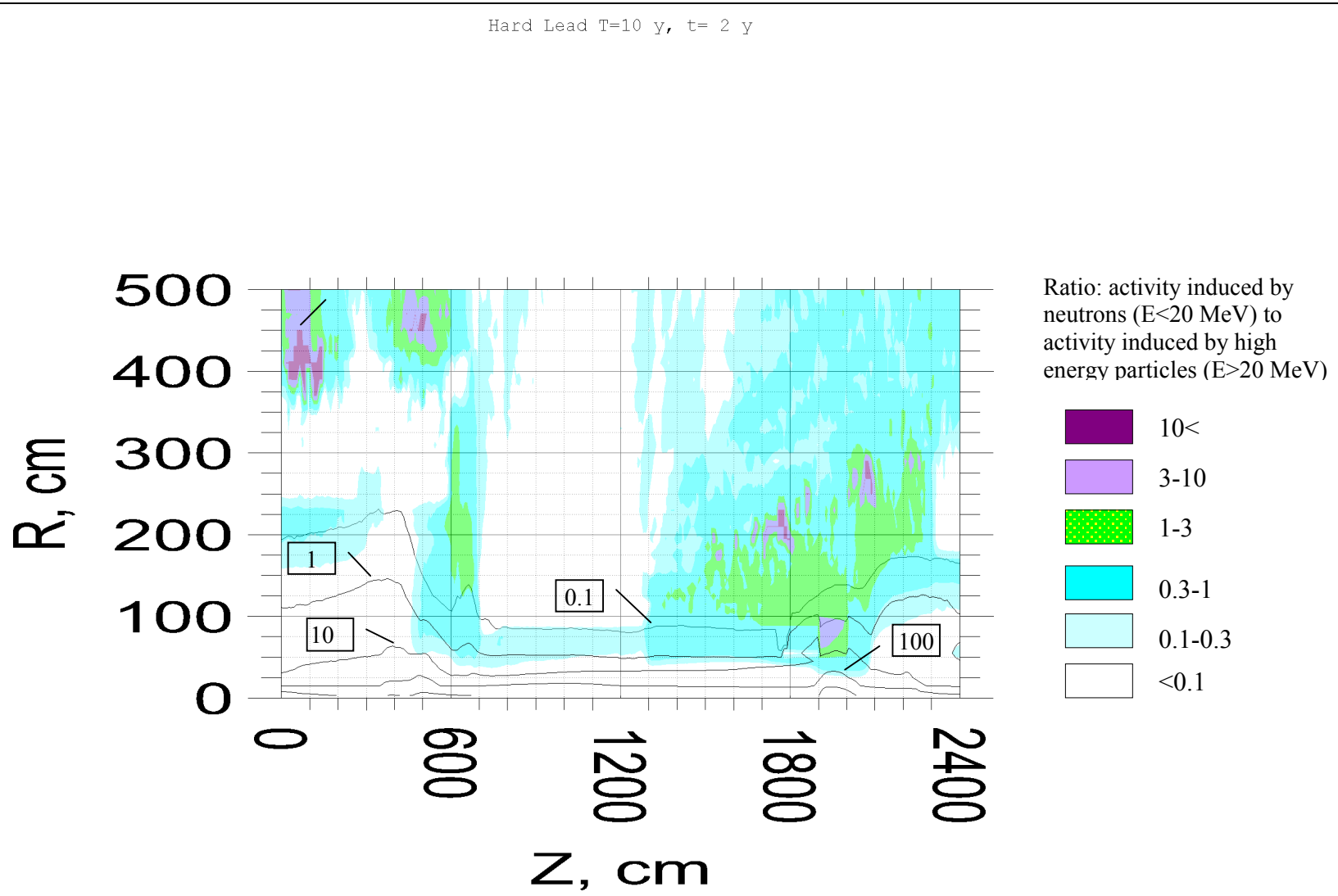

Fig .24. Distribution of induced radioactivity in Hard Lead calculated at T=10y, t=2y. The levels show contact dose rate in μSv/h.